SYNTHESIS AND EVALUATION OF C-ETHER FORMULATIONS FOR USE AS HIGH TEMPERATURE LUBRICANTS AND HYDRAULIC FLUIDS

by F. S. Clark, R. L. Green, and D. R. Miller

MONSANTO RESEARCH CORPORATION

Prepared for

NATIONAL AERONAUTICS AND SPACE ADMINISTRATION

NASA Lewis Research Center

Contract NAS3-15333

1. Report No. NASA CR-134643	2. Government Accession No.	3. Recipient's Catalog No.
4. Title and Subtitle SYNTHESIS AND EVALUATION OF C-ETHER FORMULATIONS FOR USE AS HIGH TEMPERATURE LUBRICANTS AND HYDRAULIC FLUIDS		5. Report Date December 1974
		6. Performing Organization Code
7. Author(s) F. S. Clark, R. L. Green, and D. R. Miller		8. Performing Organization Report No. MRC-SL-460
		10. Work Unit No.
9. Performing Organization Name and Address Monsanto Research Corporation 800 North Lindbergh Boulevard St. Louis, Missouri 63166		11. Contract or Grant No. NAS3-15333
		13. Type of Report and Period Covered Contractor Report
12. Sponsoring Agency Name and Address National Aeronautics & Space Administration Washington, D.C. 20546		14. Sponsoring Agency Code

15. Supplementary Notes

Project Manager, William R. Loomis, Fluid Systems Components Division, NASA Lewis Research Center, Cleveland, Ohio

16. Abstract

Blends of disiloxanes or low molecular weight C-ethers with C-ethers produce fluids with pour points of -40°C or lower. These new low pour point mixtures have evaporation losses and oxidative stability comparable to reference C-ether oils.

An unformulated C-ether lubricated an 80-mm ball bearing only about one hour at 316°C before catastrophic cage wear occurred. Additives increased the time to failure to 50 or more hours. The best additive, perfluoroglutaric acid, allowed the bearing to run 100 hours without the cage wear failure.

A Vickers PV3-044 hydraulic pump ran for three hours at 260°C using a formulated C-ether lubricant before failure of wear parts occurred. The metallurgy of these wear parts was then changed from tungsten carbide on tin bronzed M2 steel to tungsten carbide on silvered S-Monel. A formulated C-ether/disiloxane blend on the modified pump ran for nine hours at 260°C before failure of wear parts occurred.

17 Key Words (Suggested by Author(s)) C-ethers Disiloxanes Low pour point C-ethers (-40°C) 316°C Bearing tests 260°C Hydraulic pump tests		18. Distribution Statement Unclassified - unlimited	
19. Security Classif. (of this report) Unclassified	20. Security Classif. (of this page) Unclassified	21. No. of Pages 319	22. Price*

NASA-C-168 (Rev. 6-71)

FOREWORD

The research reported herein was done under NASA contract NAS3-15333 by Monsanto Research Corporation in the Monsanto Company Research Center in St. Louis, Missouri. The film thickness measurements were subcontracted to the Lubrication Laboratory of the Department of Mechanical Engineering, Imperial College, London, England.

Dr. Alastair Cameron, Director of the Lubrication Laboratory, was the consultant for the contract. He also assisted in the designing of the bearing rig as did Mr. Richard Shevshenko of Pratt and Whitney Aircraft, and Mr. William R. Loomis and Mr. Robert L. Johnson, both of NASA Lewis Research Center. The main bearing designer was Mr. Don Myers of Midwest Aero Industries Corporation, a division of Pure Carbon Company of Saint Marys, Pennsylvania. Dr. Edward O. Stejskal of Monsanto's Central Research Department designed the slow four-ball machine and the rub-block tester. Mr. Walter N. Trump and Mr. Lewis Fowler of Monsanto invented the new instrument for surface tension measurements. Mr. Ralph A. Luebke and Mr. Paul F. Pellegrin provided the capable hands for running the bearing and pump tests.

This contract was directed by the NASA Project Manager, Mr. William R. Loomis, Fluid Systems Components Division, NASA Lewis Research Center.

TABLE OF CONTENTS

TABLE OF CONTENTS (Continued)

TABLE OF CONTENTS (Continued)

TABLE OF CONTENTS (Continued)

LIST OF TABLES

LIST OF ILLUSTRATIONS

LIST OF ILLUSTRATIONS (Continued)

LIST OF ILLUSTRATIONS (Continued)

LIST OF ILLUSTRATIONS (Continued)

xiii

LIST OF ILLUSTRATIONS (Continued)

xiv

LIST OF ILLUSTRATIONS (Continued)

LIST OF ILLUSTRATIONS (Continued)

LIST OF ILLUSTRATIONS (Continued)

LIST OF ILLUSTRATIONS (Continued)

1. SUMMARY

The objectives of this contract were formulation and evaluation of C-ether fluids for use in the hydraulic and lubrication systems of the space shuttle and advanced air breathing engines. Another goal was to lower the pour point of a reference C-ether from -29°C to -40°C without changing its evaporation loss.

Use of disiloxanes mixed with C-ethers gave a -40°C pour point fluid with little change in the desired evaporation loss or in oxidative stability. A second -40°C pour point fluid containing only C-ethers was also developed.

A screening program tested lubrication additives for C-ethers and the new fluids. Six additive packages were chosen for evaluation in 316°C bearing tests, two for evaluation in 260°C pump tests.

The goal of the bearing test was a 100 hour run. The rig was a specially designed 80-mm axially loaded ball bearing. The C-ether base fluid ran only one hour at 316°C before cage wear failure occurred. The best additive blends ran 47, 94 and 100 hours. The 96 hour test gave excessive deposits. The 100 hour test had no wear failures; an unexplained loss of cage silver occurred from areas of direct fluid impingement on the cage.

Two pump tests were run using a Vickers high temperature PV3-044 pump. The critical wear parts were tungsten carbide on tin bronzed M2 steel. The first test failed after three hours due to deposits on the cylinder barrel and erosion of the piston shoes. The tin bronzed wear areas were refurbished and plated with silvered S-Monel to reduce corrosion and wear. A formulated C-ether/disiloxane fluid ran for nine hours in the modified rig (260°C). At that time excessive internal leakage occurred due to erosion or wear failure of the critical wear areas.

2.   INTRODUCTION

Aircraft currently being designed place increasingly stringent requirements on the performance of bearings, lubricants, hydraulic fluids, hydraulic system components, and other vehicle components. The space shuttle, because of its unique mission requirements, will be especially severe on the fluids and fluid systems used. It has been estimated (ref. 1) that aerodynamic heating during and following reentry will heat lubricants and hydraulic fluids to temperatures well in excess of 340°C for short periods. Such applications will require fluids with exceptional thermal stability, exceptional oxidative resistance, and low vapor pressure. Presently available fluids are of limited use in the temperature range from 260 to 340°C for various reasons, including deficient lubrication, high density, flammability, and high pour point. Several NASA and Air Force contracts (ref. 2-5) are devoted to finding fluids for this operating range.

Polyphenylethers can be made thermally and oxidatively stable at 340°C; however, they have inconveniently high pour points (near 4°C). C-ethers [modified polyphenylethers (ref. 6)] are stable to at least 260°C and to over 320°C in some tests. They have convenient pour points (near -29°C) for most terrestial uses. However, a still lower pour point is needed in the space shuttle. Both the polyphenylethers and C-ethers have low vapor pressures, high surface tensions, and high shear stabilities. The properties of the C-ethers and polyphenylethers make them promising candidates for use in various space shuttle and airframe systems. Moreover, additives and improved formulations can be expected to improve their performance as boundary lubricants and coolants.

Three examples of formulation-improved C-ethers include:

1. MCS® 2931,* a formulated C-ether, permitted a 25-mm bearing to operate satisfactorily for up to 100 hours at 316°C, whereas other C-ethers failed this test in a few minutes (ref. 4).

2. Several C-ether formulations have passed a screening test devised by SNECMA** to simulate wear of silver-plated bronze bearing cage material at 338°C (ref. 7).

---

*Monsanto Company registered trademark.
**Societe Nationale d'Etude et de Construction de Moteurs d'Aviation.

3. When excessive wear in steel/chrome-anodized aluminum journal bearings was discovered to be a problem, an additive package was found which greatly reduced the wear rate (ref. 8).

The general goals, then, of this contract were the formulation or changing of C-ethers to make them usable in the space shuttle hydraulic and lubrication systems. The resulting fluids should also have application in advanced air breathing aircraft engines. Specific goals were:

- Produce a C-ether oil with a -40°C pour point and an evaporation loss at 204°C of 10% maximum. This represents lowering the pour point of a reference C-ether by 11°C without raising its evaporation loss. Realizing this objective might not be attainable, a secondary or fallback goal was set: a -40°C pour point and a 15% evaporation loss. This is the evaporation loss of Mobil's XRM 206A hydrocarbon hydraulic fluid.

- Formulate C-ether fluids to lubricate a high speed ball bearing for 100 hours at 316°C outer race temperature.

- Test two C-ether fluids in a 260°C hydraulic pump test. The target again was to achieve 100 hours successful operation.

3

3. CONCLUSIONS AND RECOMMENDATIONS

CONCLUSIONS

1. New blend stocks extend the low temperature fluidity of a C-ether oil from -29°C to around -40°C without undue sacrifice in evaporation loss. The resulting fluids have excellent oxidative stability particularly in the absence of copper. The blend stocks are disiloxanes or low molecular weight C-ethers. Further pour point reductions are possible if evaporation loss restrictions are relaxed.

   a) One of the new fluids, blend f_3, has a -39°C pour point and an evaporation loss of 11% at 204°C. The primary contract goal was a -40°C pour point and 10% evaporation loss.

2. Unconventional additives enable a C-ether oil to lubricate high speed (2×10^6 DN) aircraft ball bearings for 100 hours at 316°C.

   a) The best bearing performance - 100 hours with no wear failures - was obtained with perfluoroglutaric acid at 0.07%; this additive was not effective in a new low pour point blend developed during the contract.

   b) Other additives produced runs of 47 and 94 hours compared with less than 10 hours for the unformulated C-ether base stock.

   c) Most bearing test failures occurred because of excessive inner race-cage wear.

   d) A reference Type II ester fluid ran the high speed bearing at 260°C for 88 to 125 hours without any lubrication problems. These runs were cleaner than the corresponding C-ether runs at 316°C.

3. The slow speed four-ball screening test was useful in choosing C-ether additives for the full-scale bearing rig. There was a reasonable but not complete correlation between the lowering of the coefficient of friction in the test and bearing life. The slow four-ball test did not predict the bearing performance of a reference Type II ester or of a formulated disiloxane/C-ether fluid. The surface tensions of candidate blends did not correlate with contact angles or bearing life.

4

4. Hydraulic pump tests of a formulated C-ether fluid and a formulated version of blend f_3 failed to run past ten hours.

RECOMMENDATIONS

1. Work out a simpler synthesis of the disiloxanes needed for blend f_3.

2. Prepare and characterize new fluids with pour points around -48°C. These are described in section 5.4.1 (page 19).

3. Develop a wear screening test to simulate the cage-race wear which caused bearing failures with C-ether blends. This instrument could be

   a) a modification of Monsanto's rub-block tester, or

   b) a new wear machine for total simulation of the cage wear.

4. Develop a rating system for bearing debris formation and improve the analysis of debris. The latter might include a deposit analysis which distinguishes between metal wear particles and organic deposits.

4. NOMENCLATURE OF C-ETHERS

C-ethers are a proprietary family of jet engine lubricants. Chemically, these products are modified polyphenylethers and they will be designated in this report by the number of benzene rings in their structure.

5.   MATERIALS

5.1   BASE STOCKS AND REFERENCE OILS

The following fluids for the contract came from existing commercial stocks:

- MCS 524:   a standard C-ether base stock unformulated except for antifoam

- 3-Ring C-ether (FH-140)

- Skylube 45C   a formulated Type II ester lubricant

The viscosities and pour points of these products are given in Table 1.

TABLE 1. - PHYSICAL PROPERTIES OF BASE STOCKS AND REFERENCE ESTER

	Viscosity, cs		
	38°C	99°C	Pour Point, °C
MCS 524	25.2	4.13	-29
3-Ring C-ether	12.4	3.5	-45
Skylube 450	28-29	5.3	-59

5.2   ADDITIVES

The additives used in the present study are listed on the next page.

5.3   FORMULATIONS/BLENDING

No special procedures were necessary in preparing formulations for the screening and bearing tests other than bearing test 14. Modest heating dissolved trichloroacetic acid and phenylphosphinic acid in the base stocks. Blends containing perfluoroglutaric acid (PFGA) took longer heat cycles. Dry PFGA was added to the fluid at 40-64°C and stirred for a day. After cooling for at least a day, filtration completed the blending. Subsequent fluorine analysis usually showed an acid concentration of 0.06 to 0.07%.

The preparation of fluids for bearing test 14 and the pump tests are given in the sections describing those tests.

7

Additive	Abbreviation	Chemical Class	Source
Trichloroacetic acid	TCA		
Additive A-88	A-88		Monsanto Co.
Perfluoroglutaric acid	PFGA		
Phenylphosphinic acid	PPA or ϕPO_2H_2		
m-Phenylmercaptophenyl-phosphinic acid	PMPPA or $\phi S\phi PO_2H_2$		Synthesized for the contract; see Appendix A
m-(m-Phenylmercapto-phenylmercapto)phenyl-phosphinic acid	PMPMPPA or $\phi S\phi S\phi PO_2H_2$		Synthesized for the contract; see Appendix A
Tetraoctyltetraphos-phetane tetrasulfide	Tetrasulfide	Sulfide	Monsanto Co.
Emcol PS-236		Organic phosphate ester	Witco Chemical
DC-473		Glycol silicone copolymer	Dow Corning
DC-472		Glycol silicone	Dow Corning
L-520		Glycol silicone	Union Carbide
CP 57347		Sterox; ethoxylated alkylphenol	Monsanto Co.
CP 57518		Sterox; propoxylated phenol	Monsanto Co.
Phenyloctadecanoic acid		Carboxylic acid	Eastman
Diphenyldimethoxysilane	$\phi_2 Si(OCH_3)_2$	Silicate	Dow Corning
Phenyltrimethoxysilane	$\phi Si(OCH_3)_3$	Silicate	Dow Corning
DC-550		Aryl silicone	Dow Corning
DC-710		Aryl silicone	Dow Corning
Versilube 1080		Large alkyl silicone	General Electric
XF-1-0307		Stearyl siloxane	Dow Corning
F-157 wax		Poly(dimethylsiloxy) stearyloxy siloxane	Dow Corning
Krytox PR 143AA		Polyperfluoropropy-lene oxide	Du Pont
UC L-77		Silicone	Union Carbide

5.4   LOW POUR POINT BASE STOCKS

This section describes the development of new low pour point fluids. Details of the laboratory syntheses needed for this work are in Appendix B. Once blend f_3 was chosen for rig tests, six gallons of this material was synthesized. The large scale preparations involved are given in Appendix C.

Generally the term pour point means the lowest temperature at which a fluid will flow. Lack of flow can be due to crystallization or to high viscosity (above around 50,000 cs). Hereafter in this study pour point will mean lack of flow due only to high viscosity; crystallization will be considered separately. For example, a pour point of -46°C (-50°F) for the 3-ring C-ether is the temperature of a supercooled sample where high viscosity inhibits flow. This compound melts at ∿19°C (66°F). Of course, all final blends must be non-crystallizing to allow use in any engine or hydraulic system.

Three approaches looked promising for lowering the pour point of C-ethers:

1.   Use of disiloxanes or silanes to give fluids or fluid components with lower pour points. The basis for using silylation is in the literature (ref. 9) and in proprietary Monsanto studies. This approach was very successful; it produced an oil with a pour point of -40°C and an evaporation loss at 204°C (400°F) of 11%. The contract goal was -40°C and 10%, respectively. Based on this silylation technology, it should be possible in the future to make products with pour points around -48°C (-55°F) and evaporation losses around 24%.

2.   Blending lower molecular weight compounds into C-ethers. This would lower the pour point but only at the expense of increasing the evaporation loss. A suitable result would then have to be a compromise between these properties. This method was also successful giving a fluid with a -40°C pour point and a 204°C (400°F) evaporation loss of 18%. This almost equals the secondary goal of a -40°C pour point with 15% evaporation loss.

3.   Introduction of a compound into the C-ethers which synergistically lowers the viscosity of the fluid. This will also lower the pour point. This approach was not successful as the largest pour point lowering was only 2°C (4°F).

5.4.1 Low Pour Point Fluids from Silylation

The following information was known at the start of the contract from reference 9 and proprietary Monsanto data:

Compound	Pour Pt., °C (°F)	Evaporation Loss @ 204°C (400°F), % (6-1/2 hr, 1 atm)
3-Ring C-ether	-46 (-50)	17
50% 3-Ring C-ether } 50% 4-Ring C-ethers	-29 (-20)	10
3-Trimethylsilyldiphenyl-ether	-52 (-62)	
1,3-bis(m-Phenoxyphenyl) tetramethyldisiloxane	-29 (-20)	

These data immediately suggested that a blend of the 3-ring C-ether and the above phenoxyphenyldisiloxane would have a pour point well below -29°C (-20°F). This was confirmed as shown below:

	Pour Pt.	Evaporation Loss @ 204°C (400°F), %
(f) 60% 3-Ring C-ether 40% 4-Ring phenoxy-disiloxane	-40°C	8

This mixture (called blend f) actually meets the primary contract goal of a -40°C pour point and a 10% evaporation loss.

To test the thermal stability of the disiloxane blend (f), a 260°C (500°F) oxidation-corrosion test was run with very encouraging results. No deposits were observed with or without copper specimens in the fluid. With copper, blend f showed a larger 38°C (100°F) viscosity increase than MCS 524 (27% versus 2%), but even so the increase was considerably lower than that typical of such base stocks as hindered esters or phosphate esters. Without copper, the viscosity increase on blend f was the same as on MCS 524, 1%.* Unfortunately, blend f crystallized extensively after ten days when seeded and then subjected to a -40°C to -19°C temperature cycle in a cold box. Gas-liquid chromatography analysis of the crystals showed 90% 3-ring C-ether and 10% 4-ring. Apparently the 3-ring C-ether is crystallizing. This crystallization precludes the use of blend f as a low temperature fluid.

---

*The above results were on a disiloxane sample of 94% purity. Using 99% pure disiloxane, the viscosity increase was 24% in the presence of copper, 2% in the absence of copper.

The calculated pour point for blend f based on <u>linear pro-</u>
<u>portionality</u> <u>of</u> <u>pour</u> <u>point</u> <u>to</u> <u>weight</u> <u>percent</u> is -39°C; that is

$$0.6 \ (-46°C) \ + \ 0.4 \ (-29°C) \ = \ 39°C$$

This is in good agreement with the observed pour point of -40°C.
Subsequent data (Table 2) showed this linear mixture rule to be
true for C-ether and silylated C-ether blends. This allowed cal-
culation of pour points from components usually to within 2°C
(4°F) of the observed pour point.

More data were needed to put the pour point work on firmer
footing; namely:

1) Pour points and evaporation losses on model C-ethers
and silylated compounds. This would confirm the
correlation between pour points and concentration of
the different components. Also, it might lead to a
correlation between pour point and molecular structure.

2) Evaluation of the physical properties of blends con-
taining promising pour point depressants from 1). This
would include pour point measurements, oxidation-corro-
sion tests and crystallization tests.

The following compounds were synthesized for the low pour
point program. Synthetic details are given in Appendix B.

Compound	Chemical Name	Abbreviated Name
<u>mm</u>φSφOφSi(CH$_3$)$_3$	3-Trimethylsilyl-3'-phenyl-mercaptodiphenyl ether	
<u>m</u>φSφSi(CH$_3$)$_3$	3-Trimethylsilyldiphenyl sulfide	2-Ring sulfur silyl
<u>mm</u>[φOφSi(CH$_3$)$_2$]$_2$O	1,3-bis(m-Phenoxyphenyl) tetramethyldisiloxane	4-Ring oxy di-siloxane
<u>mm</u>[φSφSi(CH$_3$)$_2$]$_2$O	1,3-bis(m-Phenylmercapto-phenyl)tetramethyldi-siloxane	4-Ring sulfur disiloxane
[φSi(CH$_3$)$_2$]$_2$O	1,3-bis(Phenyl)tetra-methyldisiloxane	2-Ring disiloxane
<u>m</u>φSφSi(CH$_3$)$_2$-OSi(CH$_3$)$_2$φ	1-(m-Phenylmercaptophenyl)-3-phenyltetramethyl-disiloxane	3-Ring sulfur disiloxane

<u>mm</u>...Consecutive meta orientation from the left side of the
structure.
φ = Substituted benzene ring.

11

Pour points and evaporation losses were found for most of these compounds as well as for various C-ethers and C-ether mixtures. These results are given in Table 2.

TABLE 2. - POUR POINTS, FREEZING POINTS AND EVAPORATION LOSSES OF REFERENCE COMPOUNDS AND BLENDS

mm...Consecutive meta orientation from the left side of the structure

ϕ = Substituted benzene ring

	Compound or Blend	Freezing Point, °C (°F)	Pour Point, °C (°F)	Evap. Loss @ 204°C (400°F), %
1)	2-Ring C-ether	>-7 (>20)	~-93 (-135)[a]	100
2)	3-Ring C-ether		-46 (-50)	17
3)	4-Ring C-ethers		-12 (10)	1-1/2
4)	50% 3-Ring C-ether 50% 4-Ring C-ethers		-29 (-20)	10
5)	50% 2-Ring C-ether 50% 3-Ring C-ether		-65 (-85)	
6)	50% 2-Ring C-ether 50% 4-Ring C-ethers		-57 (-70)	51
7)	$\underline{m}\phi S\phi Si(CH_3)_3$		-54 (-65)	
8)	$\phi Si(CH_3)_2 OSi(CH_3)_2 \phi$			
9)	$\underline{m}\phi O\phi S\phi$			36
10)	$\underline{mm}\phi S\phi O\phi Si(CH_3)_3$		-29 (-21)	
11)	$\underline{mm}[\phi O\phi Si(CH_3)_2]_2O$ 4-ring oxy disiloxane		-29 (-20)	
12)	$\underline{mm}[\phi S\phi Si(CH_3)_2]_2O$ 4-ring sulfur disiloxane		-33 (-28)	
13)	$\underline{m}\phi S\phi Si(CH_3)_2 OSi(CH_3)_2\phi$ 3-ring sulfur disiloxane		-56 (-68)	26

---

[a]Extrapolated.

It was not possible to measure the 2-ring C-ether pour point directly because the tilting arm in the cold box froze at the very low temperatures involved. The value of -93°c comes from the average of the linear extrapolations of the 50:50 2-3 ring mixture and the 50:50 2-4 ring mixture. The former extrapolation gives a value of -84°C for the 2-ring C-ether; the latter gives a value of -101°C. This is not very good agreement; it is the one instance where the linearity of pour points with weight percents give an inconsistent result.

The data from Table 2 show that evaporation losses are a linear function of weight percent. For example:

evaporation loss of 3-ring C-ether = 17 %

evaporation loss of 4-ring C-ethers = 1.5%

calculated evap. loss for 50:50 mixture = 9 %

observed evap. loss for 50:50 mixture = 10 %

Seven blends were characterized based on the various compounds in Table 2. Six of these contained silicon compounds, the seventh (blend b) contained only C-ethers. It is discussed further in section 5.4.2. These blends may be divided as follows:

(1) Four blends with pour points around -40°C

(2) Three blends with pour points around -46°C

A third group of blends has not been characterized but their properties are predictable with reasonable assurance from data obtained in the contract.

The compositions of the seven tested blends are given in Table 3. Their pour points, evaporation losses and crystallinity tests are summarized in Table 4 and graphically shown in Figure 1. O&C tests are reported in Tables 5 and 6. These results are discussed below.

1. -40°C Blends

Blend	Pour Point, °C (°F)	Evaporation Loss, %
b	-40 (-40)	18
f_1	-39 (-39)	19
f_2	-42 (-43)	21
f_3	-39 (-39)	11

TABLE 3. - COMPOSITION OF LOW POUR POINT BLENDS

mm...Consecutive meta orientation from the left
    side of the structure
φ = Substituted benzene ring

4-Ring sulfur disiloxane	= 1,3-bis(m-Phenylmercaptophenyl) tetramethyldisiloxane
3-Ring sulfur disiloxane	= 1-(m-Phenylmercaptophenyl)-3-phenyltetramethyldisiloxane
2-Ring disiloxane	= 1,3-bis(Phenyl)tetramethyl-disiloxane

Blend		
b	64%	3-Ring C-ether
	29%	4-Ring C-ethers
	7%	2-Ring C-ether
f_1	30%	3-Ring C-ether
	30%	m-φOφSφ
	10%	mm-φSφOφSi(CH$_3$)$_3$
	30%	4-Ring sulfur disiloxane
f_2	30%	3-Ring C-ether
	30%	m-φOφSφ
	10%	3-Ring sulfur disiloxane
	30%	4-Ring sulfur disiloxane
f_3	50%	3-Ring C-ether
	30%	4-Ring sulfur disiloxane
	10%	3-Ring sulfur disiloxane
	10%	mm-φSφOφSφ
g^1	50%	3-Ring C-ether
	30%	4-Ring sulfur disiloxane
	20%	2-Ring C-ether
j	20%	4-Ring sulfur disiloxane
	10%	3-Ring sulfur disiloxane
	30%	3-Ring C-ether
	30%	m-φOφSφ
	10%	2-Ring disiloxane
k	20%	4-Ring sulfur disiloxane
	10%	3-Ring sulfur disiloxane
	30%	3-Ring C-ether
	30%	m-φOφSφ
	10%	2-Ring C-ether

14

TABLE 4. - LOW POUR POINT BLENDS: POUR POINTS, EVAPORATION
LOSSES AND CRYSTALLINITY TESTS

Blend	Pour Point, °C (°F)	Evap. Loss @ 204°C,%(6-1/2 hr, 760 mm)	Crystallinity Test (10 day cycling between T_1 and T_2)
MCS 524	-30 (-22)	10	
Synthetic hydrocarbon MIL-H-83282 (XRM-206A)		15	
b	-40	18	No growth of seed crystal[a]
f_1	-39 (-39)	19	No growth of seed crystal[a]
f_2	-42 (-43)	21	Seed crystal dissolves after six days[a]
f_3	-39 (-39)	11	Seed crystal dissolves after six days[a],[b]
g^1	-49 (-57)	31	Seed crystal dissolves after two days[c]
j	-47 (-53)	30	Seed crystal dissolved after two days then a crop of small crystals formed in the fluid (see Fig. 2); borderline pass[c]
k	-46 (-50)	31	No crystal growth in five days. Crystal lost during sample transfer. No crystal growth during another five day period after regeneration.[c]

[a] T_1 = -40°C, T_2 = -19°C (-2°F).
[b] Also passes viscometer tube crystallinity test.
[c] T_1 = -47°C (-52°F), T_2 = -28°C (-19°F).

15
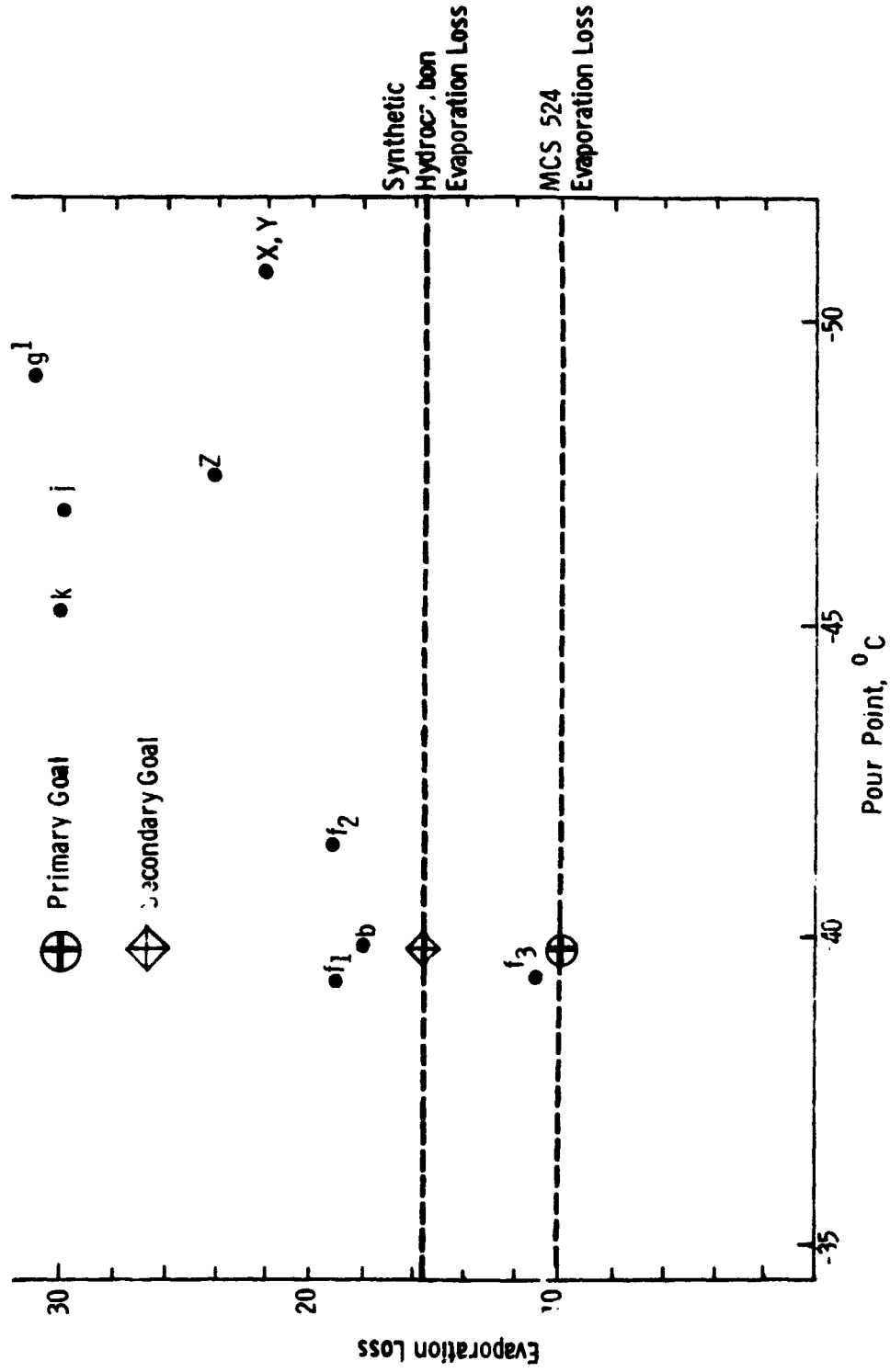
Figure 1. Pour Points and Evaporation Losses of Experimental Blends

16

TABLE 5. - OXIDATION-CORROSION TESTS ON LOW POUR POINT FLUIDS

260°C (500°F); 51 hr; (no copper coupon); 5 ℓ air/hr

Blend	Visc. Inc., %	Wt. Change, mg/cm²ᵃ Silver	Deposits	Fluid Appearance After Test
b	8	-1.0	Light coke, no sludge	Normal
f₁	3	-0.4	No coke, no sludge	Slightly opaque orange
f₂	3	-0.4	No coke, no sludge	Clear light orange
f₃	4	-0.2	No coke, no sludge	Clear orange
g¹	4	-0.6	V. lt. coke, no sludge	Normal
j	4	-0.2	V. lt. coke, no sludge	Clear light orange
k	4	-0.4	No coke, no sludge	Opaque orange-red

TABLE 6. - OXIDATION-CORROSION TESTS ON LOW POUR POINT FLUIDS

260°C (500°F); 48 hr; 5 ℓ air/hr

Blend	Visc. Inc., %	Wt. Change, mg/cm²ᵃ Cu	Ag	Deposits	Fluid Appearance After Test
b	15	-8.2	0.0	No coke, no sludge	Normal
f₃	87	-3.6	-3.3	No coke, no sludge	Normal
g¹	146	-9.0	-2.5	No coke, no sludge	Normal

ᵃNegligible weight losses for magnesium, aluminum, titanium and iron.

All of these blends pass the ten day crystallization test. [In this test, the fluid plus an FH-140 crystal are cycled between T_1 and T_2 for ten days. T_1 is roughly the pour point of the blend and T_2 is the pour point plus $\sim22°C$ (40°F). The cycle time between T_1 and T_2 is about one hour.] In addition, blend f_3 passed another type of crystallinity test without significant crystal growth. A sample of blend f_3 was put in a Cannon semi-micro 700 viscometer tube and caused to flow through the tube at various times over four days at temperatures between -45°C and -23°C. This gives a fluid motion favoring molecular alignment and hence crystallization. The fluid quickly turned turbid and a few small crystals formed. These crystals decreased in size during the test and did not obstruct the flow of the oil. The blend became clear at -8°C after a fairly rapid temperature rise.

Blend b has the desired -40°C pour point and an evaporation loss 3% higher than the secondary goal of 15%. This fluid has good oxidation-corrosion test properties with a somewhat high copper corrosion (-8 mg/cm^2) and somewhat high silver corrosion in the absence of copper (-1 mg/cm^2). It contains no silicon compounds and so will probably be less expensive than the other fluids. Also, it seems more stable in the presence of copper (15% viscosity increase vs. 87% for blend f_3).

Blends f_1, f_2, and f_3 are variations on blend f. This mixture

<div align="center">

60% 3-ring C-ether

40% 4-ring oxy disiloxane

</div>

crystallized extensively. Apparently the presence of three other components inhibits the crystallization of the 3-ring C-ether. All of these oils give excellent and comparable oxidation-corrosion test results in the absence of copper. With similar synthetic problems, the lower evaporation loss of blend f_3 makes it superior to f_1 or f_2.

2. -46°C Blends

Blend	Pour Point, °C (°F)	Evap. Loss @ 204°C, %
g^1	-49 (-57)	?1
j	-47 (-53)	30
k	-46 (-50)	30

Compared with the secondary goal (-40°C pour point, 15% evaporation loss) these blends offer a rough trade-off of an 8°C (15°F) lower pour point for a 15% higher evaporation loss. Fluids g[1] and k pass the ten day crystallization test while blend j gives a marginal pass (see Figure 2). The oxidation-corrosion properties of these blends are similar in the absence of copper.

3. Non-Characterized Blends

Attractive low pour point blends based on known disiloxane compounds would include:

Blend	Projected Pour Point, °C (°F)	Projected Evap. Loss @ 204°C, %
(X) 50% 3-Ring C-ether 50% 3-Ring sulfur disiloxane	-51 (-59)	22
(Y) 80% 3-Ring sulfur disiloxane 20% 4-Ring sulfur disiloxane	-51 (-59)	22
(Z) 50% 3-Ring C-ether 25% m-ϕSϕOϕ 25% 3-Ring sulfur disiloxane	-48 (-54)	24

5.4.2   Low Pour Point Fluids from Dilution with Lower

Molecular Weight Compounds

Blend b is:

    64% 3-ring C-ether
    19% 4-ring C-ethers
     7% 2-ring C-ether

These percentages came from a contour mapping of pour points and evaporation losses on 3-component triangular diagrams (Figure 3). The pure components are at each vertex of the triangle. The data used (taken from Table 2) are shown on page 22.
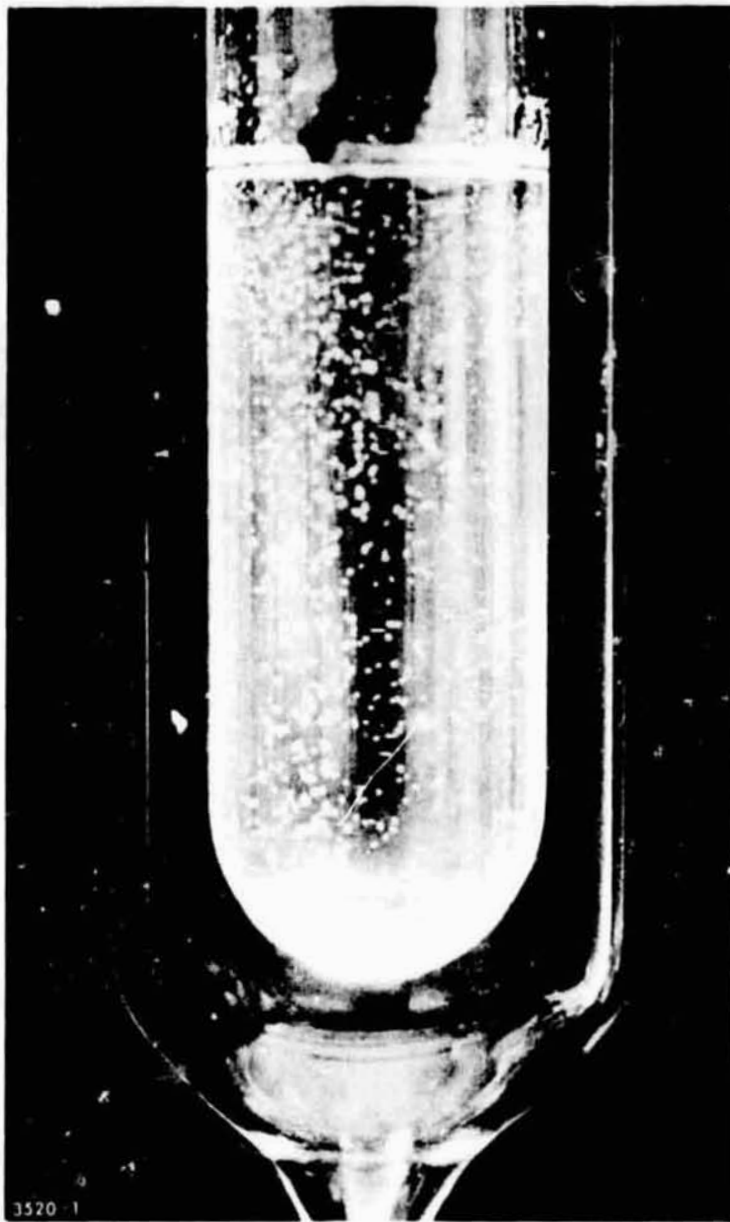
Figure 2. Blend j After the Crystallization Test
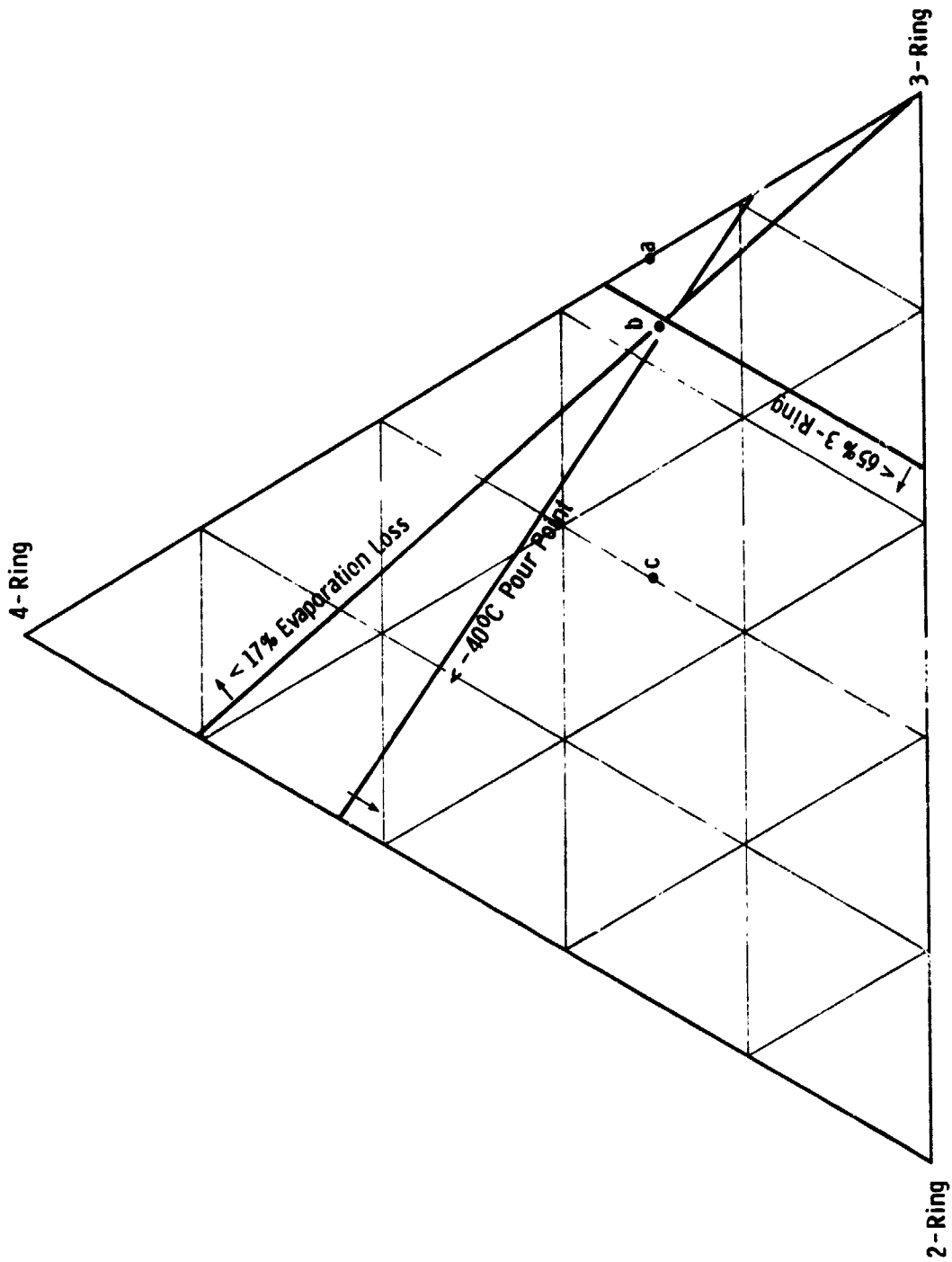
Figure 3. Three Component C-Ether Blend Diagram

REFERENCE BLEND DATA

Compound or Blend	Freezing Pt., °C (°F)	Pour Pt., °C (°F)	Evap. Loss @ 204°C(400°F), %
2-Ring C-ether (2)	>-7 (>+20)	∿-93 (-135)[a]	100[c]
3-Ring C-ether (3)	19 (66)	-46 (-50)[b]	17
4-Ring C-ethers (4)		-12 (10)	1.5
50% (3) with (4)		-29 (-20)	10
50% (2) with (3)		-65 (-85)	
50% (2) with (4)		-57 (-70)	

[a]Extrapolated.
[b]Supercooled.
[c]An assumed value of 90% was used in triangular diagram constructs.

Linearity of pour point with concentrations permitted the location of the -40°C pour point contour as shown in Figure 3. Vertex evaporation losses then established the 17% loss contour, also shown in Figure 3. Finally the 65% 3-ring ether line is highlighted as an approximate upper limit on the concentration of 3-ring ether to avoid crystallization of this component.

As demonstrated in Figure 3, the three limitations are simultaneously satisfied only in the vicinity of point (blend) b. Blends a and c represent two variations wherein one or two of the restrictions were relaxed. It may be noted that the measured pour and evaporation loss of blend b were almost exactly the values predicted from the diagram using a linear mixture rule.

	Pour Point	Evap. Loss
Observed	-40°C	18%
Predicted	-40°C	17%

5.4.3 Low Pour Point Fluids via Synergistic Viscosity Decrease

The following compounds were dissolved in MCS 524 (pour point = -30°C) to try to lower the pour point. The best result was a 2°C (4°F) lowering of the pour point, a result on the borderline of experimental accuracy.

a) Dow Corning FS-1265 fluorosilicone - This was very insoluble in MCS 524. No pour point measurements were made on the mixture.

22

b)   15-Methyl-15-phenylhentriacontane

$$\text{C}_6\text{H}_5-\overset{\overset{\displaystyle \text{CH}_3}{|}}{\underset{\underset{\displaystyle \text{C}_{14}\text{H}_{29}}{|}}{\text{C}}}-\text{C}_{16}\text{H}_{33}$$
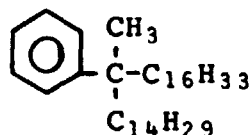
Results on a 4% mixture of this hydrocarbon in MCS 524 were:

% Hydrocarbon	Pour Point, °C (°F)
0	-30 (-22)
4	-24 (-12)

The 4% mixture was opaque at -30°C and had an emulsion-like appearance indicating a phase separation or possibly additive crystallization.

c)   2,5-(1-Methyl-1-hexylnonyl)thiophene (DAT)

$$\text{H}_{17}\text{C}_8-\overset{\overset{\displaystyle \text{CH}_3}{|}}{\underset{\underset{\displaystyle \text{C}_6\text{H}_{13}}{|}}{\text{C}}}\text{---}\underset{S}{\text{[thiophene]}}\text{---}\overset{\overset{\displaystyle \text{CH}_3}{|}}{\underset{\underset{\displaystyle \text{C}_6\text{H}_{13}}{|}}{\text{C}}}-\text{C}_8\text{H}_{17}$$
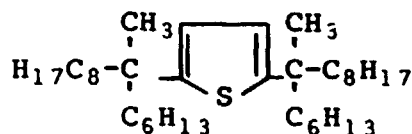
Various amounts of DAT in MCS 524 failed to lower the pour point except at 1%.

DAT, %	Pour Point, °C (°F)
0	-30 (-22)
1	-32 (-26)
5	-26 (-15)
10	-26 (-15)

No further attempts were made to prepare low pour point products by this approach.

5.4.4   Experimental: Test Methods

1. Pour Points

Initial pour point determinations at a participating laboratory were done using ASTM 97-57. The results were erratic and so different from expectations that they were discarded and a non-standard method adopted. The non-standard "cold box" method is described below.

A loaded pour point tube was mounted vertically on a tiltable framework inside a refrigerated cold chamber. The fluid was allowed to equilibrate at set temperature for 45 minutes in the forced-draft-air chamber. The tube was then tilted 90° for 5 seconds. If surface movement was observed, the chamber temperature was dropped several degrees and another tilt test performed after equilibration. The pour point was taken as the lowest temperature at which surface movement was observed.

A comparison of pour points expected and measured by the two methods is shown in Table 7.

TABLE 7. - POUR POINT COMPARISON: THEORETICAL
vs. ASTM vs. COLD BOX

Blend	Pour Point, °C		
	Expected[a]	Defective ASTM	Cold Box
a	-36	-26	-38
b	-40	-32	-40
c	-49	-43	-48
f	-39	-34, -29	-40
c	-50	-40	-48
h	-42	-40	-41
1	-49	-40	-49

[a]Based on a linear mixture rule.

To check the accuracy of the cold box, a pour point was run on MCS 524. The result (-30°C) was in good agreement with the previously run ASTM pour point of -29°C. When blend f_3 was chosen for rig tests, its cold box pour point (-39°C) was re-checked by ASTM 97-57. The result was a pour point of -40°C.

All of the pour points in this contract were done by the cold box method except the following:

24

Compound or Mixture	ASTM Pour Point, °C (°F)	Comment
a) 3-Ring C-ether	-46 (-50)	Run prior to the contract; accurate value
b) 4-Ring C-ethers	-12 (+10)	
c) mφSφSi(CH₃)₃	-54 (-65)	
d) MCS 524 + 5% DAT	-26 (-15)	
e) MCS 524 + 10% DAT	-26 (-15)	

Errors in the ASTM method are more likely at colder temperature; i.e. with (c). However, a blend of 50% 3-ring C-ether and 50% mϕSϕSi(CH$_3$)$_3$ had a cold box pour point of -49°C. This gives a calculated value of -52°C for the mϕSϕSi(CH$_3$)$_3$--good agreement with the ASTM value of -54°C. The pour points for (b), (d) and (e) should be accurate.

2. Evaporation Losses

    Method: ASTM D972-56. Conditions were 204°C (400°F), 6-1/2 hours and one atmosphere pressure.

3. Oxidation-Corrosion Tests

    The apparatus used is a modification of Method 5308 of Federal Test Method Standard 791. Tests were run at 260°C (500°F) for 48 hours with an airflow of five liters of air per hour. One test (Table 5) inadvertently ran for 51 hours.

4. Crystallinity Tests

    Two tests, a ten day temperature cycle and a viscometer tube test, were used. These are described on page 18.

6.   LUBRICANT SCREENING TESTS

6.1   TEST RIGS

The following screening tests evaluated the candidate additives and base stocks.

6.1.1   Slow Speed Four-Ball Test

This was used to study boundary lubrication. The instrument (ref. 10) is a reduced-speed version of the familiar Shell 4-Ball lubrication tester but with disk specimens in place of clamped balls and low thermal inertia specimen holders. The slow speed of rotation, typically 2.2 cm/min, and moderate load ensure boundary lubrication in a near-isothermal environment. Under these conditions wear is negligibly slow and lubrication is followed by continuously measuring the coefficient of friction.

In operation the test sample is heated from room temperature to 371°C with continuous recording of the friction coefficient. The resulting friction-temperature profile reveals any physical or chemical changes in the surface film which alter the friction coefficient. This approach has been used to study various additives in aliphatic oils. For example, a typical boundary friction curve for 0.003 molar tetradecanoic acid in tetradecane on stainless steel shows a sharp friction rise at 78°C (ref 11). This is the temperature of effective desorption of the acid additive from the steel.

Operating conditions used in this contract were:

Speed: 1 rpm (2.2 cm/min)

Load: 3 kg (about 9.65×10^8 N/m^2 or ∿140,000 psi Hz load)

Temperature: room temperature to 371°C (700°F)

Metallurgy: M50 ball on M50 disks
              M50 ball on silvered 6415 disks

After each run all parts of the instrument contacted by the fluid were cleaned in benzene in an ultrasonic cleaner.

6.1.2   Monsanto Company Rub-Block on Rotating Ring Tester

This instrument (Figures 4 and 5) utilizes a ring rotating against two stationary blocks to measure friction and/or wear. In this contract it was used to record friction as a function
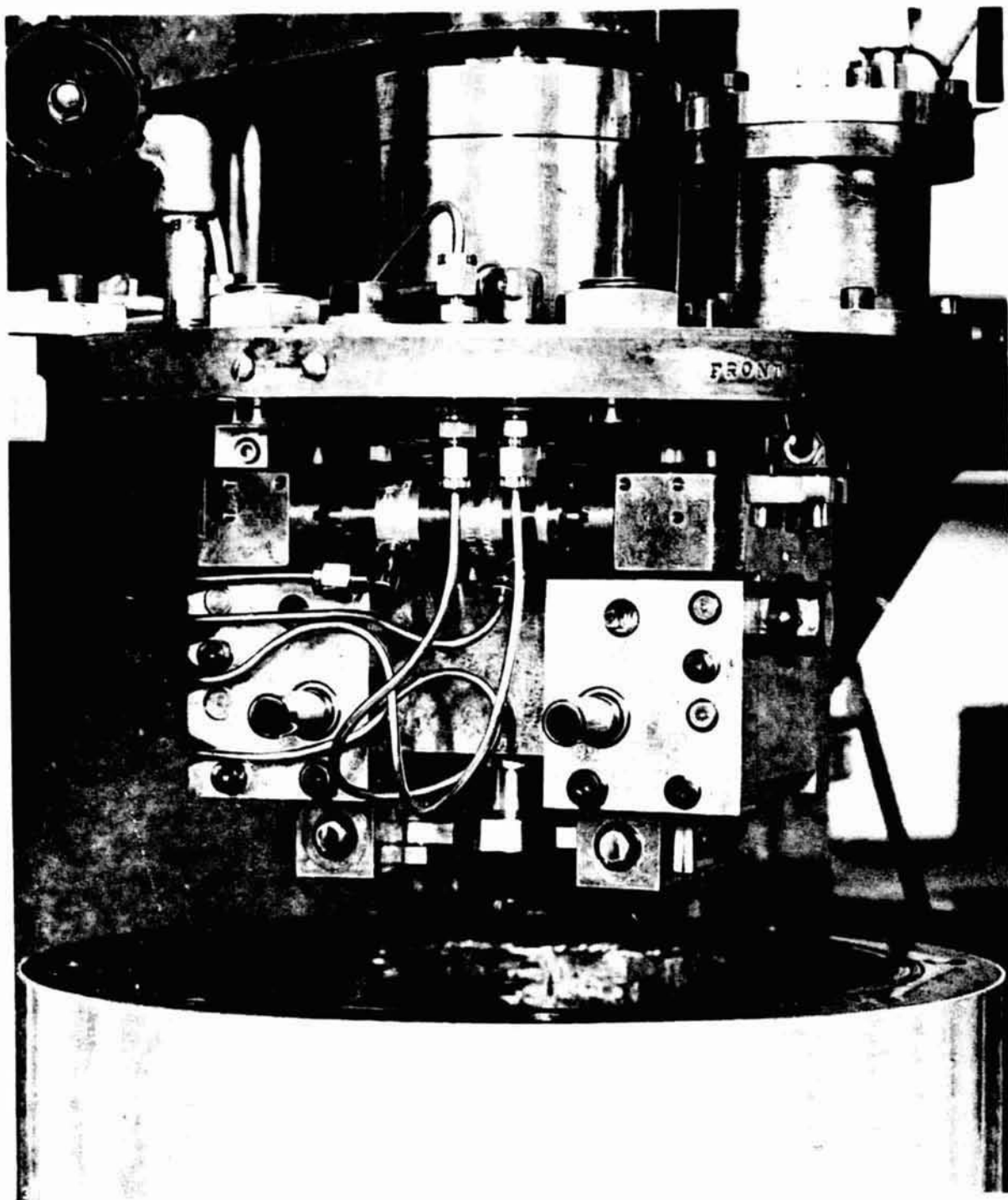
Figure 4. Internal Mechanism of the Rub-Block
on Rotating Ring Tester
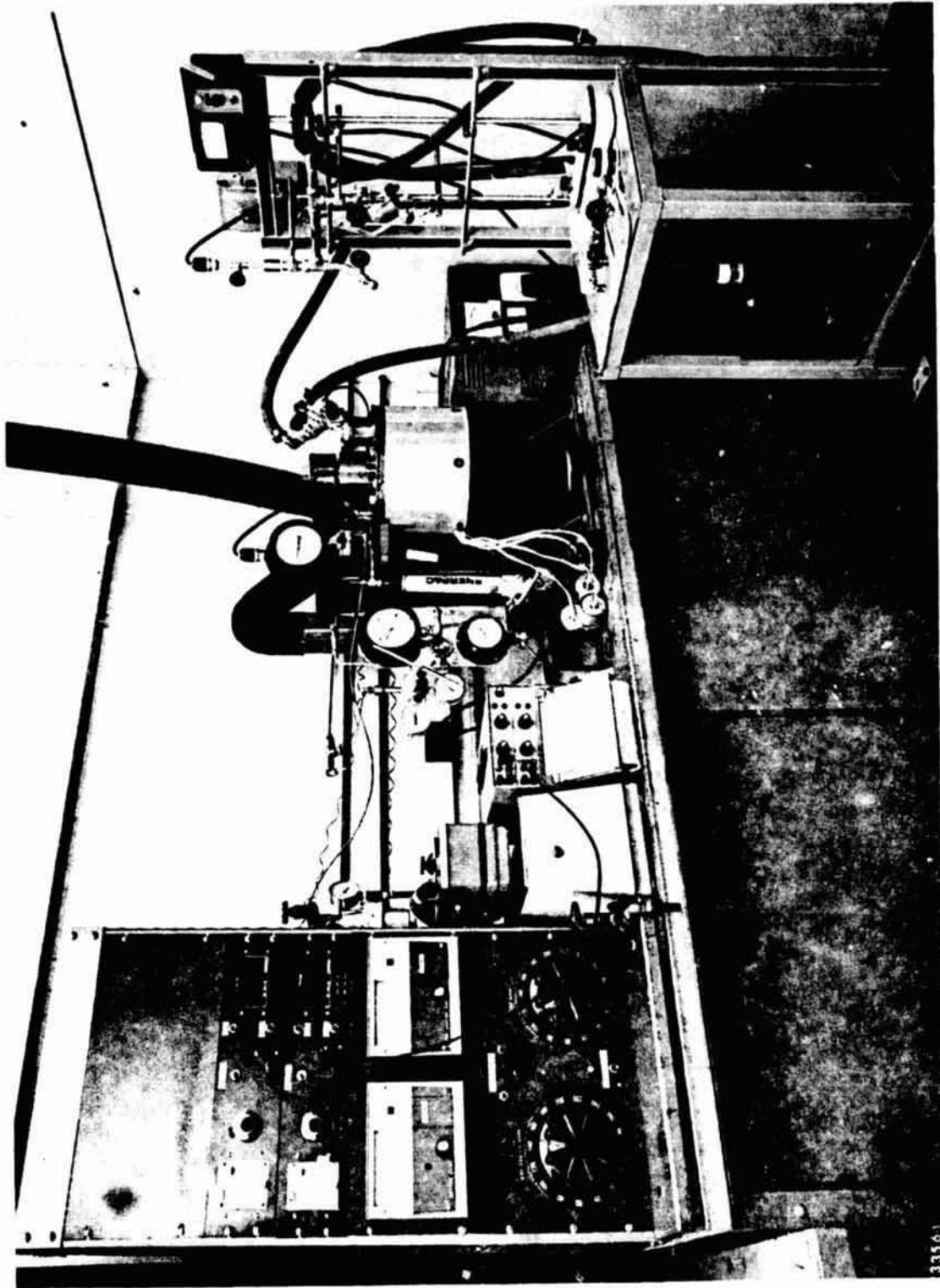
Figure 5. Overall View of the Rub-Block on Rotating Ring Tester

of speed and load. After immersing the ring and block in the test fluid, these components were brought into contact at 2.07 x 10^5 N/m^2 (30 psi) and at 1000 rpm (11,430 cm/min). The drive speed then idled down to zero rpm with continual recording of the torque. After breaking the contact, the speed cycle from 1000 to zero rpm was repeated at higher loads. Specific conditions were:

Loads: initially 2.07 x 10^5 N/m^2 (30 psi) (contact)

then 2.76 x 10^5 N/m^2 (40 psi)

then 3.79 x 10^5 N/m^2 (55 psi)

then 5.17 x 10^5 N/m^2 (75 psi)

then 7.24 x 10^5 N/m^2 (105 psi)

then 1.03 x 10^6 N/m^2 (150 psi)

The higher loads were not run if high torques occurred at lower loads.

Configuration: Line contact

Atmosphere: Air or inerted

Temperatures: 316°C (600°F) in air (to simulate aerated bearing tests on C-ethers)

340°C (650°F) under nitrogen (to simulate inerted bearing tests on C-ethers)

260°C (500°F) in air (simulating bearing tests on esters)

260°c (500°F) under nitrogen (simulating the pump tests)

Metallurgies: M50 on M50 (bearing race and ball metallurgy. Ideally, rub-block tests should also have run on the cage metallurgy, i.e. M50 on silvered 6415 steel. This was not done due to lack of funding. The cage lubrication is critical up to the point where skidding occurs, then the race lubrication becomes critical.)

Tin bronzed M2 steel on tungsten carbide (cylinder barrel and port cap metallurgy in the first pump test. No screening was done on silvered S-Monel against tungsten carbide, the metallurgy in subsequent pump tests.)

29

6.1.3   Contact Angle Measuring Device

The contact angle is the angle measured from liquid-solid to liquid-air surfaces in a liquid drop resting on a plane solid surface. The contact angle indicates the degree of adhesion of the liquid to the solid. Commonly, a liquid is said to wet a solid if the contact angle is zero or "small." The larger the contact angle, the less the wetting. The wetting properties of an oil may influence bearing performance by controlling heat transfer and lubricant starvation.

MRC measured the contact angle using the sessile drop method. A drop of liquid was placed on a horizontal metal coupon (M50 or silvered 6415) in a thermostat at 169°C (336°F). Polished M50 coupons were used since contact angle varies with roughness (ref.12). The silvered 6415 coupons (cage metallurgy) were made by plating silver on lapped 6415 disks via AMS 2412. The average surface roughness of the lapped disks was 1.27×10^{-5} cm, i.e. five microinches.

The general procedure was to photograph the drop as soon as possible once the drop was on the coupon. After cooling, the drop was removed from the suface with a Kleenex tissue, the coupon rotated, and another measurement made. Usually around four measurements were made per coupon.

Initial contact angles on C-ether fluids measured at 307°C (584°F) were very small or 0°. Subsequent tests were then run at a lower temperature (169°) to have a large enough angle for easy measurement.

6.1.4   Surface Tension Measurement Apparatus

Surface tension is equivalent to the work needed to extend a fluid surface. Surface tension is one variable that affects the ease of spreading of a liquid on a solid. This in turn may affect bearing oil starvation and/or cavitation, Also, mist properties and foaming vary with surface tension.

MRC measured the surface tensions of candidate fluids at 169°C by the maximum bubble pressure method. This is described by Sugden (ref. 13) and is based on measuring the pressure required to produce a bubble at an orifice. Using two orifices of different diameter and taking the difference of bubble pressures cancels the effect of depth of immersion in the fluid. The result is not in a mathematically closed form, however, so that it is necessary to use iteration in calculating the surface tensions or to use an approximate equation which Sugden developed. Cuny and Wolf (ref. 14), starting with an equation deduced by Schrodinger, produced a more useful approximation.

30

$$S = \frac{P}{2(1/r_1 - 1/r_2)} + \frac{gd[(r_2 - r_1)/3 - (t_1 - t_2)/2]}{1/r_1 - 1/r_2}$$

$$\frac{g^2d^2(r_2{}^3 - r_1{}^3)}{24S(1/r_1 - 1/r_2)}$$

S = surface tension

P = differential pressure

r_1 = radius of smaller orifice

r_2 = radius of larger orifice

g = gravitational constant

d = density of liquid

t_1 = immersion depth of smaller orifice

t_2 = immersion depth of larger orifice

Cuny and Wolf point out that if the apparatus is set up with $t_2 - t_1 = 2/3(r_2 - r_1)$, the second term of the equation is zero. In addition, the third term is small. Thus, extending Cuny and Wolf's derivation, S in the third term may be replaced by the approximation given by the first term alone, $S = P/2(1/r_1 - 1/r_2)$. The third term also may be modified by dropping the cube of r_1, as r_1 is expected to be much smaller than r_2. With these changes,

$$S = \frac{P}{2(1/r_1 - 1/r_2)} + \frac{g^2d^2r_2{}^3}{12P}$$

Thus the calculation of surface tension consists of multiplying the observed pressure by an apparatus constant, and adding the small correction represented by the second term above. This correction is negligible for most purposes, for ordinary organic liquids. For benzene, for example, the correction term adds 0.10% to the surface tension calculated from the first term only. However, the correction increases rapidly with increasing density of the liquid. From bromobenzene, the correction term is 0.19%, and for carbon tetrachloride, 0.41%.

Originally it was intended to duplicate the equipment described in a NASA Technical Note (ref. 15), but a slight modification of the same basic apparatus produced an instrument easier to use. Rather than applying a strain-gauge differential pressure transducer to the Sugden apparatus, with capillary

tubes at equal immersion depth, and using the transducer merely to measure the pressures across the two orifices separately, Cuny and Wolf's arrangement of capillary orifices at the calculated difference of immersion depths was used. The differential pressure transducer then measured the difference of the two orifice pressures directly. The apparatus is shown schematically in Figure 6. Air or inert gas passes through a sintered filter and thence to a pressure regulator, gauge and relief valve. The regulator is adjusted for an output pressure of about 4 psig. A relief valve opening at about 6 psig prevents the application of damaging pressure to the transducer, which is capable of withstanding 10 psi differential. The following switching valve either applies the gas to the orifice assembly, or shuts off gas flow and vents the orifices for checking of the transducer zero point. Measurements on 6 standard liquids gave an average deviation from the literature values of 0.5%, maximum deviation 0.9%, based on calibration with benzene.

6.1.5   Differential Scanning Calorimetry (DSC)

Chemical interactions between a fluid and its static solid-gas environment at elevated temperature are readily studied by DSC. The instrument detects and displays heat effects due to physical and chemical transitions occurring while the sample temperature is programmed upward. A Perkin-Elmer Model DSC-1B Calorimeter was used for these studies. Corrections between four-ball tests and thermogravimetric data are in the literature (ref. 16).

6.1.6   Oxidation and Corrosion Tester (O&C)

This instrument is a modification of Method 5308 of Federal Test Method Standard 791. It subjects fluids to heat and oxygen in the presence of metals for prolonged times and shows the fluid's ability to withstand thermal and oxidative stress. All O&C tests were run for 48 hours at 260°C with an air flow of five liters per hour.

6.1.7   Film Thickness

The film thicknesses of Skylube® 450, two C-ether fluids (FH-140 and MCS 524) and blend f_3 were measured using optical techniques. The rig is described in the literature (ref. 17). A one inch diameter tungsten carbide ball was loaded against a lubricated quartz disk coated with chromium to allow interferometry. Chromatic interferometry was used to give maximum accuracy in measuring the film thickness.

The speed of the electrically driven disk was measured digitally using a photoelectric technique, and accuracy of control and reading fell between the limits of 1 in 100 and 1 in 500.

32
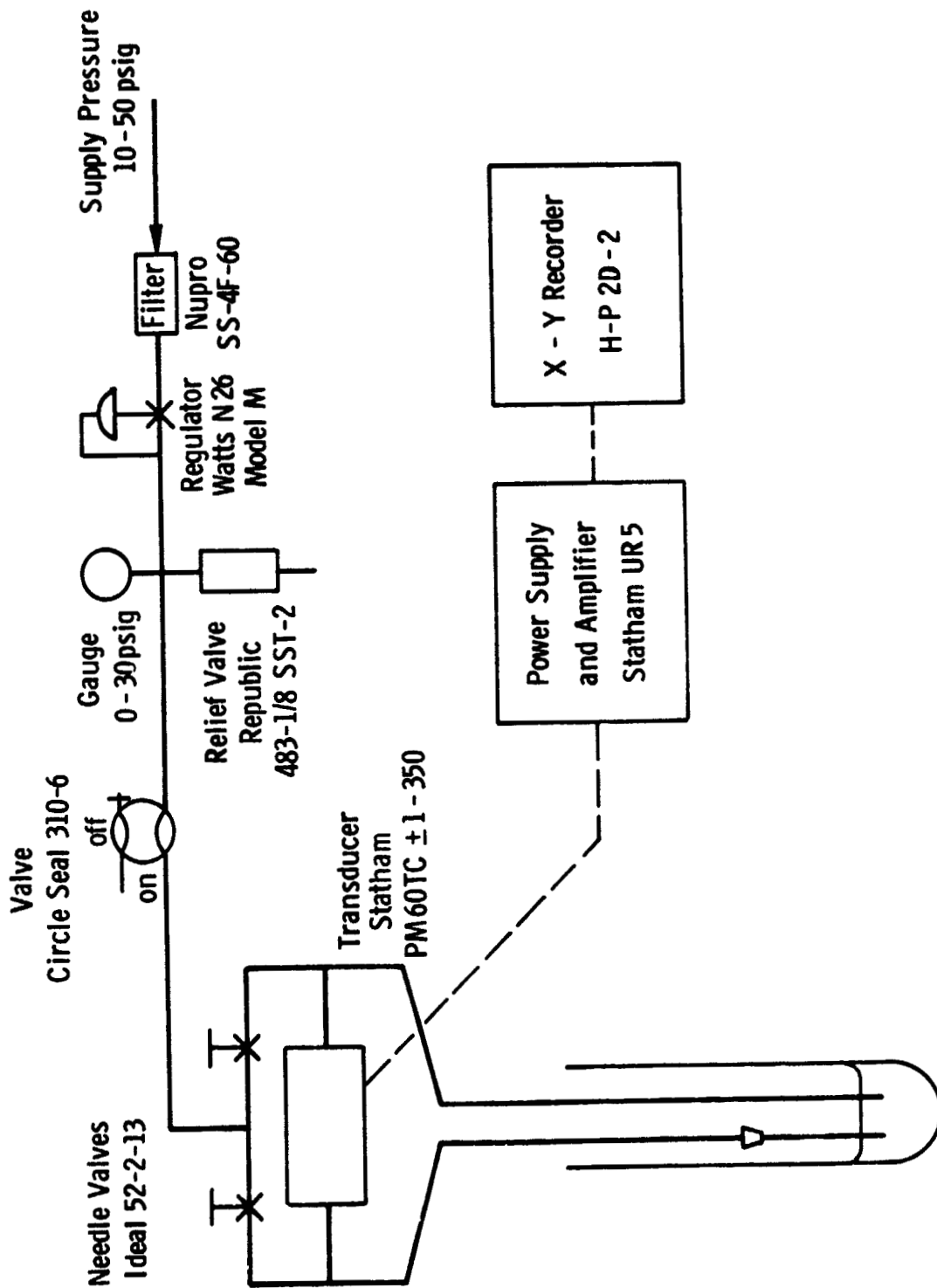
Figure 6. Surface Tension Apparatus (Schematic)

The temperature of the lubricated disk surface was measured using a trailing thermocouple and the tests were stopped temporarily if the temperature varied more than 1/2°C. Test temperatures were 19°C and 70°C.

Maximum Hertz pressures in the contacts were:

(A) 4.59×10^8 N/m^2 (66,500 psi)

(B) 5.78×10^8 N/m^2 (83,780 psi)

6.2   SCREENING TEST RESULTS

6.2.1   Slow Speed Four-Ball, M50 on M50

Twenty-four boundary friction coefficient-temperature curves on M50/M50 are shown in Appendix D.

a)   Skylube 450 (Figure D-1)

This ester gives a low coefficient of friction up to 371°C (700°F); it is lower than that of MCS 524 except around 332°C.

The literature reports the high speed friction coefficients of a C-ether fluid and a Type II ester on M50. Using a ball-on-disk apparatus, the C-ether has a higher μ from 150 to 300°C (ref. 18).

b)   MCS 524

A typical friction curve for this mixture is shown in Figure D-2. The boundary coefficient rises to ca. 177°C, levels off, then gradually drops to a fairly low value at higher temperatures. The initial rise is presumably caused by the absence of any surfactants or boundary lubrication additives in the base stock. The high temperature friction drop is probably due to an EP action by the base stock itself. This reverses the earlier friction deterioration. Since the C-ethers are stable chemically, the EP action is not effective until high temperatures.

c)   FH-140

The friction curve for this compound (Figure D-3) resembles that of MCS 524.

d)   Blend f$_3$

The curve for blend f$_3$ (Figure D-4) is similar to that for MCS 524. When blend f$_3$ was run using a setting of 80 on the heater coil variable transformer (the normal setting), fluid starvation occurred (as evidenced by a "dry cup" at run's end)

34

giving slightly different μ values at higher temperatures. Subsequent runs on f_3 were made at a setting of 100; this completes the temperature cycle more quickly and minimizes starvation.

e) MCS 524 + 0.05% Trichloroacetic Acid + 0.1% A-88

The friction (see Figure D-5) rises to a peak at 260°C ($\mu>0.7$) followed by a sharp drop which holds at the higher temperatures.

f) MCS 524 + ~0.07% Perfluoroglutaric Acid

The boundary friction of this blend (see Figure D-6) is actually higher than that of the base stock from 149 to 316°C. At the latter temperature a sharp friction drop occurs.

g) MCS 524 + 0.1% Phenylphosphinic Acid

This acid (see Figure D-7) causes a decrease in boundary friction of MCS 524 between 93°C and 232°C. The friction then reverts to that of the base stock. A second friction lowering occurs above 316°C. Presumably, these friction changes reflect two different chemical reactions by the additive.

h) Blend f_3 + 0.1% Phenylphosphinic Acid

The curve for blend f_3 plus phenylphosphinic acid on M50/M50 is shown in Figure D-8. The effect of the acid in blend f_3 is similar to its effect in MCS 524. The boundary coefficient of friction is lowered from about 132 to 249°C and from about 313 to 371°C.

i) MCS 524 + 0.1% m-Phenylmercaptophenylphosphinic Acid

This additive (see Figure D-9) gives a friction coefficient-temperature contour similar to the base stock but with a lower coefficient above 121°C. The curve for the substituted acid compared to the unsubstituted acid is shown in Figure D-10. The first reaction of the parent acid does not occur as readily with the 2-ring acid. Moreover, there is essentially no transition between the two reactions, if indeed the two reactions are occurring.

j) MCS 524 + m-(m-Phenylmercaptophenylmercapto)phenyl-
     phosphinic Acid

The boundary friction curve for MCS 524 + 0.1% of the above acid compared with MCS 524 is shown in Figure D-11. The additive blend has a generally lower friction, but the shape of the curve parallels somewhat the curve of the base stock. A second slow speed four-ball run was made using a higher acid

35

concentration (∿0.28%). This curve (Figure D-12) has a boundary
friction intermediate between that of the 0.1% concentration and
the base stock itself. Both concentrations lower the boundary
friction, but there is no obvious interpretation of this friction
reduction or of the changes in the curves due to concentration
changes.

k) MCS 524 + 0.1%* Perfluoroglutaric Acid + 0.075%*
   Phenylphosphinic Acid

The curves (Figures D-13 and D-14) for this combination
resemble that of the phenylphosphinic acid. The combination has
a slightly smoother curve, i.e. there is less transition between
the areas of chemical reaction.

l) MCS 524 + 0.1%* m-Phenylmercaptophenylphosphinic Acid
   + 0.1%* Perfluoroglutaric Acid (Figure D-15)

This blend shows a coefficient of friction reduction from
121°C to ∿221°C compared with MCS 524. This is a synergism,
since neither acid alone has this low a friction in this temper-
ature range (Figure D-16 and D-17). There is no evidence of a
high temperature synergism.

m) MCS 524 + 0.05% Tetraoctyltetraphosphetane Tetra-
   sulfide + 0.05% Emcol PS-236

The boundary friction-temperature curve is shown in Figure
D-18. Large friction coefficient lowering occurs at all temper-
atures producing hydrodynamic conditions above 288°C.

n) MCS 524 + 0.1% DC-473 (Figure D-19)

The curve for this surfactant blend closely resembles that
for MCS 524. This is not surprising since the additive, a glycol-
silicone wetting agent, should not have any EP properties.

o) MCS 524 + 0.1% Phenylphosphinic Acid + 0.1% DC-473
   (Figure D-20)

This combination gives a coefficient-temperature profile
similar to phenylphosphinic acid alone (Figure D-21). However,
there is a greater coefficient drop at 316-371°C with the acid-
surfactant combination than with the acid alone.

---

*These figures are the initial additive charge. After warming,
 cooling and filtration, the acid level, especially that of
 PFGA, is probably lower.

36

p) **MCS 524 + 0.1% Phenylphosphinic Acid + 0.1% Perfluoro-
glutaric Acid + 0.1% DC-473**

The slow speed four-ball curve for this blend is compared
with that of MCS 524 in Figure D-22. Friction lowering occurs
especially at 93-246°C and 316-371°C. [See section (p) of
6.2.2 for a discussion of interactions between these additives.]

q) **MCS 524 + 5% DC-710** (curve not shown)

The DC-710, an aryl silicone, is a wetting agent for M50
steel but not for silvered 6415 steel (see section 6.2.4.1).
This silicone does not change the slow speed four-ball curve
of MCS 524.

r) **Blend f$_3$ + ~0.07% Perfluoroglutaric Acid (Figure D-23)**

The addition of the acid raises the value of μ above that of
the base stock from ca. 150°C to ca. 316°C. A sharp lowering of
μ then occurs. This change in blend f$_3$ is very similar to that
produced by PFGA in MCS 524 (Figure D-24).

6.2.2   Slow Speed Four-Ball, M50 on Silvered 6415

**Procurement of cage material disks for the slow speed four-
ball.**-A bar of AMS 6415 steel (4340 material, hardness ~R$_C$ 21)
was sliced into 0.1 cm (0.040 inch) thick disks. These were
ground and lapped to a roughness of ca. 1.27 x 10^{-5} cm (5 micro-
inches), then silver plated according to AMS 2412. Twenty-two
curves for the above metallurgy are presented in Appendix E.

a) **Skylube 450**

This ester has a low friction coefficient until ~204°C
whereupon a sharp rise occurs. This rise peaks at ~260°C, then
decreases slightly (Figure E-1).

b) **MCS 524**

This curve is shown in Figure E-2. The coefficient of
friction rises more or less steadily to 277°C whereupon a sharper
friction rise occurs. The final coefficient is 0.57. This high
temperature friction rise contrasts with the high temperature
friction drop using M50 balls and disks and implies the cage
metallurgy is more inert then M50 to the C-ethers at high
temperatures.

c) **FH-140**

This friction curve (Figure E-3) resembles that of MCS 524.
An even sharper friction rise occurs at 271°C than occurs with
MCS 524.

37

d)   Blend f₃

The curve for this mixture closely resembles that for MCS 524 (see Figure E-4).

e)   MCS 524 + 0.05% Trichloroacetic Acid + 0.1% A-88

This combination of additives (Figure E-5) gives two friction decreases, one at 121-260°C and one at 316-371°C. The curve resembles that of phenylphosphinic acid in MCS 524.

f)   MCS 524 + ∿0.07% Perfluoroglutaric Acid

This acid (see Figure E-6) causes a continuous coefficient of friction lowering up to ∿277°C. The coefficient then rises but remains lower than the base stock over the remaining temperature range.

g)   MCS 524 + 0.1% Phenylphosphinic Acid

This additive (see Figure E-7) gives two pronounced areas of friction lowering. The first is from 149 to 210°C; a very distinct friction lowering occurs above 260°C. Presumably, these friction reductions are due to two different chemical reactions by the additive.

h)   Blend f₃ + 0.1% Phenylphosphinic Acid

This curve is shown in Figure E-8. Again the effect of the additive is similar to its effect in MCS 524; friction lowering occurs between 199 and 254°C and between 302 and 371°C. The friction below 121°C is above that of blend f₃.

i)   MCS 524 + 0.1% m-Phenylmercaptophenylphosphinic Acid

The curve for this blend is compared with that for MCS 524 in Figure E-9. Figure E-10 compares the above acid with unsubstituted phenylphosphinic acid. The two-ring acid does not lower the friction between 149 and 204°C. It does give a sharp friction lowering starting around 343°C. If this is due to the same high temperature reaction as with the unsubstituted ac`.`, it is occurring at an even higher temperature with the two-ring acid.

j)   MCS 524 + ∿0.28% m-(m-Phenylmercaptophenylmer-
     capto)phenylphosphinic Acid

This acid additive (Figures F-11 and E-12) eliminates the high temperature friction rise of the base stock above 260°C but does not give a sharp friction lowering like the other phosphinic acids.

38

k) MCS 524 + 0.1%* Perfluoroglutaric Acid + 0.075%* Phenylphosphinic Acid (Figure E-13)

This acid combination causes a great decrease in boundary friction at all temperatures above 121°C.

l) MCS 524 + 0.1%* m-Phenylmercaptophenylphosphinic Acid + 0.1%* Perfluoroglutaric Acid

This combination is compared with MCS 524 in Figure E-14. A high temperature coefficient drop occurs at ∿335°C. The corresponding drop for the phosphinic acid alone in MCS 524 is ∿360°C (Figure E-15), so the fluoro acid lowers the temperature of the friction drop. (The arrows in Figure E-15 mark the initial point of friction lowering.)

m) MCS 524 + 0.05% Tetraoctyltetraphosphetane Tetra-sulfide + 0.05% Emcol PS-236 (Figure E-16)

These additives cause large lowering of the friction co-efficient at all temperatures giving hydrodynamic conditions above 260°C.

n) MCS 524 + 0.1% DC-473 (Figure E-17)

This curve is essentially equivalent to that for MCS 524. The additive, a wetting agent, does not change the boundary friction.

o) MCS 524 + 0.1% Phenylphosphinic Acid + 0.1% DC-473

This blend has a curve very similar to that of phenyl-phosphinic acid alone. (See Figure E-19 for a comparison with phenylphosphinic acid and Figure E-18 for a comparison with MCS 524.) This result implies the phosphinic acid is preferentially adsorbed on the surfaces.

p) MCS 524 + 0.1% Phenylphosphinic Acid + 0.1% Perfluoro-glutaric Acid + 0.1% DC-473

The boundary friction profile is shown in Figure E-20. This curve closely resembles that for phenylphosphinic acid alone (Figure E-7); it differs from the curves for perfluoroglutaric acid alone (Figure E-6) and from the combination of phenyl-phosphinic acid and perfluoroglutaric acid (Figure E-13). This suggests an interference between the glycol-silicone

_____

*These figures are the initial additive charge. After warming, cooling and filtration, the acid level, especially that of PFGA, is probably lower.

39

wetting agent and the perfluoroglutaric acid, i.e. the wetting agent prevents the fluoro acid from reacting at the surface. This interference may be due to a reaction between the wetting agent and the fluoro acid. When DC-473 is added to a blend of phenylphosphinic acid in MCS 524, the glycol-silicone quickly and cleanly dissolves. When the silicone is added to a mixture of phenylphosphinic acid and perfluoroglutaric acid, there is an instantaneous heavy opaqueness. Presumably the glycol is reacting with the fluoro acid giving water and hence opaqueness. Why the glycol reacts with the fluoro acid but not with the phosphinic acid is an interesting question.

q) **MCS 524 + 5% DC-710** (curve not shown)

The DC-710, an aryl silicone, is a wetting agent for M50 steel but not for silvered 6415 steel (see sections 6.2.4 and 6.2.5). It does not change the slow speed four-ball curve of MCS 524.

r) **Blend f_3 + ~0.07% Perfluoroglutaric Acid (Figure E-21)**

The acid produces a lowering of μ from roughly 150 to 290°C. The acid produces a similar lowering in MCS 524 (Figure E-22).

6.2.3 Variable-Speed, Incremental-Load Rub-Block Tests

6.2.3.1 **M50 on M50 in air, 316°C** (one test at 260°C).- Friction-speed X-Y recordings for 12 runs are shown in Figures F-1 through F-12 of Appendix F. Figures F-1, F-2 and F-3 show that the torques for the C-ethers at 316°C (600°F) are as good or better than Skylube 450 at 260°C (500°F). The best additive for M50/M50 in air at 316°C was m-(m-phenylmercaptophenylmercapto)-phenylphosphinic acid (Figure F-8). At maximum load and zero speed with this blend, the coefficient of friction equivalent to the observed torque was 0.04, indicating modest boundary lubrication. Good curves were also obtained with perfluoroglutaric acid (Figure F-5) and with A-88 plus trichloroacetic acid (Figure F-4). Other results included:

- MCS 524 + $\underline{m}$-$\phi S\phi PO_2H_2$ + PFGA (Fig. F-10)

  This combination gives a good curve but it is not better than PFGA by itself (Fig. F-5)

- phenylphosphinic acid (Fig. F-6) ⎤
- phenylphosphinic acid + PFGA (Fig. F-9) ⎥ some
- phenylphosphinic acid + DC-473 (Fig. F-11) ⎥ friction
- phenylphosphinic acid + PFGA + DC-473 (Fig. F-12) ⎦ lowering

- $\underline{m}$-phenylmercaptophenylphosphinic acid (Fig. F-7) ⎤ no friction lowering

40

6.2.3.2 <u>M50 on M50, inerted (N_2), 343°C</u> (one test at 316°C).
-Friction-speed X-Y recordings for 13 runs are given in Appendix
G.

For M50/M50 steel, inerting raises the friction of C-ether
base stocks (compare Figure G-2 with Figure F-2 of Appendix F).
However, this friction rise under inerted conditions is less at
343°C that at 316°C (cf. Fig. G-1 and Fig. G-2). Apparently
an EP action of the base stock assists lubrication at very high
temperatures. This effect also occurs with the pump metallurgy
(see Figures H-3 and H-4 of Appendix H).

The best additive for M50/M50 inerted at 343°C was m-(m-
phenylmercaptophenylmercapto)phenylphosphinic acid (Figure G-8).
At maximum load and zero speed with this acid, the coefficient
of friction was 0.02. This is almost as low as a hydrodynamic
coefficient. Very good friction lowering also occurred with
A-88 + trichloroacetic acid (Figure G-4), m-phenylmercapto-
phenylphosphinic acid (Figure G-7) and phenylphosphinic acid +
PFGA + DC-473 (Figure G-13). This latter curve had pronounced
friction lowering at the higher speeds. More modest friction
lowering occurs with m-phenylmercaptophenylphosphinic acid +
perfluoroglutaric acid, phenylphosphinic acid + DC-473, per-
fluoroglutaric acid, phenylphosphinic acid + perfluoroglutaric
acid, and phenylphosphinic acid (Figures G-10, G-12, G-5, G-9
and G-6).

6.2.3.3 <u>Tin bronzed M2 on tungsten carbide, inerted (N_2),
260°C</u> (one test at 316°C).-Fourteen friction-speed
X-Y recordings are reproduced in Appendix H. Most of the C-
ether base stocks and blends had high frictions on these metals.
The best additive for the pump metallurgy was A-88 + trichloro-
acetic acid (Figure H-5). This additive package in MCS 524
gave a friction profile about like that of Skylube 450 (Figure
H-1). Some modest friction lowering occurred with

· phenylphosphinic acid (Fig. H-7)

· m-phenylmercaptophenylphosphinic acid (Fig. H-8)

· m-phenylmercaptophenylphosphinic acid + PFGA (Fig. H-11)

The other additives tested were ineffective.

The A-88 + trichloroacetic acid combination is the most
consistently good package in all three conditions run on the
rub-block tester. A friction coefficient of 0.11 was measured
with this additive package on the pump metallurgy at maximum
load and zero speed. This is a boundary regime.

To see if a wetting agent would improve this friction
profile, two rub-block tests were run on MCS 524 + 0.1% A-88
+ 0.05% trichloroacetic acid + 0.1% DC-473. The blend

41

containing the DC silicone has a slightly inferior friction curve on M50/M50 inerted at 343°C (Figure G-4 vs. Figure G-11 of Appendix G). This is still a better friction than that of the base fluid. The wetting agent curve on tungsten carbide/tin bronzed M2 steel is good but no improvement over the blend without the wetting agent (Figure H-12 vs. Figure H-5 of Appendix H). However, the wear during the rub-block test seemed lower with the wetting agent added, possibly due to a protective deposit formed on the bronze. Further testing of the wetting agent formulation stopped with it was found that the DC-473 is a profoaming agent in MCS 524. This additive increases both foam tendency and foam stability beyond reasonable limits.

6.2.4   Contact Angle Measurements on Polished M50

6.2.4.1 Screening of wetting agents in MCS 524.-Glycol-silicone copolymers were found to increase the wetting of MCS 524 on M50 steel at 169°C. One of these polymers, DC-473 fluid, reduced the contact angle from 22° to 0°. However, this additive promotes foaming in MCS 524 and so was not evaluated in any rig tests. Various other surfactant types (Steroxes, carboxylic acids, silicones, alkoxysilanes, polyperfluoropropylene oxide, and stearoxy siloxanes) were not effective wetting agents at 0.1 wt. %. One silicone, DC-710, did lower the contact angle at a higher concentration (5%). This additive did not improve the wetting on silvered 6415 (see Table 10).

The results on M50 are given in Table 8. All concentrations were 0.1% unless noted otherwise. The contact angle of MCS 524 without a surfactant is 22°.

6.2.4.2 Contact angles of test fluids on M50.-The results are given in Table 9. At 169°C the C-ethers do not totally wet M50 steel, giving angles around 20°. The arylphosphinic acids are adsorbed on the surface and increase the wetting of the metal.

6.2.5   Contact Angles on Silvered 6415

Reproducibility was a problem in measuring the contact angles on silvered 6415 steel at 169°C. Initial runs on several C-ether base stocks (MCS 524, FH-140, and blend f_3) generally gave small contact angles (<8°). Later runs on these base stocks gave higher angles ($\sim$20°). The reason for this discrepancy is not known; the higher values are believed correct since four subsequent runs of MCS 524 on different silvered coupons consistently gave angles around 20°. The contact angle of MCS 524 at 307°C is 9° and at 343 is about 0°.

All of the arylphosphinic acids lowered the contact angle on silvered 6415 at 169°C as they did on M50. The DC-473 is a very good wetting agent on both surfaces. (This is the silicone which promotes foaming.) The DC-710 aryl silicone which causes

42

TABLE 8. - SURFACTANTS IN MCS 524: CONTACT ANGLES ON M50 STEEL AT 169°C

Change in Contact Angle	Surfactant	Chemical Class	Contact Angle
Large reduction	DC-473	Glycol silicone copolymer	0°
	DC-710 (5%)	Aryl silicone	6°
	DC-472	Glycol silicone	13°
	L-520	Glycol silicone	14°
No significant change	CP 57347	Sterox; ethoxylated alkylphenol	19°
	CP 57518	Sterox; propoxylated phenol	23°
	Phenylocta-decanoic acid	Carboxylic acid	22°
	$\phi_2\mathrm{Si(OCH_3)_2}$	Silicate	21°
	$\phi\mathrm{Si(OCH_3)_3}$	Silicate	22°
	DC-550	Aryl silicone	22°
	DC-710	Aryl silicone	22°
	Versilube 1080	Large alkyl silicone	20°
	XF-1-0307	Stearyl siloxane	26°
	F-157 wax	Poly(dimethylsiloxy) stearyloxy siloxane	28°
	Krytox PR 143AA (0.05%)	Polyperfluoropropylene oxide	28°
Increase	UC L-77	Silicone	33°

TABLE 9. – CONTACT ANGLES OF TEST FLUIDS ON M50 STEEL AT 169°C

Fluid	Contact Angle	Comments
Skylube 450	$\sim0°$	
MCS 524	22°	Average of 3 runs
FH-140	18°	Average of 2 runs
Blend f_3	16°	
MCS 524 + 0.1% A-88 + 0.05% trichloroacetic acid	17°	
MCS 524 + $\sim$0.07% perfluoro-glutaric acid (PFGA)	16°	
MCS 524 + 0.1% $\phi PO_2 H_2$	9°	
MCS 524 + 0.1% $\phi S \phi PO_2 H_2$	9°	Spreading after formation of the drop
MCS 524 + 0.1% $\phi S \phi S \phi PO_2 H_2$	12°	
MCS 524 + 0.075%[a] $\phi PO_2 H_2$ + 0.1%[a] PFGA	18°	
MCS 524 + 0.1%[a] $\phi S \phi PO_2 H_2$ + 0.1%[a] PFGA	12°	Spreading after formation of the drop
MCS 524 + 0.1% $\phi PO_2 H_2$ + 0.1% DC-473	$\sim4°$ (21°)	
MCS 524 + 0.1% $\phi PO_2 H_2$ + 0.1% PFGA + 0.1% DC-473	15°	
Blend f_3 + 0.1% $\phi PO_2 H_2$	$\sim5°$	

[a]Initial additive charge.

wetting of M50 steel does not induce wetting on silvered 6415!
Finally, 1,3-bis(phenyl)tetramethyldisiloxane was tried as a
wetting agent. This compound has a higher volatility and lower
surface tension than MCS 524 (29 vs. 47 dynes/cm at room temper-
ature). This combination of properties can produce wetting
(ref. 19) but none was observed here.

44

All the angles are given in Table 10. From these data several tenative conclusions can be drawn:

- Perfluoroglutaric acid is strongly adsorbed on silver and is oleophobic; it presents a layer of oleophobic fluorine atoms to the oil

- The arylphosphinic acids are adsorbed on the surface, the 2-ring more strongly than the 1-ring compound, and to about the same degree as PFGA

- DC-473 adsorbs on the silver surface less strongly than the arylphosphinic acids

6.2.6 Surface Tension Measurements

The values are given in Table 11. Most of the additives had little effect on the surface tension. There is no simple correlation between wetting and surface tension. The silicones DC-473 and DC-710 lower the tension from ~32 to ~28 dynes/cm. The former wets M50 and silver, the latter only M50. Blend f_3 (γ ~29 dynes/cm) wets neither. The phosphinic acids do not change the surface tension but do lower the contact angles on M50 and on silver.

6.2.7 Differential Scanning Calorimetry (DSC) on Test Fluids

DSC curves on four base stocks were run in a gold pan -

(i)   in air in the absence of metals

(ii) in air in the presence of M50 and silver wool

(iii) under nitrogen in the presence of these metals

The results are uninspiring in that none of the thermograms of C-ethers show much detail. This is not too surprising since the base stocks are expected to have good thermal stability. The only exception is a strong endotherm by blend f_3 at 155-254°C in air and metals.

a)   <u>Skylube 450</u>

All runs had pan rupture (>11000 mm Hg) below 442°C.

(i)   strong exotherm at 401°C

(ii) featureless drift (exo or endo depending on base line slope)

(iii) exothermic drift

45

TABLE 10. - CONTACT ANGLES OF TEST FLUIDS ON SILVERED 6415 STEEL AT 169°C

Fluid	Contact Angle	Comments
Skylube 450	$\sim 1°$	
MCS 524	22°	Average of 4 runs; ignores initial run of 7°
FH-140	19°	Ignores initial run of 5°
Blend f_3	22°	Average of 2 runs; ignores initial runs of 7 and 6°
MCS 524 + 0.1% A-88 + 0.05% trichloroacetic acid	20°	
MCS 524 + $\sim$0.07% perfluoro-glutaric acid	30°	
MCS 524 + 0.1% ϕPO_2H_2	10°	Average of 3 runs
MCS 524 + 0.1% $\phi S\phi PO_2H_2$	10°	Average of 2 runs; spreading after formation of the drop
MCS 524 + 0.1% $\phi S\phi S\phi PO_2H_2$	12°	Spreading after formation of the drop
MCS 524 + 0.075%[a] ϕPO_2H_2 + 0.1%[a] PFGA	23°	Average of 2 runs
MCS 524 + 0.1%[a] $\phi S\phi PO_2H_2$ + 0.1%[a] PFGA	16°	Spreading after formation of the drop
MCS 524 + 0.1% DC-473	6°	Average of 2 runs
MCS 524 + 0.1% ϕPO_2H_2 + 0.1% DC-473	12°	Average of 3 runs
MCS 524 + 0.1% ϕPO_2H_2 + 0.1% PFGA + 0.1% DC-473	17°	Average of 3 runs
MCS 524 + 5% DC-710	25°	Average of 2 runs
MCS 524 + 1% $(\phi Si)_2O$	26°	
MCS 524 + 5% $(\phi Si)_2O$	27°	
Blend f_3 + 0.1% ϕPO_2H_2	<5°	

[a]Initial additive charge.

46

TABLE 11. — SURFACE TENSIONS OF TEST FLUIDS AT 169°C ± 1°

Sample	γ, dynes/cm	
	N_2	Air
Skylube 450	19.9	20.1
MCS 524	31.5	32.3
FH-140	32.3	31.9
Blend f_3	28.8	28.4
MCS 524 + 0.1% A-88 + 0.05% TCA	32.5	33.0
MCS 524 + ∿0.07% perfluoroglutaric acid	33.2	33.3
MCS 524 + 0.1% ϕPO_2H_2	33.2	33.4
MCS 524 + 0.1% $\phi S\phi PO_2H_2$	33.3	33.1
MCS 524 + 0.1% $\phi S\phi S\phi PO_2H_2$	32.9	32.1
MCS 524 + 0.1%[a] PFGA + 0.075%[a] ϕPO_2H_2	33.1	33.4
MCS 524 + 0.1%[a] PFGA + 0.1%[a] $\phi S\phi PO_2H_2$	33.2	33.2
MCS 524 + 0.1% ϕPO_2H_2 + 0.1% DC-473	32.1	32.1
MCS 524 + 0.1% ϕPO_2H_2 + 0.1% PFGA + 0.1% DC-473	32.8	33.2
MCS 524 + 0.05% tetraoctytetraphosphetane tetrasulfide + 0.05% Emcol PS-236	32.8	32.8
MCS 524 + 0.1% DC-473	27.2	27.6
MCS 524 + 5% DC-710	28.0	28.1
Blend f_3 + 0.1% ϕPO_2H_2	29.0 (28.2)	28.5

[a] Initial additive charge.

47

b) MCS 524

    (i) and (ii) show a featureless endothermic
               drift above ∿400°C

    (iii) an exothermic drift starts around 480°C

c) FH-140

    (i) endothermic onset at 407°C - becomes
        a strong effect

    (ii) exothermic drift - some question of
         reproducibility

    (iii) featureless exothermic drift

d) Blend f₃

    (i) a featureless exothermic drift increas-
        ing above 417°C

    (ii) strong endotherm (155-254°C); presumably
        this represents an interaction of the
        fluid and the metals since (i) above
        did not have this transition

    (iii) endothermic drift - becomes strong

DSC curves were also run on the fluids used in bearing
tests 9 through 14. Many of these curves show exothermic peaks
or drifts and some of these correspond fairly well to transition
points on the slow speed four-ball friction-temperature plots.
In air, the exotherms are at high temperatures (above 232°C) and
probably represent chemical reactions between the fluid and the
metal(s) rather than physisorption-desorption of the additives.
Some of the DSC curves show exotherms above the 371°C upper
limit of the slow four-ball curves. The DSC curves in nitrogen
differ from those in air.

The results are summarized belo   All fluids were run in
air and nitrogen in the presence of silver and M50 steel. A
curve on MCS 524 + PFGA + phenylphosphinic acid is included.

   1) MCS 524 + 0.1% ↓SφPO₂H₂ (Bearing Test 9)

Air - no distinct transitions were seen. A general, strong
endothermic drift began at 238°C and continued to 500°C.

Nitrogen - There were no definite transitions. There was
an endothermic drift starting at 141°C. There was slight exo-
thermic activity at 207°C.

48

2) MCS 524 + 0.1% A-88 + 0.05% TCA (Bearing Test 10)

Air - A broad exothermic peak occurred starting at 307°C (shoulder at 328°C). A slow, four-ball friction (μ) lowering occurs on M50/silver at 316°C and a large friction coefficient drop on M50/M50 between 227 and 316°C.

Nitrogen - A small exotherm has an onset at 172°C. An exothermic drift starts at 209°C and levels off at 279°C. An endothermic peak occurs at 348°C.

3) MCS 524 + ∿0.07% Pε fluoroglutaric Acid (Bearing Test 11)

Air - An exothermic peak occurs from 272 to 324°C; a friction coefficient (μ) lowering occurs on M50/M50 at 316°C and a μ rise on M50/silver at ∿277°C. Other exothermic peaks start at 331°C and 397°C.

Nitrogen - There are no definite peaks. There is an endothermic drift that levels off at 285°C.

4) MCS 524 + 0.1% Phenylphosphinic Acid (Bearing Test 12)

Air - A series of exotherms occurs beginning at 264, 336, 384 and 470°C. Slow four-ball friction lowerings occur at 260°C on M50/silver and at 316°C on M50/M50.

Nitrogen - An endothermic drift starts at 137°C. There is a slight exotherm at 289°C. From that temperature on there is increasing endothermic drift.

5) MCS 524 + 0.05% Tetraoctyltetraphosphetane
    Tetrasulfide + 0.05% Emcol PS-236 (Bearing Test 13)

Air - No distinct peaks are seen. There is exothermic activity starting at 208°C. At 284°C there is an increase in exothermic activity, and at 337°C there is another increase. There is a friction coefficient lowering on M50/silver at 210°C. A general exotherm is consistent with the overall μ lowering on M50/M50 at all high temperatures. Actually, the μ lowering on M50/M50 begins well below 208°C.

Nitrogen - There were no definite transitions. There is an exothermic drift starting at 123°C.

6) Blend f₃ + ∿0.07% Perfluoroglutaric Acid (Bearing Test 14)

Air - The DSC shows no distinct transitions; the pan leaked at high temperatures where an endothermic drift occurred.

Nitrogen - Shows no distinct transitions; there was endothermic drift at high temperatures.

7) MCS 524 + 0.075%* Phenylphosphinic Acid + 0.1%*
   Perfluoroglutaric Acid

__Air__ - Featureless endothermic drift begins at 305°C.

__Nitrogen__ - Featureless endothermic drift begins at 198°C,
becomes strong.

6.2.8   Oxidation-Corrosion Tests

Test results on bearing test fluids and various candidate
blends are presented in Table 12. All of the oils give good
results in that deposits are minimal and viscosity increases are
low.

6.2.9   Film Thickness (Base Stocks)**

The film thicknesses of four base stocks are given in
Table 13. The fluids are:

Skylube 450

MCS 524

FH-140

Blend f_3

MCS 524 and lend f_3 have greater film thickness than
Skylube 450, which in turn is thicker than FH-140. The tests
were run at 19°C and 70°C and at speeds up to 7.5 m/s (18,000
in./min).

6.2.10   Choice of the Best Additives Based on Screening Tests

A ranking of the additives was needed to choose fluids for
the bearing tests. This was done by a desirability function
analysis of the screening data. The method is outlined below.
The blend with phenylphosphinic acid was the best blend.

Each screening test is transformed into a desirability
scale (d). This scale is a dimensionless number representing the
inherent value of a given property to the fluid. We chose a
range of d between 0.0 and 1.0 such that d = 0.0 is completely

---

*Initial additive charge.

**This work was subcontracted to the Lubrication Laboratory,
  Department of Mechanical Engineering of Imperial College,
  London, England.

50

TABLE 12. – OXIDATION-CORROSION TESTS ON CANDIDATE OILS

260°C (500°F), 48 hr, 5 ℓ air/hr

Fluid	Visc. Inc., %	Wt. Change, mg/cm²[a]		Deposits
		Cu	Ag	
MCS 524	4.0	-2.3	-0.5	No coke, no sludge
	0.4	(b)	-0.3	No coke, no sludge
MCS 524 + 0.1% A-88 + 0.05% trichloroacetic acid	4.8	-3.0	-0.6	Lt. coke, lt. sludge
	3.2	(b)	-0.1	Lt. coke, lt. sludge
MCS 524 + ᵥ0.07% per-fluoroglutaric acid	6.0	-2.3	-0.6	No coke, few black specks
MCS 524 + 0.1% phenyl-phosphinic acid	6.0	-4.9	-0.9	No coke, no sludge
	4.0	(b)	-0.6	No coke, no sludge
MCS 524 + 0.1% m-phenyl-mercaptophenylphos-phinic acid	14.0	-9.1	-0.05	Lt. coke, no sludge
	2.8	(b)	-0.02	No coke, no sludge
MCS 524 + 0.05% tetraoctyl-tetraphosphetane tetra-sulfide + 0.05% Emcol PS-236	9.8	-3.1	-1.2	Lt. coke, no sludge
	3.6	(b)	-0.04	Lt. coke, no sludge
MCS 524 + 0.1% DC-473	6.8	-1.7	+0.06	Lt. coke, no sludge
	4.4	(b)	-0.01	No coke, no sludge
MCS 524 + 5% DC-710	2.0	-1.4	-0.4	No coke, no sludge
	7.0	(b)	-0.3	Trace coke, no sludge
Blend f₃ + 0.1% phenyl-phosphinic acid	7.5	(b)	-0.3	No coke, no sludge
Blend f₃ + ᵥ0.07% per-fluoroglutaric acid	99.4	-4.2	-2.4	No coke, no sludge
	4.3	(b)	-0.2	No coke, no sludge

---

[a]Negligible weight loss for magnesium, aluminum, titanium and iron.
[b]No copper coupon present.

51

TABLE 13. - FILM THICKNESSES OF FOUR BASE STOCKS

A: 4.59×10^8 N/m^2 (66,500 psi)
B: 5.78×10^9 N/m^2 (83,780 psi)

Film Thickness, m	Speed, m/s[a]			
	19.0°C		70.0°C	
	A	B	A	B
Skylube 450				
1.37×10^{-7}	0.216	0.258	1.21	1.33
1.85	0.334	0.384	1.80	2.02
2.33	0.479	0.549	2.66	2.92
2.95	0.690	0.748	3.66	4.04
3.22	0.829	0.885	4.45	4.79
3.84	1.10	1.12	5.84	6.28
4.18	1.23	1.27	6.74	7.18
4.59	1.44	1.51		
5.21	1.79	1.87		
5.89	2.17	2.31		
MCS 524				
1.20×10^{-7}	0.103	0.114	1.33	1.49
1.62	0.150	0.161	1.94	2.16
2.03	0.204	0.225	2.62	2.92
2.57	0.286	0.308	3.59	3.89
2.81	0.352	0.364	4.12	4.41
3.35	0.435	0.472	5.24	5.68
3.65	0.520	0.554	5.98	6.58
4.00	0.610	0.647	6.95	7.40
4.55	0.706	0.744		
5.15	0.831	0.883		
FH-140				
1.20×10^{-7}	0.256	0.273	1.56	1.69
1.62	0.388	0.413	2.35	2.55
2.03	0.551	0.592	3.22	3.44
2.57	0.750	0.755	4.56	4.79
2.81	0.857	0.954	5.24	5.54
3.35	1.15	1.21	6.74	7.18
3.65	1.30	1.38		
4.00	1.50	1.59		
4.55	1.83	1.95		
5.15	2.21	2.31		
Blend f$_3$				
1.22×10^{-7}	0.135	0.153	0.554	0.614
1.64	0.217	0.231	0.860	0.920
2.07	0.292	0.329	1.10	1.29
2.61	0.414	0.449	1.65	1.72
2.86	0.486	0.546	1.91	2.02
3.40	0.650	0.691	2.43	2.62
3.71	0.748	0.778	2.77	2.96
4.07	0.863	0.913	3.27	3.49
4.62	1.04	1.09	4.01	4.35
5.23	1.35	1.42	5.17	5.62

[a]Rolling speed at indicated film thickness.

undesirable and d = 1.0 is completely desirable. The relation-
ship between d and any specific property may be linear or non-
linear. Establishing this relationship is subjective, a judge-
ment based on data, intuition, and experience.

Once d is found for each screening test, the desirability
function, D, for each blend is the geometric mean of the de-
sirability values.

$$D = \sqrt[N]{d_1 \times d_2 \ldots d_n} \qquad (N = 4)$$

The screening tests were:

slow speed four-ball friction, M50/M50

slow speed four-ball friction, M50/silvered 6415

rub-block friction-speed X-Y recordings, M50/M50
@ 316°C in air

contact angle on M50 and on silvered 6415 steel

Surface tension data were not included in the analysis. All of
the tests received equal weight relative to each other. The
wetting test comprised the contact angles on both M50 and
silvered 6415 since the wetting of each metal is important.

The desirability curves are shown in Figure 7. The solid
line relates the slow speed four-ball test and the rub-block
test to d. The dotted line is for the contact angle test.

For the slow speed four-ball test, M50/M50, a significantly
lower μ than MCS 524 (BS) at all temperatures was g in an
abscissa value of 10 (i.e. d = 1). Friction loweri   at high
temperatures was considered more valuable than low t .ction at
intermediate or at low temperatures. That is, the desirability
curve is shaped to weight most critically what happens at high
temperatures.

Friction Profile	Abscissa
Low μ at all temperatures	10
Low μ at high and intermediate temperature	8
Low μ at high temperature only	7
Unchanging μ below MCS 524	7
Low μ at low temperature only	5
μ = MCS 524	4
μ above MCS 524 at high temperature	0

53
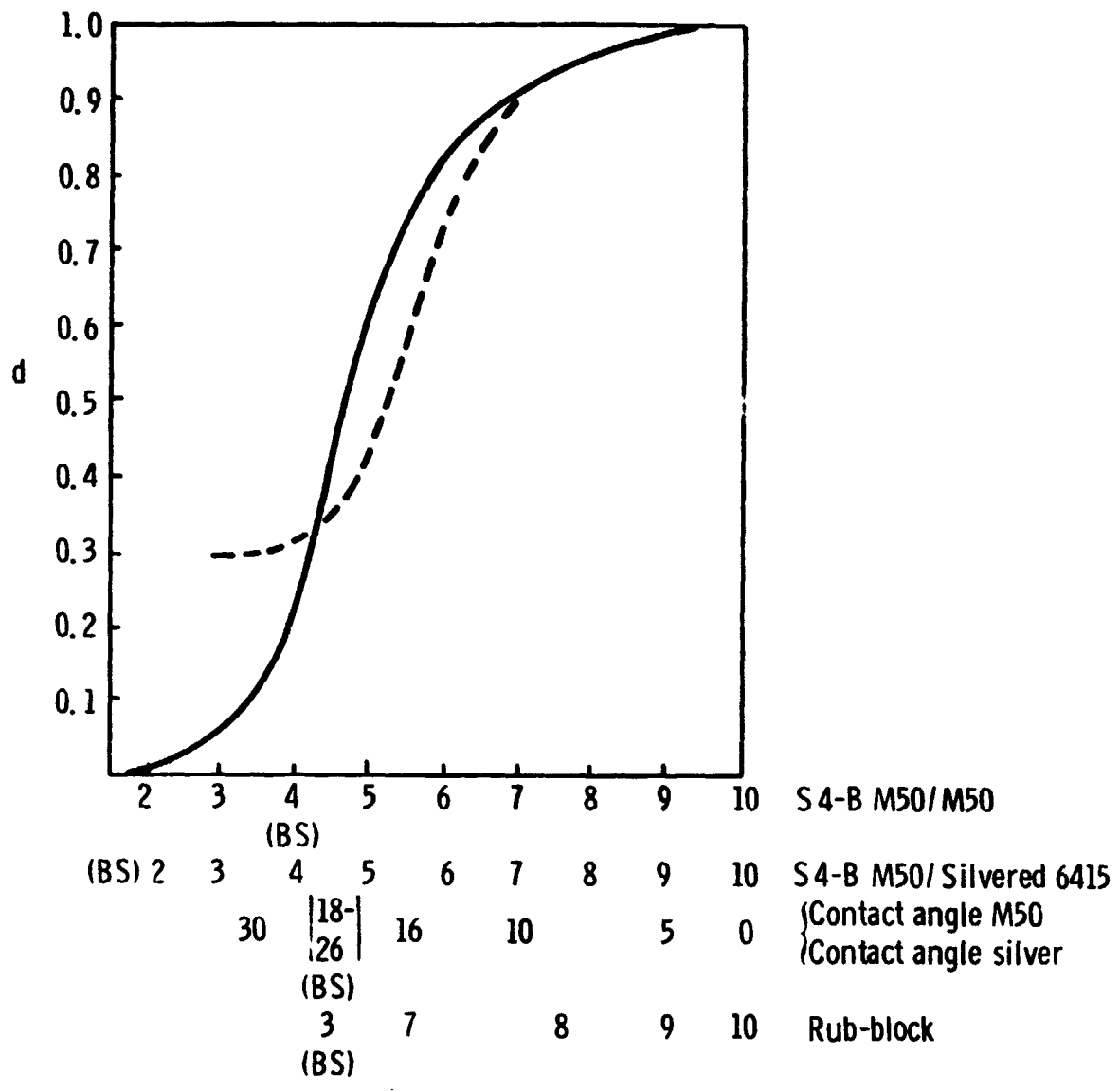
Figure 7. Desirability Curves for Screening Tests

For the slow speed four-ball test, M50/silvered 6415, again a large μ lowering vs. MCS 524 at all temperatures was given an abscissa value of 10 (d = 1).

Friction Profile	Abscissa
Low μ at all temperatures	10
Low μ at high and intermediate temperature	8
Low μ at high temperature only	7
Modest μ lowering at high temperature	4
Low μ at low temperatures	0
μ = MCS 524	0

Contact angles above or around that of the base stock are given low d values; contact angles below 5° are given high d values.

For the rub-block test, the friction-speed curve for the best additive ($\phi S\phi S\phi PO_2H_2$) was given a value of 10 and the curve for MCS 524 a value of 3. The corresponding d values are 1.0 and 0.43. The other blends were given intermediate values.

The data and d values are summarized in Table 14.

This analysis did rather well in that it predicted good performance for phenylphosphinic acid and for the A-88/trichloro-acetic acid combination. The former (in MCS 524) had a bearing life of 96 hours, and its failure was due more to excessive deposits than to a lubrication deficiency per se. The latter ran for 47 hours compared with one hour for MCS 524. The analysis failed to predict a good performance by perfluoroglutaric acid, which ran 100 hours. The reason for the low ranking of PFGA in the desirability analysis was its high contact angle (i.e. poor wetting). It should be remembered that the contact angles were measured at 169°C while the bearing hot-spot was 316°C. The wetting of the test fluid in the rig at the higher temperature was doubtless better than that given by the screening test.

6.2.11 Selection of Fluids for Bearing and Pump Tests

The following additives were chosen for bearing tests after stabilization of the rig with damper supports:

> m-phenylmercaptophenylphosphinic acid
> A-88 + trichloroacetic acid
> perfluoroglutaric acid
> phenylphosphinic acid
> tetraoctyltetraphosphetane tetrasulfide
>   + Emcol PS-236

55

TABLE 14. - TEST RATINGS AND D-VALUES

Additive	S4-Ball M50/M50	S4-Ball M50/Silvered 6415	Contact Angle M50	Contact Angle Silver	Rub-Block	D
A-88 + TCA	7 0.90	8 0.95	17° $\dfrac{0.53 + }{}$	20° $\dfrac{0.43}{2}$	9 0.98	$\sqrt[4]{0.486}$
ϕPO_2H_2	8 0.95	8 0.95	9° $\dfrac{0.92 + }{}$	10° $\dfrac{0.90}{2}$	7 0.74	$\sqrt[4]{0.608}$
$\phi S\phi PO_2H_2$	7 0.90	7 0.92	9° $\dfrac{0.92 + }{}$	10° $\dfrac{0.90}{2}$	3 0.43	$\sqrt[4]{0.324}$
$\phi S\phi S\phi PO_2H_2$	7 0.90	4 1/2 0.40	12° $\dfrac{0.84 + }{}$	10° $\dfrac{0.90}{2}$	10 1	$\sqrt[4]{0.313}$
PFGA	6 0.82	8 0.95	16° $\dfrac{0.58 + }{}$	30° $\dfrac{0.30}{2}$	9 0.98	$\sqrt[4]{0.336}$
ϕPO_2H_2 + PFGA	8 0.95	9 1/2 0.98	17° $\dfrac{0.55 + }{}$	23° $\dfrac{0.33}{2}$	7 0.74	$\sqrt[4]{0.303}$
$\phi S\phi PO_2H_2$ + PFGA	6 0.83	7 1/2 0.93	12° $\dfrac{0.90 + }{}$	16° $\dfrac{0.75}{2}$	7 0.74	$\sqrt[4]{0.474}$
ϕPO_2H_2 + DC-473[a]	8 1/2 0.97	8 0.95	4° $\dfrac{0.98 + }{}$	12° $\dfrac{0.84}{2}$	7 0.74	$\sqrt[4]{0.621}$
ϕPO_2H_2 + PFGA + DC-473[a]	8 1/2 0.97	8 0.95	15° $\dfrac{0.70 + }{}$	17° $\dfrac{0.55}{2}$	7 0.74	$\sqrt[4]{0.430}$
Emcol PS-236 + tetrasulfide	10 1	10 1	No data		No data	---

[a] Promotes foam.

56

The three-ring phosphinic acid gave an excellent M50/M50 rub-block friction test. However, the preparation of this acid gave such low conversions that there was not enough available for rig tests. Blends containing DC-473 were dropped due to foaming problems. The combination of phenylphosphinic acid plus perfluoroglutaric acid was dropped because the phosphinic acid by itself produced heavy deposits. The blend of the tetrasulfide plus Emcol PS-236 was run instead even though this fluid was only partially characterized.

The first pump test used MCS 524 + A-88 + trichloroacetic acid since this blend had the best friction curve on the pump metallurgy (see Figure H-5, Appendix H). Subsequent tests used blend f_3 plus perfluoroglutaric acid because rig data were desired on the new fluid and because the fluoro acid was the best additive in the bearing tests.

7. BEARING LUBRICATION TESTS

7.1 BEARING TEST APPARATUS

Bearing lubrication tests were performed on a specially designed high speed rig depicted schematically in Figure 8. The drive train consists of an Erdco universal test stand (ref. 20) modified by the substitution of a 10:1 helical-geared speed increaser for the original 3:1 speed increaser. This change permitted the 50 horsepower drive motor to turn test bearings at continuously variable speed to past 30,000 rpm.

7.1.1 Test Bearings

Test bearing design was fixed in consultation with bearing specialists at NASA, Pratt & Whitney and Midwest Aero Industries Corporation.* It is an 80-mm bore, ABEC Class 7 angular (25°) contact 18-ball bearing typifying current aircraft engine practice. Ball-to-raceway conformity is 52%. The cage, designed to ride on the inner race, has an imbalance limit of 3 g-cm at the land riding surface. Inner (split) and outer races are fabricated of M50 tool steel with a specified R_c 60 hardness and rms roughness of 15.2×10^{-6} cm (6×10^{-6} in.). The balls (1.428 cm or 0.5625 in. diameter) are also M50 steel of R_c 60 hardness. Their specified rms roughness is 5.08×10^{-6} cm (2×10^{-6} in.). The cage is fabricated of AMS 6415 steel of R_c 28-30 hardness silver plated to a depth of 2.54×10^{-3} to 5.08×10^{-3} cm (0.001-0.002 in.).

The 25 bearings acquired under this contract were manufactured from single heats by Marlin Rockwell Corporation, and were stabilized for 340°C running. Photographs of an unused bearing are included in Figures 9-11 for comparison with later photographs of used bearings.

7.1.2 Test Head

The test head was designed and fabricated by 'lidwest Aero Industries Corporation with the advice and agreement of Monsanto Research Corporation and the bearing specialists identified earlier. A view of the head and the associated test oil system in operating position is given in Figure 12.

The test head was designed to accommodate 2×10^6 DN (mm bore x rpm) operation of an 80-mm bore bearing, with provision for future 3×10^6 DN operation of a 100-mm bore bearing.

_____

*Then of Royal Oak, Michigan - more recently a division of Pure Carbon Co. of St. Marys, Pennsylvania.
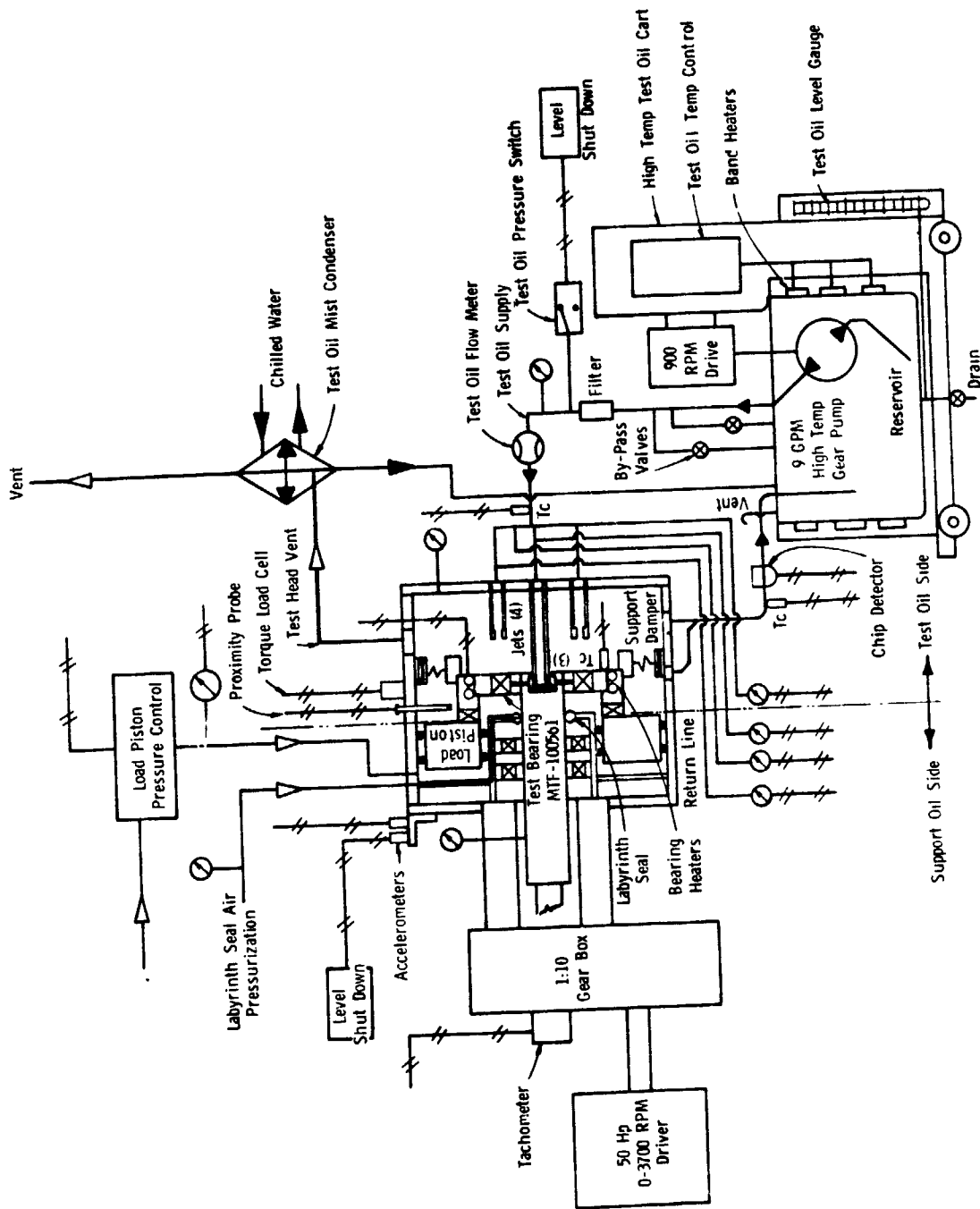
Figure 8. Bearing Test Rig

59
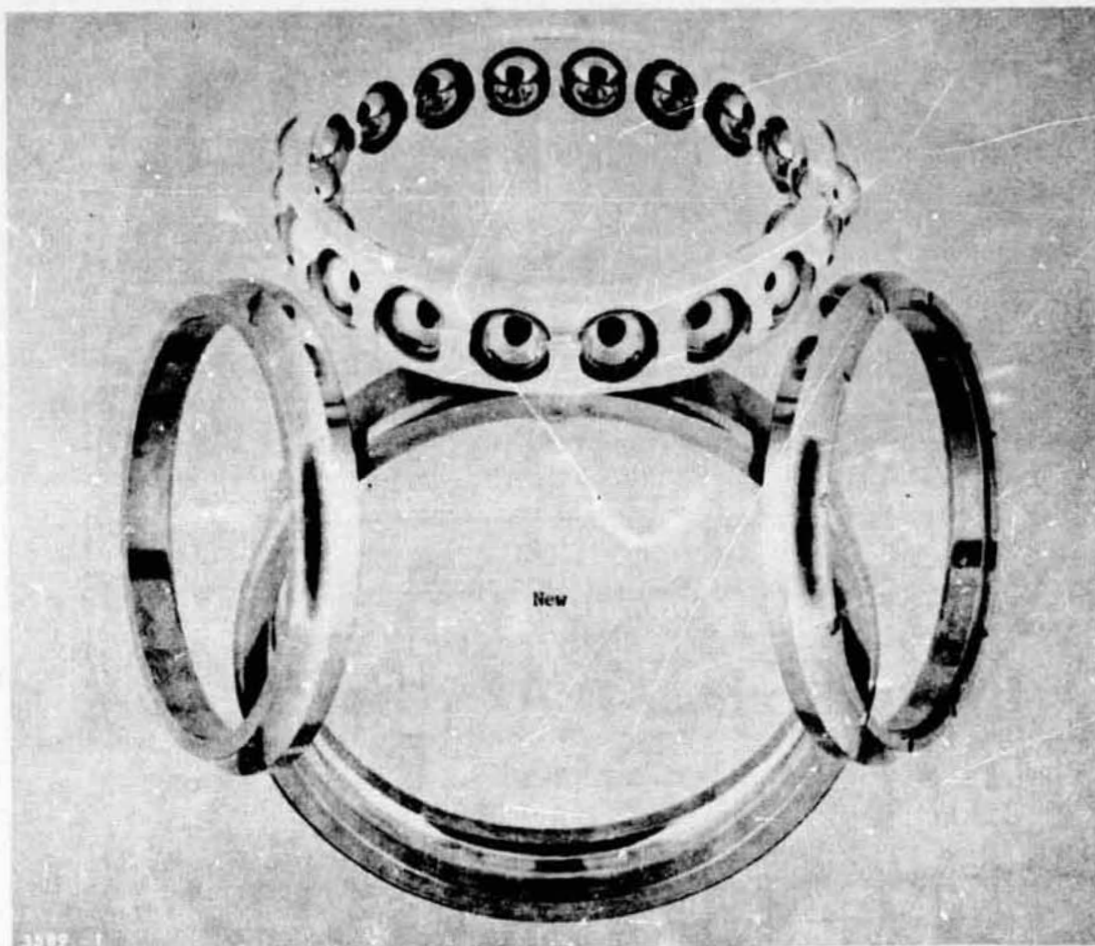
Figure 9.   Composite View of New Test Bearing

Figure 10. Bearing Cage Land Riding Area Viewed from
Direction of Test Oil Supply (New Bearing)

Figure 11. Bearing Cage Face Area Viewed from
Test Oil Outlet Area (New Bearing)
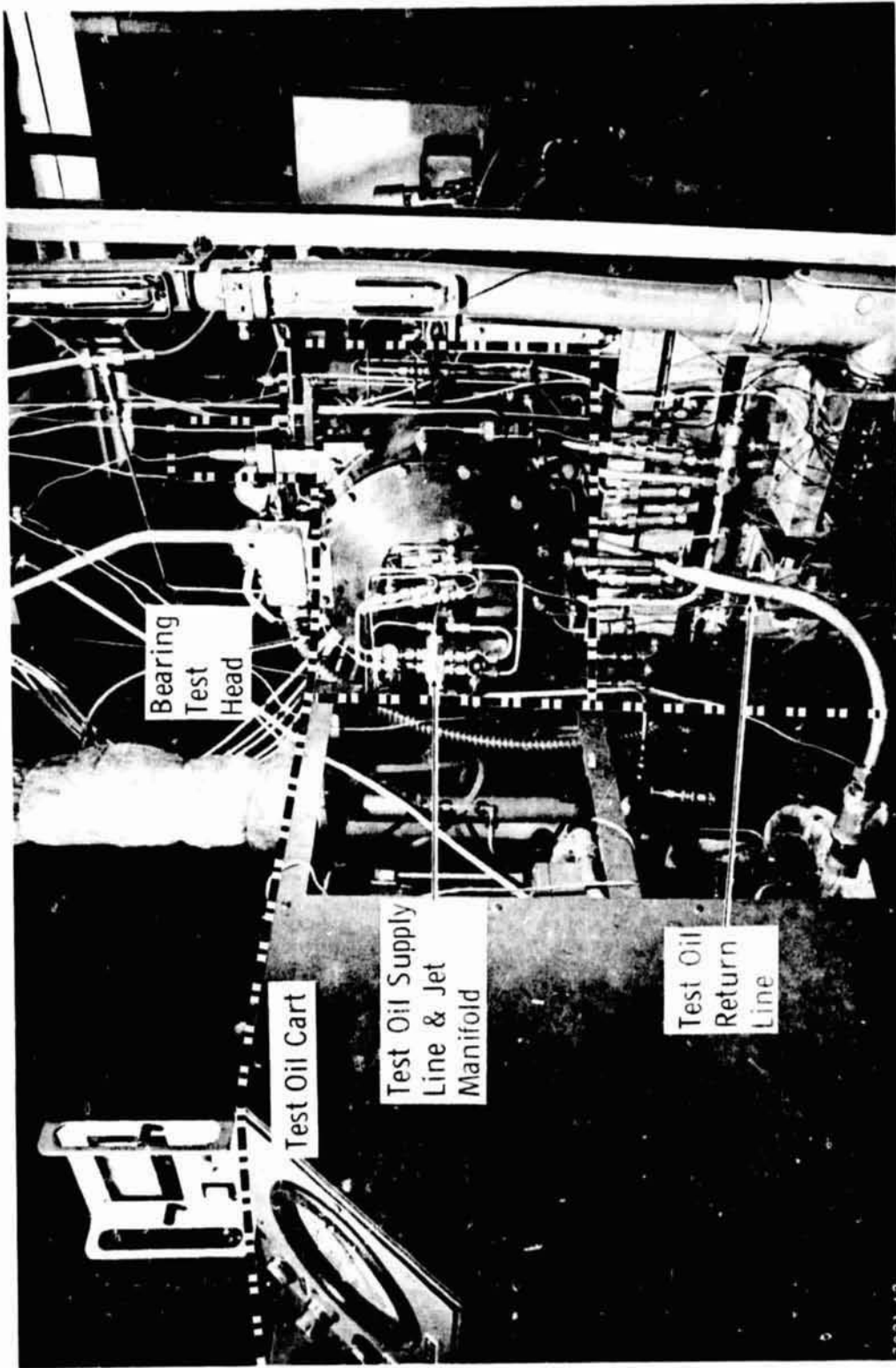
Figure 12. View of Assembled Bearing Test

Bearing Test Head

Test Oil Cart

Test Oil Supply Line & Jet Manifold

Test Oil Return Line

3821-62

Bearing support heaters allow 340°C maximum temperature control. A pneumatic loading piston provides thrust loading of the inner ring to 2.07 x 10^9 N/m^2 (300,000 psi) maximum contact stress under high speed operation. The cantilever design feature allows unobstructed observation of the bearing under test (through a housing window) and easy access to the bearing before and after testing.

An exploded view of the bearing and its mounting mechanisms appears in Figure 13. The large ring (with bolts, belleville springs and rollers) is a stabilizing device not part of the original design. It was added after bearing test No. 6 to suppress excessive radial/torsional vibrations in the outer (stationary) bearing support. A view of the assembly in its housing is given in Figure 14.

7.1.3 Lubricant System

Lubrication of the test bearing was accomplished by pumping the test oil into the bearing partly through a single nozzle jetting axially onto the bearing cage and partly into the split inner race oil passage. The lubricant departs from both front and back of the bearing and returns by gravity to the reservoir through a chip detector. The reservoir is electrically heated and insulated to control the lubricant supply temperature. Lubricant is returned to the bearing by a 9 gpm submerged gear pump through a cartridge filter.

7.1.4 Bearing Test Procedures and Conditions

Procedures employed in conducting the bearing lubrication tests are given in detail in Appendix I. Conditions of testing were as follows:

Contractual

Test duration	100 hours or prior lubrication failure
Bearing speed	2 x 10^6 mm-rpm (DN)
Contact stress	1.38 x 10^9 N/m^2 (200,000 psi) maximum, inner race
Test oil inlet temperature	204°C for Skylube 450 260°C for C-ether oils
Bearing outer race temp.	260°C for Skylube 450 316°C for C-ether oils

Figure 13. Exploded View of Test Bearing and Housing

BEARING HOUSING

BEARING HEATER

TEST BEARING

SUPPORT DAMPER

BEARING RETAINING NUTS
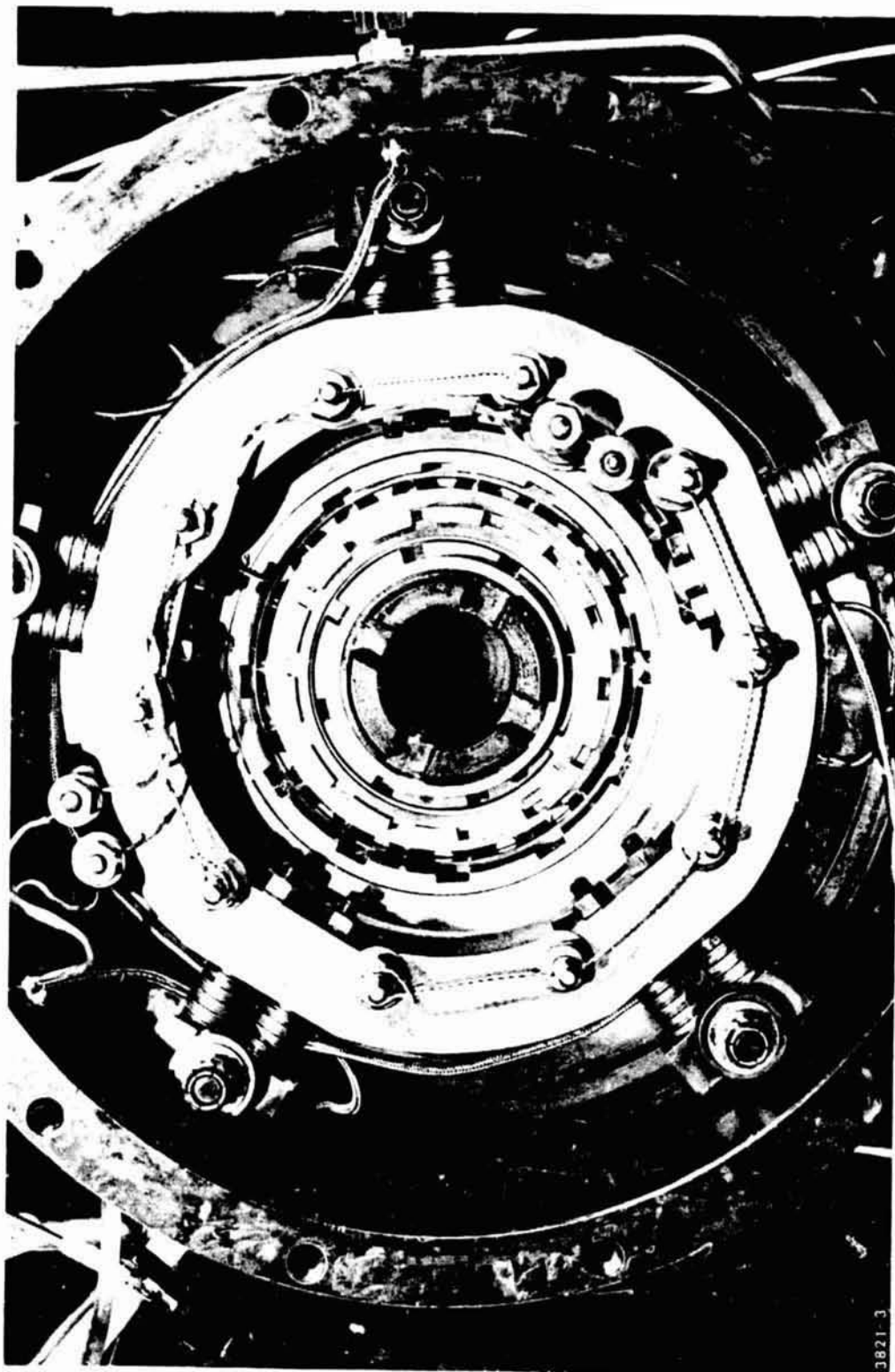
Figure 14. Assemble View of Test Bearing, Bearing Housing and Radial Support Damper in Bearing Test Head

3821-3

65

Test oil flow rate	$5.17 \times 10^{-5} m^3 s^{-1}$ (0.82 gpm)
Test oil flow through jet	60% of above
Initial test oil charge	7000 cc
Test oil filter	none, tests 1 through 3
	200 µm SS screen, tests 4-8
	10 µm depth (small), tests 9-10
	10 µm depth (large), tests 10-15

7.2   TEST RESULTS - SUMMARY

Fifteen tests were completed involving six formulated C-ether oils, the C-ether base stock (MCS 524) and the reference commercial oil (Skylube® 450). These tests are briefly summarized in Table 15.

Excessive vibrations of the test head were experienced in the first six tests. These vibrations caused termination of the three C-ether tests (4-6) before attaining contract running conditions. In the case of the Skylube 450 tests (1-3), however, the vibrations were less severe, especially at operating speed, and did not interfere with satisfactory completion of 100 hours operation.

At the termination of Test 6, a bearing support damper was installed to stiffen the radial support of the bearing outer race and add to its mass. This major modification succeeded in greatly reducing vibration, and it was therefore employed in the remaining nine tests (7-15). For this reason, most of the remaining presentation of results is limited to Tests 7 through 15.

No lubrication failures occurred during any test using Skylube 450. The C-ether base stock, MCS 524, ran only 0.6 hour before failure (Test 15). The failure was signaled by overheating of the outer race; examination of the bearing showed loss of silver from the cage and wear between the cage and inner race. Continued running past one hour (Test 8) produced excessive wear debris. This cage-race wear was the predominant failure mode of the C-ether blends. Additives produced large extensions of the bearing life, with one blend eliminating the gross wear failure altogether. An unexplained loss of silver occurred during the latter test from the side of the cage facing the fluid jet. This fluid (MCS 524 + PFGA) also gave the cleanest C-ether test. Generally, the C-ethers gave more filter pluggings, decomposition products and/or wear debris than the reference oil, which was run at a 56°C lower bearing temperature.

TABLE 15. - RESULTS OF BEARING TESTS

Test No.	Fluid	Bearing Serial No.	Outer Race Temp., °C	Stand Config.	Hours Run	Failure Mode; Comments
1	Skylube 450	14	241	No damper support	106.6	No failure
2	Skylube 450	1	260	No damper support	125.2	No failure
3	Skylube 450	3	260	No damper support	100	No failure
4	MCS 524	15		No damper support	0	Rig vibrational instability
5	MCS 524	13		No damper support	0	Rig vibrational instability
6	MCS 524 + TCA + A-88	5		No damper support	0	Rig vibrational instability
7	Skylube 450	6	260	Damper support	87.9	No failure
8	MCS 524	7	316	Damper support	14.1	Loss of cage silver; cage-race wear
9	MCS 524 + $\phi S\phi PO_2 H_2$	8	316	Damper support	14	Loss of cage silver; cage-race wear
10	MCS 524 + TCA + A-88	9	316	Damper support	47.4	Loss of cage silver; cage-race wear
11	MCS 524 + PF'A	12	316	Damper support	100.4	No failure
12	MCS 524 + $\phi PO_4 H_2$	11	316	Damper support	93.5	Overheated bearing
13	MCS 524 + Emcol PS-236 + sulfide	15	316	Damper support	0.3	Loss of cage silver; cage-race wear
14	Blend f_3 + PFGA	16	316	Damper support	0.3	Loss of cage silver; cage-race wear
15	MCS 524	17	316	Damper support	0.6	Loss of cage silver; cage-race wear

7.3   BEARING WEAR MEASUREMENTS

Bearing test failures were found due to the cage wearing against the inner race land riding area. With the exception of Test 8, serious wear was not observed in the bearing rolling contact areas, but some surface polishing and denting from particulate debris was noted. Wear was gauged from measurements of the cage inside diameter wear path cord and the maximum wear depth of the inner race land riding area. Using these dimensions, the wear area, wear mass and imbalance centrifugal cage force were calculated with the results presented in Table 16. These calculations assume all wear is from the cage which is rigid (non-conforming to the inner ring) and that the cage speed is 9,800 rpm under contract conditions. Where the wear extends over half the circumference of the cage, calculations of weight loss are in error. By weighing each bearing cage and calculating its difference from a reference bearing (S/N 19), the imbalance force is reduced as shown in Table 16. The bearing specification imbalance does not exceed 3 gram-centimeters at 500 rpm on the land riding surface. At the contract running conditions this imbalance force would be 31.6 N (7.103 lb_f). The relative sliding speed between the inner ring and cage land riding areas then is 78.28 m/sec (256.8 ft/sec).

The cage land wear track is approximately 0.714 cm and the projected (cord) wear track length is between 3.6 and 9.5 cm. The radial imbalance force on the cage ranges from the specification 31.6 N (7.103 lb_f) to 291.60 N (65.55 lb_f) due to the cage land wear on Test 8. The resulting load pressures between the inner ring and cage contact are 1.229 x 10^5 N/m^2 (174.8 psi) and 4.299 x 10^5 N/m^2 (611.3 psi) respectively. The corresponding PV products are 9.621 x 10^6 N/m-sec (4.489 x 10^4 lb_f/ft-sec) and 3.365 x 10^7 N/m-sec (1.570 x 10^5 lb_f/ft-sec).

7.4   BEARING TEST DETAILS - TESTS 7 to 15

This section includes the following information for Tests 7 through 15:

- a descriptive history of the test run

- visual analyses of the bearings

- a qualitative description of deposits and wear

- chemical and physical analyses of test fluids and deposits

Monitoring acid number (TAN), viscosity buildup, metal content and gravimetric deposits revealed the extent of fluid breakdown. Fluid stability is also reflected in the amount of deposits formed during a run. However, these results are only indications

68

TABLE 16. - MTF-100561 BEARING CAGE WEAR AND APPROXIMATE RESULTING IMBALANCE FORCES FROM TESTS 1-15

(All measurements taken after test termination.)

Bearing Test No.	Bearing serial No.	Measured Data		Calculated Results					Measured Values			
		Cage Land Riding Wear Area Cord Dimension, cm	Measured Cage Land Wear Depth, cm	Wear Intersection of Inner Race and Cage Riding Lands (Aw),[a] cm²	Wear Mass Removed from Cage (Mw),[b] g	Centrifugal Imbalance Force Due to Cage Wear (F)[c] N	(lbf)		Wear Mass Removed from Cage (Mw),[d] g	Centrifugal Imbalance Force Due to Cage Wear (F)[c] N	(lbf)	
1	14	3.6	6.4×10^{-3}	5.215×10^{-3}	2.930×10^{-2}	1.466	0.330				
2	1	5.5	1.3×10^{-3}	2.75×10^{-2}	1.596×10^{-1}	7.731	1.738				
3	3	5.3	2.5×10^{-3}	$2.328 \times 10^{-}$	1.308×10^{-2}	6.542	1.471				
4	15	(e)									
5	13	(e)									
6	5	(e)									
7	6	4.5	5.1×10^{-3}	1.186×10^{-2}	6.664×10^{-2}	3.333	0.749				
8	7	9.5	1.07×10^{-1}	~ 4.174	23.45	1173.0	263.7		5.18	259	58.24
9	8	9.5	$6.99 \times 10^{-}$	~ 4.174	23.45	1173.0	263.7		3.42	171	38.45
10	9	9.5	$5.59 \times 10^{-}$	~ 4.174	23.45	1173.0	263.7		1.92	96.0	21.59
11	12	7.2	3.8×10^{-1}	$6.999 \times 10^{-}$	3.933×10^{-1}	19.67	4.422		3.06	153	34.40
12	10	8.4	1.02×10^{-2}	1.893×10^{-1}	1.064	53.20	11.96		(0.19)	(9.5)	(2.14)
13	11	9.5	$8.00 \times 10^{-}$	4.174	23.45	1173.0	263.7		3.56	178	40.02
14	16	9.5	$6.35 \times 10^{-}$	4.174	23.45	1173.0	263.7		3.440	172	38.67
15	17	9.5	$4.19 \times 10^{-}$	4.174	23.45	1173.0	263.7		2.158	107	24.17

[a] Assumes rigid cage and no inner race (ring) wear.

[b] Total wear track width for both land riding areas of the cage is ~0.714 cm.

[c] Assumes imbalance weight is at ID of cage; density of steel ~7.87 g/cm³, ball orbital speed = 9.800 rpm with shaft speed = 25,000 rpm.

[d] Mass difference between test bearing cage and reference bearing S/N 19.

[e] Test terminated due to bearing housing vibration; light contacts around cage indicate bouncing contacts.

of test oil performance since filters removed most of the solid debris and since large amounts of makeup fluid were added during most tests. The gravimetric analysis then represents only finely suspended particles in the fluid or sludge, particularly any sludge soluble at higher temperatures but insoluble at ambient conditions. This material is collected on 0.8 micron filter paper and subsequently weighed. The fluid metal content was found by atomic absorption.

Additive depletion was followed by periodic analysis of the fluid for an element in the additive such as phosphorus or fluorine. (Acidic degradation of the base stock would inter- fere with analysis of acid additives by titration). Nuclear magnetic resonance was used to find aliphatic moieties in the fluids. Various techniques characterized solid deposits; these included x-ray fluorescence (XRF), x-ray diffraction (XRD), infrared, elemental analysis, and optical emission spectroscopy (OES).

7.4.1 Test No. 7 - Skylube 450 (Test Duration 87.9 hr)

After installation of the bearing damper support, a base- line run with Skylube 450 ran without fluid related incident for 87.9 hours at which time the test was terminated due to a drive system malfunction.

Photographs of the used bearing are shown in Figures 15-18, while a description of the deposits is given in Table 17. Results of the usual lubricant analyses are in Table 18. No other analyses were made. The iron content rises to 10.2 ppm at 87 hours; this is still a very low value.

7.4.2 Test No. 8 - MCS 524 (Test Duration 14.1 hr)

The bearing housing vibration was 4.06×10^{-5} m (1.6 mils) at the start of the test indicating good damper support per- formance. At 2.6 hours the test oil chip detector was bridged by fine wear particles; the bearing heater power was 820 W, but this dropped to 440 W at 5 hours. At 14.1 hours the test oil pressure was low due to plugging of the oil strainer (200 micron nominal). The chip detector resistance fell to 300 ohms but did not close the alarm relay. During the last eight minutes of the test the bearing temperature increased by 28°C. Visual inspec- tion through the test head window indicated cage wear. Figures 19 through 25 are photographs of the chip detector, wear debris and the bearing. Table 19 describes the deposits formed during the run and Table 20 gives the lubricant analyses results.

Test 8 produced the greatest cage wear of any test, yet the gravimetric analysis was only 68 mg per ℓ. This reemphasizes that most of the wear debris was caught in the 200 ℓ filter.

70

Figure 15. Bearing Test 7. Overall View of Bearing and Housing Viewed from Direction of Test Oil Supply

Figure 16. Test 7. Composite View of Test Bearing

Figure 17.   Test 7.   Bearing Cage Land Riding Area Viewed
from Direction of Test Oil Supply
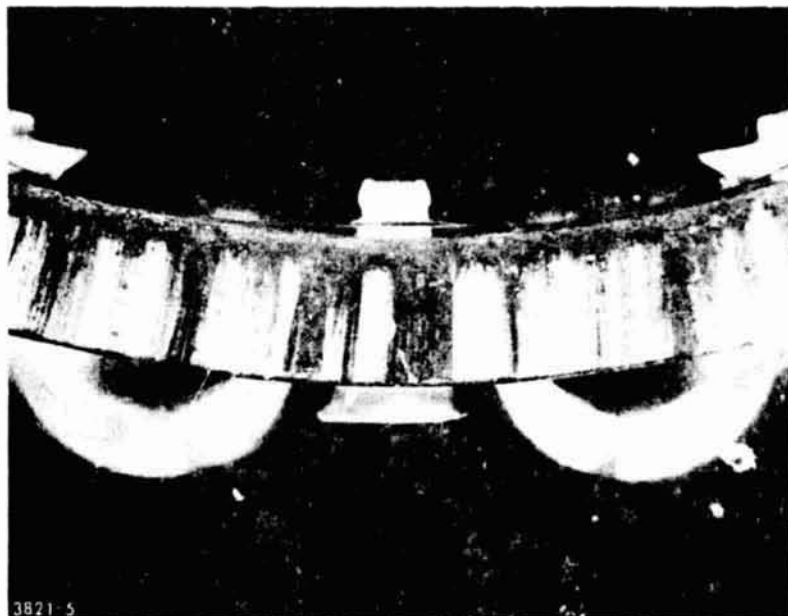
Figure 18.   Test 7.   Bearing Cage Face Area Viewed
from Test Oil Outlet Area

72

TABLE 17. - VISUAL DESCRIPTION OF DEPOSITS AND WEAR: TEST 7

Bearing Support and Housing Deposits:

    Staining and light varnish with trace of medium varnish

Bearing Deposits and Wear:

    Inner ring ball track -

        Light frosting, discoloration, and pitting

    Inner ring outside ball track -

        Very light deposit

    Outer ring ball track -

        Light frosting and staining

    Outer ring outside ball track -

        Light varnish and heat coloring

    Cage -

        Land wear area silver polished with light sludge on
        cage face; rest of cage lightly stained

TABLE 18. - LUBRICANT ANALYSES OF BEARING TEST NO. 7

Test lubricant: Skylube 450 (QA 44)

Sample number:	1	2	3	4	5
Time taken, hours:	New	1	40	65	87
Metal content, ppm:					
Ni	<0.1	<0.1	<0.1	<0.1	0.1
Fe	<0.1	0.1	1.2	1.7	10.2
Mg	<0.1	<0.1	0.1	0.1	0.4
Cu	<0.1	0.1	0.1	0.2	0.3
Ag	<0.1	0.2	0.2	0.2	<0.1
Cr	<0.1	<0.1	<0.1	<0.1	0.9
Al	0.1	0.2	0.3	0.4	0.4
Si	3.0	4.8	3.6	3.5	4.7
Ti	<0.1	<0.1	<0.1	<0.1	<0.1
Kinematic viscosity (centistokes) at 37.8°C (100°F)	29.05	28.69	31.52	34.00	39.91
TAN (mg KOH/g)	0.06	0.08	0.68	0.80	3.76
Gravimetric analysis (mg solid/ liter fluid)					not run

Figure 19.   Bearing Test 8.   Chip Detector at 14.1 Hours
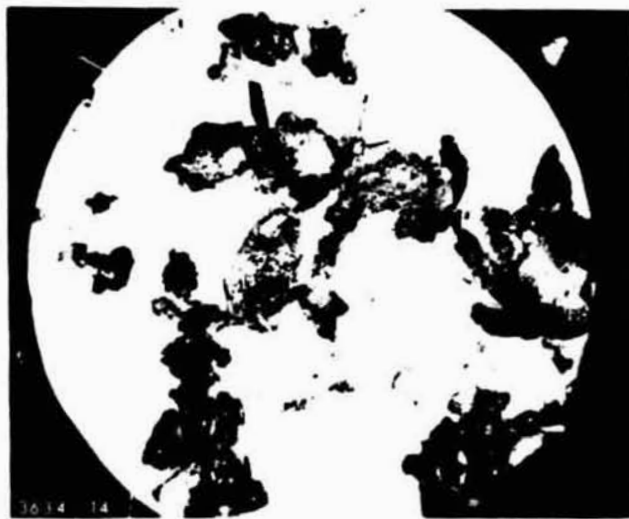
Figure 20.   Test 8.   Large Particle Wear Debris from
Test Oil Chip Detector and Strainer

Figure 21. Test 8. Overall View of Bearing and Housing
Viewed from Direction of Test Oil Supply

Figure 22. Test 8. Composite View of Test Bearing

Figure 23.   Test 8.   Typical Flaking Areas of Ball
Thrust Path of Inner Ring

Figure 24. Test 8. Bearing Cage Land Riding Area Viewed
from Direction of Test Oil Supply
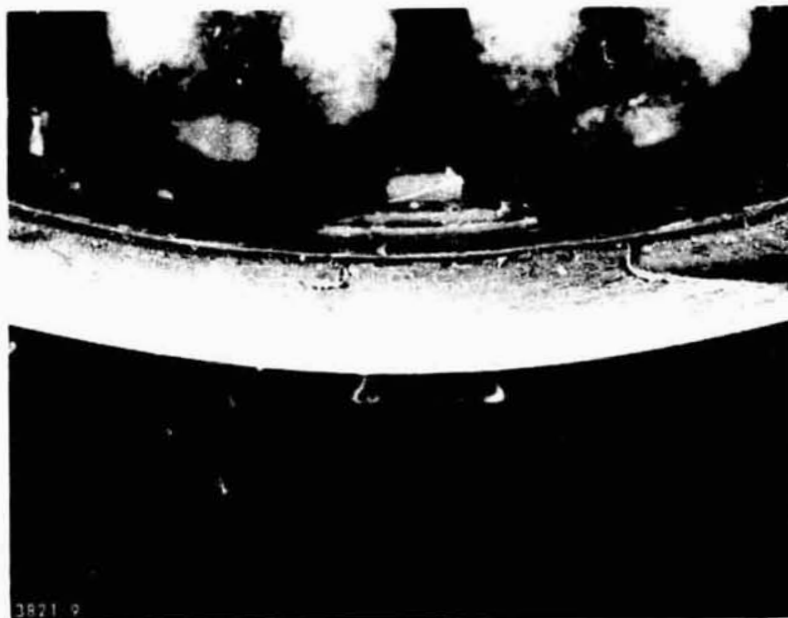
Figure 25. Test 8. Bearing Cage Face Area Viewed
from Test Oil Outlet Area

C-2

TABLE 19. - VISUAL DESCRIPTION OF DEPOSITS AND WEAR: TEST 8

Bearing Support and Housing Deposits:
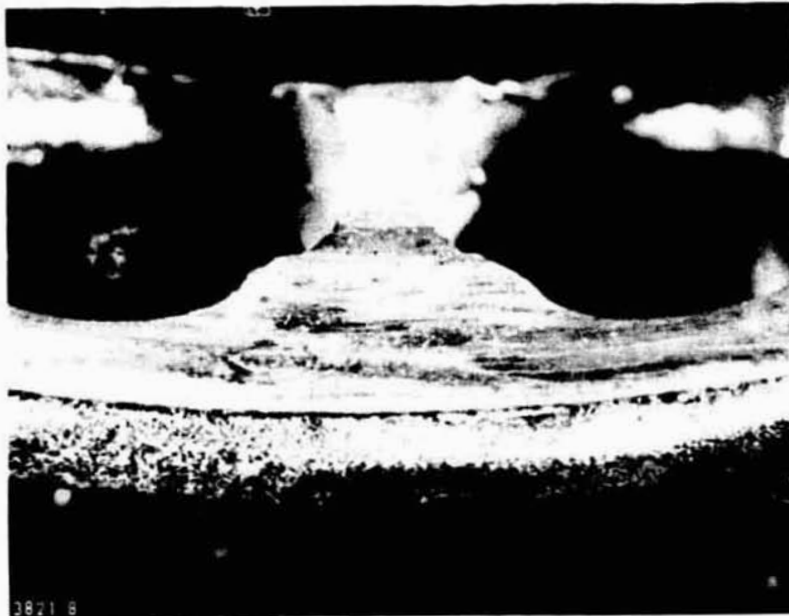
Light to medium varnish covers the entire housing

Bearing Deposits and Wear:

Inner ring ball track -

Light carbon deposits with ball path sites showing
metal flaking

Inner ring outside ball track -

Light carbon deposits with debris rolled into surface

Outer ring ball track -

Light carbon with debris rolled into ball track

Outer ring outside ball track -

Light carbon

Cage -

Gross wear of land riding area with blackest carbon
deposits near wear area; silver plating peeled back
on cage face near wear area

TABLE 20. – LUBRICANT ANALYSES OF BEARING TEST NO. 8

Test lubricant: MCS 524

Sample number:	1	2	3	4
Time taken, hours:	New	0	11	14.1
Metal content, ppm:				
Ni	4.2	4.2	4.2	5.0
Fe	0.9	3.5	7.9	55.0
Mg	<0.1	0.2	0.5	0.5
Cu	<0.1	<0.1	0.2	0.4
Ag	<0.1	1.8	19.2	19.9
Cr	<0.1	<0.1	<0.1	0.4
Al	0.1	0.3	0.4	0.3
Si	12.1	12.6	12.5	12.6
Ti	<0.1	<0.1	0.1	0.3
Kinematic viscosity (centistokes) at 37.8°C (100°F)	25.17	25.40	27.60	29.62
TAN (mg KOH/g)	0.02	0.02	0.08	0.17
Gravimetric analysis (mg solid/ liter fluid)				68

80

Between 12 and 14 hours the fluid silver concentration remained constant while the iron content increased by a factor of seven. Thus gross iron wear occurred after loss of the cage silver. This was the only test in which ring wear occurred. The inner ring ball path (Figure 23) showed large surface rupturing and extreme dark color formation and surface staining. This may have been due to bearing overheating.

7.4.3   Test No. 9 - MCS 524 + 0.1% m-Phenylmercaptophenyl-phosphinic Acid (PMPP Acid) (Test Duration 14 hr)

At 0.25 hour a new 10 micron depth filter plugged, causing low test oil pressure shutdown. The bearing was removed and showed no sign of unusual wear. At 8.8 hours the test oil level was low due to a pressure imbalance on the shaft seal caused by closing an air vent in the support oil system. Two liters of new fluid were added and the test proceeded until 14.0 hours when the test oil filter plugged. During the last 15 minutes the bearing temperature rose from 316°C to 332°C. Again the cage showed severe wear. This is seen in the photographs of the bearing and cage (Figures 26 through 29). The deposits and wear are summarized in Table 21.

The lubricant metal analysis (Table 22) shows a large copper content in the used fluid. The copper corrosion of this fluid in a 260°C oxidation-corrosion test was the highest of any test oil (-9.1 mg/cm^2).

Phosphorus analysis of the centrifuged used fluid showed 117 ppm vs. a theoretical of 124 ppm for the starting blend. Apparently little loss of the acid occurred. This is surprising in that both the contact angle and slow four-ball tests showed this acid was strongly adsorbed on metal surfaces.

7.4.4   Test No. 10 - MCS 524 + 0.1% A-88 + 0.05% Trichloroacetic Acid (Test Duration 47.4 hr)

Before contract conditions were reached there were three successive filter pluggings. After test start, additional filter pluggings were experienced at 0.3 hour, 13.6 hours, 15.8 hours and 19.3 hours. After then changing to a larger capacity 10 micron filter the test proceeded to 47.4 hours, after which there were two successive filter pluggings. Between 0.5 and 1.2 hours the bearing heater power dropped from 890 W to 590 W and gradually decreased to 420 W at 13.1 hours. Two liters of test oil were added at 11.6 hours and 1 liter was added at 30.0 hours. The metal chip detector was bridged at 24.5 hours and 39.5 hours by large metal flakes and fine agglomerates as shown in Figures 30 and 31. Despite all these interruptions, the bearing ran smoothly until shortly before failure.
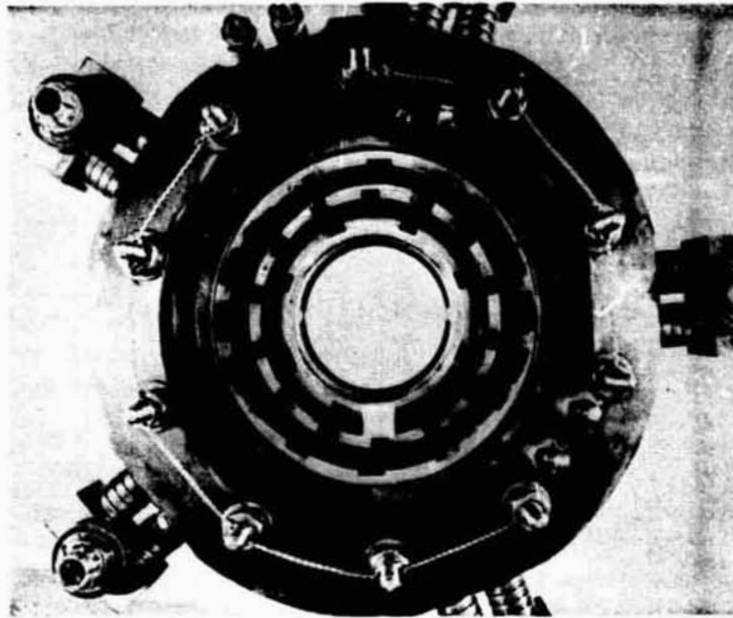
Figure 26. Bearing Test 9. Overall View of Bearing and
Housing Viewed from Direction of Test Oil Supply

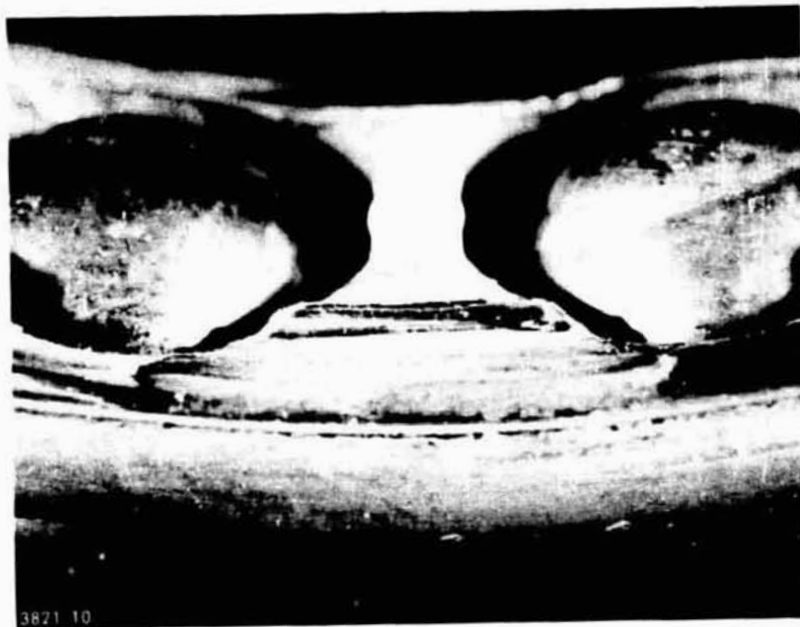Figure 27. Test 9. Composite View of Test Bearing

Figure 28.   Test 9.   Bearing Cage Land Riding Area Viewed
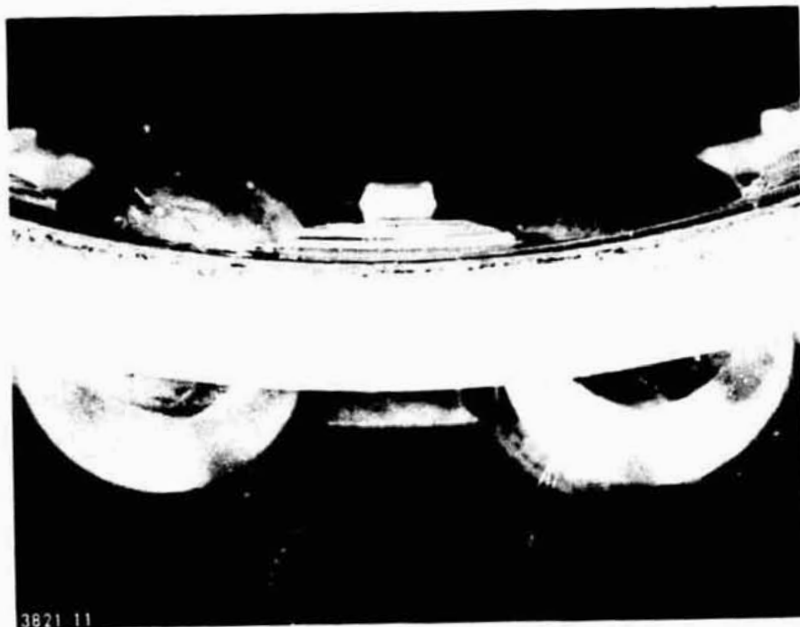from Direction of Test Oil Supply

Figure 29.   Test 9.   Bearing Cage Face Area Viewed
from Test Oil Outlet Area

TABLE 21. - VISUAL DESCRIPTION OF DEPOSITS AND WEAR: TEST 9

Bearing Support and Housing Deposits:

Light varnish and staining

Bearing Deposits and Wear:

Inner ring ball track -

Dark staining, very light carbon, ball track lightly frosted

Inner ring outside ball track -

Light carbon deposit and dark staining

Outer ring ball track -

Light staining, very light frosting in ball track

Outer ring outside ball track -

Light staining

Cage -

Heavy wear on land riding areas; light carbon deposits and silver plating peeled back outside wear area; rest of cage lightly pitted

TABLE 22. - LUBRICANT ANALYSES OF BEARING TEST NO. 9

Test lubricant: MCS 524 + 0.1% PMPP Acid

Sample number:	1	2	3
Time taken, hours:	1/4	10	14
Metal content, ppm:			
Ni	4.0	8.5	8.5
Fe	10.0	106.0	110.0
Mg	0.5	1.6	1.7
Cu	2.8	13.0	12.5
Ag	7.1	41.6	43.0
Cr	0.4	0.4	0.5
Al	0.2	0.3	0.2
Si	16.6	16.9	16.8
Ti	0.1	0.1	0.1
Kinematic viscosity (centistokes) at 37.8°C (100°F)	24.82	29.51	27.26
TAN (mg KOH/g)	0.19	0.14	0.14
Gravimetric analysis (mg solid/ liter fluid)			1800

Figure 30.   Bearing Test 10.   Chip Detector
Bridging at 24.5 Hours

Figure 31.   Test 10.   Chip Detector
Bridging at 39.5 Hours

During the last 10 minutes of the test (before the final two filter pluggings) the bearing temperature rose 11°C. Since the cage showed considerable wear, it was decided to terminate the test. Figures 32-35 are photos of the bearing and cage; descriptive comments on the deposits and wear are in Table 23.

Fluid metal analysis (Table 24) shows a small increase in iron content and no increase in copper. The silver pickup in the fluid was erratic. The amount of solids centrifuged from the fluid was small after 16 hours but fairly large after 40.5 hours. The major metallic element in this centrifuged residue at 40.5 hours was silver (OES); silver was also the major metal of the first filter plugging. The XRF analysis of the filter plugging also detected:

>iron (second)
>molybdenum (third)
>copper
>zinc
>chromium
>potassium
>calcium
>sulfur
>phosphorus

A quick loss of additive from the fluid was observed. Phosphorus analysis of the fluid showed greater than 85% removal of A-88 at 16 hours. Chlorine analyses were all above the theoretical chlorine for 0.05% trichloroacetic acid, so there was a chlorinated impurity in the fluid.

$$\begin{aligned}
\text{Theoretical phosphorus} &= 186 \text{ ppm} \\
\text{at 16 hr} &= 15 \text{ ppm} \\
\text{at 47 hr} &= 24 \text{ ppm} \\
\\
\text{Theoretical chlorine} &= 325 \text{ ppm} \\
\text{at 16 hr} &= 625 \text{ ppm} \\
\text{at 40 hr} &= 535 \text{ ppm} \\
\text{at 47 hr} &= 500 \text{ ppm}
\end{aligned}$$

The significance of rapid additive depletion is discussed in section 7.5.

7.4.5   Test No. 11 - MCS 524 + ~0.07% Perfluoroglutaric Acid (Test Duration 100.4 hr)

During this test 1 liter of makeup fluid was added at 19.5 hours, 36.3 hours, 70.9 hours and 94.2 hours. Filter pluggings were experienced at 30.1 hours and 76.4 hours. At 76.4 hours it was noticed that 75% of the silver from the cage
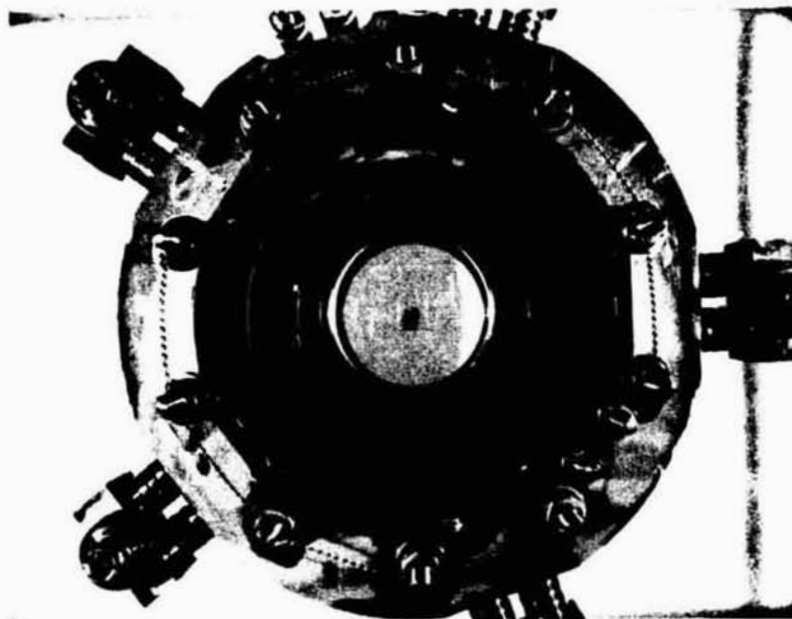
Figure 32. Test 10. Overall View of Bearing and Housing
Viewed from Direction of Test Oil Supply

Figure 33. Test 10. Composite View of Test Bearing

Figure 34. Test 10. Bearing Cage Land Riding Area Viewed
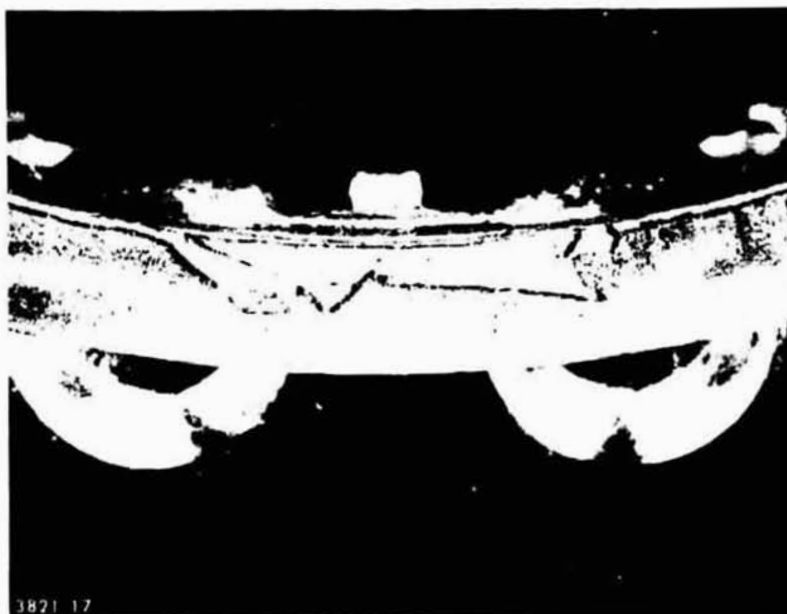from Direction of Test Oil Supply

Figure 35. Test 10. Bearing Cage Face Area
Viewed from Test Oil Outlet Area

TABLE 23. - VISUAL DESCRIPTION OF DEPOSITS AND WEAR: TEST 10

Bearing Support and Housing Deposits:

    20% light, 50% medium and 20% heavy varnish; 10% light
    carbon, sludge

Bearing Deposits and Wear:

    Inner ring ball track -

        Ball path lightly frosted with light carbon deposits

    Inner ring outside ball track -

        Heavy varnish to light carbon deposits

    Outer ring ball track -

        Carbon deposits in ball track

    Outer ring outside ball track -

        Light to medium varnish

    Cage -

        Heavy wear in land riding area; total cage covered
        with light to medium sludge

TABLE 24. - LUBRICANT ANALYSES OF BEARING TEST NO. 10

Test lubricant: MCS 524 + 0.1% A-88 + 0.05% TCA acid

Sample number:	1	2	3	4	5
Time taken, hours:	0	1.2	16	40.5	47.4
Metal content, ppm:					
Ni	4.0	4.1	3.7	3.9	3.9
Fe	1.3	1.6	1.6	2.4	6.0
Mg	<0.1	<0.1	<0.1	<0.1	<0.1
Cu	0.3	0.3	0.3	0.6	0.3
Ag	1.3	1.7	8.8	55.0	1.6
Cr	<0.1	<0.1	<0.1	<0.1	0.2
Al	0.2	0.2	0.3	0.2	0.2
Si	18.1	17.29	16.7	16.8	16.6
Ti	<0.1	<0.1	<0.1	<0.1	<0.1
Kinematic viscosity (centistokes) at 37.8°C (100°F)	25.29	25.14	25.88	29.60	33.98
TAN (mg KOH/g)	0.03	0.03	0.05	0.15	0.24
Gravimetric analysis (mg solid/ liter fluid)				3268	

area of test oil jet impingement was removed. At 94.2 hours the chip detector bridged. At 100.4 hours the test was terminated with little noticeable wear of the cage to inner race contact area, while all the silver in the cage jet impingement area was removed. This was the cleanest C-ether run. The bearing and cage are shown in Figures 36-39, and a qualitative summary of deposits and wear is given in Table 25.

The fluid showed (Table 26) an early and almost linear pickup of silver with a much later increase of copper and iron. As discussed later, the "soluble" silver may represent a beneficial corrosive loss of this metal from the cage, or it may represent flaked silver subsequently ground into fine particles in the contact regions. The amount of centrifugable matter in the fluid is fairly small until the 76.4 hour sample. Likewise, the acid number, viscosity and iron content increased between the 53 and 76 hour analyses. The fluid was apparently quite clean for 60 to 70 hours.

The centrifuged solids at 94 hours contained chloroform-soluble and chloroform-insoluble fractions. An infrared spectrum of the soluble portion showed mostly aromatic absorption but also revealed minor peaks associated with aliphatic and carbonyl groups. The presence of alkyl groups is surprising. Support oil contamination of the C-ether fluid would explain aliphatic impurities. This was unlikely, however, since no aliphatic peaks were detected by nuclear magnetic resonance in the base stock after 94 hours. Fein (ref. 21) has shown that aromatic materials can generate aliphatic moieties under boundary lubrication conditions. This may have happened in the C-ether oil under the harsh environment of a 100 hour test.

The centrifuged residue at 76 hours contained 14% ash. Optical emission showed the main metal of the centrifuged solids at 100 hours was silver. Silver was also the major component of highly metallic (78% ash) particles left after filtration of the fluid at 76 hours. XRF identified silver metal per se in these deposits. These metallic flakes may have come from the side of the cage where there was direct fluid impingement on the silver plating. At the end of the test silver was completely removed from this area, while the remainder of the cage retained its silver plating except in three ball pockets.

The bearing gave indications of fatigue failure initiation with the formation of small pits in the contact path of the outer ring.

Fluorine content of the fluid was very low after 50 hours, hence the fluoro acid was no longer in the fluid.
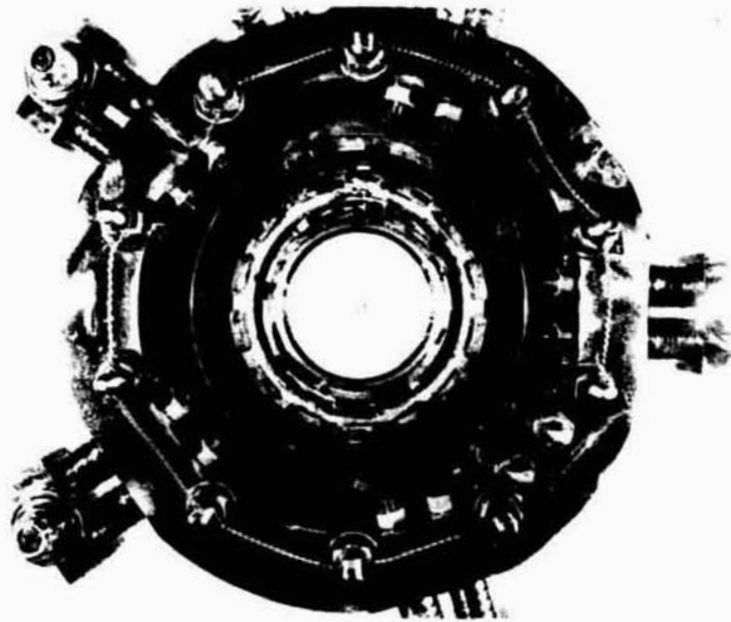
92

Figure 36. Bearing Test 11. Overall View of Bearing and Housing Viewed from Direction of Test Oil Supply

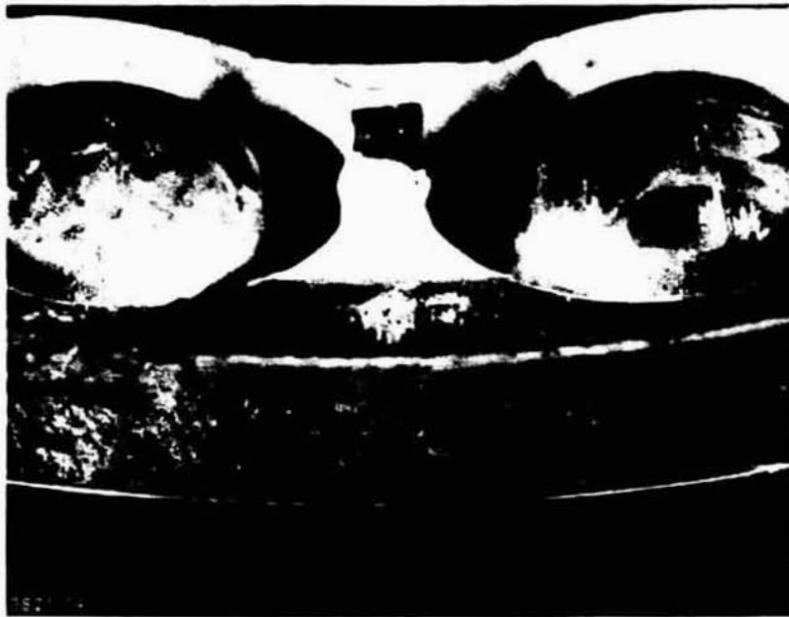Figure 37. Test 11. Composite View of Test Bearing

93

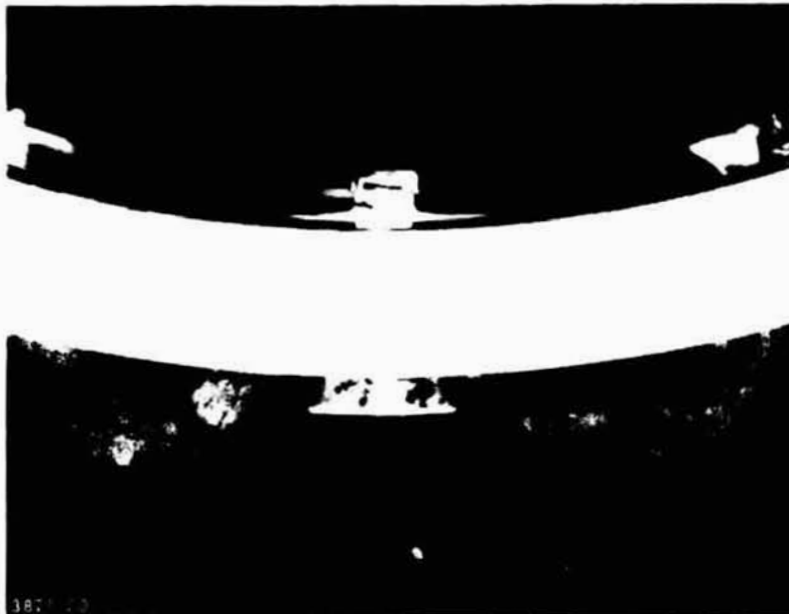Figure 38. Test 11. Bearing Cage Land Riding Area Viewed from Direction of Test Oil Supply

Figure 39. Test 11. Bearing Cage Face Area Viewed from Test Oil Outlet Area

TABLE 25. - VISUAL DESCRIPTION OF DEPOSITS AND WEAR: TEST 11

Bearing Support and Housing Deposits:

   40% medium and 50% heavy varnish; 10% light sludge

Bearing Deposits and Wear:

   Inner ring ball track -

      Light frosting of ball path, light varnish

   Inner ring outside ball track -

      Light varnish

   Outer ring ball track -

      Light varnish and small pits in ball path

   Outer ring outside ball track -

      Light to medium varnish

   Cage -

      Cage is lightly worn with only silver removed; silver
      on cage face totally removed in jet impingement area;
      rest of cage in clean condition with little deposit
      on silver plate

TABLE 26. - LUBRICANT ANALYSES OF BEARING TEST NO. 11

Test lubricant: MCS 524 + ∿0.07% perfluoroglutaric acid

Sample number:	1	2	3	4	5	6	7
Time taken, hours:	0	19.5	30.4	53.4	76.4	94.2	100.4
Metal content, ppm:							
Ni	3.3	3.4	3.5	3.5	4.0	4.0	4.8
Fe	2.4	1.9	3.1	2.1	19.4	31.2	27.0
Mg	<0.1	<0.1	0.1	0.2	0.2	0.2	0.2
Cu	2.8	3.1	2.9	6.0	12.5	13.5	12.0
Ag	4.5	70.0	100.0	180.0	240	320	300
Cr	<0.1	<0.1	<0.1	<0.1	0.3	0.5	0.4
Al	0.3	<0.1	0.7	0.9	1.5	2.1	1.9
Si	17.4	17.5	16.6	16.7	17.5	17.6	17.5
Ti	<0.1	<0.1	<0.1	<0.1	<0.1	<0.1	<0.1
Kinematic viscosity (centistokes) at 37.8°C (100°F)	25.30	28.76	29.39	33.07	45.80	48.42	45.51
TAN (mg KOH/g)	0.12	0.29	0.25	0.34	0.54	0.56	0.50
Gravimetric analysis (mg solid/ liter fluid)							2680

Hours	% PFGA
0	0.07
19.5	0.008
53.4	<0.004
94.2	<0.004

As discussed later, this does not necessarily imply loss of effective boundary film. However, the almost complete removal of the acid at 50 hours must mean at least some loss of acid after establishment of the initial equilibrium. The water content of the oil remained reasonably constant at ∿0.02%.

Hours	ppm Water
19.5	201
53.4	155
94.2	148

7.4.6 Test No. 12 - MCS 524 + 0.1% Phenylphosphinic Acid (Test Duration 93.5 hr)

During this test there were four filter pluggings, at 2.3 hours, 18.0 hours, 41.7 hours and 54.0 hours. At 18 hours the test head cover was removed and heavy sludge was found on all continuously wetted parts, but the cage showed little wear. One liter of makeup oil was added at 18.0 hours, 37.0 hours, 56.0 hours and 84.8 hours. During the first 56 hours of this test the bearing heater power fluctuated between 900 W and 190 W. Between 41.7 hours and 54 hours the bearing temperature changed from 316°C to 343°C. At 56 hours the bearing temperature again reached 343°C and shut down the test. Inspection of the bearing head interior indicated little change from the 18 hour inspection. The test was restarted with fan cooling of the test oil reservoir and bearing head. The bearing temperature reached 321°C equilibrium temperature at a 260°C oil inlet temperature with no power being supplied to the outer race heaters. After addition of one liter of test oil at 84.8 hours the bearing temperature and test oil temperature climbed at an increasing rate until at 93.4 hours the test oil reached 316°C and the bearing temperature became 399°C. Viewing the bearing through the test head window revealed some cage wear.

This test did not show gross wear or loss of silver from direct fluid impingement. However, it gave the greatest amount of deposits of any test with a particularly high gravimetric analysis. Photographs of the cage and bearings appear in Figures 40 through 43, and Table 27 outlines the deposits and wear.
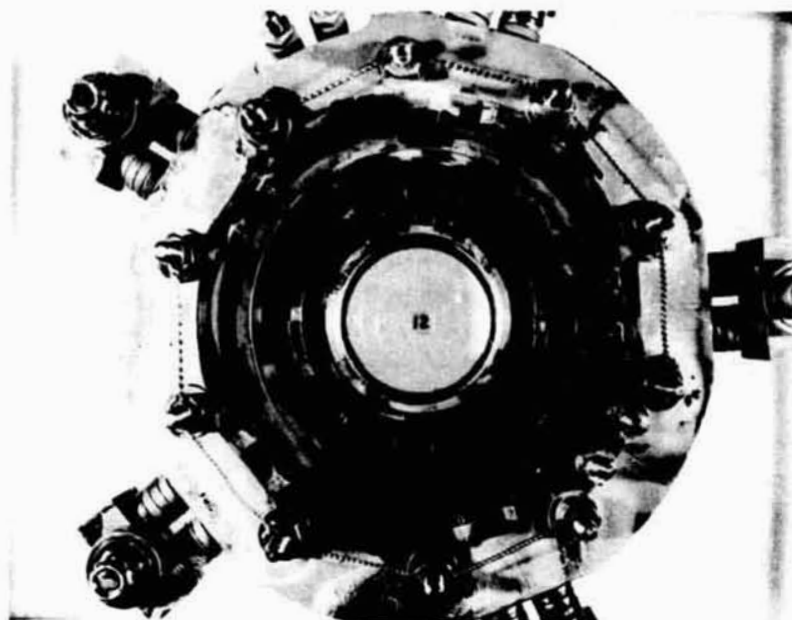
97

Figure 40. Bearing Test 12. Overall View of Bearing and Housing Viewed from Direction of Test Oil Supply

Figure 41. Test 12. Composite View of Test Bearing

Figure 42. Test 12. Bearing Cage Land Riding Area
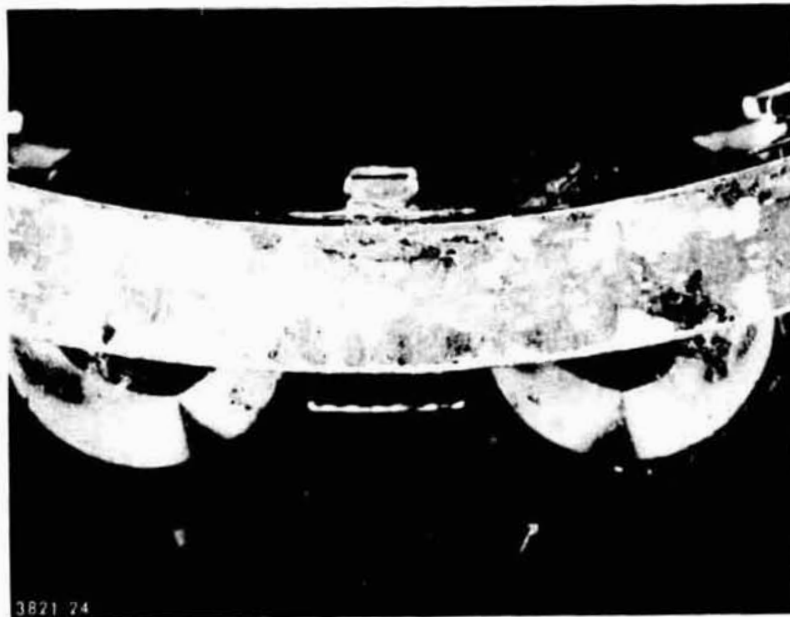Viewed from Direction of Test Oil Supply

Figure 43. Test 12. Bearing Cage Face Area
Viewed from Test Oil Outlet Area

TABLE 27. - VISUAL DESCRIPTION OF DEPOSITS AND WEAR: TEST 12

Bearing Support and Housing Deposits:

    30% medium and 50% heavy varnish; 20% light sludge

Bearing Deposits and Wear:

    Inner ring ball track -

        Frosting and dark staining of ball track

    Inner ring outside ball track -

        Medium varnish

    Outer ring ball track -

        Washboarding of the ball track and heavy varnish

    Outer ring outside ball track -

        Heavy varnish

    Cage -

        Cage land riding area has moderate wear with medium
        varnish covering cage

The fluid showed a linear rise in silver content (Figure 56) with fair amounts of copper and iron after 50 hours. The data are reported in Table 28.

Although the cage silver did not wear except in the normal wear area, and there was no loss of silver due to impingement, the filter pluggings and the sludge contained ash. The filter residue was more metallic (ca. 45% ash vs. ca. 30% for the sludges). More detailed characterizations of the filter pluggings and two sludges are presented in Appendix J. There was no aliphatic material in the fluid after 54 hours even though some was detected in the filter residue. Possible sources of aliphatic groups are discussed in section 7.4.5 (Test 11).

Loss of ∿90% of the original phosphorus in the fluid was very rapid.

Starting fluid = 216 ppm (theory is 218)

0 hr = 25 ppm

10 hr = 26 ppm

54 hr = 32 ppm

The phosphinic acid must quickly react at the bearing surfaces, protecting the silver and iron from wear. This additive also reacts with the base stock (possibly after or during the reaction on the metal surface), producing sludge. All of this happens quickly. A wiping of the sludge at 18 hours was visible at 94 hours.

It is interesting that the related phosphinic acid used in Test 9 did not give sludge and also did not provide sufficient lubrication. Its rate of depletion was much less than that of phenylphosphinic acid, probably because of its greater solubility. Hence it did not give as much of either the beneficial or detrimental surface reactions.

7.4.7   Test No. 13 - MCS 524 + 0.05% Emcol PS-236 + 0.05% Tetra-
octyltetraphosphetane Tetrasulfide (Test Duration 0.33 hr)

At 0.33 hour the bearing speed was jogging, the bearing temperature was rising rapidly past 338°C and the test oil filter was plugging. Visual inspection revealed cage wear. The bearing and cage are pictured in Figures 44-47; Table 29 gives comments on the deposits and wear and Table 30 presents the fluid analyses data.

The fluid picked up much more iron than silver. These two elements were the main metals of two filter residues. These deposits were highly metallic (∿80% ash); their elemental analyses and XRD lines are in Appendix K; XRD did not lead to identification of the solids.

TABLE 28. - LUBRICANT ANALYSES OF BEARI`G TEST NO. 12

Test lubricant: MCS 524 + 0.1% phenylphosphinic acid

Sample number:	1	2	3	4	5	6
Time taken, hours:	0	10	18	37	54+	93.5
Metal content, ppm:						
Ni	5.3	4.2	3.6	4.0	3.9	4.6
Fe	23.1	10.8	5.7	5.5	17.3	55.7
Mg	0.5	0.3	0.2	0.2	0.3	0.4
Cu	4.0	0.4	0.4	1.8	2.1	9.2
Ag	5.3	9.7	17.2	38.7	60.0	105.0
Cr	0.3	0.1	0.2	0.3	0.8	0.8
Al	0.2	0.2	0.4	1.5	1.5	1.5
Si	15.2	15.3	17.0	17.5	16.7	16.6
Ti	0.3	0.2	0.2	0.5	1.0	2.5
Kinematic viscosity (centistokes) at 37.8°C (100°F)	25.42	27.17	29.03	34.94	39.61	51.95
TAN (mg KOH/g)	0.33	0.22	0.22	0.40	0.35	0.35
Gravimetric analysis (mg solid/ liter fluid)						10,000 2 ml sample
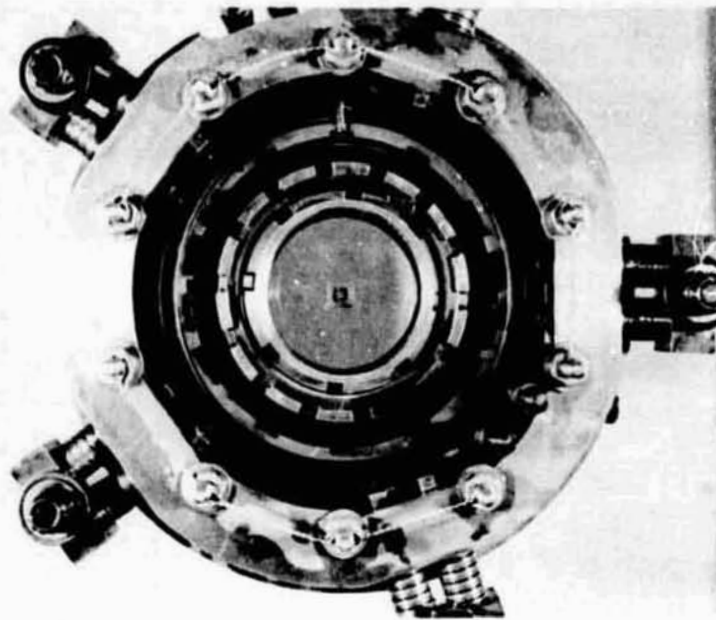
Figure 44.   Bearing Test 13.   Overall View of Bearing and
              Housing Viewed from Direction of Test Oil Supply

Figure 45.   Test 13.   Composite View of Test Bearing

103
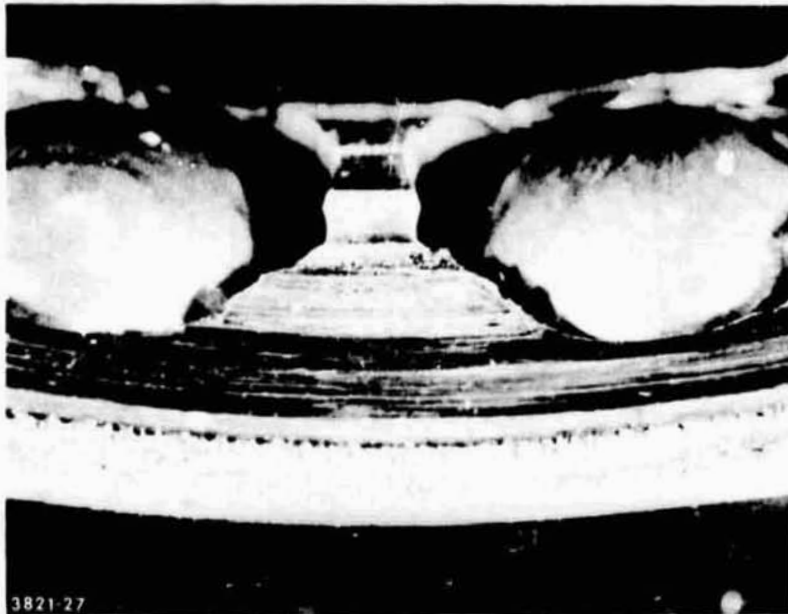
Figure 46.   Test 13.   Bearing Cage Land Riding Area
Viewed from Direction of Test Oil Supply
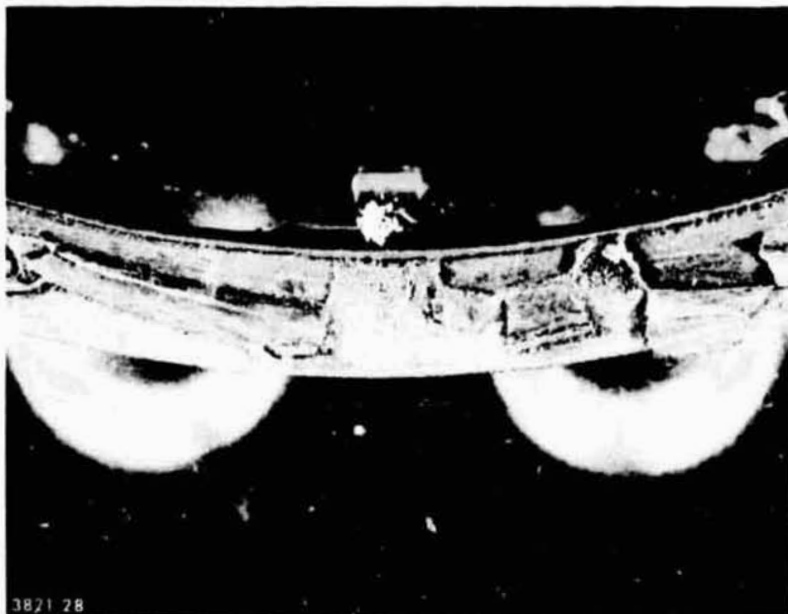
Figure 47.   Test 13.   Bearing Cage Face Area
Viewed from Test Oil Outlet Area

TABLE 29. - VISUAL DESCRIPTION OF DEPOSITS AND WEAR: TEST 13

Bearing Support and Housing Deposits:

Light to medium varnish covers the housing

Bearing Deposits and Wear:

Inner ring ball track -

Ball p... lightly frosted and stained

Inner ring outside ball track -

Very light varnish

Outer ring ball track -

Light staining

Outer ring outside ball track -

Light staining

Cage --

Cage heavily worn in land riding area which has silver
plate peeling; cage covered by light carbon sludge
and varnish

TABLE 30. – LUBRICANT ANALYSES OF BEARING TEST NO. 13

Test lubricant: MCS 524 + 0.05% Emcol PS-236 + 0.05% tetrasulfide

Sample number: 1

Time taken, hours: 0 (after failure)

Metal content, ppm:

Ni	5.0
Fe	51.0
Mg	0.1
Cu	0.6
Ag	1.8
Cr	0.1
Al	0.5
Si	15.2
Ti	0.2

Kinematic viscosity   25.28
(centistokes) at
37.8°C (100°F)

TAN(mg KOH/g)   0.08

Gravimetric anal-   240
ysis (mg solid/
liter fluid)

The unused fluid had 106 ppm of phosphorus and the used fluid 24 ppm. These analyses inadvertently were not run until ca. 12 months after completion of the test and hence are a bit suspect.

7.4.8 Test No. 14 - Blend f_3 + ~0.07% Perfluroglutaric Acid (Test Duration 0.3 hr)

Due to the scarcity of blend f_3, the fluid used in pump test No. 4 was refurbished and used as the base stock in bearing test No. 14. The pump test fluid (238 ppm fluorine) was

a)   filtered

b)   treated under nitrogen with 3.5% of 28-48 mesh alumina for 5 hours at 100-114°C

The filtered liquid contained 59 ppm fluorine. After the addition of 0.1% PFGA and a subsequent 1 μ Millipore filtration, antifoam addition with Dispersator stirring finished the formulation. The nylon Millipore filter (NRWG 14250) plugged several times during the filtrations. The final fluorine titre prior to antifoam addition was 345 ppm (0.07% PFGA).

After operating conditions were attained, the bearing temperature rose past 327°C with no bearing heater power. The bearing showed high cage to inner race wear. The bearing photographs (Figures 48-51), descriptions of the deposits and wear (Table 31) and fluid analyses (Table 32) follow.

The used fluid contained 85% of the original fluoro acid (292 ppm fluorine vs. 345 ppm). Additive depletion was low compared to Test 11, and probably wasn't the main cause of the failure.

7.4.9 Test No. 15 - MCS 524 (Lot QB-39) (Test Duration 0.6 hr)

For the first 30 minutes the operating conditions were stable, after which the bearing temperature rose quickly to 332°C without external heating. The cage again showed wear.

The bearing and cage photographs are in Figures 52-55. The summation of deposits and wear is in Table 33 and the fluid analyses are presented in Table 34.

7.5 DISCUSSION OF BEARING TEST RESULTS

Disregarding filter pluggings, the best C-ether blend was MCS 524 plus perfluoroglutaric acid (Test 11). This ran for 100 hours with no lubrication failure. The maximum cage wear depth for this C-ether blend compared favorably with the ester
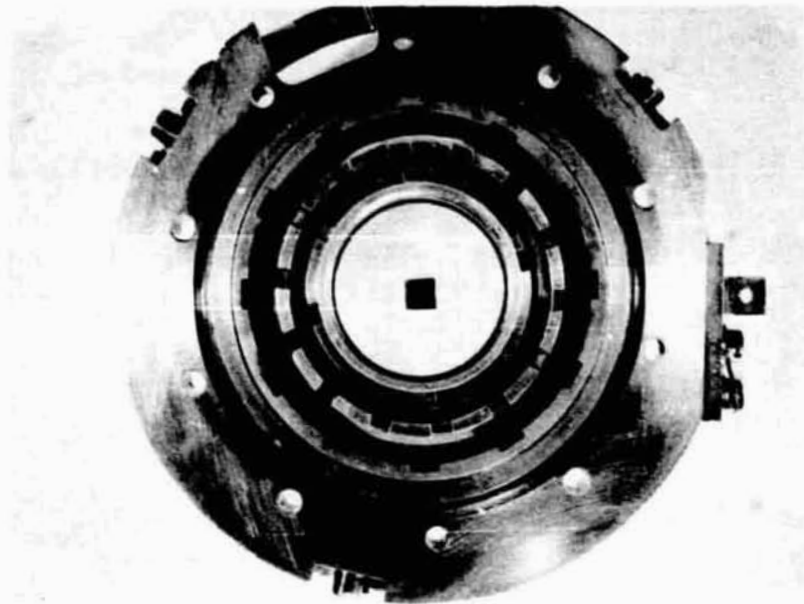
Figure 48.   Bearing Test 14.   Overall View of Bearing and
Housing Viewed from Direction of Test Oil Supply

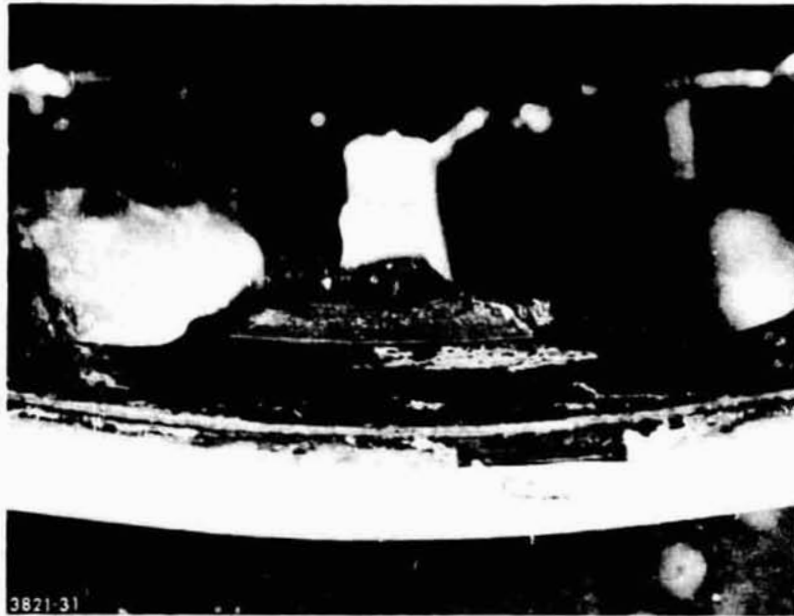Figure 49.   Test 14.   Composite View of Test Bearing

Figure 50.   Test 14.   Bearing Cage Land Riding Area Viewed
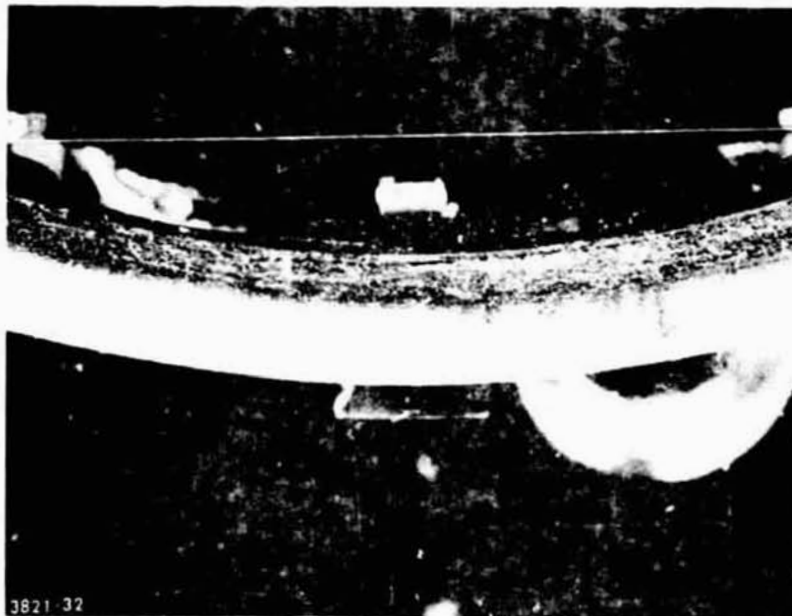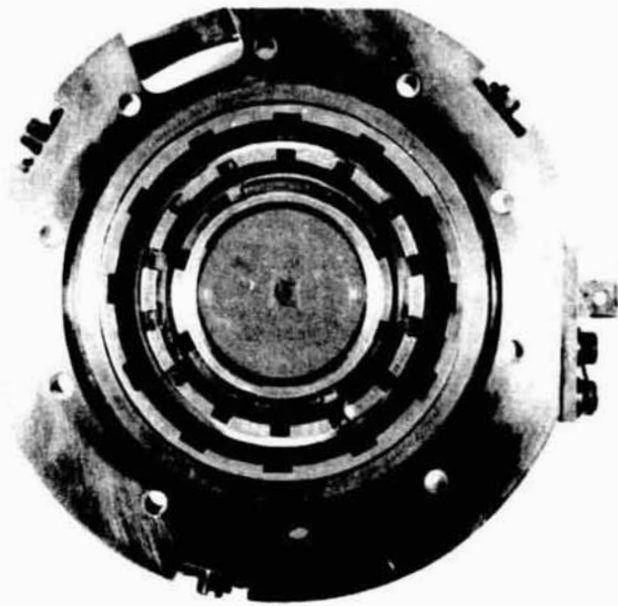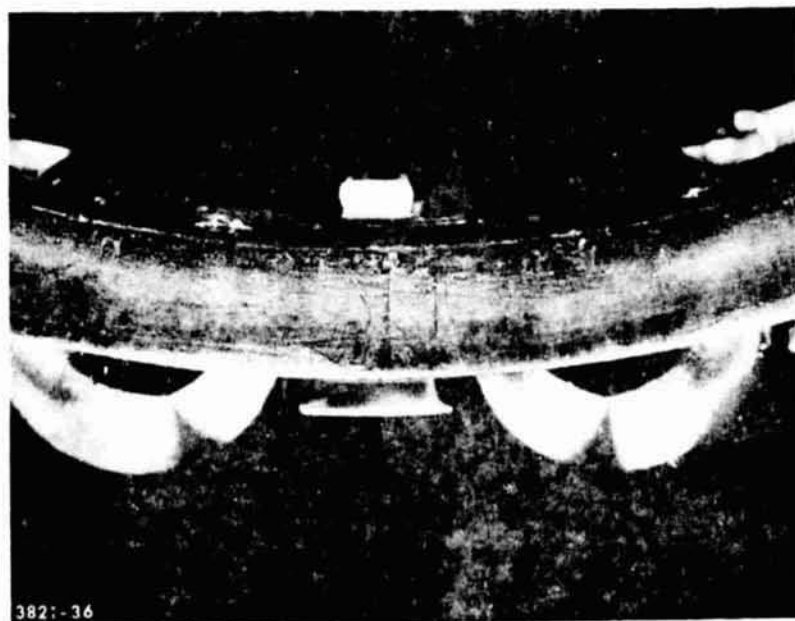from Direction of Test Oil Supply

Figure 51.   Test 14.   Bearing Cage Face Area
Viewed from Test Oil Outlet Area

TABLE 31. - VISUAL DESCRIPTION OF DEPOSITS AND WEAR: TEST 14

Bearing Support and Housing Deposits:

No deposits, light staining

Bearing Deposits and Wear:

Inner ring ball track -

Light staining

Inner ring outside ball track -

Light staining

Outer ring ball track -

Light staining

Outer ring outside ball track -

Light staining

Cage -

Silver peeled from the heavily worn land riding area;
light staining of the silver plating

110

TABLE 32. - LUBRICANT ANALYSES OF BEARING TEST NO. 14

Test lubricant: blend f_3 + $\sim$0.07% perfluoroglutaric acid

Sample number:	1
Time taken, hours:	0.2

Metal content, ppm:

Ni	5.2
Fe	65.3
Mg	<0.1
Cu	1.8
Ag	12.5
Cr	0.4
Aℓ	1.1
Si	67,800
Ti	0.4

Kinematic viscosity (centistokes) at 37.8°C (100°F)	18.74
TAN (mg KOH/g)	0.34
Gravimetric analysis (mg solid/ liter fluid)	406.0

111

Figure 52.   Bearing Test 15.   Overall View of Bearing and
Housing Viewed from Direction of Test Oil Supply

Figure 53.   Test 15.   Composite View of Test Bearing

Figure 54. Test 15. Bearing Cage Land Riding Area Viewed from Direction of Test Oil Supply

Figure 55. Test 15. Bearing Cage Face Area Viewed from Test Oil Outlet Area

113

TABLE 33. - VISUAL DESCRIPTION OF DEPOSITS AND WEAR: TEST 15

Bearing Support and Housing Deposits:

    No deposit, light staining

Bearing Deposits and Wear:

    Inner ring ball track -

        Light staining

    Inner ring outside ball track -

        Light staining

    Outer ring ball track -

        Light staining

    Outer ring outside ball track -

        Light staining

    Cage -

        Moderate to heavy wear of land riding area

TABLE 34. - LUBRICANT ANALYSES OF BEARING TEST NO. 15

Test lubricant: MCS 524 (QB-39)

Sample number:	1
Time taken, hours:	0.7

Metal content, ppm:

Ni	3.0
Fe	66.2
Mg	0.2
Cu	0.9
Ag	7.6
Cr	0.3
Al	0.5
Si	245.0
Ti	0.1

Kinematic viscosity (centistokes) at 37.8°C (100°F)	25.23
TAN (mg/KOH/g)	0.03
Gravimetric analysis (mg solid/ liter fluid)	208.0

oil (3.8 and 5.1 x 10^{-5} m respectively). However, the fluoro acid was not an effective additive with the low pour point fluid, blend f_3. The next best formulation was MCS 524 plus phenylphosphinic acid (Test 12) where the last two makeup fluid additions caused hotter bearing operation, presumably due to increasing frictional losses between the cage and inner ring. The wear depth in this run was 1.02 x 10^{-4} m. The largest wear depth (1.07 x 10^{-3} m) occurred with MCS 524 in Test 8 which ran 14 hours; this was nearly half the original cage thickness.

Some general conclusions and speculations about the tests include:

1) Rapid additive depletion from the test oils occurs with many but not all additives. However, there is no correlation between bearing life and additive depletion since the longest test runs all revealed rapid loss of additives from the fluid.

Test No.	Hours Run	Additive Left
10	47	<13% (A-88) at 16 hr
11	100	<12% at 19 hr
12	94	<12% at 0 hr

Obviously the loss of the additive is not always detrimental to performance. This can be rationalized in the case of perfluoroglutaric acid. This additive doubtless reacts at the bearing surface, and the equilibrium between the dissolved and adsorbed acid may well favor the adsorbed species.

$$\text{soluble acid} \; \underset{\longleftarrow}{\overset{\longrightarrow}{\qquad}} \; \text{acid on surface}$$
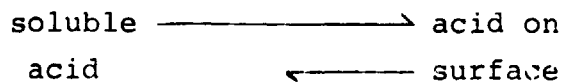
This would remove the acid from the fluid, but a subsequent low acid analysis would not mean total additive depletion or absence of an effective additive film on the bearing surfaces.

The rapid additive loss during successful runs may represent a chemical break-in of the bearing surfaces, i.e. a chemical reaction which accomplishes the equivalent of a mechanical break-in. Once this occurs, little further additive is needed in the system.

116

2) The two tests which did not have lubrication failures revealed a more or less linear fluid pickup of silver with time. This is shown graphically in Figure 56.

This must be finely suspended silver and may represent a beneficial corrosive loss of silver rather than a destructive wear loss. Alternatively, at least in Test 11, fine silver may have come from larger particles lost from areas of fluid impingement and then pulverized in the contact zones. Silver was the major metal present in solids centrifuged from the oils of bearing Tests 10 and 11.

3) The C-ether fluids withstood the bearing tests rather well in that viscosity increases and acid buildup were low. For example, after running 100 hours in Test 11, the fluid's viscosity increase was 80% and the acid number only 0.5.

4) Correlation of deposit formation with fluid stability is difficult because of the great variations in the duration of the various C-ether tests, Also, the wear failures may have produced deposits, particularly cage deposits. Bearing housing deposits tended to vary with running time except for Test 13 which had light varnish and sludge formation after 0.3 hour. The phenylphosphinic acid blend produced the greatest amount of deposits.

7.6 CORRELATION OF SLOW FOUR-BALL CURVES (CAGE METALLURGY) WITH BEARING PERFORMANCE

The main mode of lubrication failure with the C-ethers was loss of the cage silver with subsequent wear between the inner race and the cage. The screening test dealing directly with cage lubrication was the slow four-ball test. Qualitative correlations between this test and bearing performance are given on age 119.

Except for the last two fluids, the curves gave reasonable correlations with the bearing results. The Skylube 450 curve shows a surprisingly high μ considering that no lubrication failures occurred during four bearing tests. The blend containing the tetrasulfide and Emcol PS-236 may have failed due to too much EP action by the additives. A rapid chemical attack on the silver and/or iron may have peeled off chunks of metal and produced a large imbalance in the bearing.
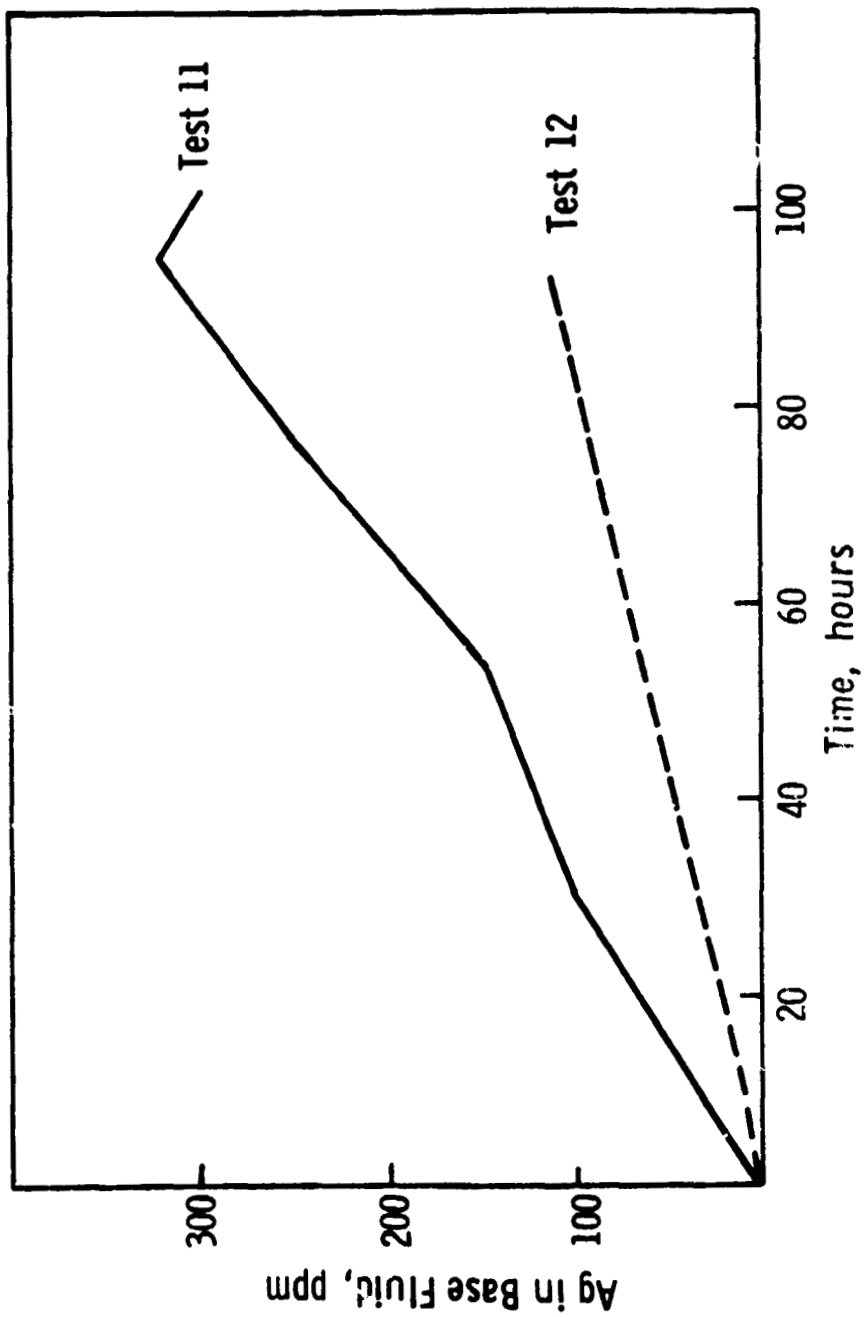
Figure 56.   Bearing Tests 11 and 12, Fluid Silver Content vs. Time

Bearing Test No.	Fluid	Appendix E Figure No.	Prediction	Observed
8	MCS 524	E-2	High μ;* trouble at high temp.	Loss of silver; cage-race wear; failure at 01 hr
9	MCS 524 + φSφPO$_2$H$_2$	E-9	μ lowering only above 360°C; beneficial reaction may not occur at a low enough temp. to prevent failure	Failure at 14 hr
10	MCS 524 + A-88 + trichloro-acetic acid	E-5	Improvement vs. MCS 524	Failure at 47 hr
11	MCS 524 + PFGA	E-6	Significant improvement vs. MCS 524	Ran 100 hr
12	MCS 524 + φPO$_2$H$_2$	E-7	Improvement vs. MCS 524; curve similar to Test #10; should run 50 to 100 hr	Ran 94 hr; failure due to bearing overheating; not wear
13	MCS 524 + tetra-sulfide + Emcol PS-236	E-16	Very large μ lowering; should run well	Failure at 1/2 hr
1,2,3 &7	Skylube 450	E-1	μ jump above 206°; may have problems	No lubrication failures

*Coefficient of friction in slow 4-ball test.

A major unanswered question is why the blend of MCS 524 plus perfluoroglutaric acid ran 100 hours while the same acid in blend f₃ ran only 0.3 hour. The slow four-ball curves of these fluids on the cage metallurgy as well as on M50/M50 are very similar. (These plots are compared directly in Figure E-22 of Appendix E and Figure D-24 of Appendix D.) Moreover, the fluoro acid produces similar changes in the slow four-ball curves of both base stocks. On the cage metallurgy, both MCS 524 and blend f_3 are converted from oils giving a more or less constantly rising friction coefficient to blends with a friction minimum around 290°C. (See Figures E-6 and E-21 of Appendix E.) On M50/M50, the acid generates a friction coefficient rise in both base stocks from about 150°C to 316°C, then a sharp lowering of the coefficient occurs (Figures D-6 and D-23 of Appendix D). Nevertheless, the bearing performance was very different. In theory the fluoro acid could be used up by reacting with the disiloxane molecules of blend f_3. However, 85% of the acid was in the recovered fluid after bearing Test 14, so this was probably not the cause of the test failure. Possible reasons for the short run include:

1) There may be a minimum or critical viscosity below which the additive will not function.

2) Variations in humidity may have affected the bearing test results. Humidity has a profound effect on wear by aliphatic oils (ref. 22). It has also been shown to alter the lubrication of a C-ether base stock containing perfluoroglutaric acid (ref. 16). This blend showed lower wear at low temperatures and higher wear at high temperatures (above 200°C) in moist air as compared to a dry air atmosphere. An air drier in the test head supposedly kept the humidity low (<20%) and constant during all the tests.

3) The silver corrosion of blend f_3 plus perfluoroglutaric acid is about twelve times greater in the presence of copper than in the absence of copper. The data from the 260°C oxidation-corrosion test are as follows:

	Silver Loss, mg/cm²	
	With Copper	Without Copper
Blend f_3 + PFGA	-2.4	-0.2
MCS 524 + PFGA	-0.6	—

120

This may have been important if the test fluid came in contact with the copper flashing layer beneath the silver.

8. HYDRAULIC FLUID EVALUATION

Two pump tests on different C-ether blends were planned on a contractor selected high temperature pump. Projected operating conditions were:

Pump discharge pressure	=	2.07×10^7 N/m^2 (3000 psig)
Outlet flow rate	=	3.16×10^{-4} m^3/sec (5 gal/min)
Hottest system temperature	=	260°C (500°F)
Test duration	=	100 hours

Pump and fluid performance were to be recorded during the runs.

The chosen pump, a Vickers PV3-044 aircraft pump, is described in Appendix L. A summary of a qualification run using a hydrocarbon oil at 260°C is in Appendix M.

8.1   PUMP TEST RESULTS AND DISCUSSION

8.1.1   Test No. 1

After the one hour qualification test with MLO 072-34 at 260°C (Appendix M), the pump was disassembled and found to be within dimensional specifications. The pump was then photographed before assembly for the start of the first C-ether pump test. Photographs of the critical components of the pump are shown in Figures 57 through 66.

The test stand components were individually washed and rinsed in hexane and air dried. The pump was reassembled with MCS 524 base fluid. Nearly five gallons of MCS 524 + 0.1% A-88 + 0.05% trichloroacetic acid blend was filtered through a one-micron membrane filter, and the test fluid was flushed and drained through the pump and test stand at low temperature. Approximately 15.5 kg of fluid was charged to the test stand and the test was started under a nitrogen atmosphere. The pump characteristics obtained at 260°C (500°F) are shown in Table 35.

During 30 minutes of operation at an outlet pressure of 2.07×10^7 N/m^2 (3000 psig) and with the main flow at 2.52×10^{-4} m^3/sec (4 gal/min), the case flow increased from 6.31×10^{-5} m^3/sec (1 gal/min) to 9.48×10^{-5} m^3/sec (1.5 gal/min). At this time a fine mist was leaking from the porting surface between the valve porting plate and the pump case. Suddenly a full spray emerged and the test was shut down.
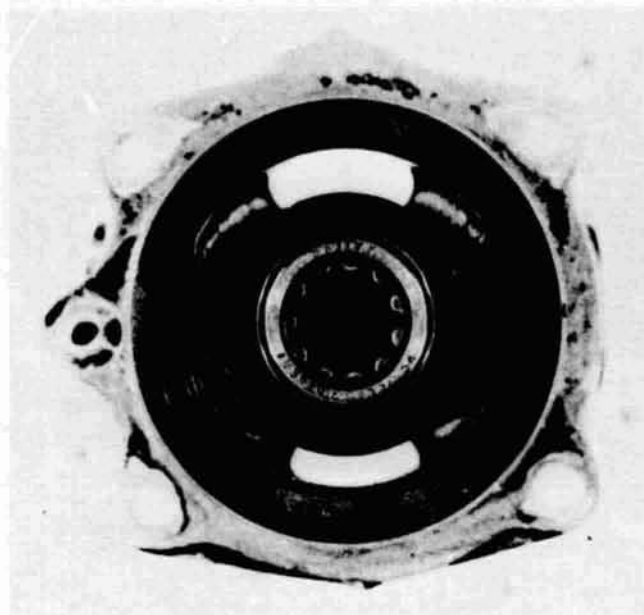
Figure 57. Valve Plate, Vickers PV3-044 Pump
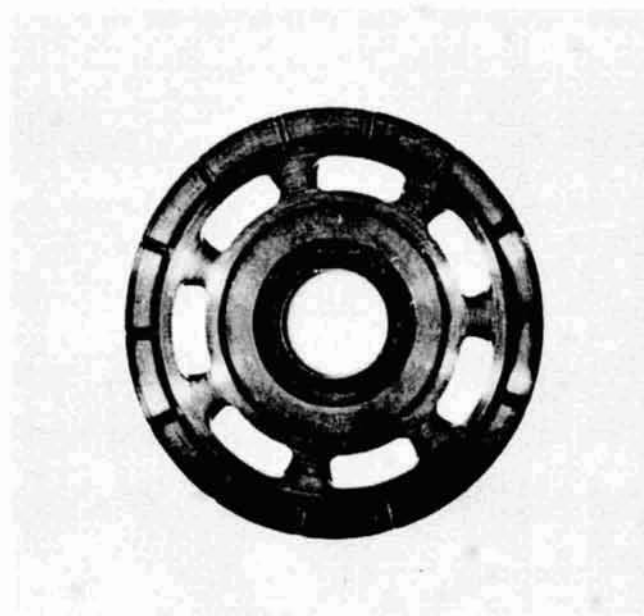
Figure 58. Cylinder Block, Vickers PV3-044 Pump
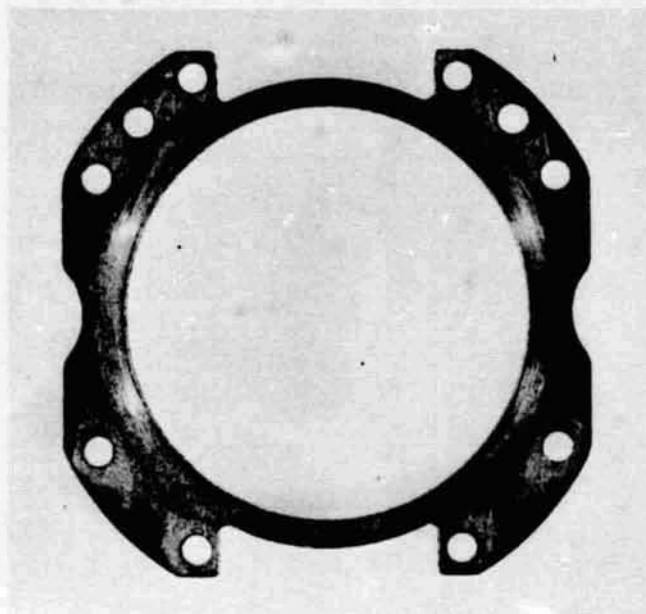
Figure 59. Shoe Hold-Down Plate Retainer,
Vickers PV3-044 Pump
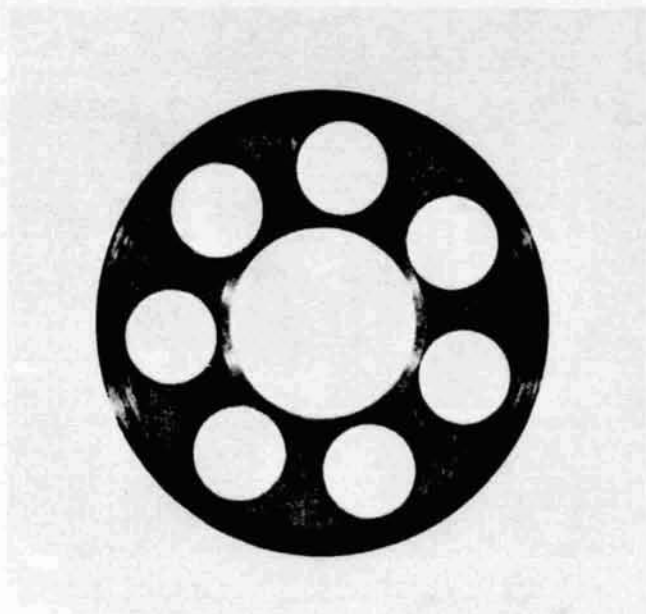
Figure 60. Shoe Hold-Down Plate, Vickers PV3-044 Pump

Figure 61. Piston and Shoe Assembly in Hold-Down Plate, Vickers PV3-044 Pump
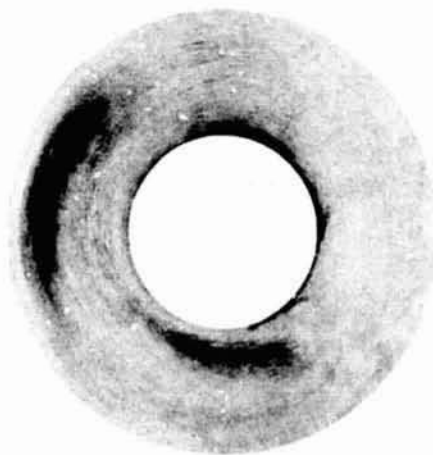
Figure 62. Shoe Wear Plate, Vickers PV3-044 Pump

Figure 63.   Carbon Seal and Mating Ring, Vickers PV3-044 Pump
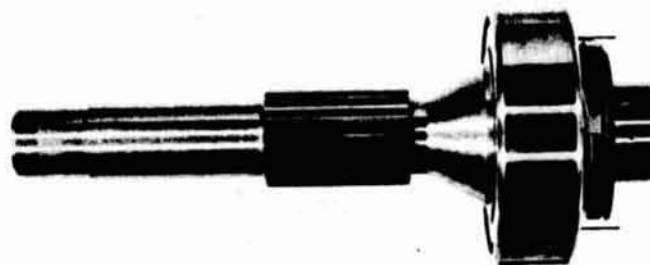
Figure 64.   Drive Shaft and Bearing, Vickers PV3-044 Pump

Figure 65. Pump Housing, Vickers PV3-044 Pump
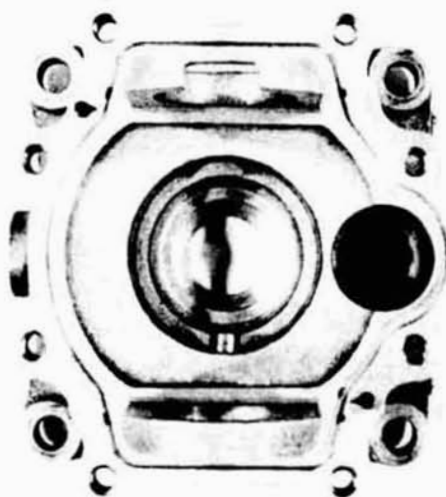
Figure 66. Mounting Flange, Vickers PV3-044 Pump

TABLE 35. - HIGH TEMPERATURE PV3-044 PUMP CHARACTERISTICS AT START
OF MCS 524 + 0.1% A-88 + 0.05% TRICHLOROACETIC ACID
PUMP TEST AT PUMP TEMPERATURE OF 260°C

Pump compensation pressure = 2.07 x 10^7 N/m^2 (3000 psi)

Pump Outlet Pressure		Main Flow		Case Flow	
N/m^2 x 10^7	psig	m^3/sec x 10^4	gpm	m^3/sec x 10^4	gpm
1.03	1500	3.6	5.7	0.47	0.75
1.38	2000	3.5	5.5	0.57	0.90
1.72	2500	3.3	5.25	0.66	1.05
1.93	2800	3.2	5.1	0.73	1.15
2.00	2900	3.2	5.0	0.79	1.26
2.07	3000	3.0	4.7	0.88	1.40
2.10	3050	0	0	1.1	1.73

Examination of the pump revealed the mounting bolts P/N 16 to be loose. Replacing "O" rings P/N 30 and 31, tightening the screws, and restarting the test produced a similar failure. Further investigation showed the failure to be caused by coiled thread inserts pulling out of the aluminum housing. These inserts were replaced with solid steel inserts which distribute the bolt stresses along the entire length of the screw. The cylinder block visually had what appeared to be wear (see Figure 67) and was replapped and polished to the condition seen in Figure 68. The total test time was 0.9 hour at this point.

The test was restarted, at which time the test fluid was noted to have a hazy appearance. Table 36 shows the pump characteristics that were obtained with the pump outlet pressure at 2.07×10^7 N/m^2 (3000 psig) and fluid temperature at 260°C (500°F).

During the test, the case drain flow continually increased at a uniform rate for 1.25 hr, at which time it exceeded the maximum chart reading of 1.58×10^4 m^3/sec (2.5 gpm). At 1 hr the main flow was manually reduced to maintain 2.07×10^7 N/m^2 (3000 psi) pressure. When the main flow had been reduced to 0.95×10^4 m^3/sec (1.5 gpm) the test was halted at 3.0 total test hours.

The after-test photographs of the pump parts are in Figures 69 through 82. The areas of most surface distress are the cylinder block and piston shoe which are presented in Figures 81 and 82. The cause of the high case leakage can be seen on the cylinder block. The area between the piston ports had a deposit which had been wiped on causing the cylinder block to become separated from the valve plate. Gross leakage then occurred readily outward and inward of the piston ports. Note that the areas radial from the piston ports are clean due to the washing by the leakage flow and short flow path. The area between the piston ports collects deposit since there is little net flow to the pump case, causing fluid containing the insoluble material to be wiped on the area by shearing motion. As deposits form, this area becomes a more efficient filter due to the close clearance between the deposit and valve plate. The piston shoe shows evidence of cavitation erosion possibly augmented by deposits which cause separation from the wear plate followed by localized erosion channels where the deposit washes out.

No signs of excessive wear were found on the pump. Other deposits were found on the tungsten carbide wearing surfaces of the valve plate. Deposits caused the cylinder block bores to decrease 60 microinches and the piston diameters to "grow" 40 microinches; these growths are visibly evident by the marks left on the cylinder barrel base by the base gauge plowing through the deposit.
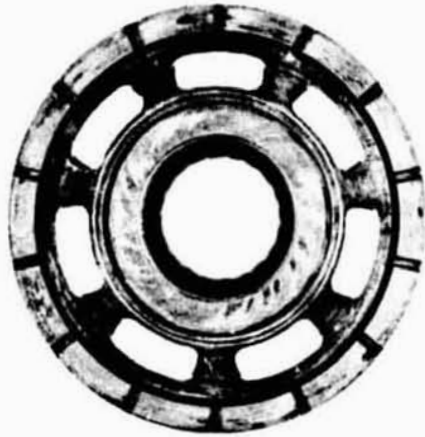
Figure 67. Worn Cylinder Block, Pump Test 1
(P/N 45 of Fig. L-1)

Figure 68. Resurfaced Cylinder Block, Pump Test 1
(P/N 45 of Fig. L-1)

TABLE 36. - HIGH TEMPERATURE PV3-044 PUMP CHARACTERISTICS AT 1 HR OF THE MCS 524 + 0.1% A-88 + 0.05% TRICHLOROACETIC ACID PUMP TEST

Pump compensation pressure = 2.07×10^7 N/m^2 (3000 psi)

Pump Outlet Pressure		Main Flow		Case Flow	
N/m^2 x 10^7	psig	m^3/sec x 10^4	gpm	m^3/sec x 10^4	gpm
1.03	1500	3.2	5.1	0.80	1.27
1.38	2000	3.1	4.9	0.95	1.50
1.72	2500	2.9	4.6	1.1	1.70
1.93	2800	2.8	4.4	1.2	1.88
2.00	2900	2.7	4.3	1.23	1.95
2.07	3000	2.6	4.1	1.3	2.10
2.10	3040	0.32	0.5	1.5	2.37
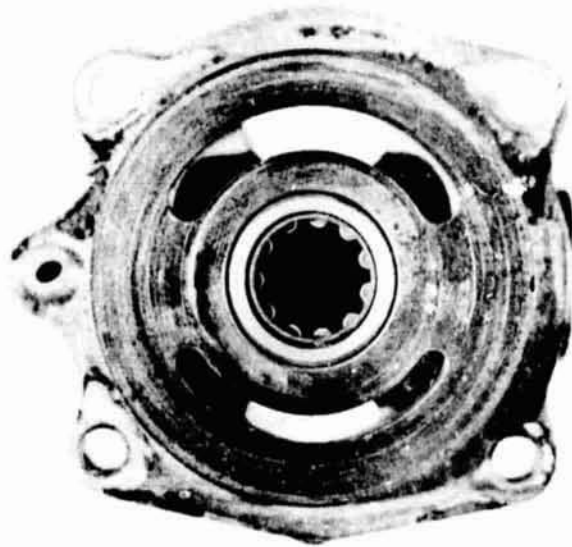
Figure 69.   Valve Plate, Pump Test 1 (P/N 28 of Fig. L-1)
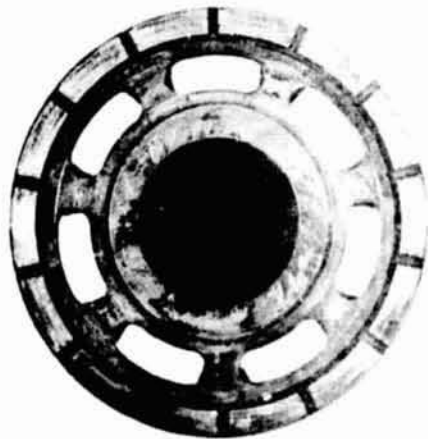
Figure 70.   Cylinder Block, Pump Test 1
(P/N 45 of Fig. L-1)
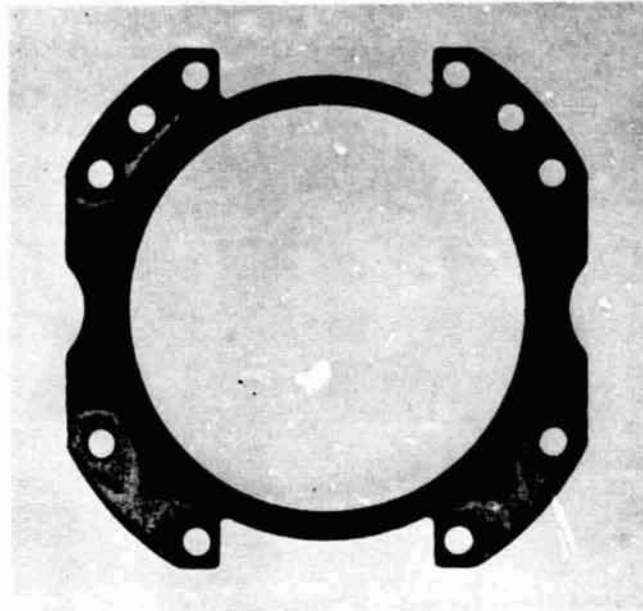
Figure 71.   Shoe Hold-Down Plate Retainer, Pump Test 1
(P/N 47 of Fig. L-1)
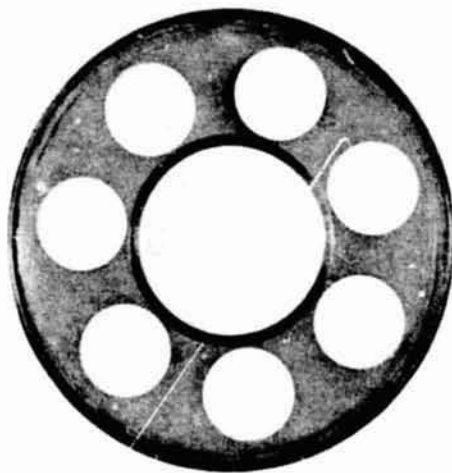
Figure 72.   Shoe Hold-Down Plate, Pump Test 1
(P/N 50 of Fig. L-1)
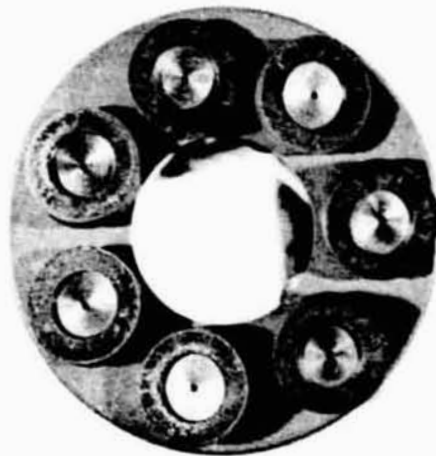
Figure 73.   Piston and Shoe Assembly in Hold-Down Plate,
Pump Test 1 (P/N 46 of Fig. L-1)

Figure 74.   Shoe Wear Plate, Pump Test 1
(P/N 51 of Fig. L-1)
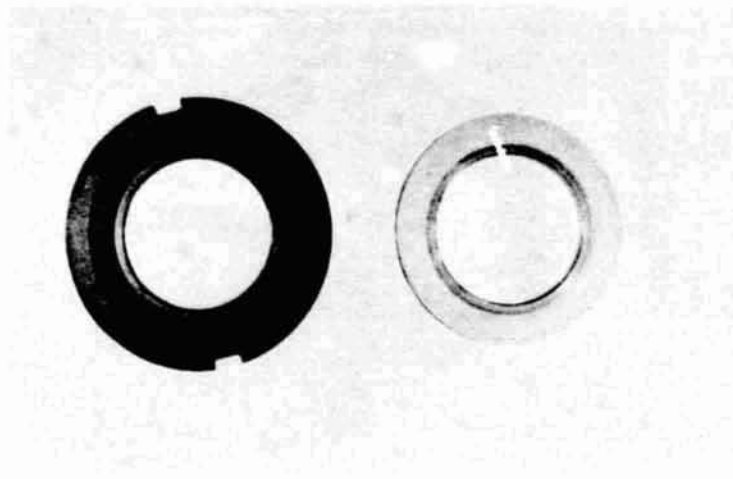
Figure 75.   Carbon Seal and Mating Ring, Pump Test 1
             (P/N 59 and 71 of Fig. L-1)
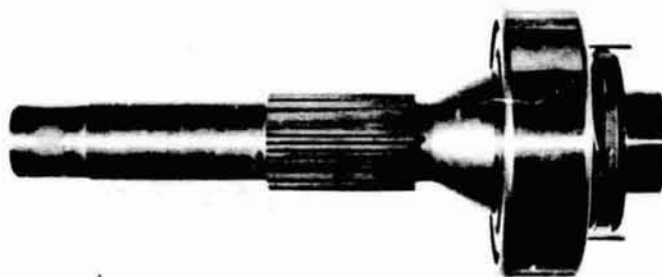
Figure 76.   Drive Shaft and Bearing, Pump Test 1
             (P/N 67 and 65 of Fig. L-1)
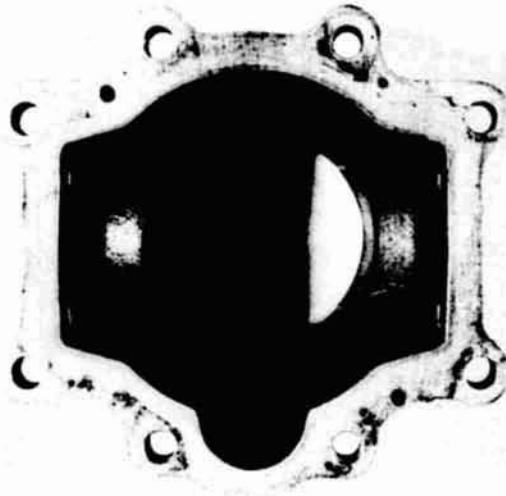
Figure 77.   Pump Housing, Pump Test 1
(P/N 39 of Fig. L-1)
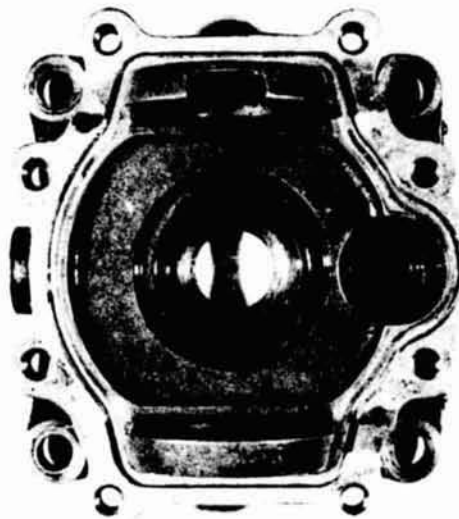
Figure 78.   Pump Mounting Flange, Pump Test 1
(P/N 79 of Fig. L-1)
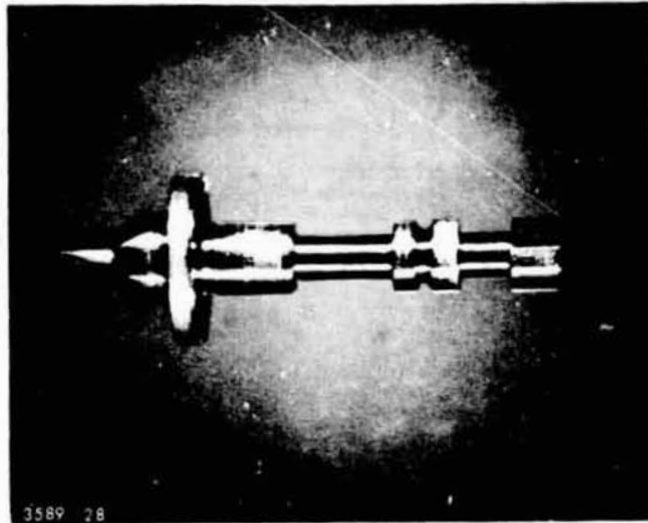
X12

Figure 79. Pilot or Compensator Valve, Pump Test 1
(P/N 27 of Fig. L-1)
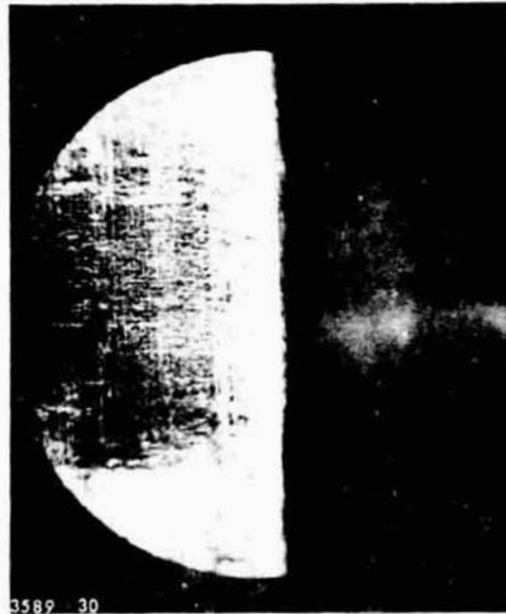
X100

Left - Supply to Control Pressure Orifice Edge
Right - Control to Return Orifice Edge

Figure 80. Compensator Valve Spool, Pump Test 1
(P/N 27 of Fig. L-1)

137

X12

Figure 81. Cylinder Barrel Deposit, Pump Test 1

X6

Figure 82. Piston Shoe Erosion, Pump Test 1

138

The fluid when filtered through a one micron filter was clarified, thus indicating that the insoluble material had grown from submicron size or was formed during the high temperature pump operation. The flush fluid was clear when drained. The fluid insoluble can be removed by centrifugation but the amount of centrifugate is very small. Infrared analysis of this dark oil showed the presence of a phosphorus acid, either a phosphinic or phosphonic acid. This type of compound was not present in the starting fluid.

The deposits were scraped from the tin bronze surface of the cylinder block and the tungsten carbide piston shoe wear plate. X-ray fluorescence of the deposits showed:

	Elements Present		
Deposit Source	Major	Minor	Trace
cylinder block	Cu	Cr, Rh	Fe, Co
wear plate	Cu	Co, Cr Fe, Rh	Sn

Copper and tin elements are most likely from the cylinder barrels while cobalt and rhodium are present in the sintered tungsten carbide as binders.

Infrared analysis detected little organic character for the cylinder block deposit and gave strong indication of silica. A micro-wet chemical analysis confirmed the deposit to be silica. Examination under an optical microscope showed the deposits to be very small particles which were mostly transparent and isotropic.

The possible sources of silica contamination are:

(1) silica treatment and process contamination of C-ether base fluid or additives

(2) contamination of pump test stand

The first source is most likely since the flush fluid was clear and no similar test stand contamination has been seen on other pump tests using similar cleaning procedures. Silica gel treatment was used on the MCS 524 base fluid and submicron particles would escape process filtration.

8.1.2   Test No. 2

Fluid for pump test No. 2 (blend f_3 plus $\sim 0.07\%$ PFGA): blend f_3 was heated to 71°C and 10 ppm antifoam was added with paddle stirring. Agitation continued for 2-3/4 hours at 71-74°C.

The resulting blend was reasonably clear showing incomplete addition of the antifoam. Dry PFGA (0.1%) was added at room temperature. Following 12 hours of stirring at 44°C, the temperature was then raised to 60°C over 9-3/4 hours. Four days later the blend was given a 1 μ Millipore filtration. The nylon filter (NRWG 14250) quickly plugged and stuck to the filter holder. After replacement, the rate of filtration became very slow but gradually increased. The fluid was refiltered through a 1 μ Millipore nylon filter. Antifoam (10 ppm) was then added using Dispersator stirring. Two fluorine analyses on this product averaged 270 ppm fluorine or 0.057% PFGA.

It was felt that the tin bronze surfaces might be too reactive at 260°C, so it was decided to plate the cylinder barrel, piston shoes and shoe retainer plate with silvered S-Monel. The test was started with the f_3 blend + ∿0.07% perfluoroglutaric acid and lasted two hours before failure. During the calibration measurements taken when the case drain temperature reached 260°C (500°F), sharp cracking noises emanated from the pump. After two hours the case drain flow was excessive and the main flow and out pressure could not be maintained.

Examination of the pump (Figures 83 through 92) indicated that the plating head flaked from the cylinder barrel (Figure 86). This opened a flow passage to case drain. There was smearing of the silver plating on the port cap (Figure 84). There was partial flaking from the retainer plate and piston shoes (Figures 87 and 89). Fluorine analysis of the used fluid indicated no additive depletion (270 ppm fluorine new to 269 ppm used,* i.e. 0.06% acid).

Consultation with the plating source revealed a good possibility that the parts were not cleaned before plating, causing poor ⌐dherence.

8.1.3   Test No. 3

Fluid preparation (blend f_3 + ∿0.07% PFGA): the fluid from pump test No. 2 was filtered through Whatman #1 paper and used directly in the next pump test. The residue was a small amount of foreign matter and an even smaller amount of fine particles. Two fluorine analyses of the filtrate showed 253 and 284 ppm of fluorine. A third analysis gave a value of 375 ppm.

The pump parts were thoroughly cleaned to improve adhesion and replated with silvered S-Monel. Scratching of reference coupons indicated acceptable plating. Test No. 2 was repeated and ran 9.5 hours before another high case drain leakage failure.

---

*An average of two analyses; a third analysis showed 375 ppm fluorine or 0.08% acid.

140

Figure 83.   Port Cap, Pump Test 2 (Note heavy, smeared
plating from cylinder barrel)

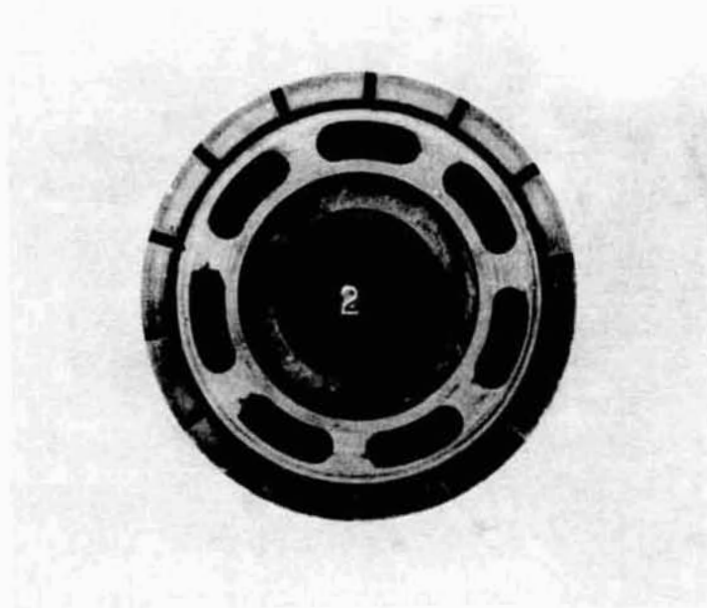Figure 84.   Close-Up of Smeared Port Cap Area, Pump Test 2

Figure 85.   Cylinder Block, Pump Test 2

Figure 86.   Cylinder Block Kidney Ports, Pump Test 2 ($\sim$6X)
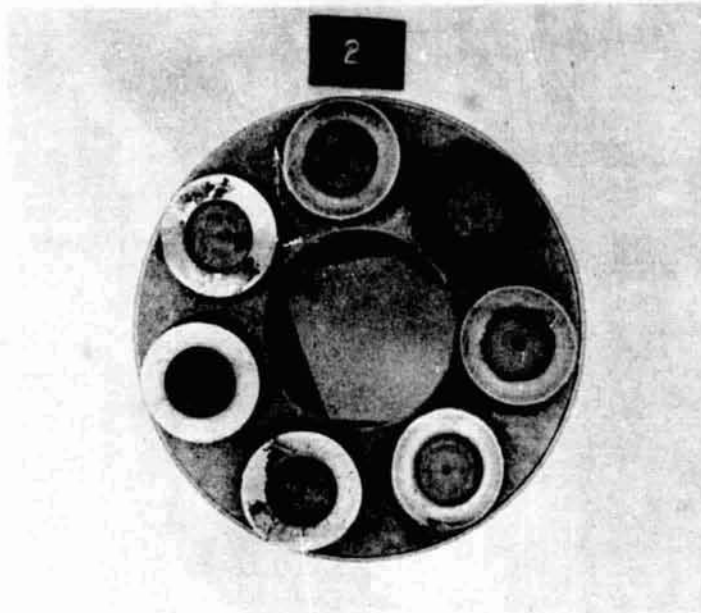(9:00 Position in Fig. 85)

142

Figure 87. Shoe Retainer Plate and Shoes, Pump Test 2
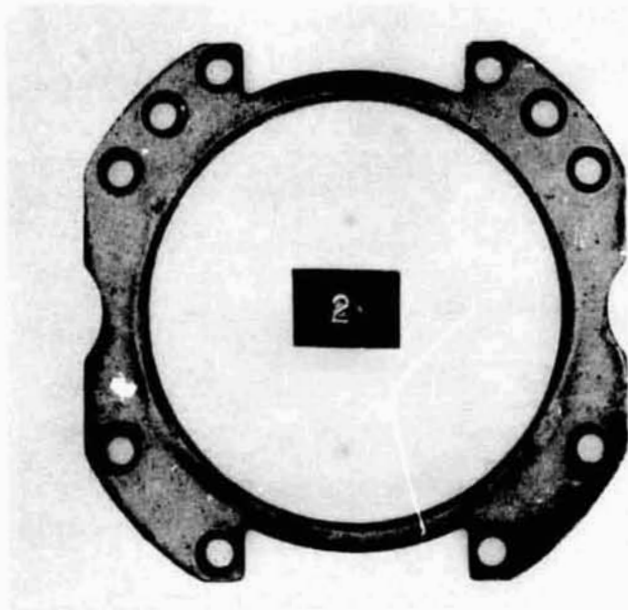

Figure 88. Wear Plate, Pump Test 2

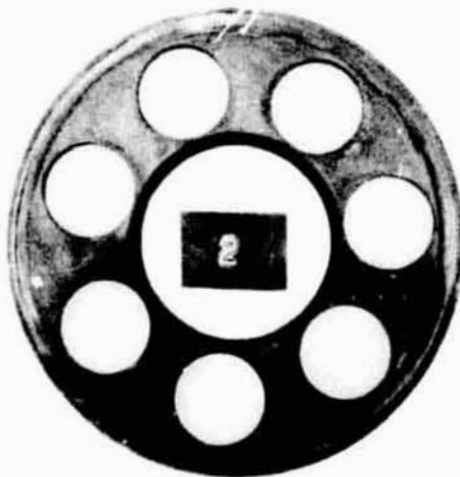143

Figure 89.   Shoe Hold-Down Plate Retainer, Pump Test 2
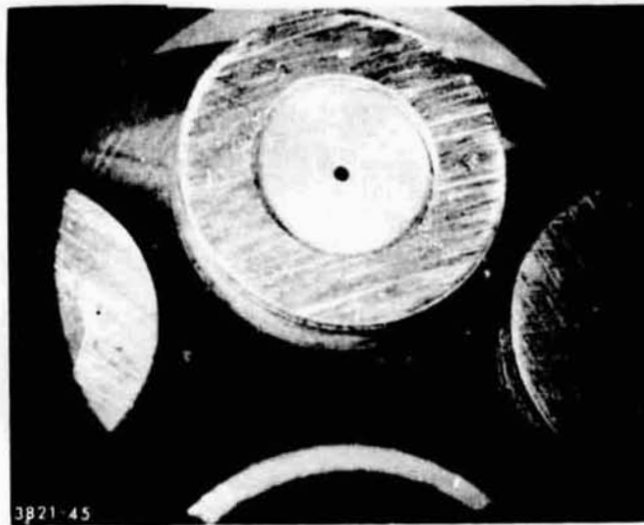

Figure 90.   Shoe Hold-Down Plate, Top Side, Pump Test 2

Figure 91. Pre-Test 2 Shoe Condition (Note chips)

Figure 92. Typical Piston Shoe After Test 2 ($\sim$3X)

145

As seen in Figures 93 through 100, the plating and some of the tin bronze were removed by erosion from the piston shoes and cylinder barrel; this opened the hydrostatic passages, producing loss of flow efficiency. The fluid condition showed no viscosity change and a slight reduction in total acid number (from 0.31 mg KOH g^{-1} to 0.24 mg KOH g^{-1}). Major elements in the filter residues were Ag, Ni, Cu, Fe and S (XRF analysis). Final titre of fluorine on the used oil was 379 ppm (0.08% acid).

8.1.4 Test No. 4

Fluid for pump test No. 4 (blend f_3 + ~0.07% PFGA): the recovered oil from pump test No. 3 (379 ppm fluorine) was given a 1 μ Millipore filtration. No filter plugging occurred.

All the silvered S-Monel plating was removed by lapping and another f_3 blend + PFGA test was started with a quick case flow leakage failure. It was discovered that lapping of the valve porting plate had removed some of the cobalt binder leaving some large tungsten carbide particles protruding from the surface. This caused gross machine wear of the cylinder barrel bronze plating. Fluorine analysis indicated a slight reduction in perfluoroglutaric acid from 0.08% to 0.05%. Major metals in the filtered solids were Sn, Ag and Cu.

Test photographs appear in Figures 101 to 106.

146
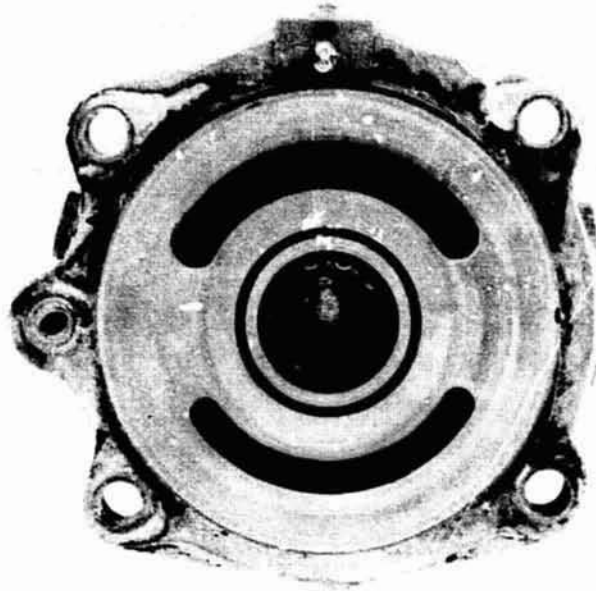
Figure 93. Port Cap, Pump Test 3
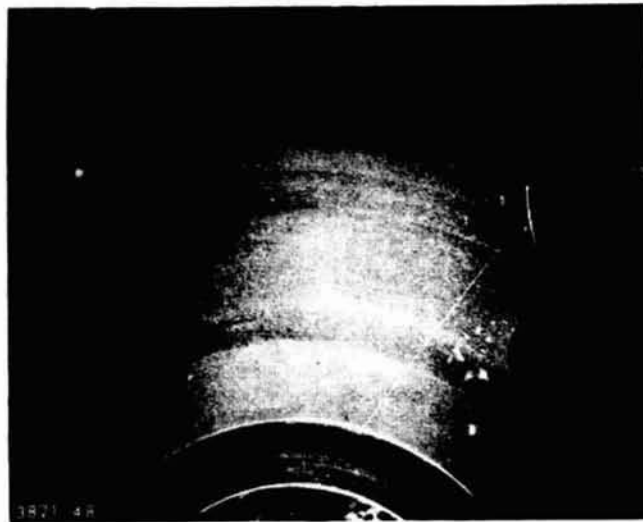
Figure 94. Port Cap, Pump Test 3 (9:00 Position
in Fig. 93) (∿3X)

147

Figure 95.   Cylinder Block, Pump Test 3 (Note leak
             paths, plating, smearing and removal)

Figure 96.   Cylinder Block, Pump Test 3
             (7:00 in Fig. 95) (∿3X)
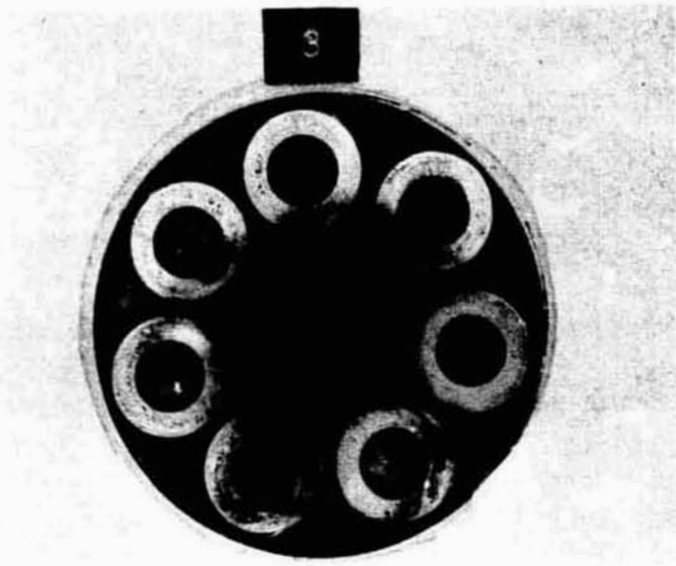
Figure 97.   Shoe Retainer Plate and Shoes, Pump Test 3
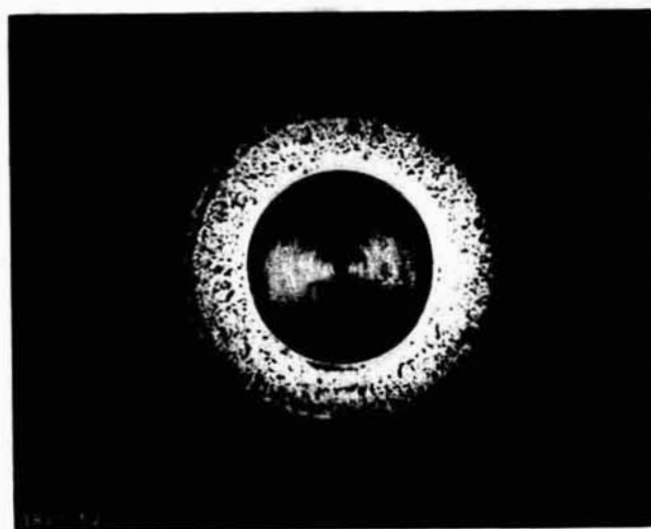
Figure 98.   Typical Shoe from Pump Test 3
Showing Erosion ($\sim$3X)
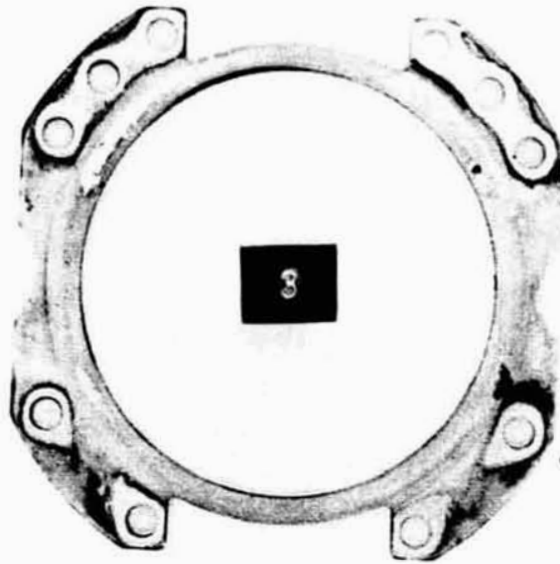
Figure 99.   Shoe Hold-Down Plate Retainer, Pump Test 3

Figure 100.   Shoe Hold-Down Plate Retainer, Pump Test 3
(2:00 in Fig. 99) (∿3X)
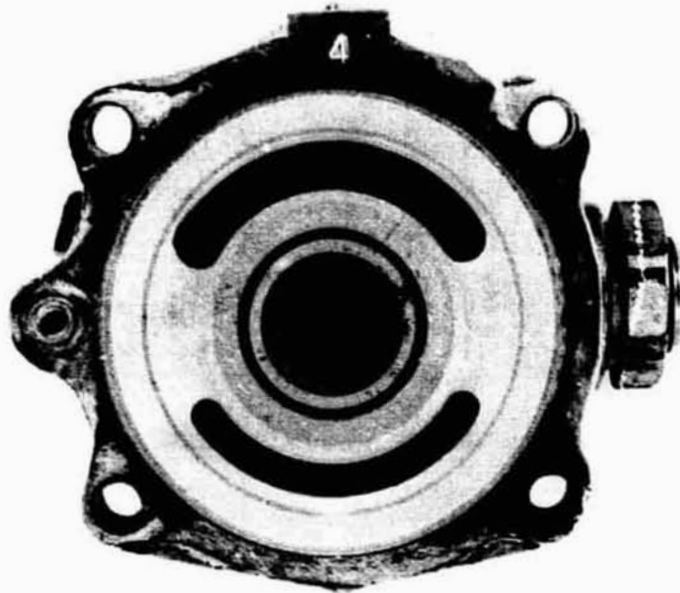
Figure 101. Port Cap, Pump Test 4 (Note flakes of bronze)
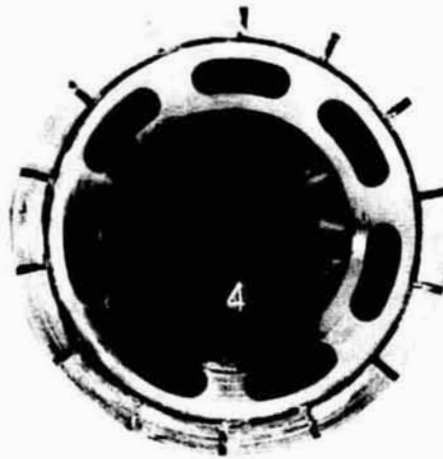
.gure 102. Cylinder Block, Pump Test 4
(Note wear, smearing)
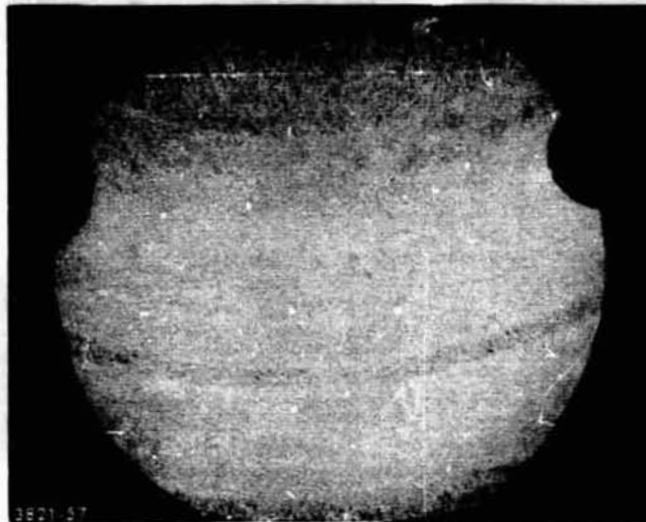
Figure 103. Port Cap, Pump Test 4 (9:00 in Fig. 101) (~3X)
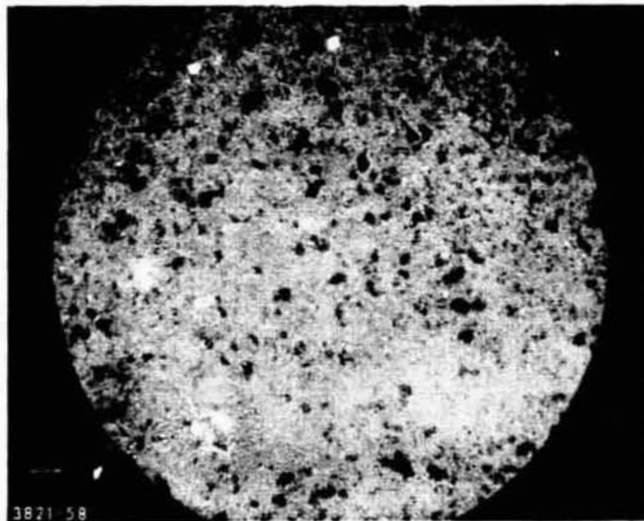
Figure 104. Port Cap Inner Non-Riding Area, Pump Test 4
(12:00 in Fig. 103) (~25X)
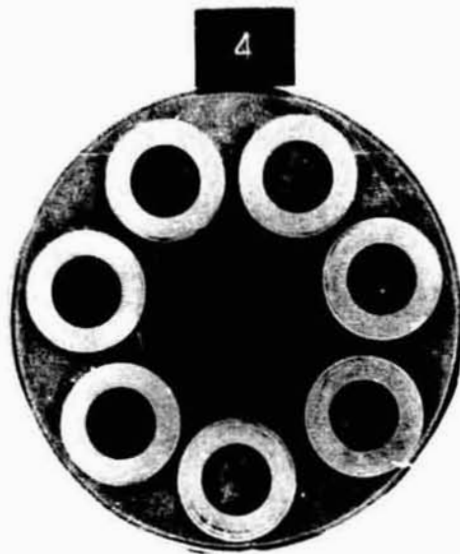
Figure 105.   Shoe Retainer Plate and Shoes,
Pump Test 4 (Light wear)
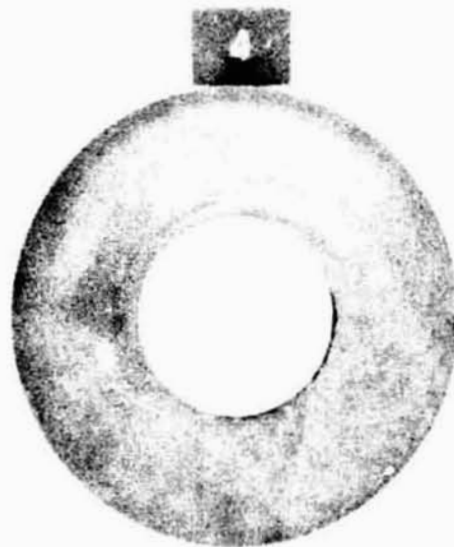
Figure 106.   Wear Plate, Pump Test 4

APPENDIX A: SYNTHESIS OF ADDITIVES

It was of interest to see if increasing the molecular weight of an acid additive would improve lubrication; hence the task of preparing the following additives:

A. m-Phenylmercaptophenylphosphinic acid was made by a proprietary method starting with 3-bromodiphenyl sulfide. The conversions ranged from 40 to 10%. The product was an oil which did not crystallize. Nuclear magnetic resonance and carbon-hydrogen analysis confirmed the structure. Typical results were:

Anal: Calculated for $C_{12}H_{11}O_2PS$: C, 57.6; H, 4.4

Found: C, 57.5; H, 4.3

Peaks for P-H, P-OH, and aryl hydrogens were found in the nuclear magnetic resonance spectrum. The observed versus the theoretical areas were:

	Observed	Theory
P-H	0.83	1.0
P-OH	1.1	1.0
aryl H	9.1	9.0

B. m-(m-Phenylmercaptophenylmercapto)phenylphosphinic acid was made by a proprietary method in a very low conversion (∼3%).

Anal: Calculated for $C_{18}H_{15}O_2PS_2$: C, 60.3; H, 4.2

Found: C, 60.5; H, 4.4

The NMR spectrum was consistent with the proposed structure.

	Observed Area	Theoretical Area
P-H	0.80	1
P-OH	0.87	1
aryl H	13	13

The NMR detected a small amount of an unknown impurity containing a P-CH₃ group. The level of this impurity was probably around 5%.

APPENDIX B: LAB SCALE SYNTHESES FOR LOW POUR POINT FLUIDS

A. **3-Trimethylsilyldiphenyl sulfide** was made by condensing the Grignard reagent of 3-chlorodiphenyl sulfide with trimethyl-chlorosilane:
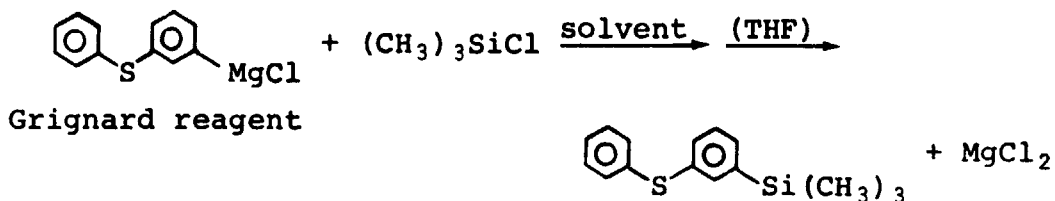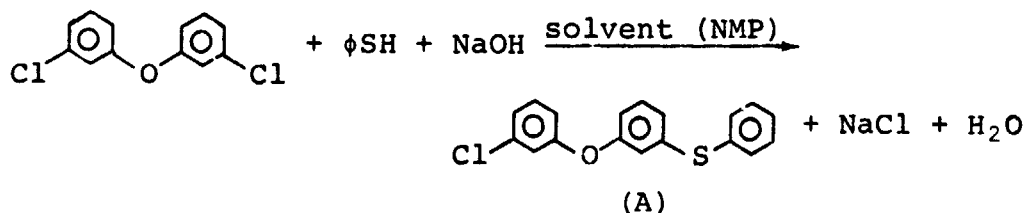

Grignard reagent

Trimethylchlorosilane (114 g, 1.05 moles) in 50 ml of tetra-hydrofuran was added dropwise under nitrogen to the Grignard reagent of 3-chlorodiphenyl sulfide (made from 0.97 mole of the halide) in tetrahydrofuran. After three hours at 70°C, the reaction was cooled, hydrolyzed with about 30 ml of water, acidified with 30 g of ammonium chloride in 270 ml of water and then with about 5 g of ammonium chloride in 50 ml of water. After filtration, the organic layer and two benzene extracts of the aqueous layer were combined and dried briefly over sodium sulfate. Vacuum distillation gave 105.5 g (41%) of the desired product (b.p. 124°C/0.6).

Anal. Calculated for $C_{15}H_{18}SSi$: C, 69.7; H, 7.0

Found: C, 71.2; H, 7.2

GLC analysis showed 98.9% purity. No attempt was made to improve the rather low conversion.

B. **3-Trimethylsilyl-3'-phenylmercaptodiphenyl ether** was made in two steps:

1. Condensation of 3,3'-dichlorodiphenyl ether with thiophenol to give 3-chloro-3'phenylmercaptodiphenyl ether (A):

(A)

2. Reaction of the Grignard reagent of (A) with trimethyl-chlorosilane to give the corresponding trimethylsilyl compound (B):

PRECEDING PAGE BLANK NOT FILMED

+ (CH$_3$)$_3$SiCl $\xrightarrow{\text{solvent}}$ (THF)

(B)

+ MgCl$_2$
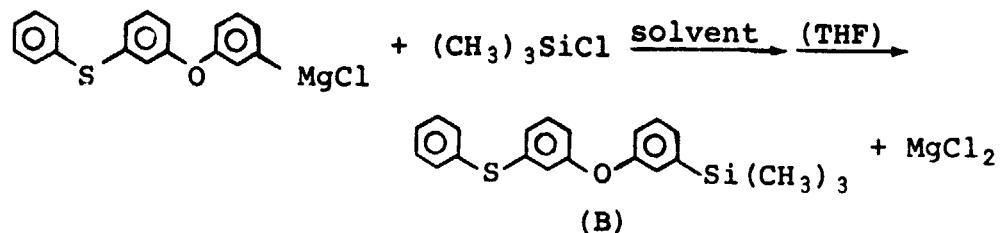
3-Chloro-3'-phenylmercaptodiphenyl ether (A). Sodium thio-phenate was prepared from benzenethiol (125 g, 1.13 moles) and sodium hydroxide (46.7 g, 1.13 moles of 97% pellets) in N-methylpyrrolidone (300 ml). Water was distilled from the pot through a small column until the pot temperature was 226°C and the vapor temperature 170°C. 3,3'-Dichlorodiphenyl ether (382 g, 1.6 moles) was charged at 170°C and stirring continued overnight at 193°C, then at 210°C for one hour. The reaction was quenched with 300 ml of 2% lye at 70°C. The organic layer was combined with a 200 ml benzene extract of the aqueous layer, washed with 250 ml of water, stripped of benzene and vacuum distilled. This gave 234.8 g (66%) of the desired chloroether (b.p. 195.5-6°C/0.7). GLC showed a purity of 99.5%.

3-Trimethylsilyl-3'-phenylmercaptodiphenyl ether (B). Tri-methylchlorosilane (81.5 g, 0.75 mole) in 50 ml of THF was added dropwise under nitrogen to the Grignard reagent of 3-chloro-3'-phenylmercaptodiphenyl ether. (The Grignard was made from 233.5 g or 0.747 mole of halide and was in about 550 ml of tetrahydrofuran.) After this addition and one hour of reflux, the solids in the pot were so thick that stirring was ineffective. More THF (200 ml) was added and reflux con-tinued overnight. The reaction was hydrolyzed with water (35 ml) and acidified with 5% HCl (200 ml). The usual work-up gave 156.3 g (60%) of the desired ether (b.p. 189.5-195°C/0.5). GLC showed a purity of 99.0%.

Anal. Calculated for C$_{21}$H$_{22}$OSSi: C, 71.9; H, 6.3

Found: C, 72.4; H, 6.1

C. (m-Phenylmercaptophenyl)dimethylchlorosilane. This compound is an intermediate in the synthesis of the 3- and 4-ring sulfur disiloxanes. Two methods were used to prepare it:

1. Addition of the Grignard reagent of 3-chlorodiphenyl sulfide to dimethyldichlorosilane:

+ Cl$_2$Si(CH$_3$)$_2$ $\longrightarrow$ + MgCl

158
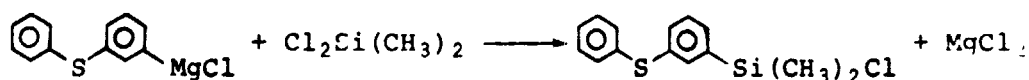
This procedure gave typical conversions of 45 to 54%.

The Grignard solution (from 1.36 moles of halide) was added under nitrogen to 452 g (3.5 moles) of dichlorodimethylsilane in 150 ml of xylene. This addition ($\sim$3 hours) was done with occasional cooling which kept the temperature below 35°C and was followed by four hours of stirring.

The reaction mixture was filtered twice and THF and unreacted chlorosilane stripped to a pot temperature of 160°C. After another filtration, xylene was stripped under water aspirator pressure to a pot temperature of 155°C. The residue was vacuum distilled through a five inch packed column, giving 204 g (54%) of the desired chlorosilane (b.p. 135-145°C/0.5-0.3).

2. In situ reaction of the Grignard reagent of 3-chlorodiphenyl sulfide and dimethyldichlorosilane:
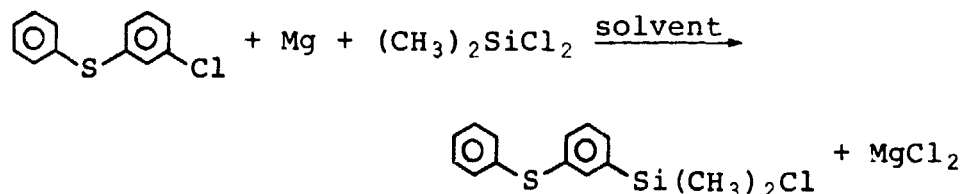
Magnesium metal (40 g), dimethyldichlorosilane (17 g) and tetrahydrofuran (THF) were heated to 40°C under a nitrogen blanket. To this mixture was added, over seven hours, a solution of 3-chlorodiphenyl sulfide (300 g), dimethyldichlorosilane (576 g) and 110 ml of THF. After stirring at about 50°C for 14 hours and refluxing at 78°C for one hour, the reaction was cooled and filtered. Unreacted solvent and silane were stripped to a pot temperature of 105°C. After another filtration, the filtrate was vacuum distilled to give 137 g (37%) of the chlorosilane (b.p. 142-4°C/0.3).

D. 1,3-Bis(m-phenylmercaptophenyl)tetramethyldisiloxane was made by hydrolysis of (m-phenylmercaptophenyl)dimethylchlorosilane:
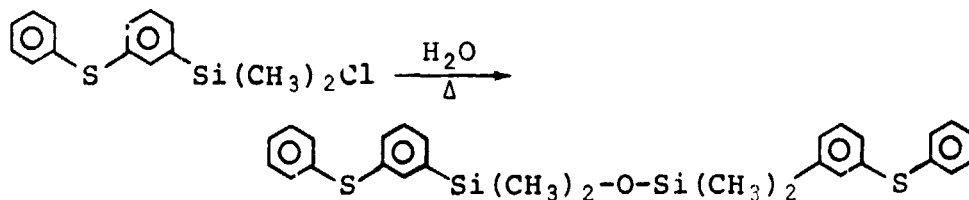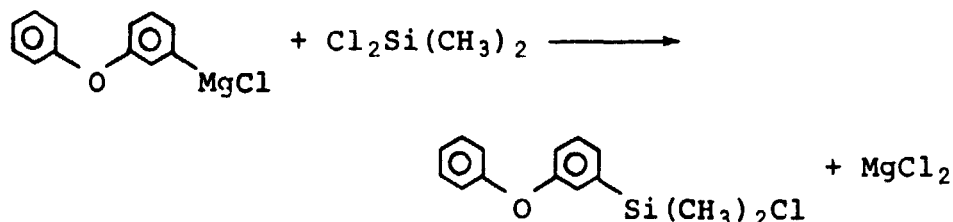

(m-Phenylmercaptophenyl)dimethylchlorosilane (203.6 g) was added to 310 ml of water and 338 ml of ether. After four hours of reflux, distillation of the dried organic layer gave 187 g of crude disiloxane (b.p. 155-265°C/$\sim$0.6). Ammonia gas

159

was bubbled through a well stirred solution of the crude product in water (364 ml) and ether (728 ml) for 15 minutes. Distillation after toluene-azeotrope drying gave 160 g (87%) of the tetramethyldisiloxane (b.p. 252°C/0.6).

Anal. Calculated for $C_{28}H_{30}OS_2Si_2$: C, 66.9; H, 6.0

Found: C, 67.0; H, 6.1

Typical GLC purity was 99%.

E. (m-Phenoxyphenyl)dimethlychlorosilane. This compound is an intermediate in the synthesis of the 4-ring oxy disiloxane. A Grignard reaction was used in making this silane:

The procedure was similar to that used for (m-phenylmercaptophenyl)dimethylchlorosilane [prep. C(1) above]. Less excess dimethyldichlorosilane was used; the ratio of dimethyldichlorosilane to starting 3-chlorodiphenyl ether was 1.75:1.5. This gave a 45% conversion to the desired chlorosilane (b.p. 123-8°C/0.4). The reported boiling point is 105°C/0.03 (Monsanto proprietary data).

F. 1,3-Bis(m-phenoxyphenyl)tetramethyldisiloxane was made by hydrolysis of m-phenoxyphenyldimethylchlorosilane:
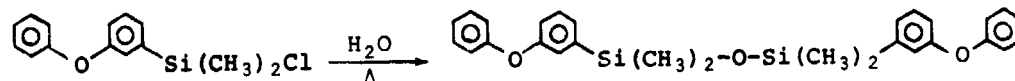
The previously described hydrolysis procedure (prep. D) gave a 77% conversion of halosilane to tetramethyldisiloxane (b.p. 216°C/0.4). The reported boiling point is 206°C/0.03 (Monsanto proprietary data).

G. Phenyldimethylchlorosilane. This compound is an intermediate used to make the 3-ring sulfur disiloxane and also 1,3-bis-(phenyl)tetramethyldisiloxane. It was made by reacting phenyl magnesium chloride and dimethyldichlorosilane:

160

Phenyl magnesium chloride (506 ml of 2.47N Grignard, Fisher
P402, 1.25 moles) was added to dimethyldichlorosilane (416 g,
3.2 moles) in 138 ml of benzene. After overnight stirring,
the reaction was filtered twice and benzene, THF, and un-
reacted silane were stripped to 160°C. After another fil-
tration, vacuum distillation gave 108.9 g (51% conversion) of
phenyldimethylchlorosilane (b.p. 66°C/5.2). Literature boil-
ing points are 197°C/766 (ref. 23) and 97-100°C/33 (ref. 24.)

H. 1,3-Bis(phenyl)tetramethyldisiloxane and 1-(m-Phenylmercapto-
    phenyl)-3-phenyltetramethyldisiloxane were made by co-hydrol-
    ysis of phenyldimethylchlorosilane and (m-phenylmercapto-
    phenyl)dimethylchlorosilane:
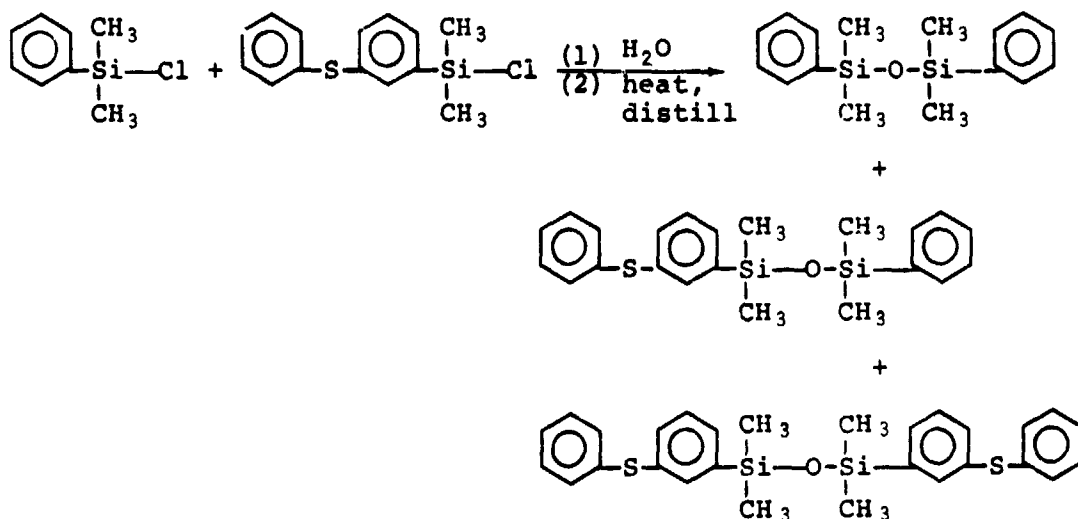
(m-Phenylmercaptophenyl)dimethylchlorosilane (85 g, 0.305 mole)
and phenyldimethylchlorosilane (52.1 g, 0.305 mole) were mixed
and added to 209 ml of water and 261 ml of ether. After four
hours of reflux, vacuum distillation of the dried organic
layer gave 17.4 g of 1,3-bis-(phenyl)tetramethyldisiloxane
(b.p. 104°C/0.35). The literature boiling point is 110°C/1
(ref. 23).

GLC showed a purity of 99.0%.

Further distillation produced 46.6 g of the 3-ring sulfur
disiloxane (b.p. 175°C/0.35). GLC showed a purity of 99.1%.

    Anal. Calculated for $C_{22}H_{26}OSSi_2$: C, 67.0; H, 6.6
                              Found: C, 67.2; H, 6.7

# APPENDIX C: INTERMEDIATES FOR SIX GALLONS OF BLEND f$_3$

The large scale syntheses below gave enough intermediates to make six gallons of blend f$_3$ for rig tests.

A. 3,3'-Bis(phenylmercapto)diphenyl ether was made by reacting sodium thiophenate and 3,3'-dichlorodiphenyl ether:
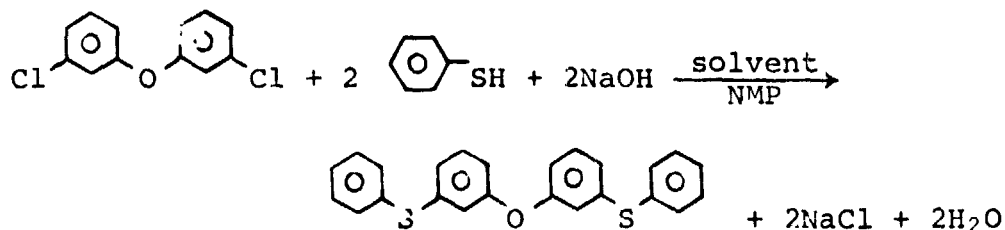
Thiophenol (2.49 kg, 22.6 moles), N-methylpyrrolidone (4.76 kg) and sodium hydroxide (0.907 kg, 22.2 moles of 98% pellets) were charged to a 22 liter round bottom fla. joined to a short Vigreux column and take-off head. Water, NMP and some water insoluble material were stripped from the system until the pot temperature was 215°C and the vapor temperature 186°C. After cooling to 160°C, 3,3'-dichlorodiphenyl ether (2.46 kg, 10.3 moles) was charged in roughly half pound portions. After four and one half hours and at pot temperature of 210°C, some material (100 to 200 ml) had boiled into a receiver below the take-off head. This may have been due to an exotherm. The reaction was stirred overnight as it cooled to 180°C, heated to 198°C for a few hours, and then quenched at 100°C with 4.1 kg of ~1% lye. The organic layer plus a toluene extract of the aqueous layer were washed with about four liters of water. Water was azeotroped from the organic layer; vacuum distillation gave 2.86 kg (71% conversion) of the desired ether (b.p. 261-5°C/0.8). GLC showed a purity above 99.5%. After filtration from a little hazy matter, this material was used directly in making blend f$_3$.

B. Phenyldimethylchlorosilane (see method G of Appendix B). The previously described reaction of phenyl Grignard and dimethyldichlorosilane gave 3.45 kg of phenyldimethylchlorosilane (b.p. 71-3°C/11-12). This was a 51% conversion based on the 39.5 equivalents of Grignard used.

C. (m-Phenylmercaptophenyl)dimethylchlorosilane. The first approach was the addition of the Grignard of 3-chlorodiphenyl sulfide to dimethyldichlorosilane [method C(1) of Appendix B]:

$$\phi S\phi Cl + Mg \longrightarrow \phi S\phi MgCl$$
$$\phi S\phi MgCl + (CH_3)_2 SiCl_2 \longrightarrow \phi S\phi Si(CH_3)_2 Cl$$

163
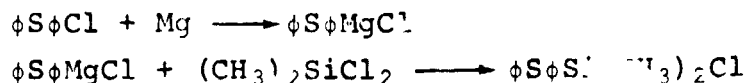
Four large scale runs using 21.8 moles of aryl halide gave the following conversions:

| Run	%
I	6
II	0
III	33
IV	30

Normal lab conversions were 45-54%. The low conversions of runs I and II were due to condensations of various silicon chlorides catalyzed by magnesium chloride. Greater care in filtering this salt gave the improved conversions of runs III and IV.

Next, the Grignard and dimethyldichlorosilane were reacted in situ [method C(2) of Appendix B]. Conversions from four large scale runs using 6 to 9 kg of aryl halide were:

R	%
V	25
VI	44
VII	8
VIII	low

The low conversions of VII and VIII were probably caused by an inhibiting coating formed on the surface of the magnesium. Runs III, IV, V and VI together with redistillation of various intermediate cuts, filter washes, and residues gave about 16 kg of the desired chlorosilane. Purity ranged from 82 to 95%. The main impurity was 3-chlorodiphenyl sulfide; this did not interfere with the subsequent hydrolysis of the chlorosilane.

D. 1-(m-Phenylmercaptophenyl)-3-phenyltetramethyldisiloxane and 1,3-Bis(m-phenylmercaptophenyl)tetramethyldisiloxane were made by co-hydrolysis of phenyldimethylchlorosilane and (m-phenylmercaptophenyl)dimethylchlorosilane (method H of Appendix B). For the large scale preps, the mole ratio of the starting chlorosilanes was adjusted to give a product with 3.1 times the weight of 4-ring as of 3-ring disiloxane. That was a molar ratio of 0.83 to 0.17 (2-ring chlorosilane to 1-ring chlorosilane). Thus, a typical reaction mixture (added to water and ether over ∿1/2 hour) was:

$$\phi S\phi Si(CH_3)_2Cl: \quad 6014 \text{ g}$$

$$\phi Si(CH_3)_2Cl: \quad 75' \text{ g}$$
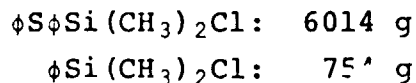
Vacuum topping of the crude product lowered the amount of 1,3-bis(phenyl)tetramethyldisiloxane and unreacted 3-chlorodiphenyl sulfide to below 1.5%. The residue contained around 94% of the two disiloxanes. Several such residues were used to make blend f_3 after filtration through Super Filtrol (grade #1) to remove a little foreign matter which formed on standing. GLC analysis of the filtered residues showed:

low boilers:	1.2%
3-ring sulfur disiloxane:	21.6%
	0.1%
	1.1%
	0.2%
4-ring sulfur disiloxane:	72.0%
high boilers:	2.7%
	0.7%
	0.3%
	0.1%

The properties of blend f_3 made from the topped disiloxanes (prior to Filtrol treatment) compared very well with lab samples made from distilled disiloxanes.

	"Distilled" f_3	"Topped" f_3
Visc. at -18°C (0°F), cs:	2860	3193
at 38°C (100°F), cs:	18.75	18.64
Pour point (cold box):	-39°C (-39°F)	-41°C (-41°F)
Oxidation-corrosion test (260°C);		
visc. change at 38°C (100°F)		
with copper:	87%	96%
without copper:	4%	1/2%
copper loss, mg/cm^2:	-3.6	-4.4
silver loss, mg/cm^2:	-3.3	-4.3
deposits:	none	none

There is a slightly higher copper and silver corrosion with the topped blend f_3.

APPENDIX D:

SLOW FOUR-BALL COEFFICIENT OF FRICTION

VS. TEMPERATURE CURVES, M50 ON M50
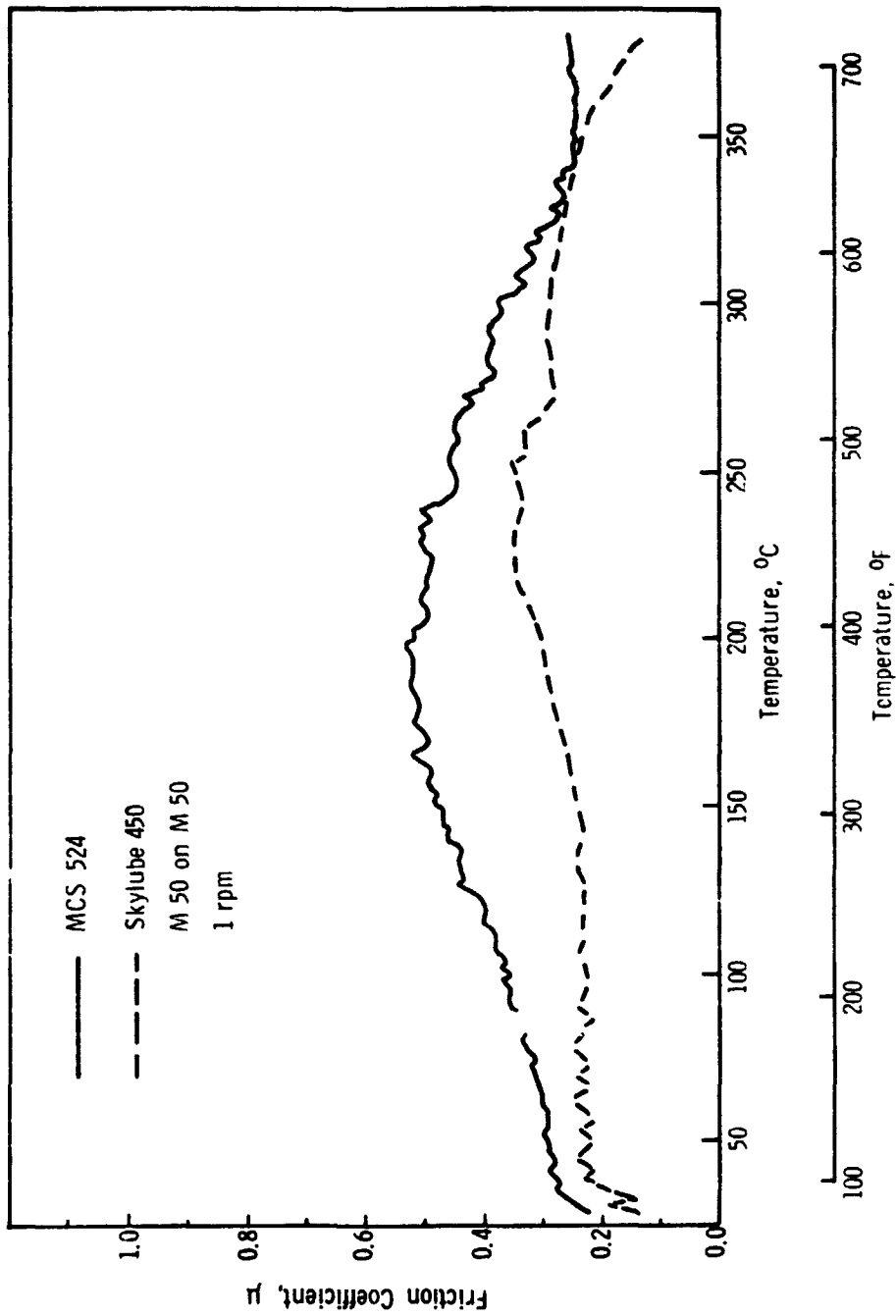
Figure D-1. Friction Curves for MCS 524 and Skylube 450

168
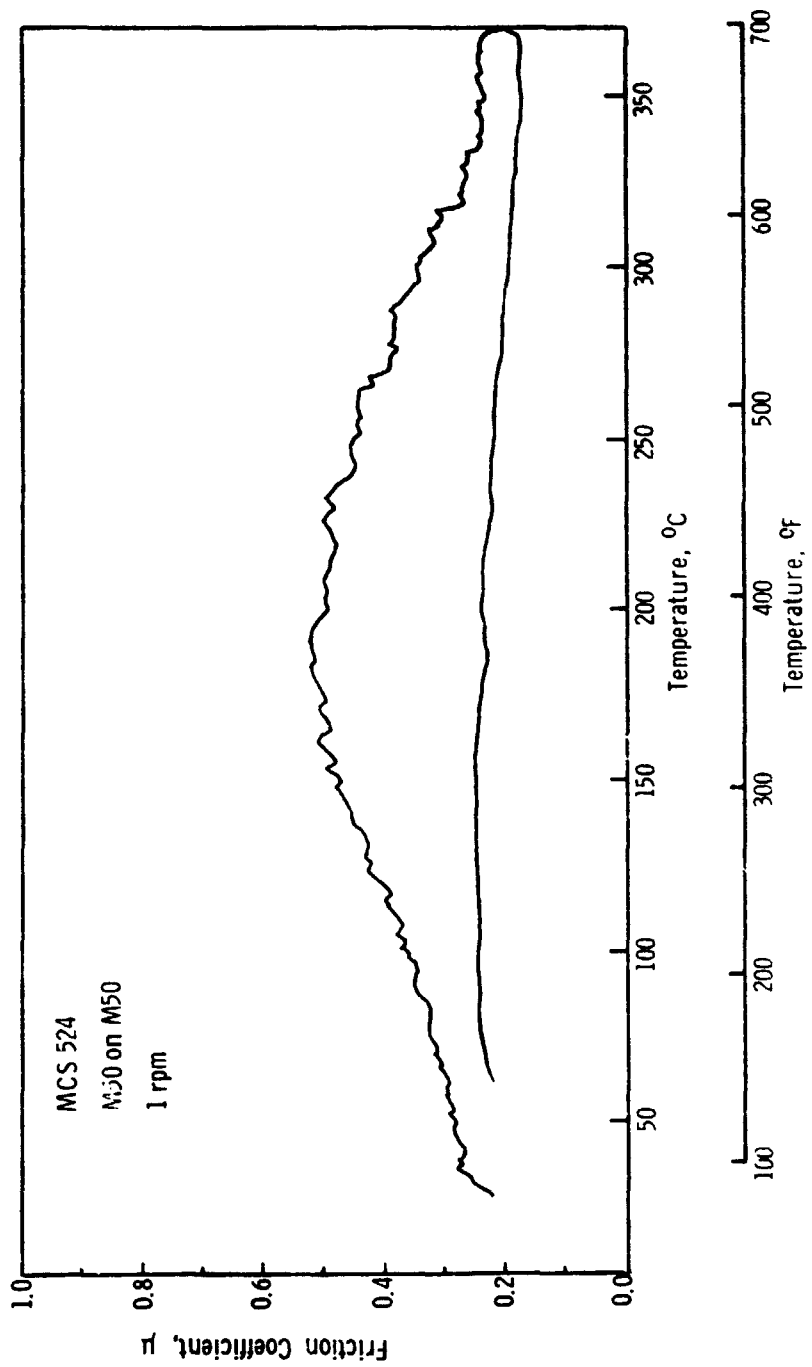
Figure D-2. Friction Curve for MCS 524

The figure shows a plot with:
- Y-axis: Friction Coefficient, μ (from 0.0 to 1.0)
- X-axis (top): Temperature, °C (50 to 350)
- X-axis (bottom): Temperature, °F (100 to 700)

Labels on the plot:
MCS 524
M50 on M50
1 rpm
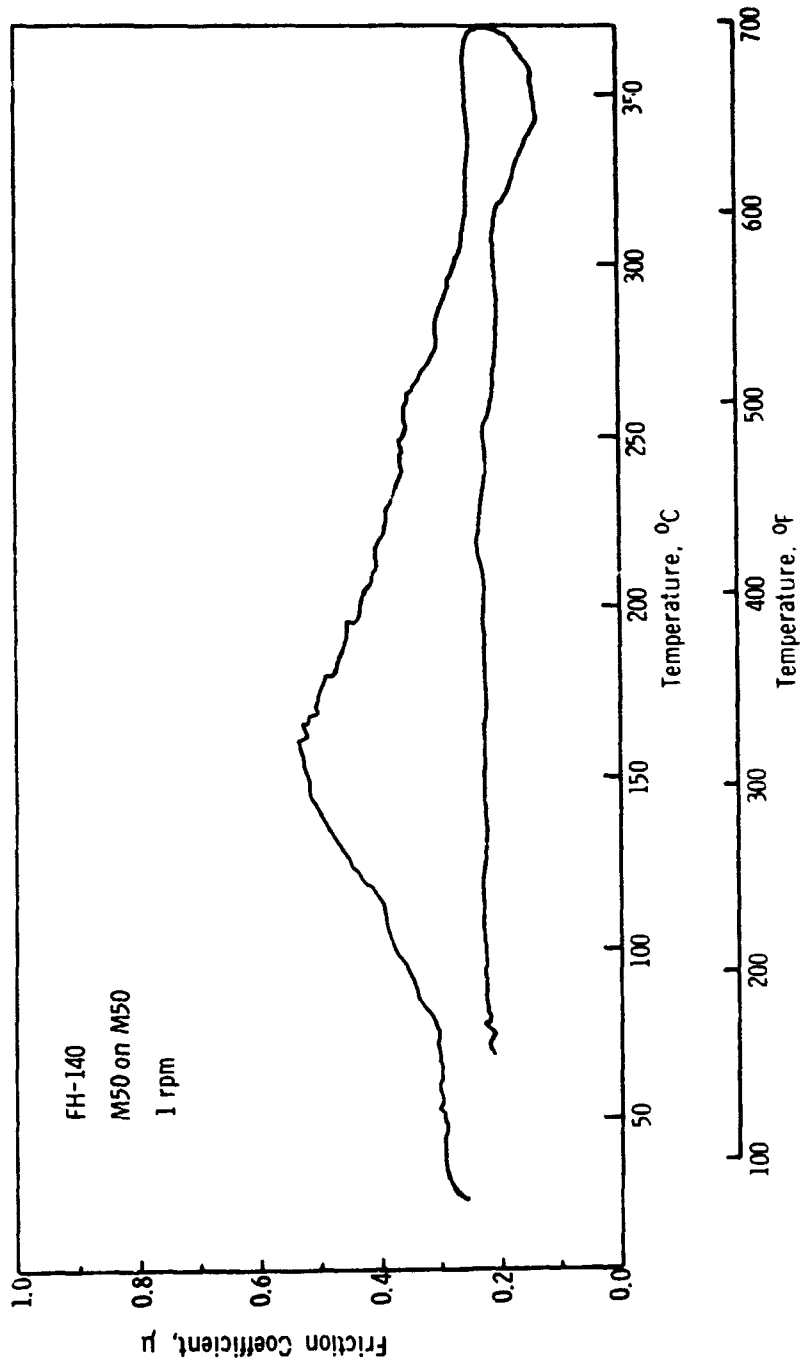
Figure D-3. Friction Curve for FH-140
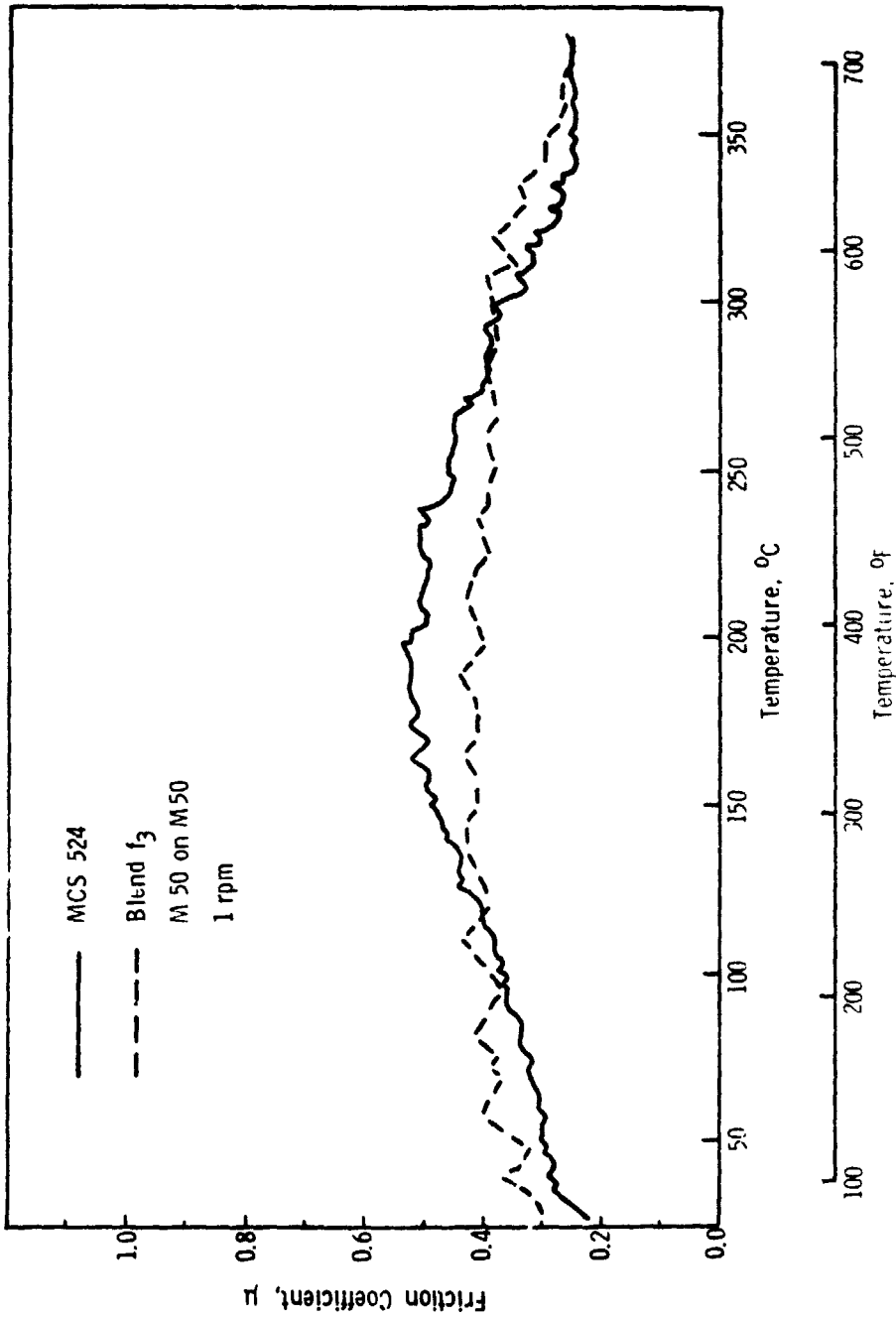
Figure D-4. Friction Curves for MCS 524 and Blend f_3

171
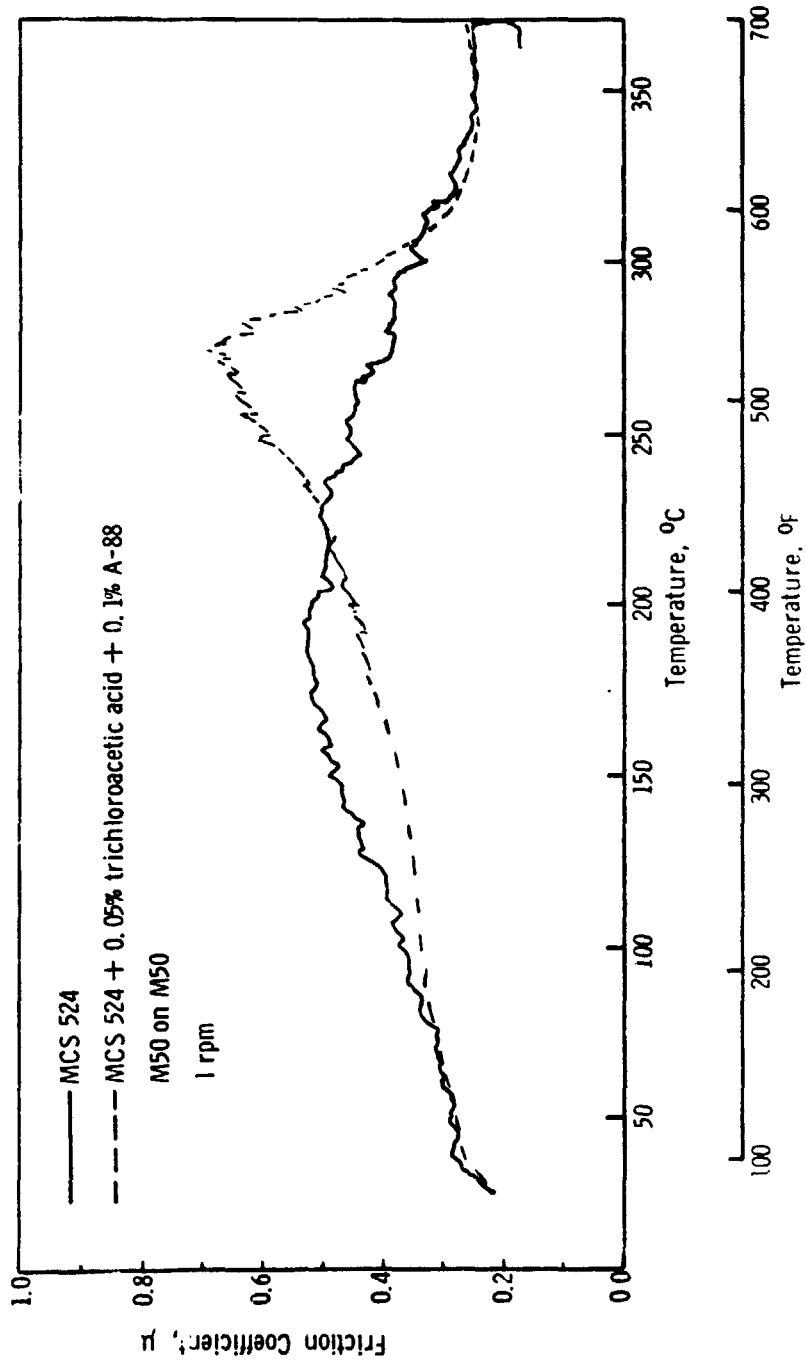
Figure D-5. Friction Curves for MCS 524 and MCS 524
+ 0.05% Trichloroacetic Acid + 0.1% A-88

172
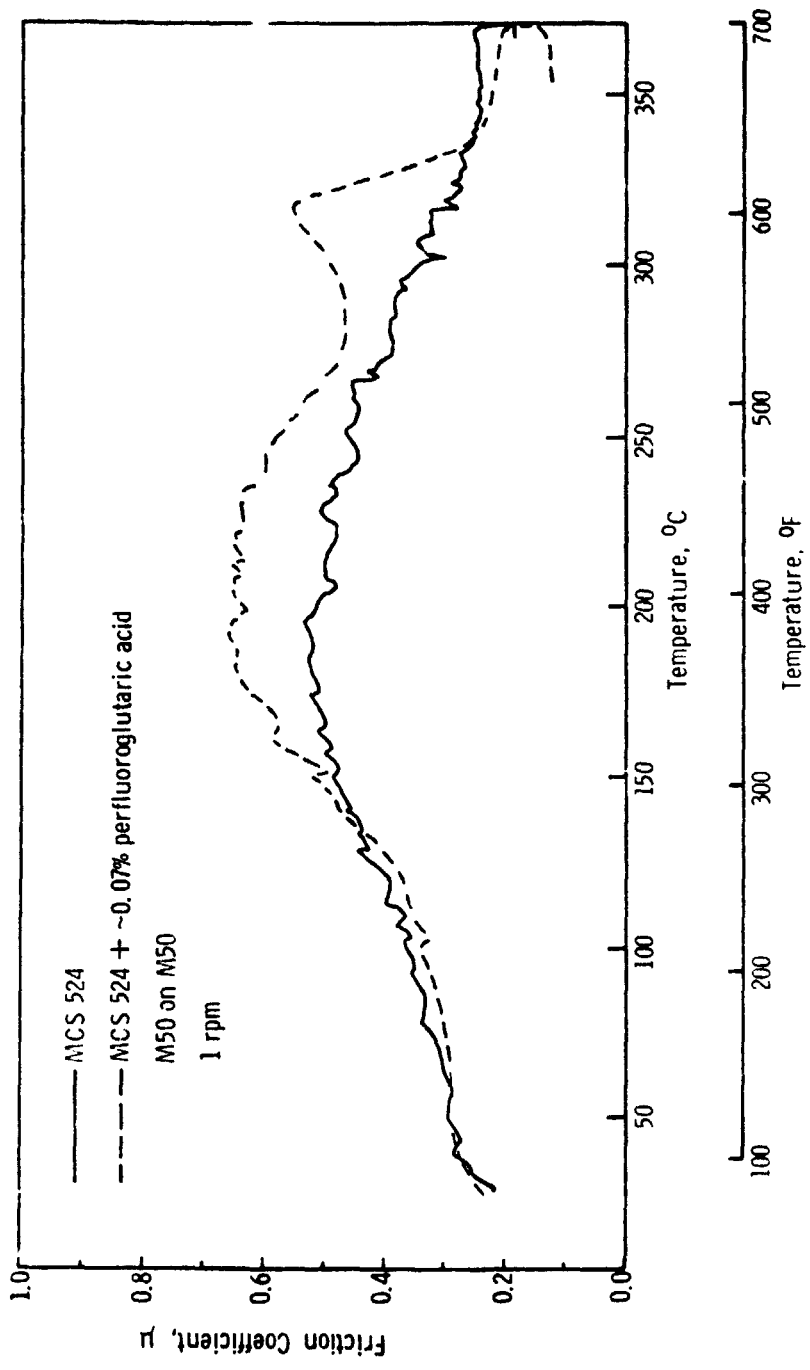
Figure D-6. Friction Curves for MCS 524 and MCS 524 + ~0.07% Perfluoroglutaric Acid
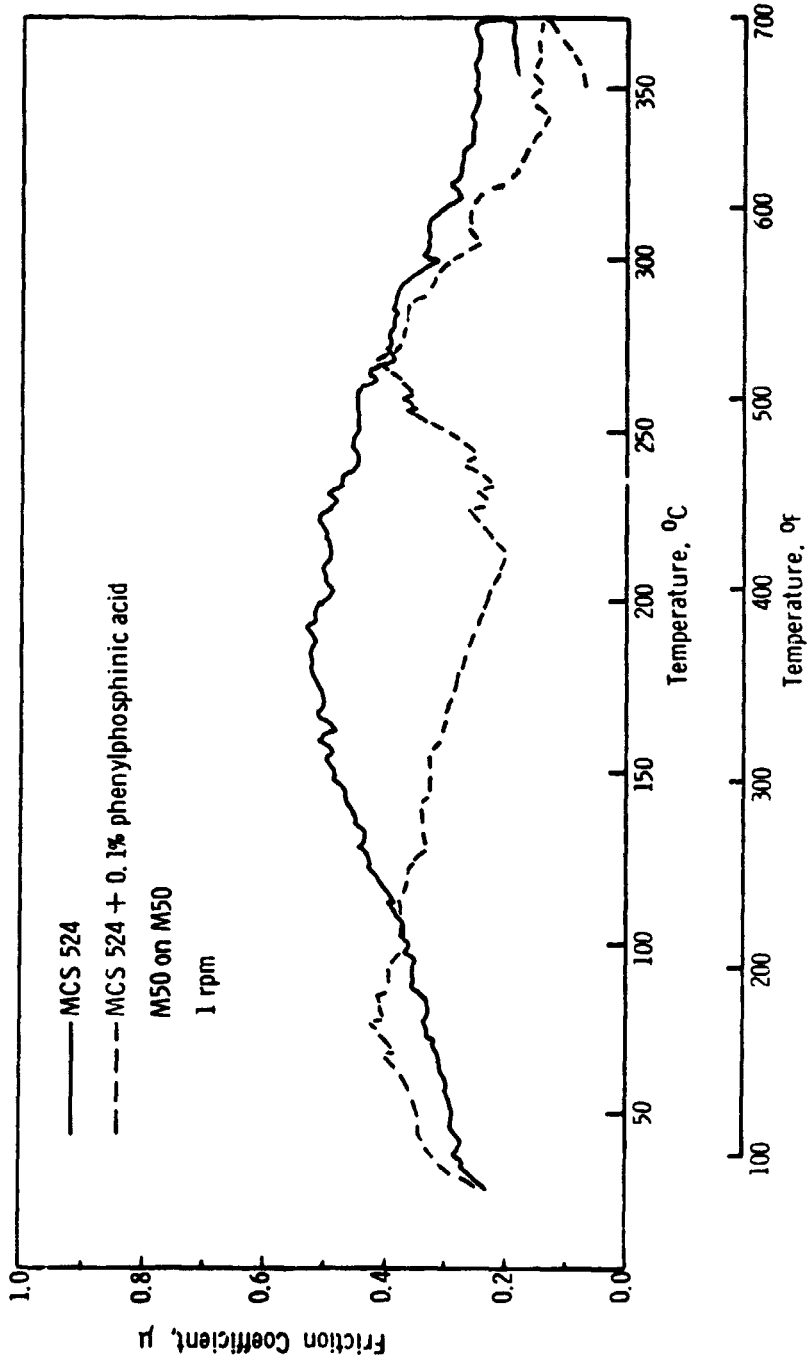
Figure D-7. Friction Curves for MCS 524 and MCS 524 + 0.1% Phenylphosphinic Acid

174
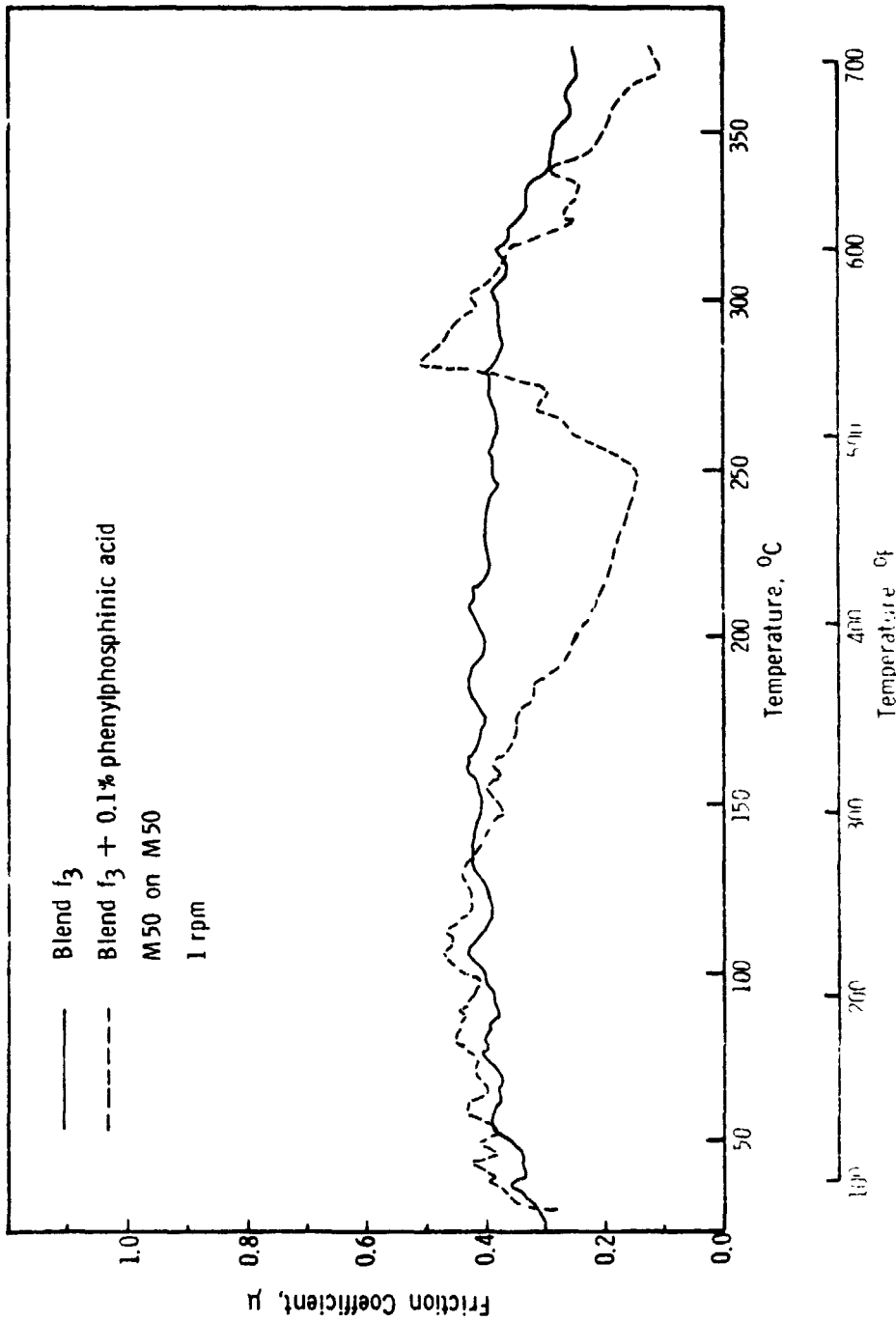
Figure D-8. Friction Curves for Blend f_3 and Blend f_3 + 0.1% Phenylphosphinic Acid
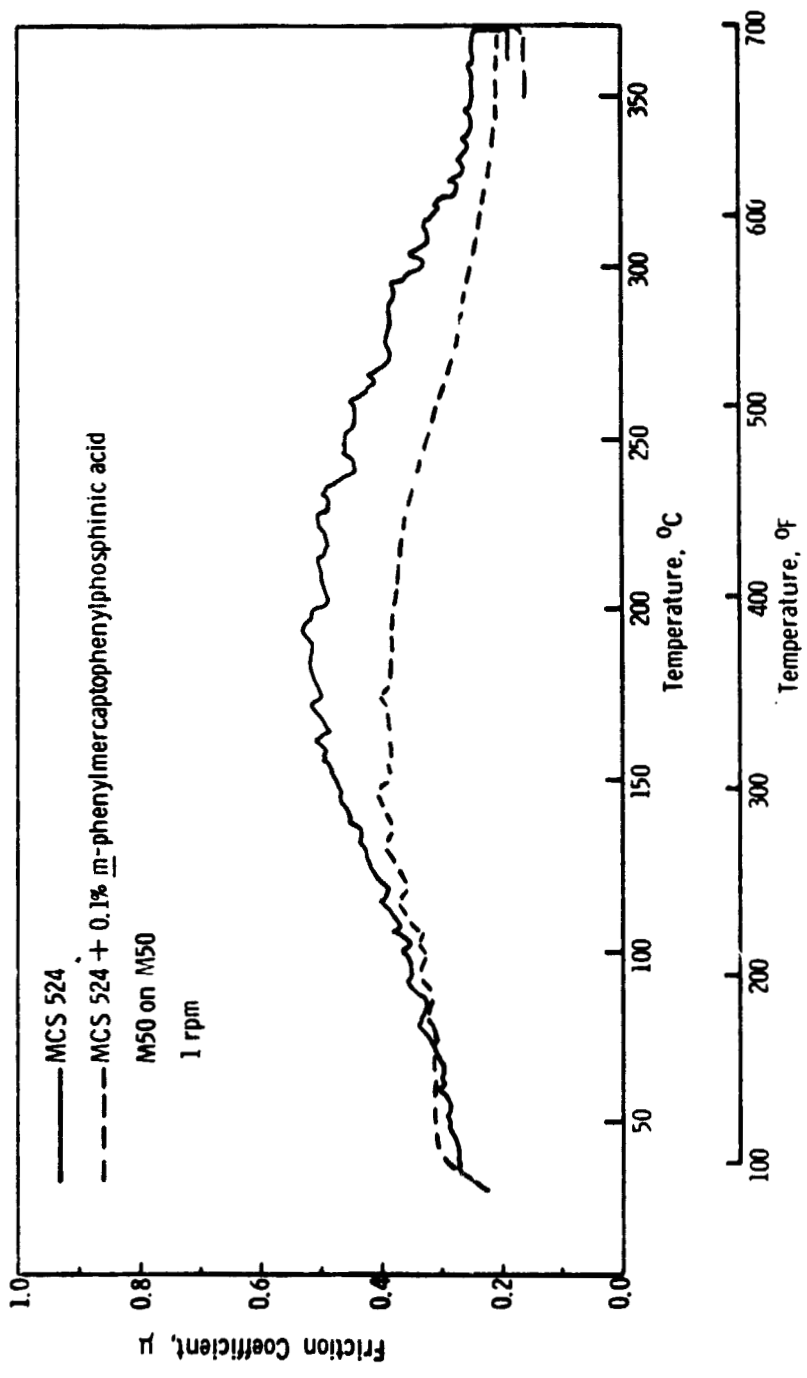
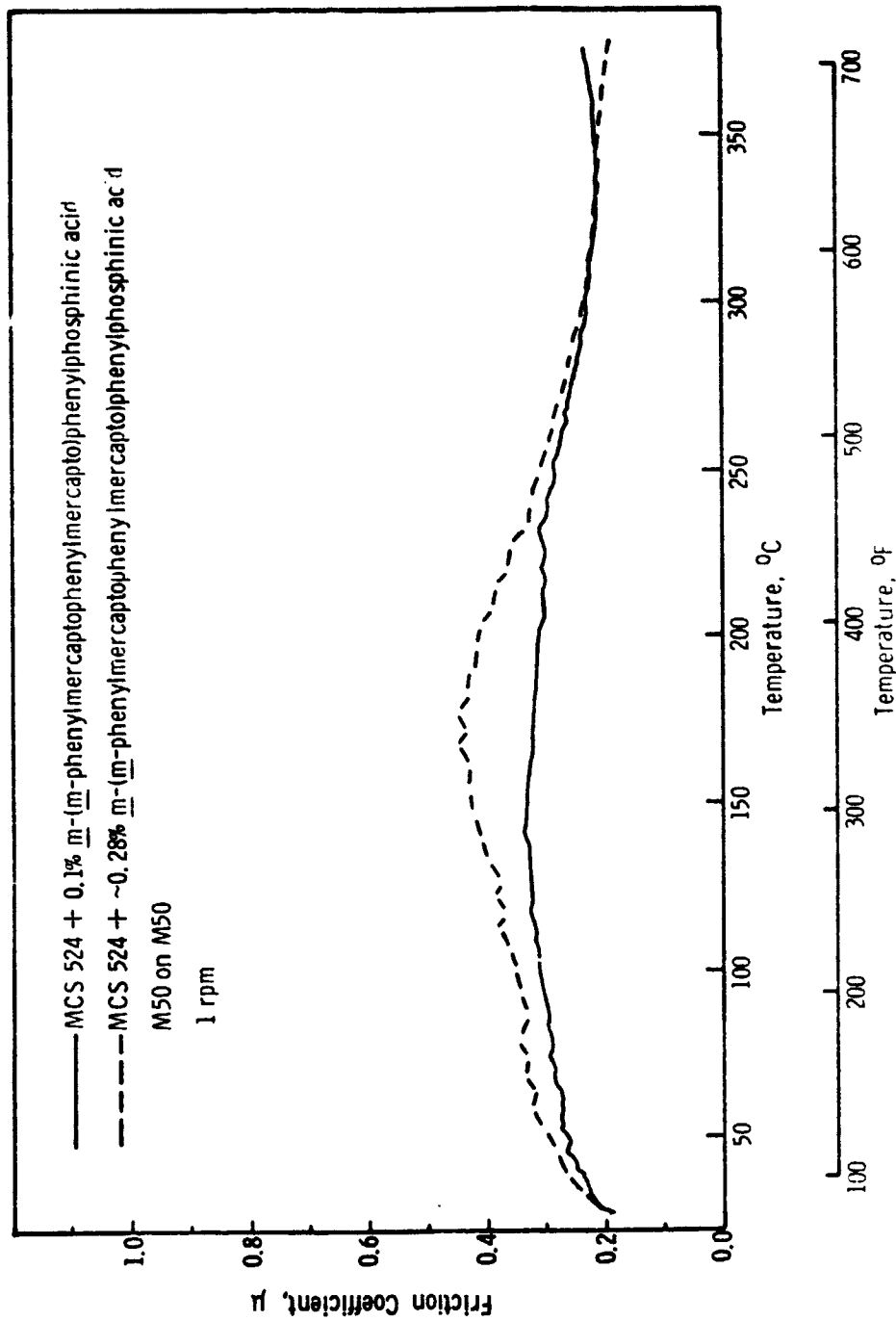Figure D-9. Friction Curves for MCS 524 and MCS 524 + 0.1% m-Phenylmercaptophenylphosphinic Acid

176
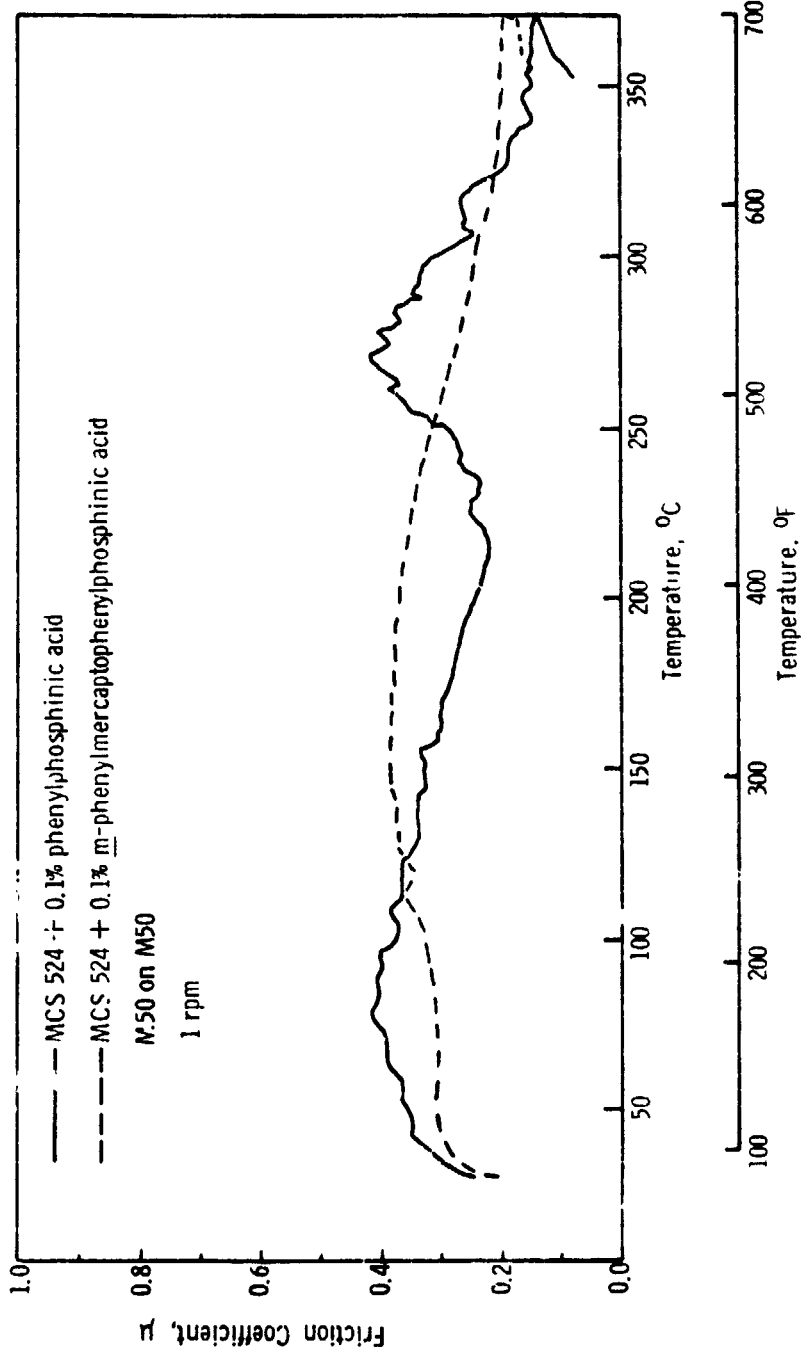
Figure D-10. Friction Curves for MCS 524 + 0.1% Phenylphosphinic Acid and MCS 524 + 0.1% m-Phenylmercaptophenylphosphinic Acid
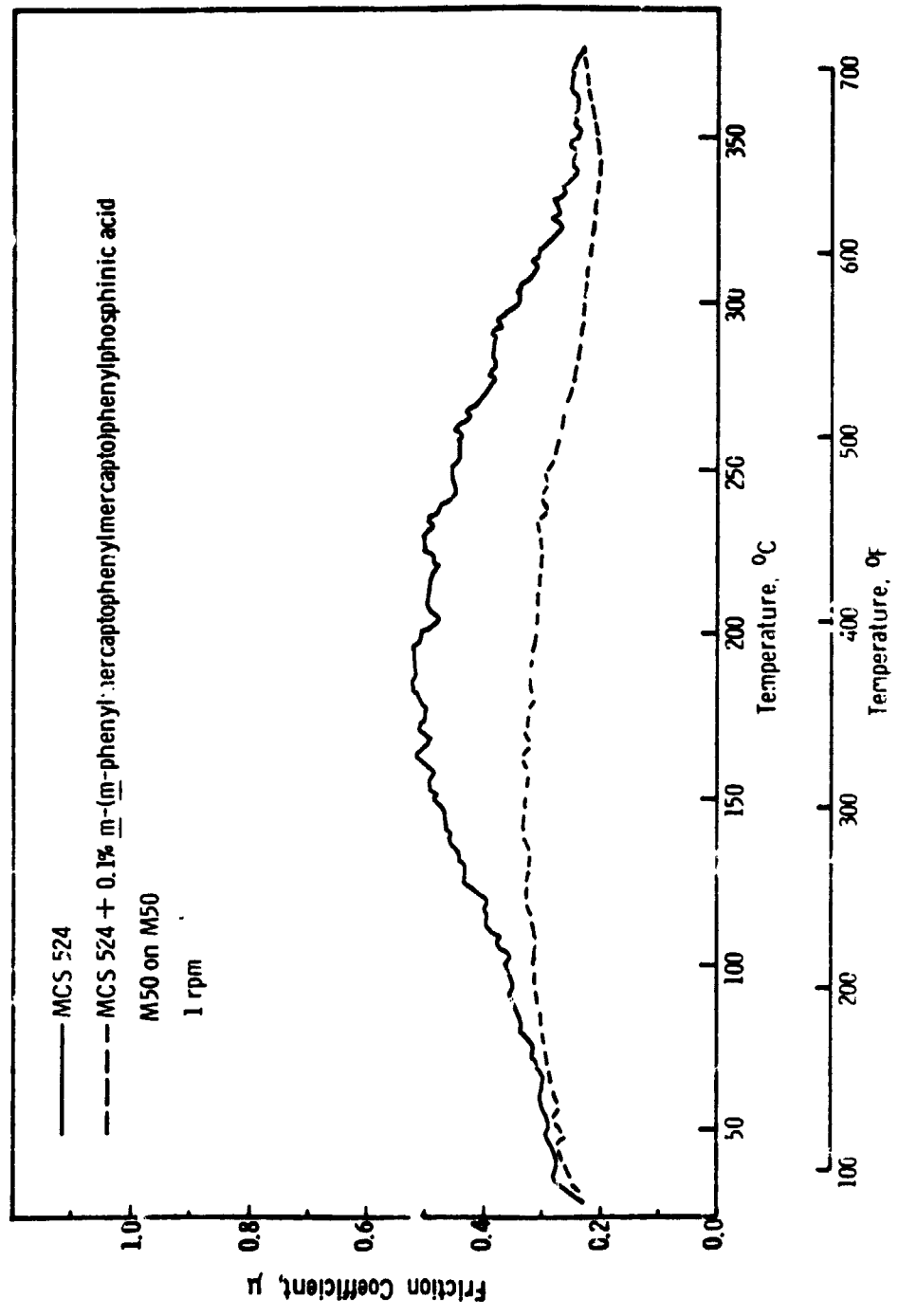
Figure D-11. Friction Curves for MCS 524 and MCS 524 + 0.1% m-(m-Phenyl-mercaptophenylmercapto)phenylphosphinic Acid

178

Figure D-12. Friction Curves for MCS 524 + 0 1% m-(m-Phenylmercaptophenylmercapto)-phenylphosphinic acid and MCS 524 + ~0.28% m-(m-Phenylmercaptophenyl-mercapto)phenylphosphinic Acid
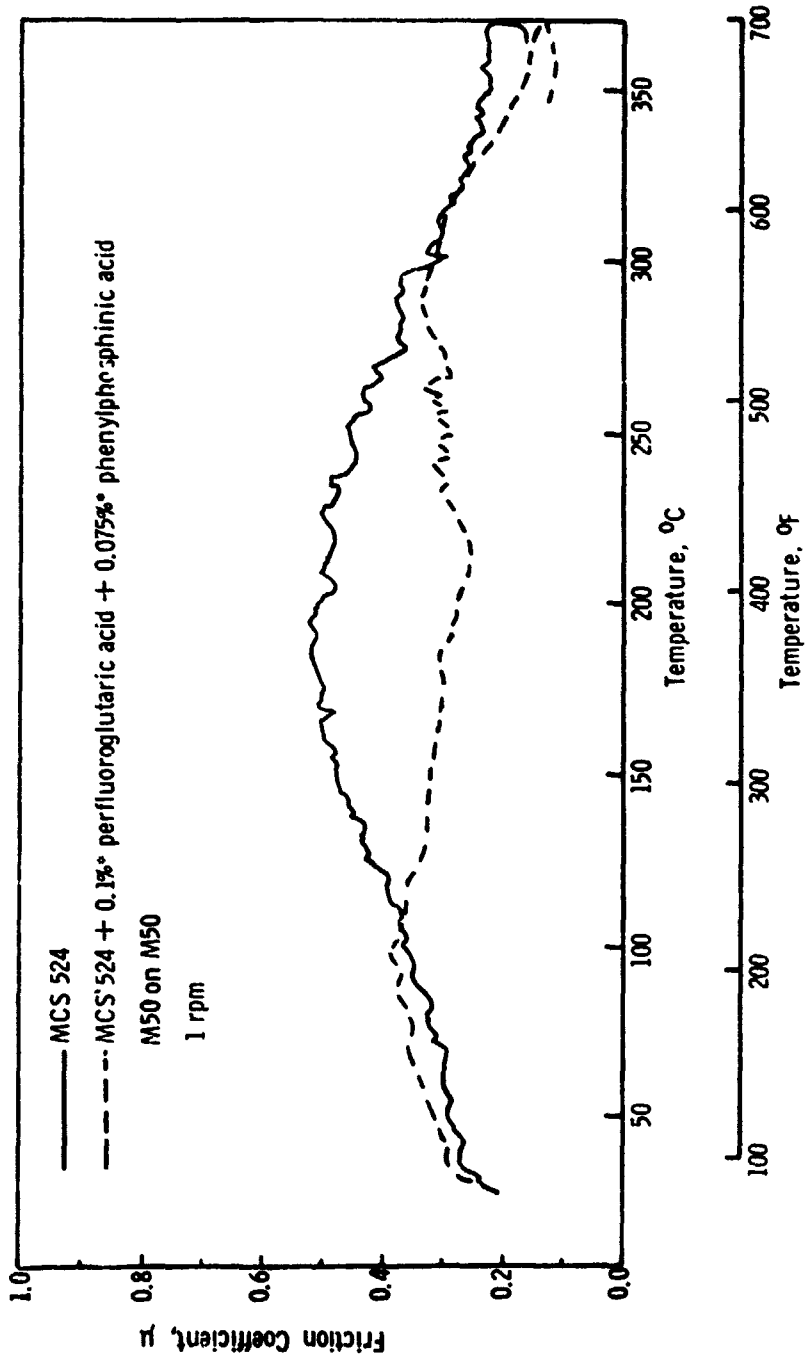
179

Figure D-13. Friction Curves for MCS 524 and MCS 524 + 0.1%* Per-
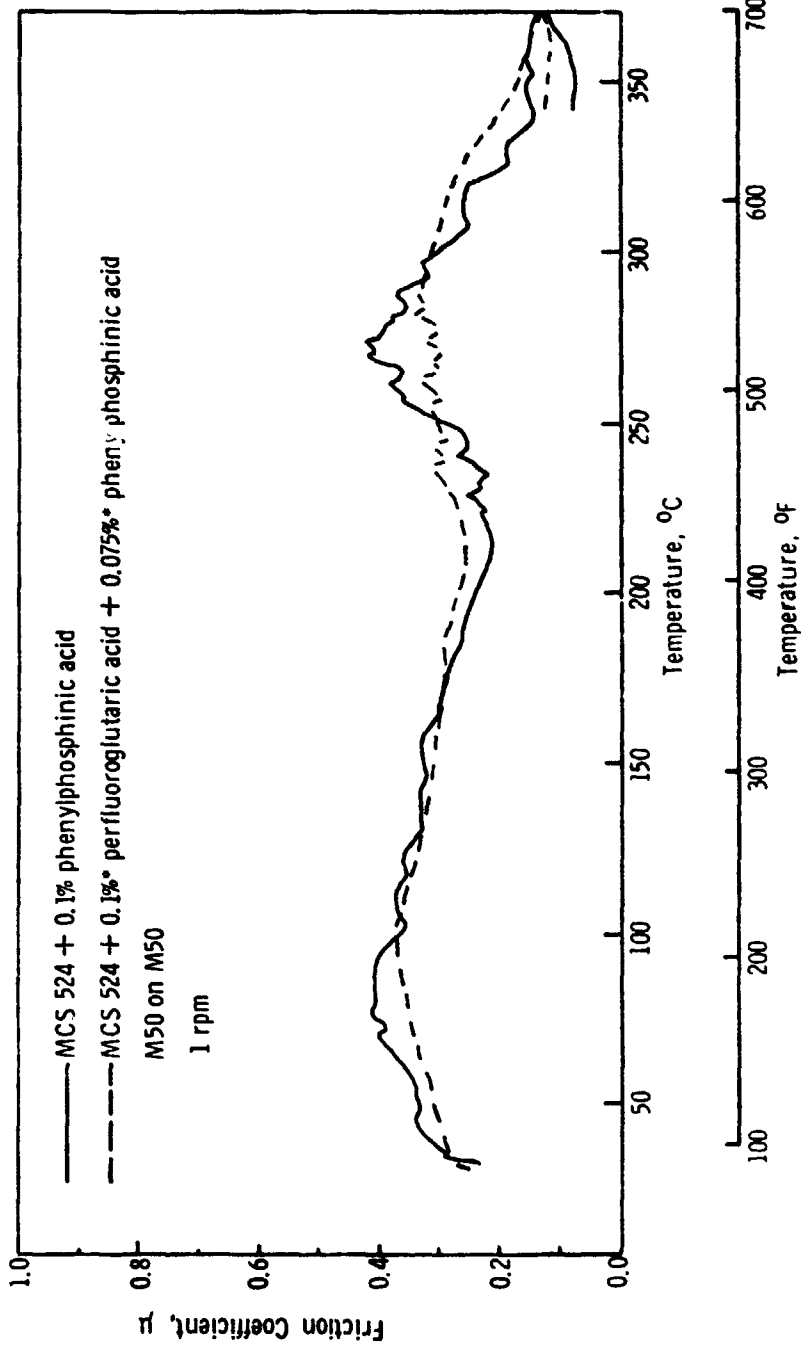fluoroglutaric Acid + 0.075%* Phenylphosphinic Acid

*Initial additive charge.

Figure D-14. Friction Curves for MCS 524 + 0.1% Phenylphosphinic Acid and MCS 524 + 0.1%* Perfluoroglutaric Acid + 0.075%* Phenylphosphinic Acid
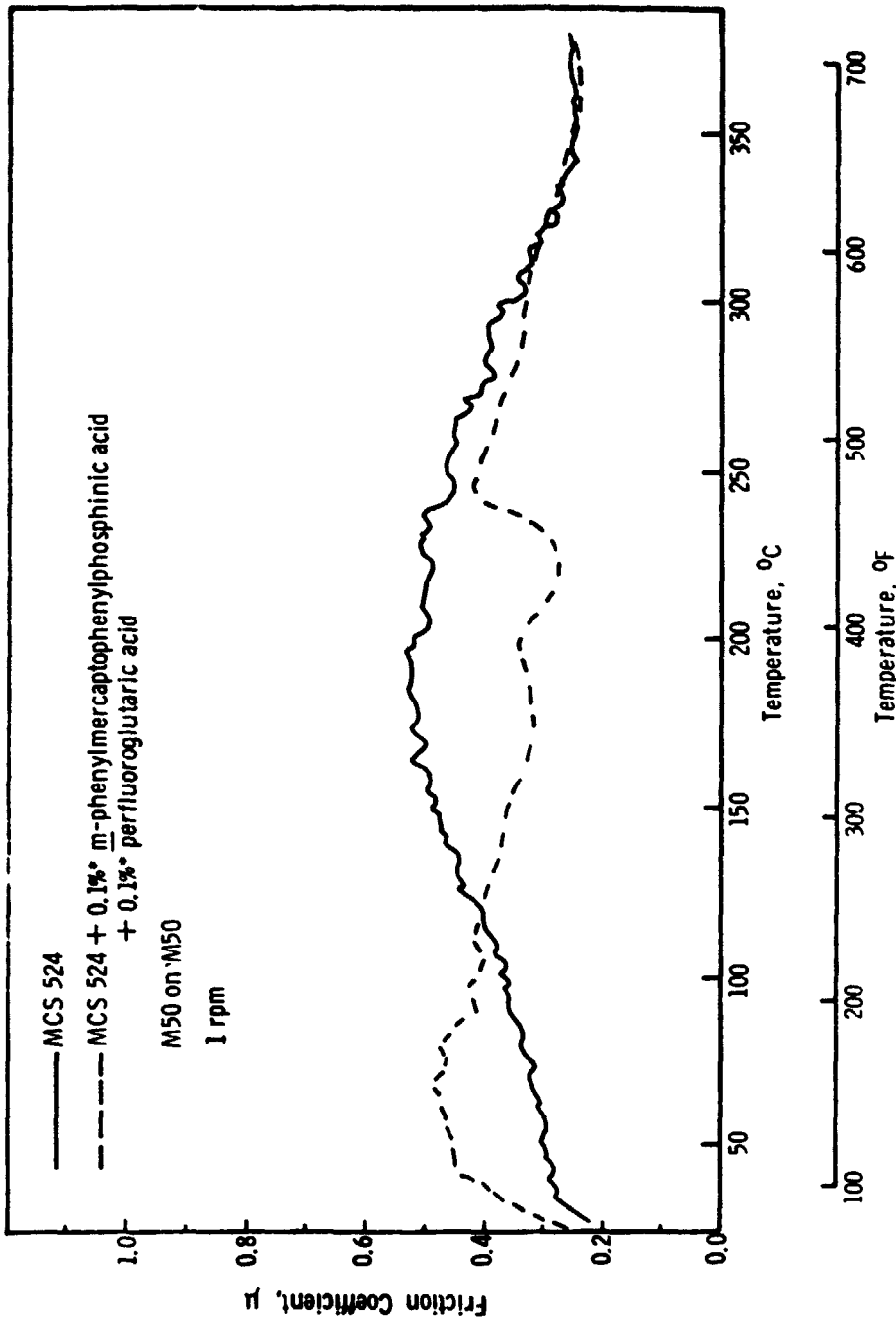
*Initial additive charge.

Figure D-15. Friction Curves for MCS 524 and MCS 524 + 0.1%* m-Phenylmercapto-phenylphosphinic Acid + 0.1%* Perfluoroglutaric Acid

―――――――

*Initial additive charge.
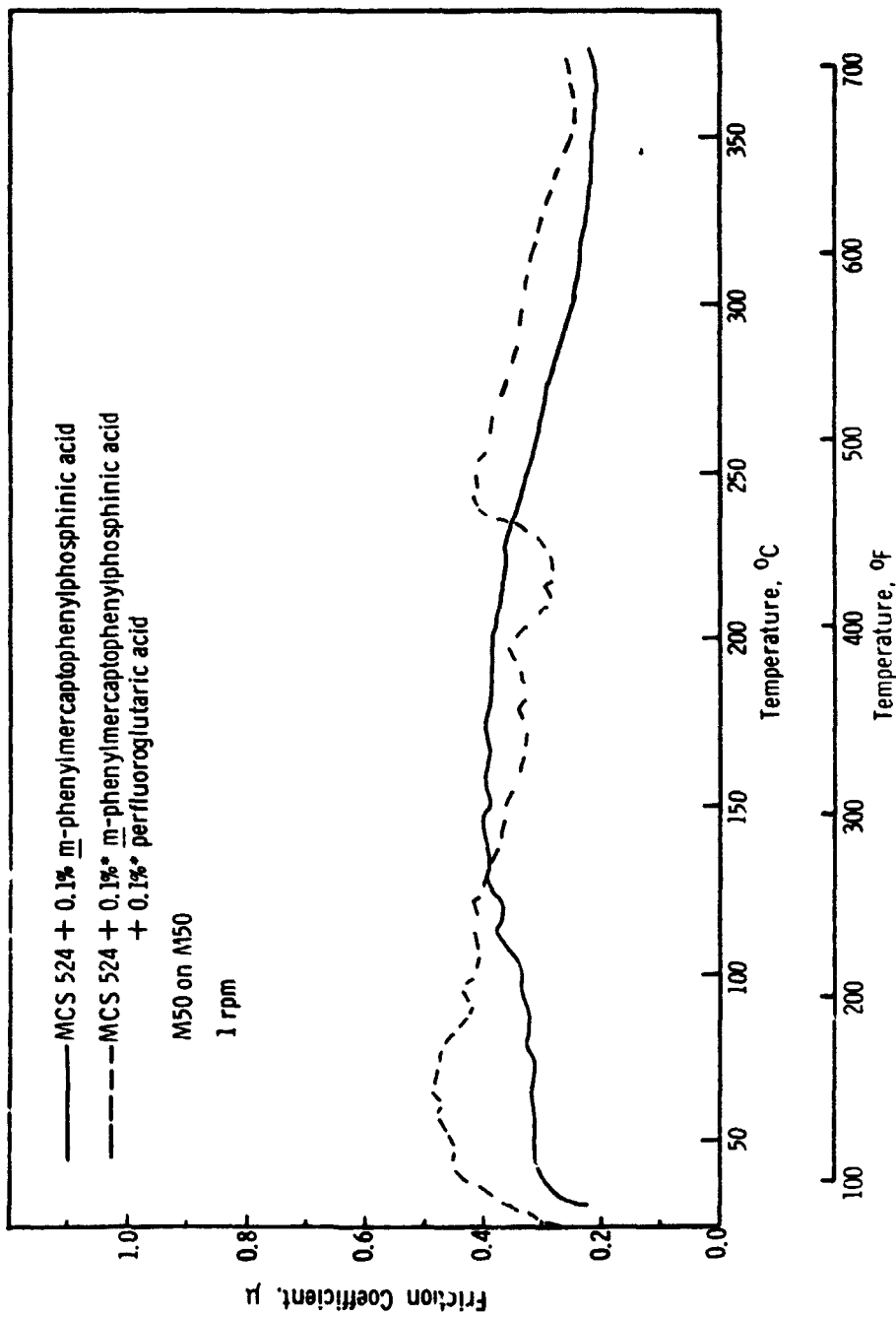
Figure D-16. Friction Curves for MCS 524 + 0.1% m-Phenylmercaptophenylphosphinic Acid and MCS 524 + 0.18* m-Phenylmercaptophenylphosphinic Acid + 0.18* Perfluoroglutaric Acid
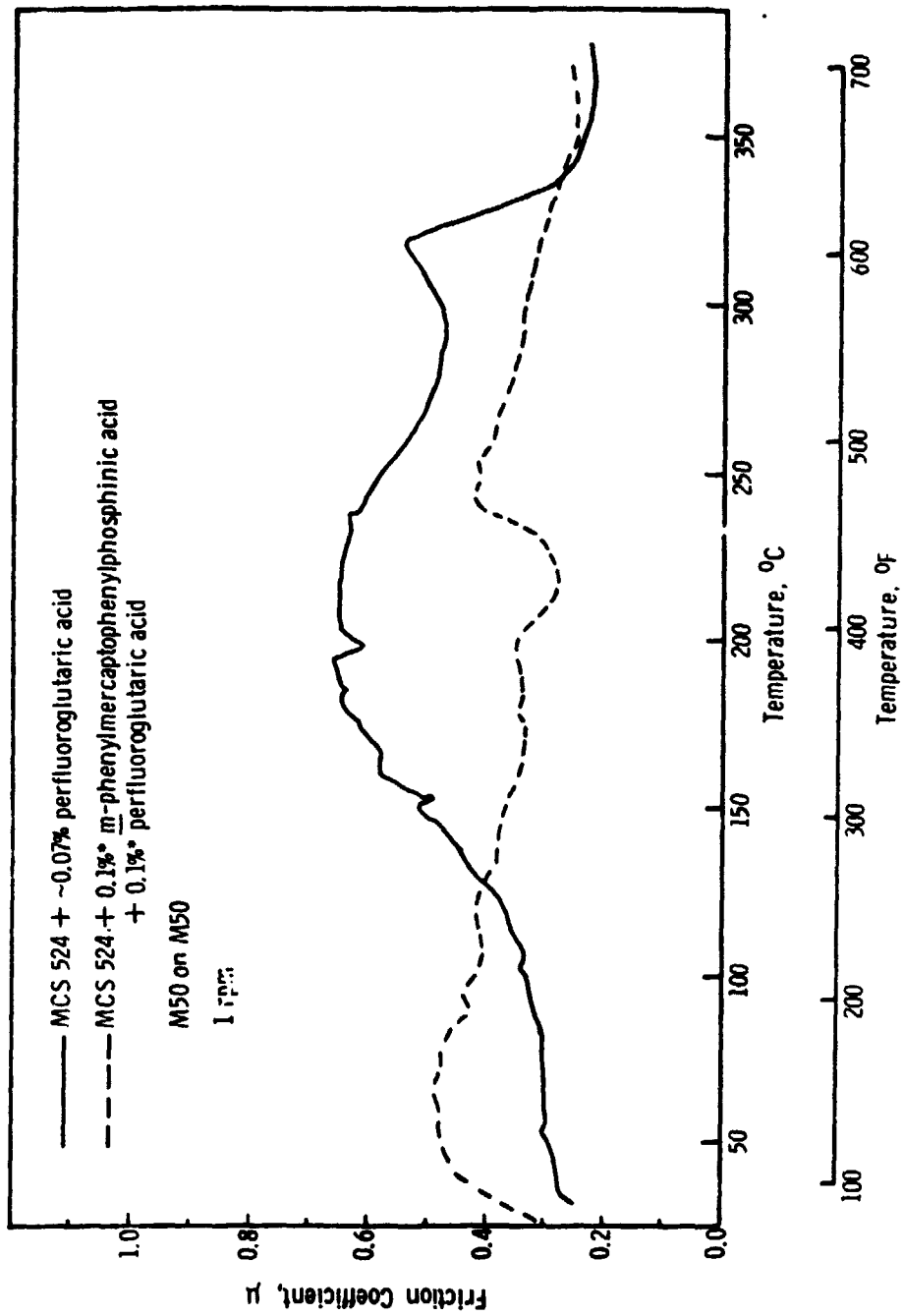
*Initial additive charge.

Figure D-17. Friction Curves for MCS 524 + ~0.07% Perfluoroglutaric Acid and MCS 524 + 0.1%* m-Phenylmercaptophenylphosphinic Acid + 0.1%* Perfluoroglutaric Acid
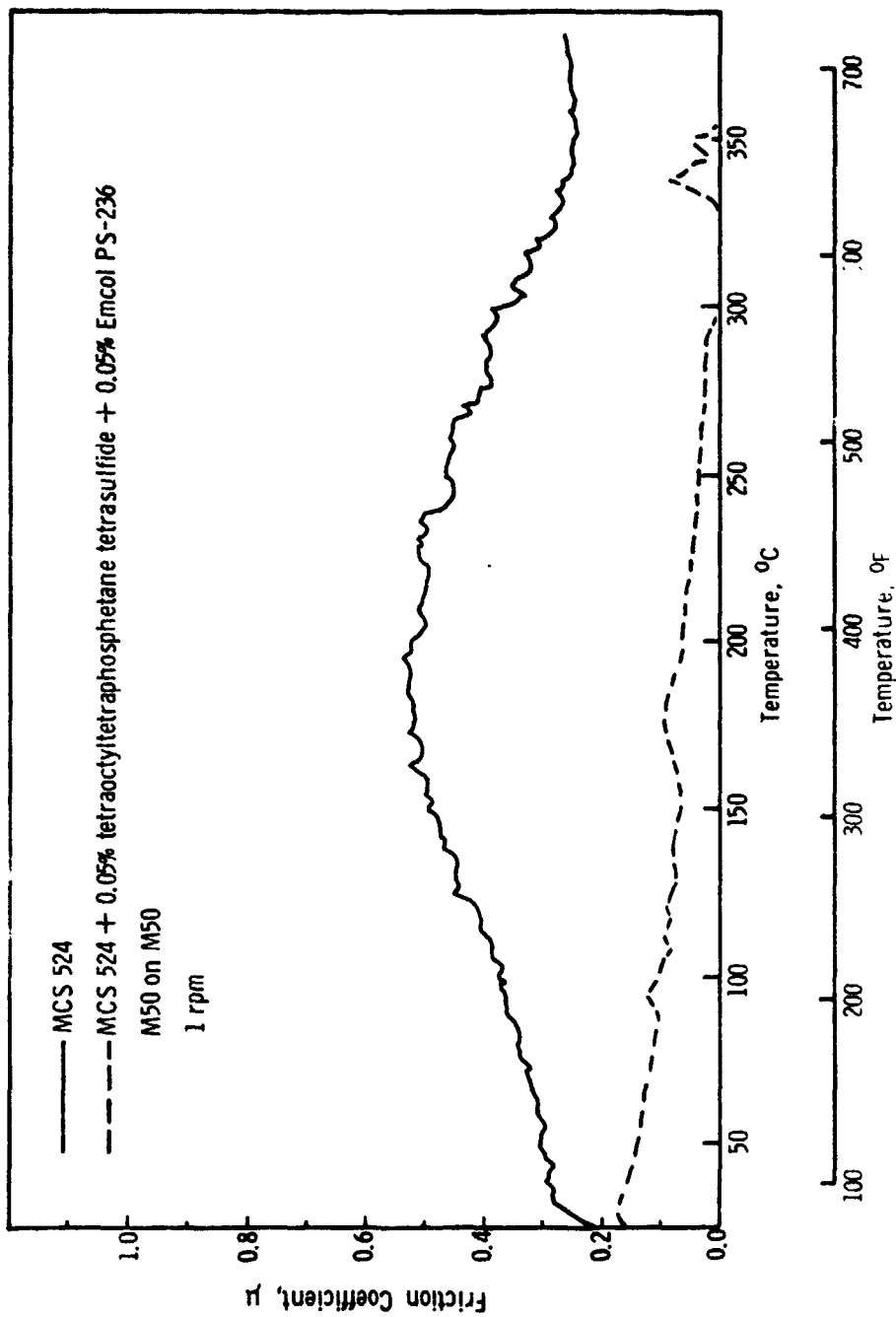
*Initial additive charge.

184

Figure D-18. Friction Curves for MCS 524 and MCS 524 + 0.05% Tetraoctyltetra-phosphetane Tetrasulfide + 0.05% Emcol PS-236
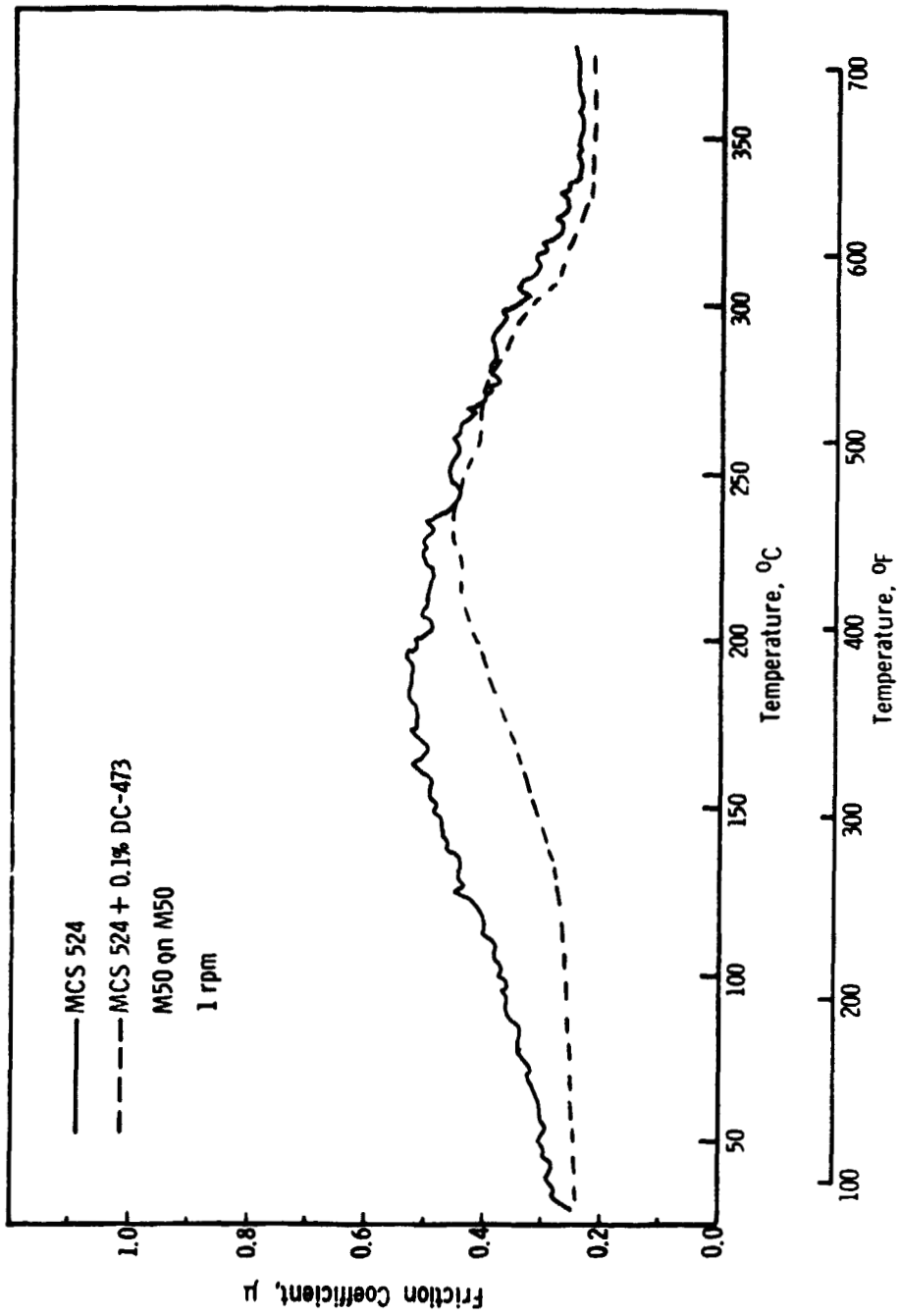
185

Figure D-19. Friction Curves for MCS 524 and MCS 524 + 0.1% DC-473
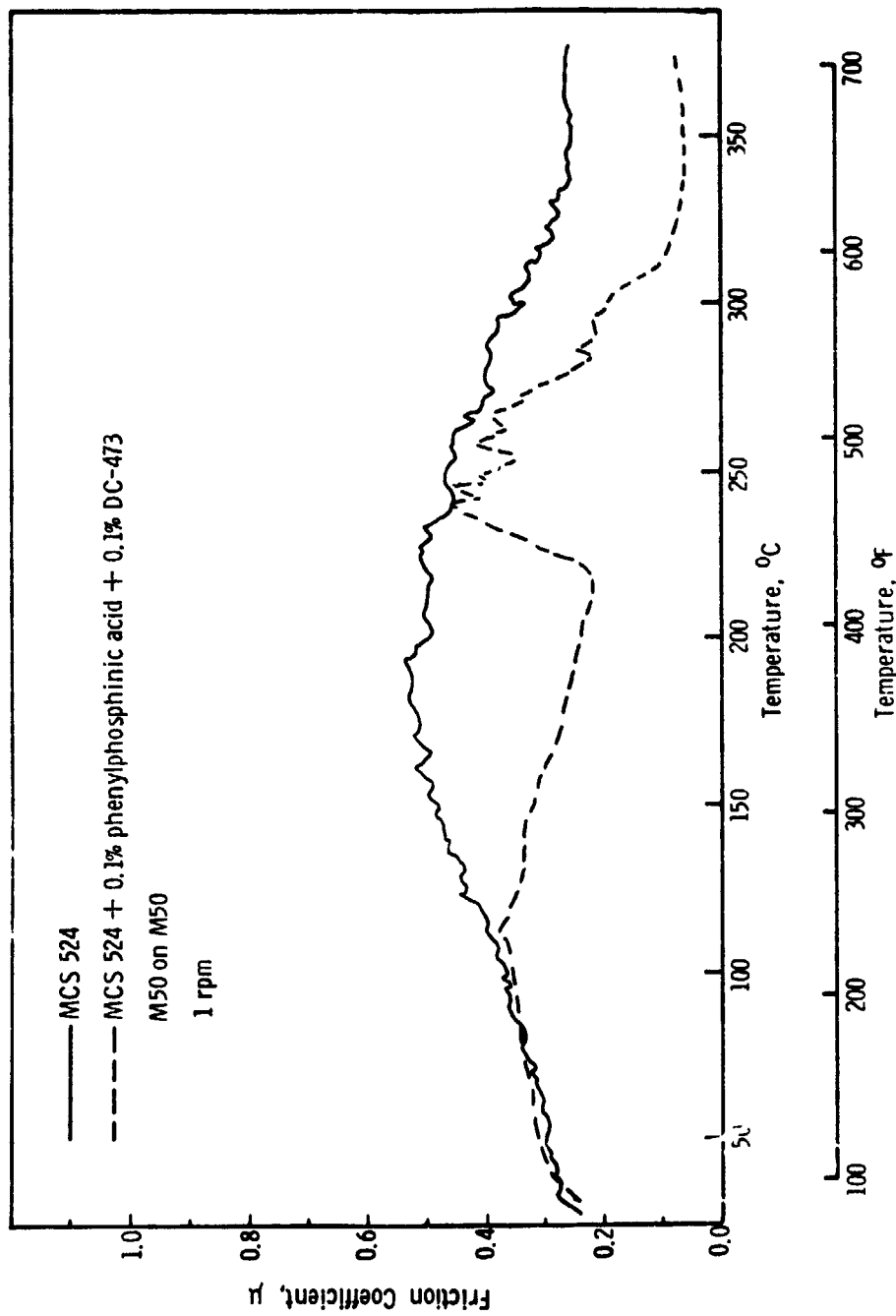
Figure D-20. Friction Curves for MCS 524 and MCS 524 + 0.1% Phenyl-
phosphinic Acid + 0.1% DC-473

187
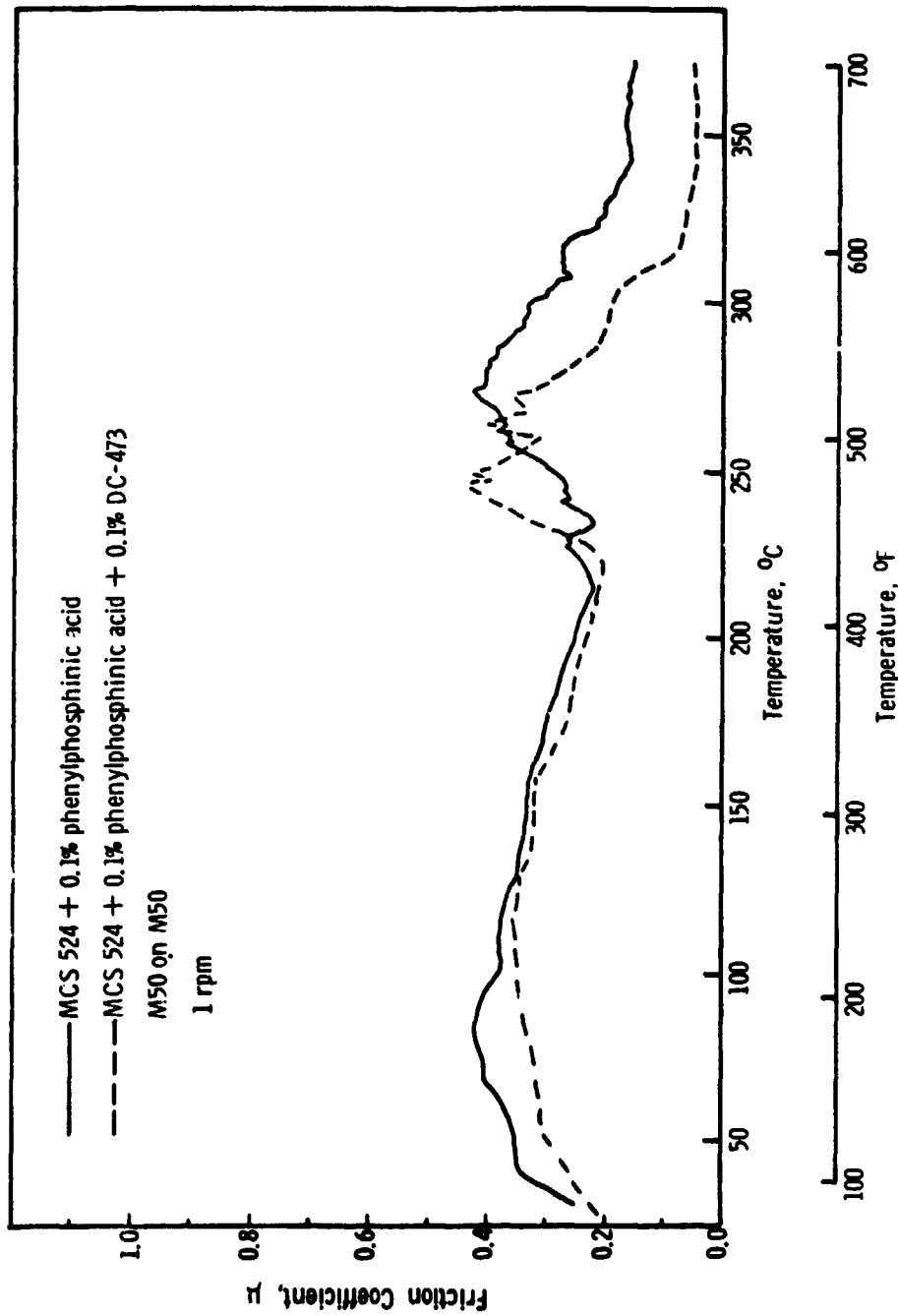
Figure D-21. Friction Curves for MCS 524 + 0.1% Phenylphosphinic Acid and MCS 524 + 0.1% Phenylphosphinic Acid + 0.1% DC-473

188
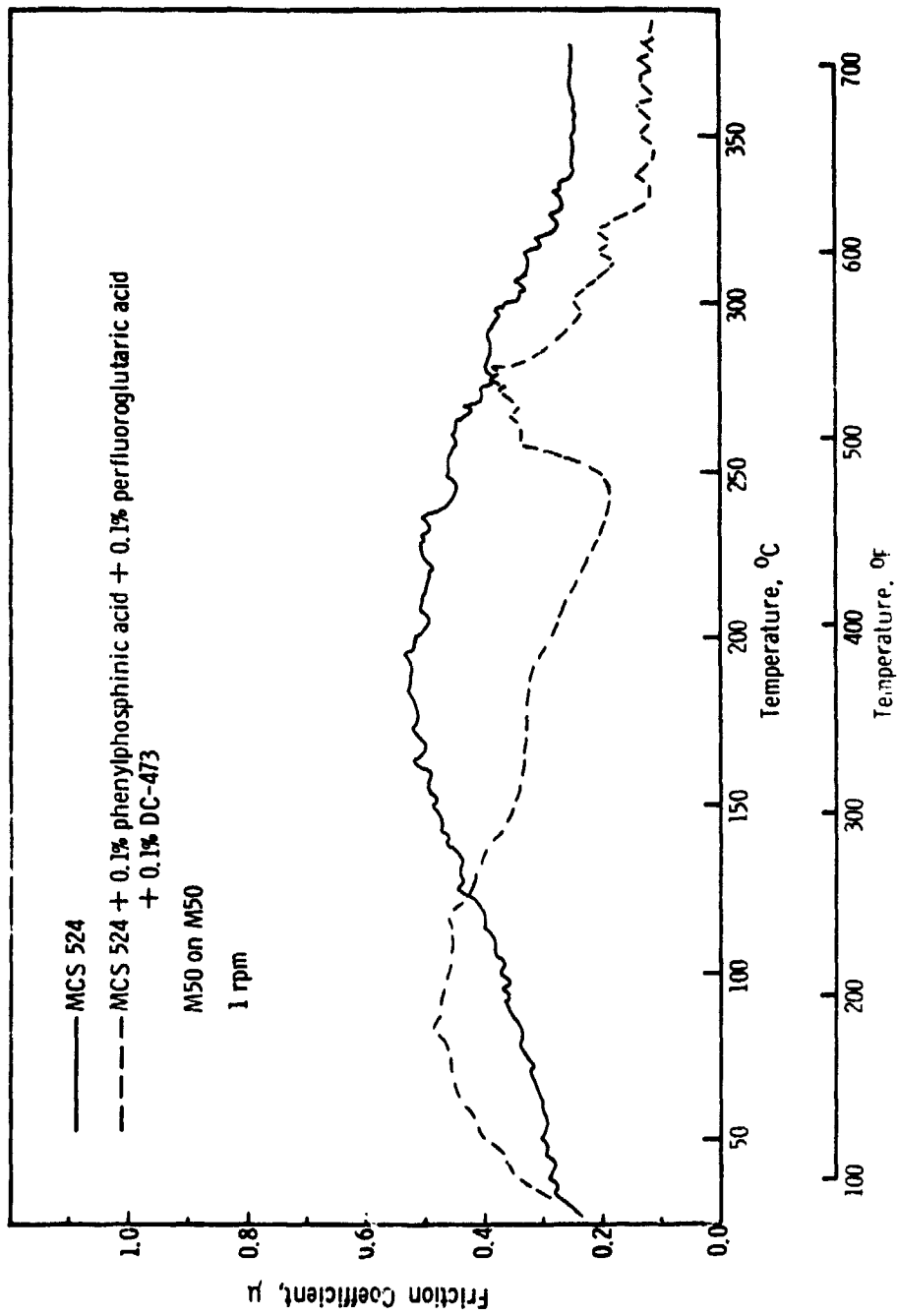
Figure D-22. Friction Curves for MCS 524 and MCS 524 + 0.1% Phenylphos-phinic Acid + 0.1% Perfluoroglutaric Acid + 0.1% DC-473

189
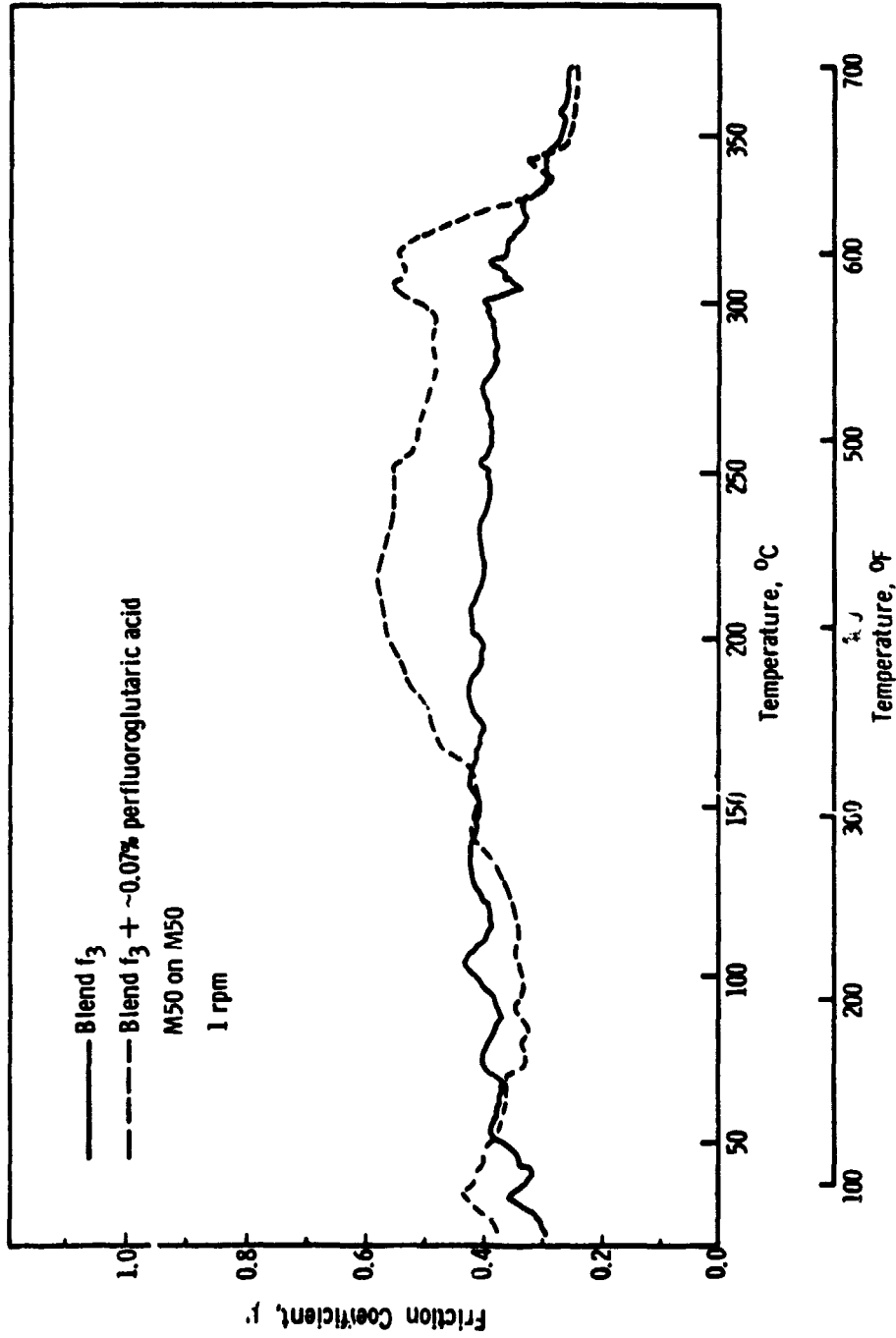
Figure D-23. Friction Curves for Blend f_3 and Blend $\bar{f}_3$ + ~0.07% Perfluoroglutaric Acid

190
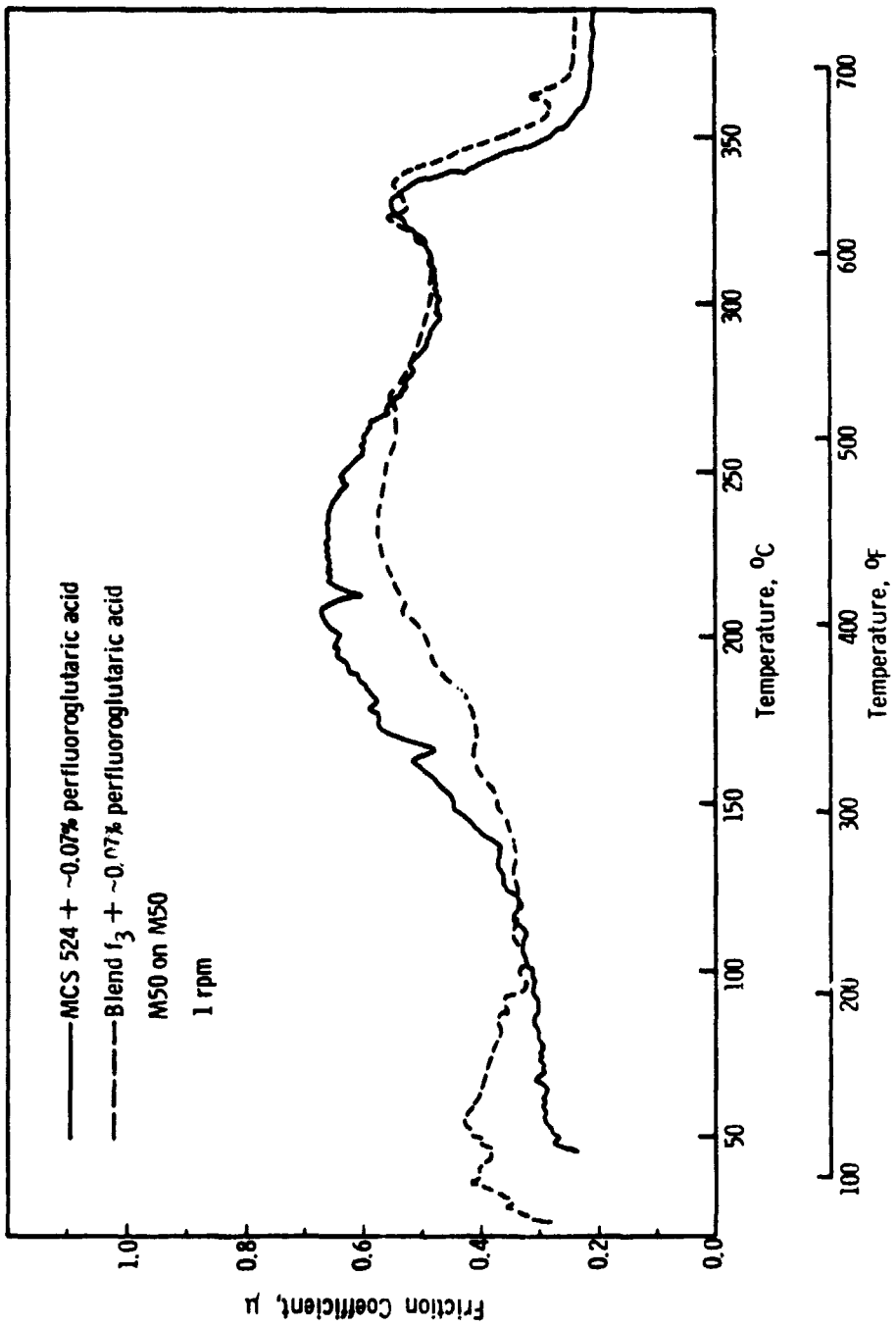
Figure D-24. Friction Curves for MCS 524 + ~0.07% Perfluoroglutaric Acid and Blend f₃ + ~0.07% Perfluoroglutaric Acid

APPENDIX E:

SLOW FOUR-BALL COEFFICIENT OF FRICTION VS.

TEMPERATURE CURVES, M50 ON SILVERED 6415
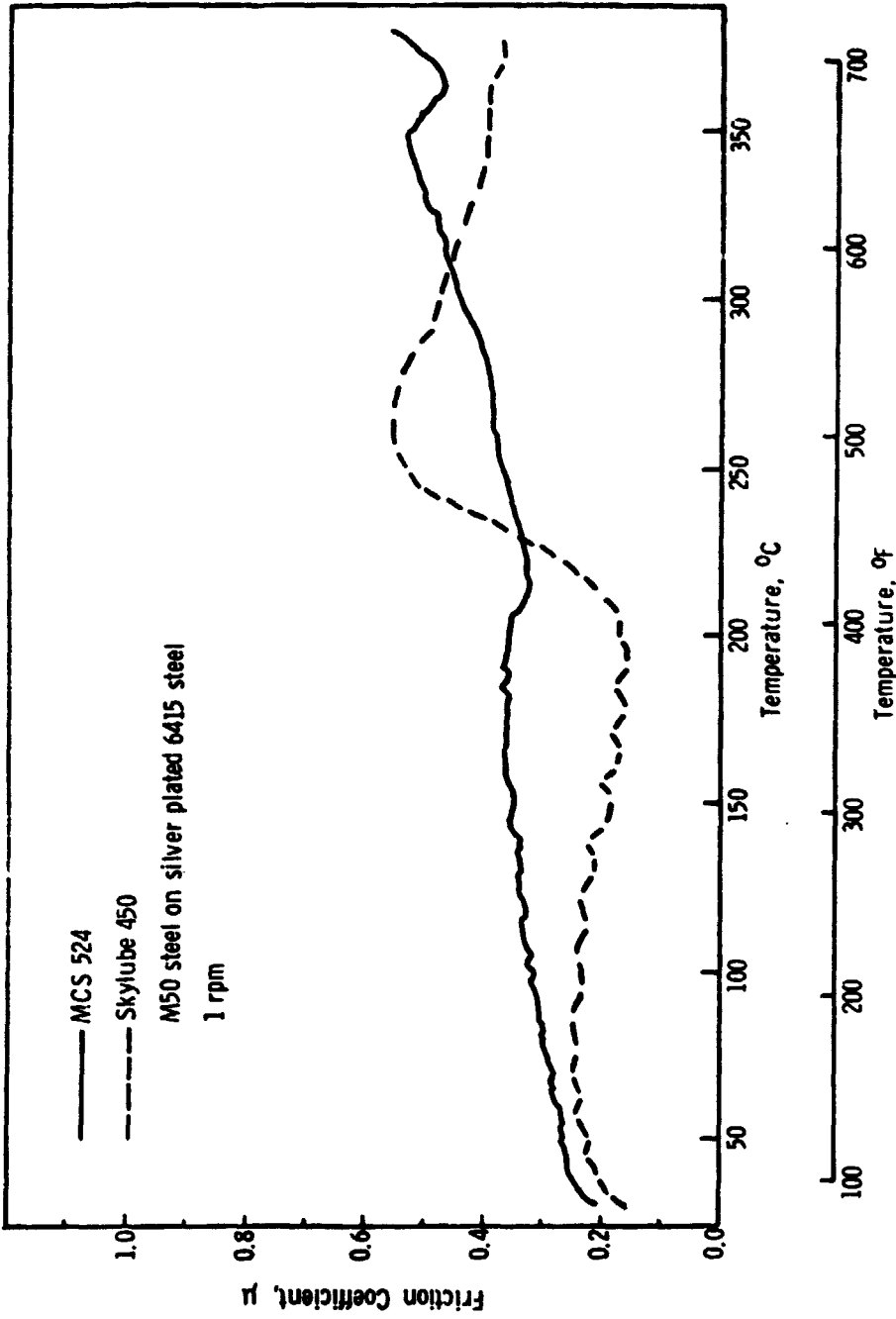
Figure E-1. Friction Curves for MCS 524 and Skylube 450

194
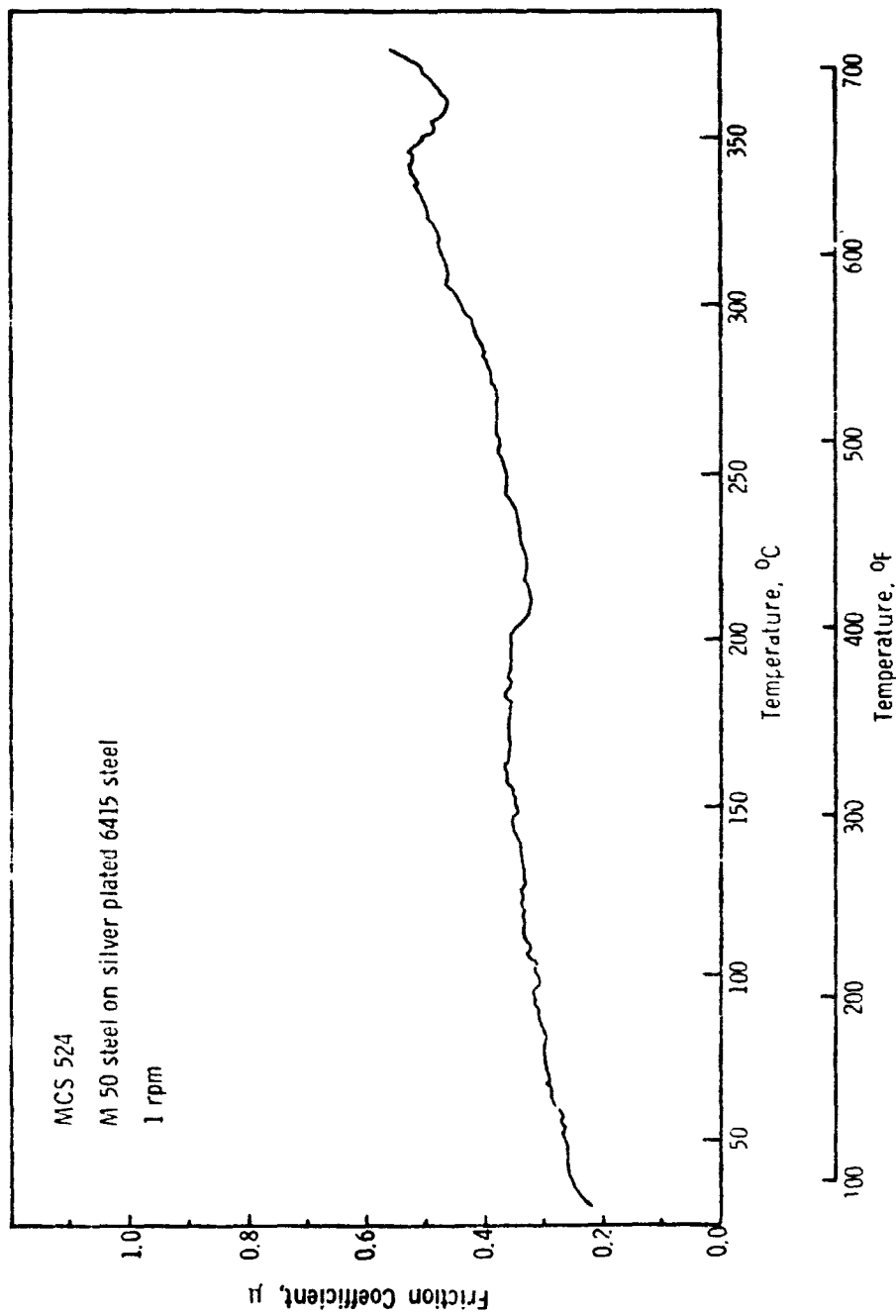
Figure E-2. Friction Curve for MCS 524

MCS 524

M 50 steel on silver plated 6415 steel

1 rpm

195
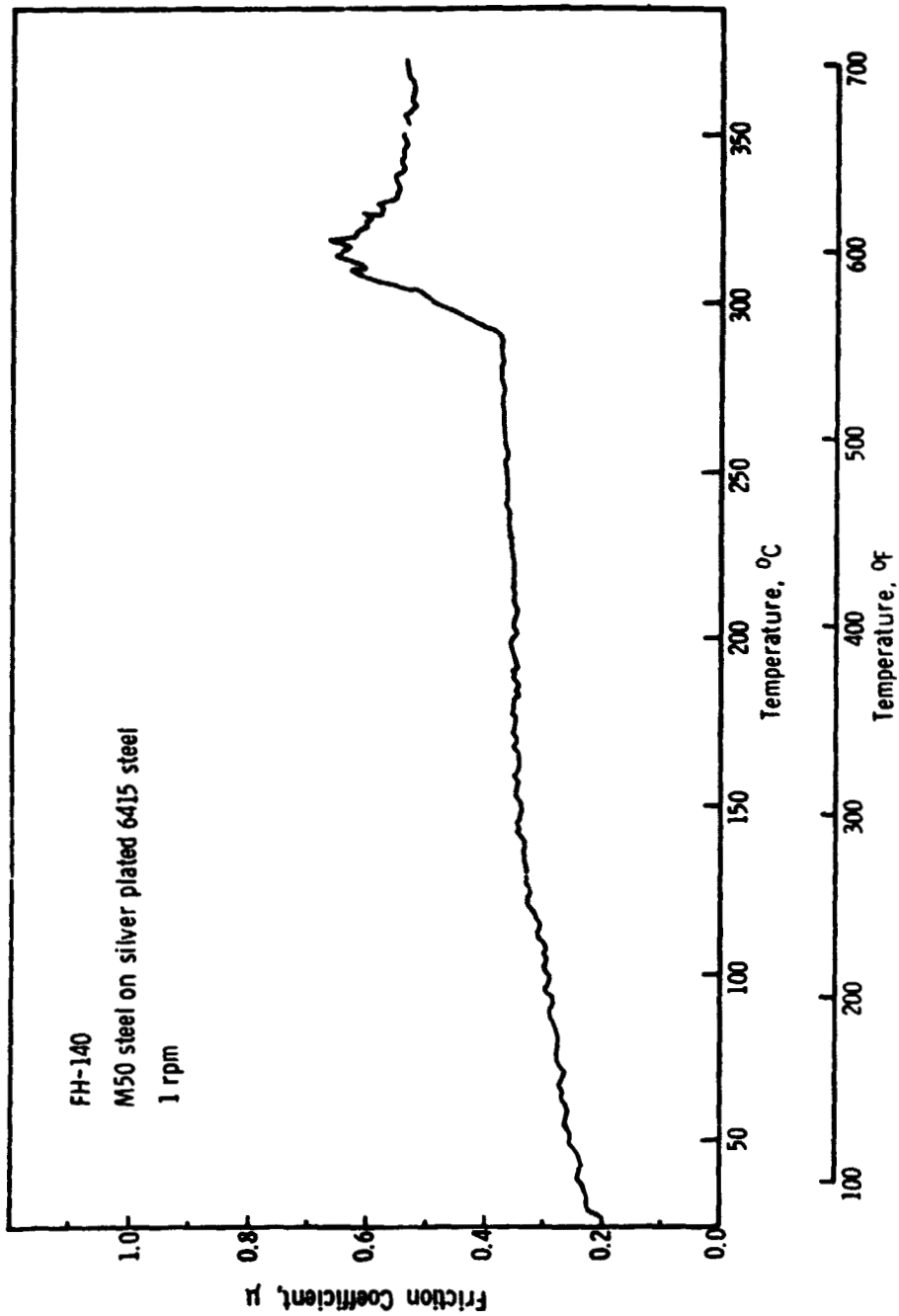
Figure E-3. Friction Curve for FH-140
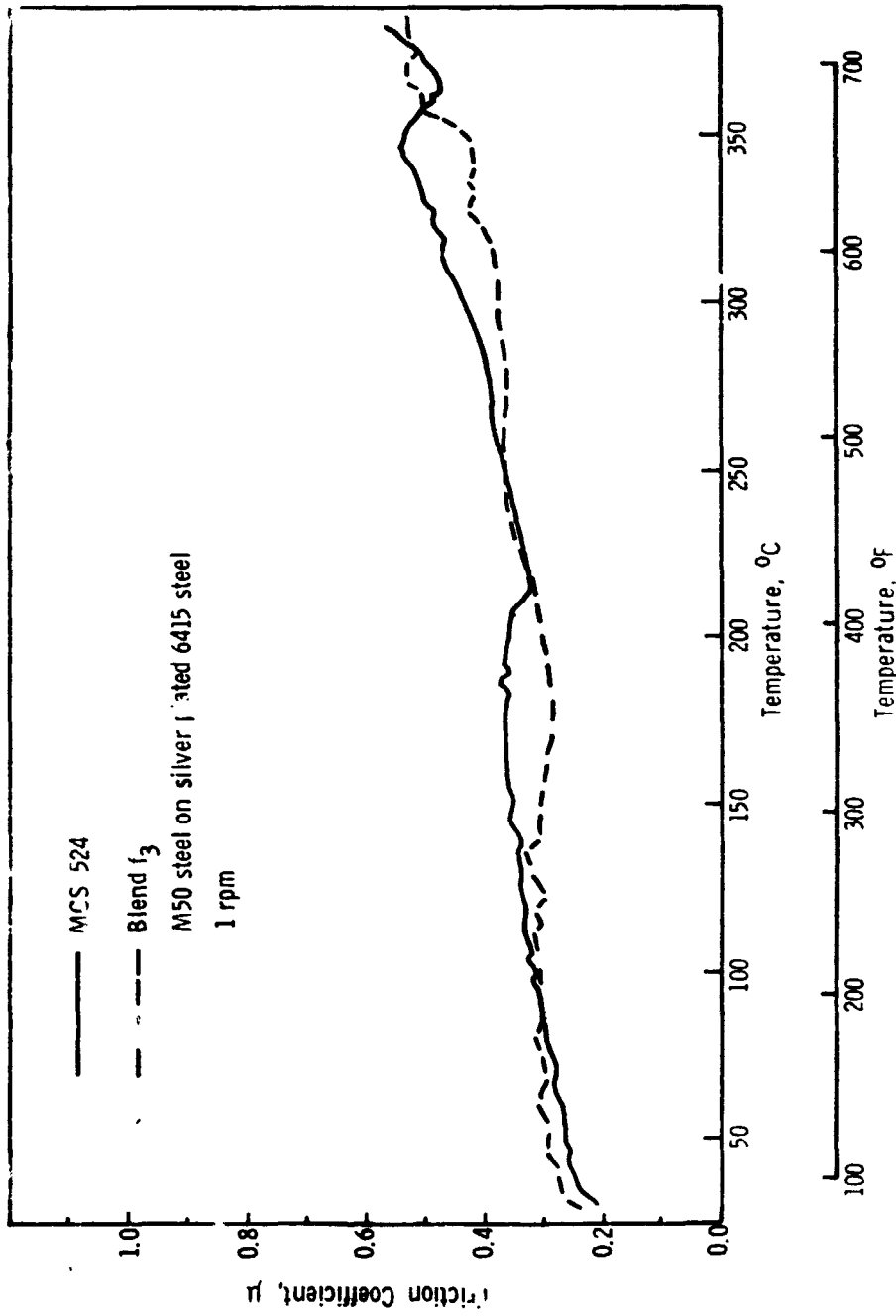
Figure E-4. Friction Curves for MCS 524 and Blend f_3
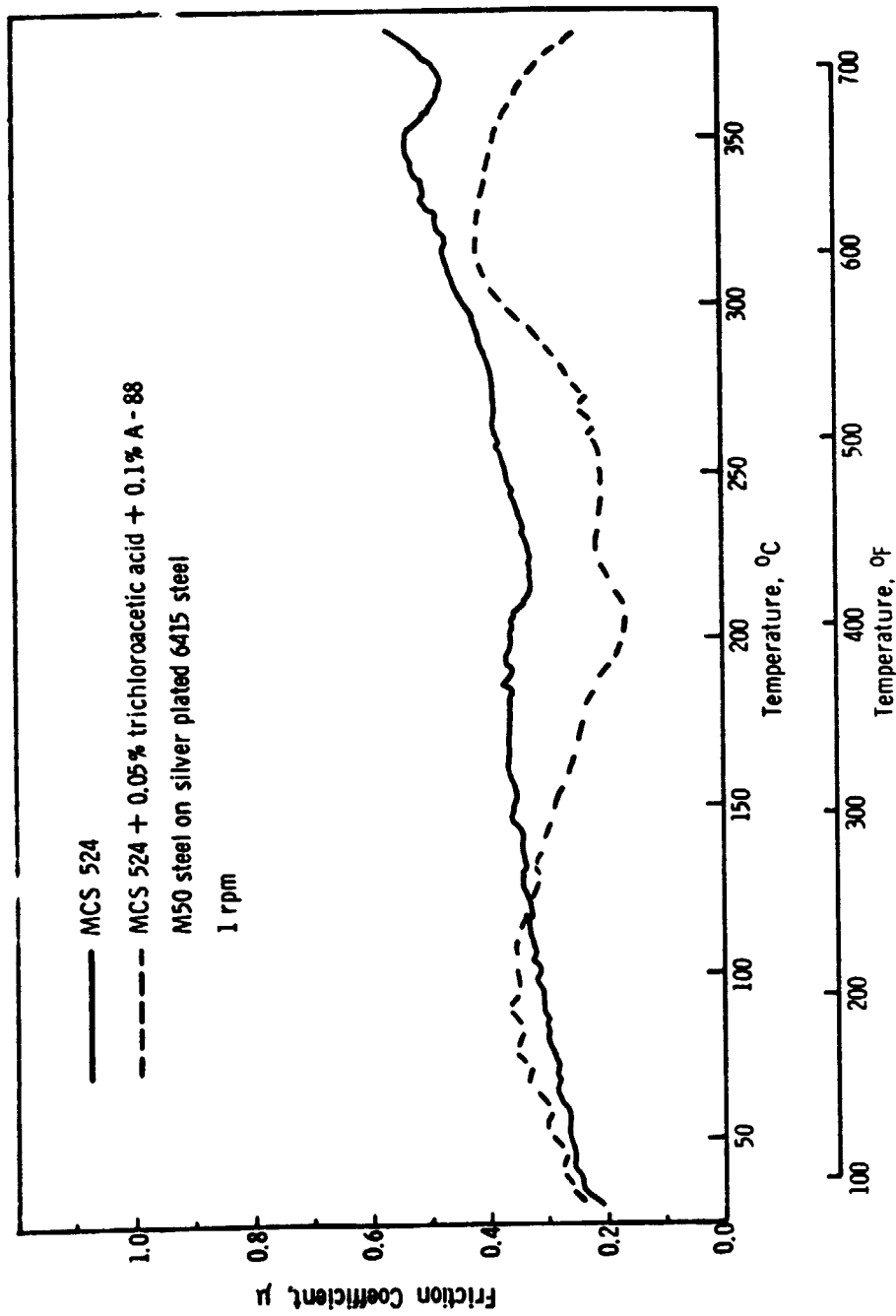
Figure E-5. Friction Curves for MCS 524 and MCS 524 + 0.05% Trichloroacetic Acid + 0.1% A-88

198

Figure E-6.   Friction Curves for MCS 524 and MCS 524 + ~0.07% Perfluoroglutaric Acid
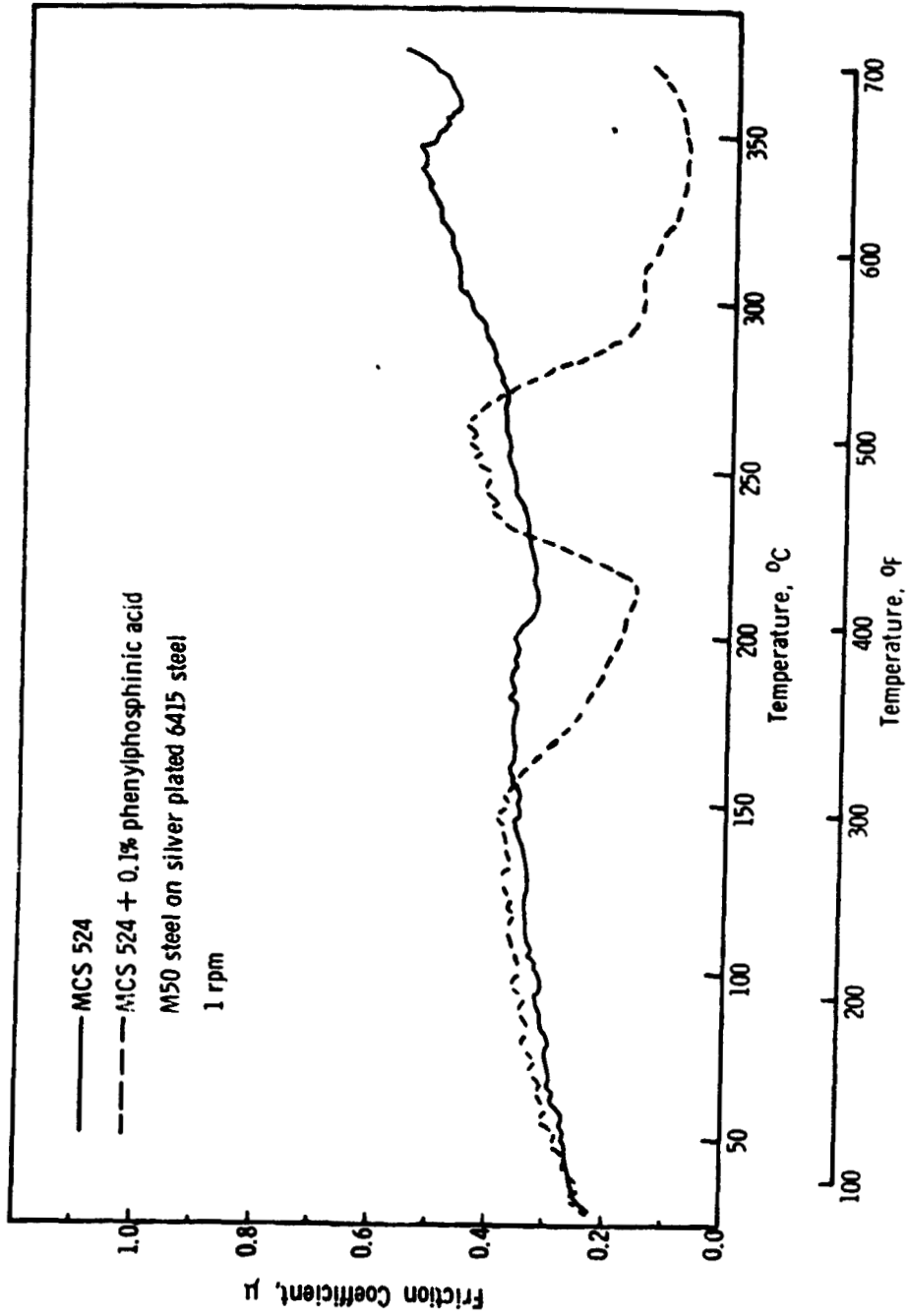
Figure E-7. Friction Curves for MCS 524 and MCS 524 + 0.1% Phenylphosphinic Acid
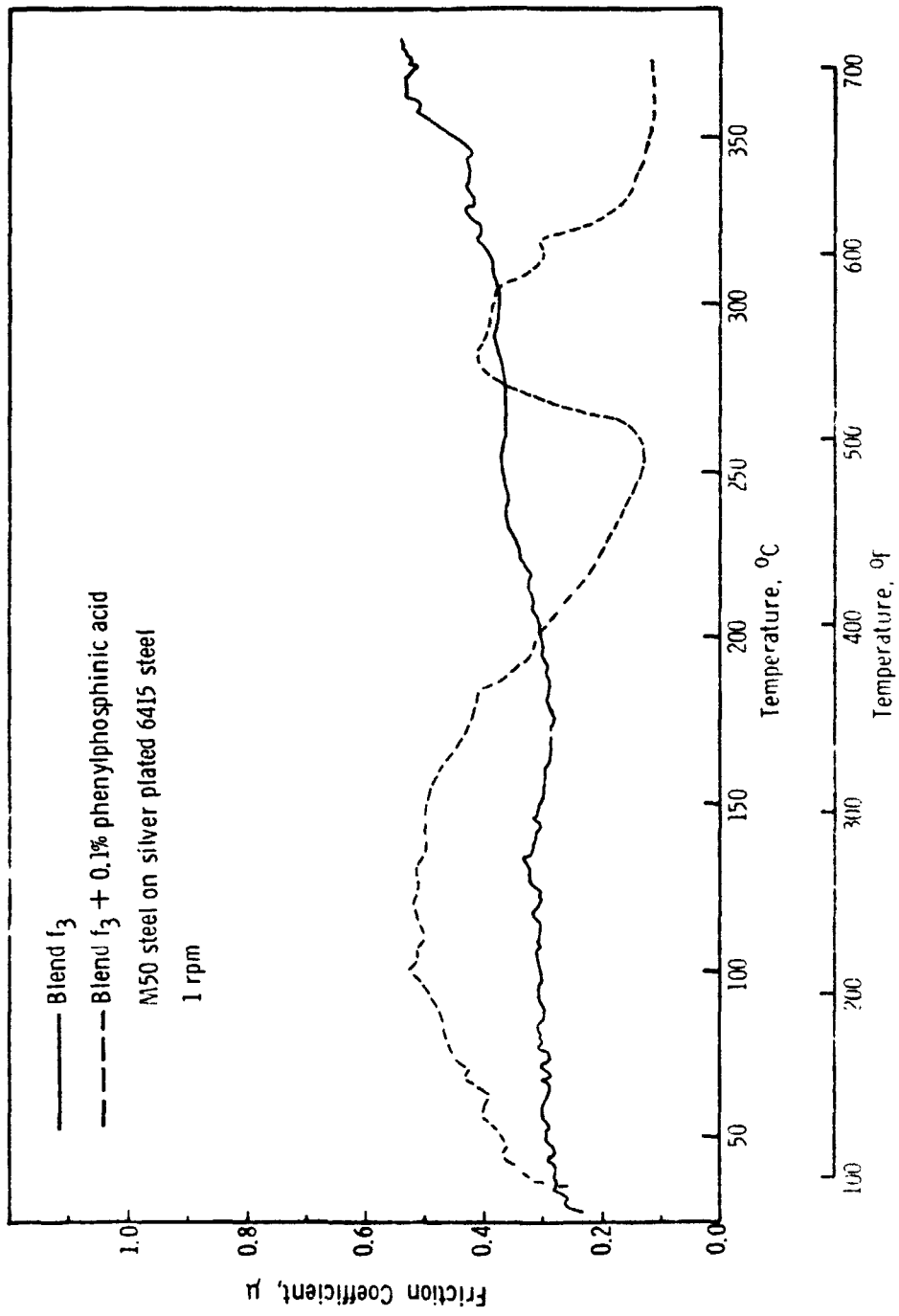
Figure E-8. Friction Curves for Blend f_3 and Blend f_3 + 0.1% Phenylphosphinic Acid
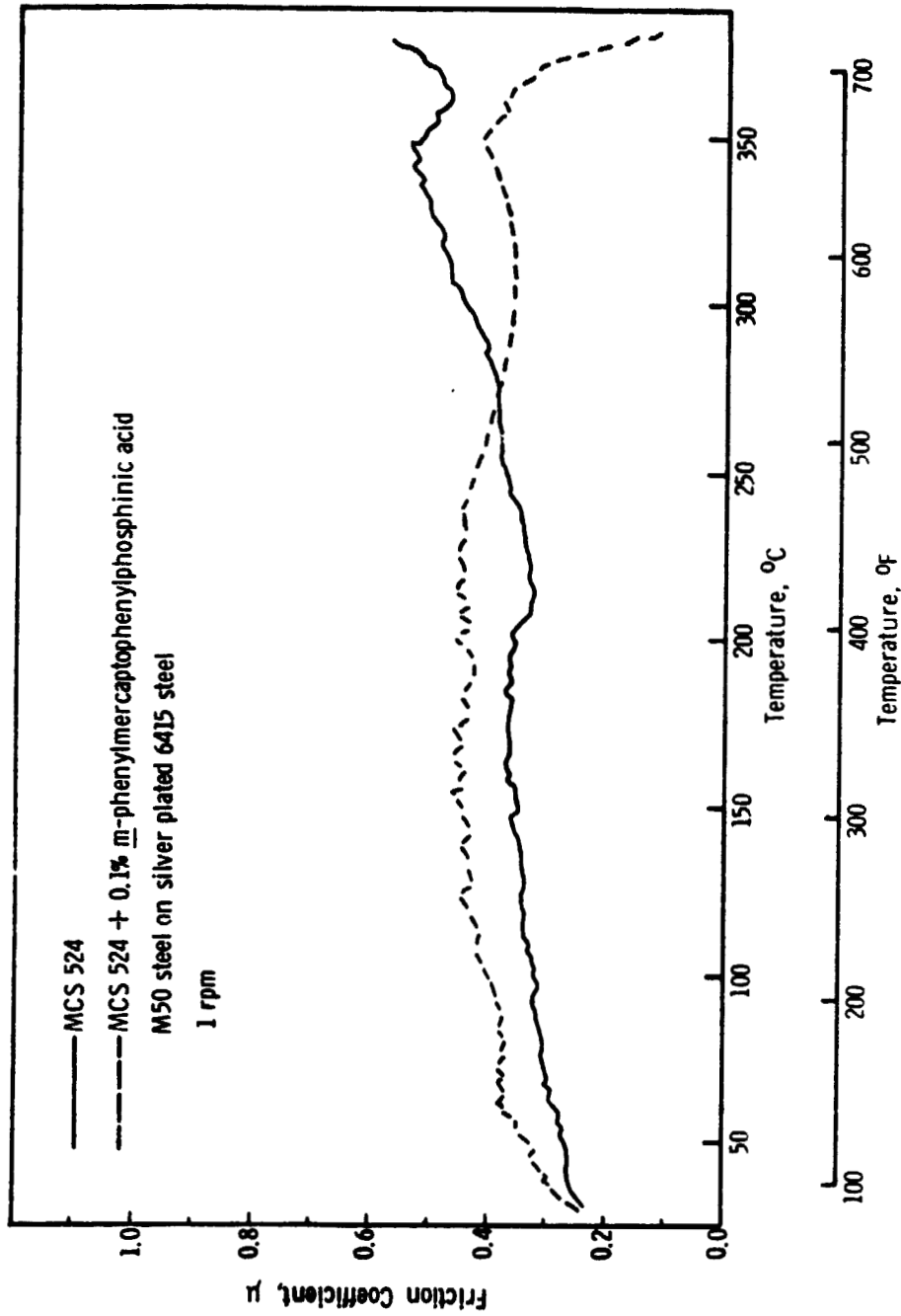
Figure E-9. Friction Curves for MCS 524 and MCS 524
+ 0.1% m-Phenylmercaptophenylphosphinic Acid

202
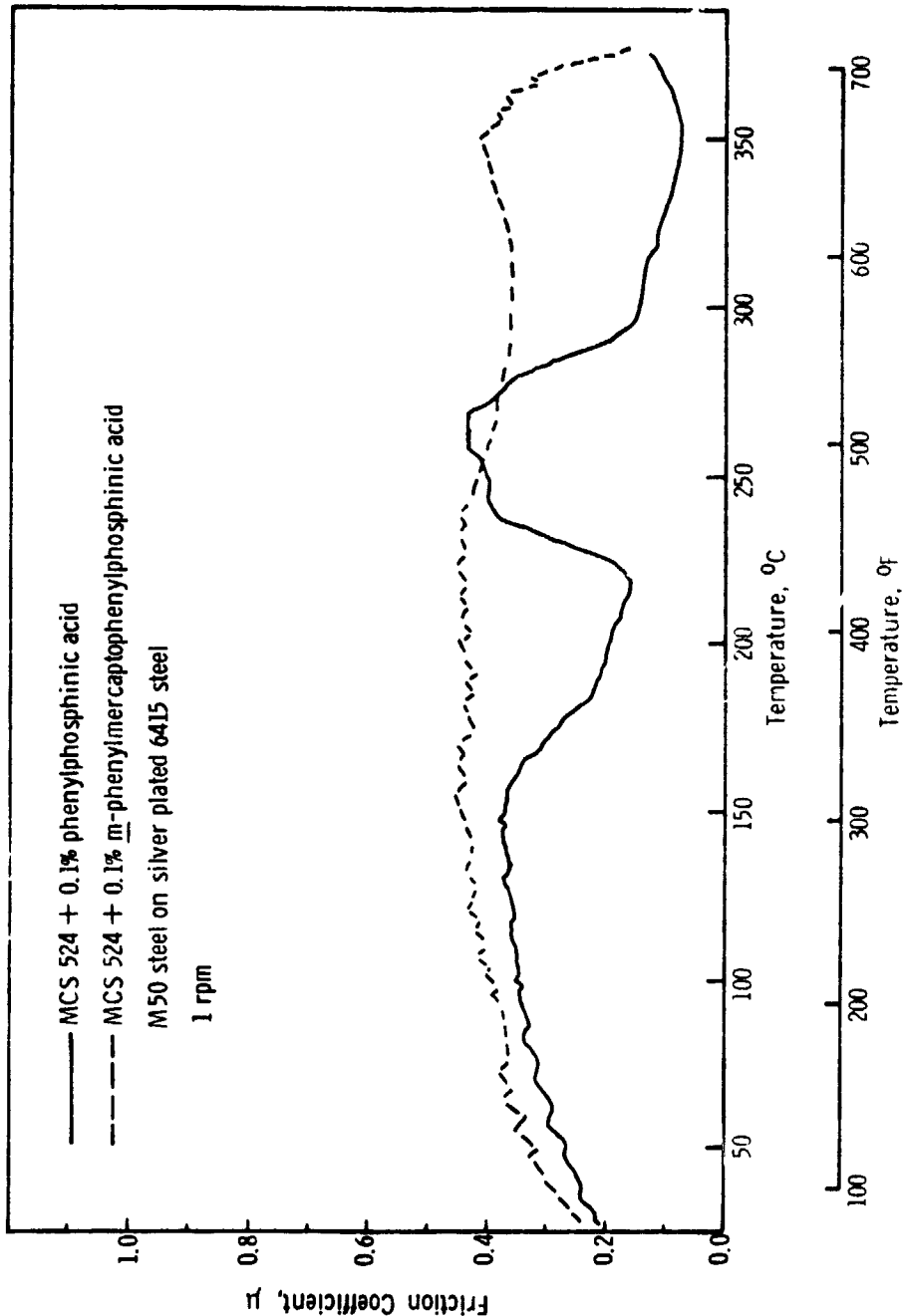
Figure E-10. Friction Curves for MCS 524 + 0.1% Phenylphosphinic Acid and MCS 524 + 0.1% m-Phenylmercaptophenylphosphinic Acid

203
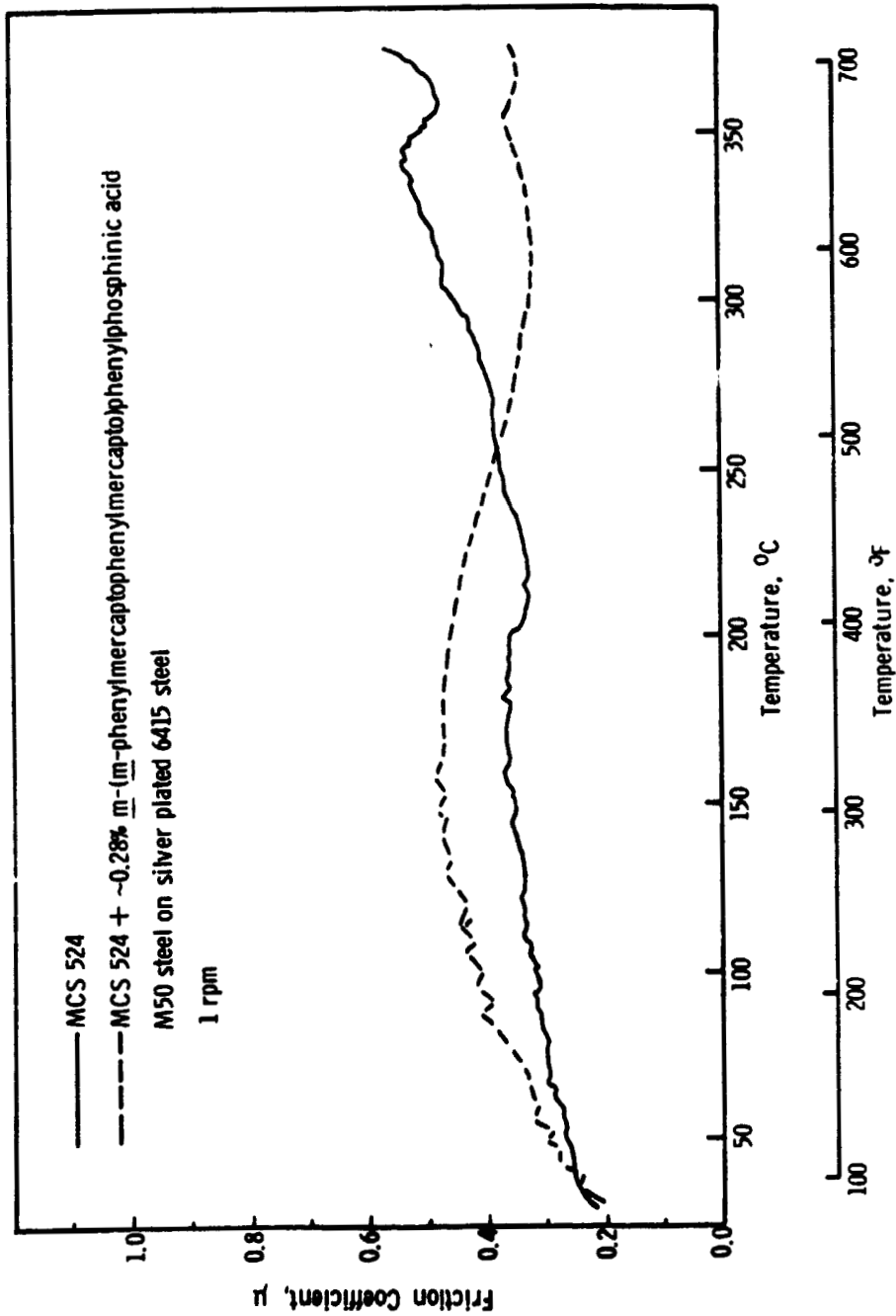
Figure E-11. Friction Curves for MCS 524 and MCS 524 + ~0.28% m-(m-Phenyl-mercaptophenylmercapto)phenylphosphinic Acid

204
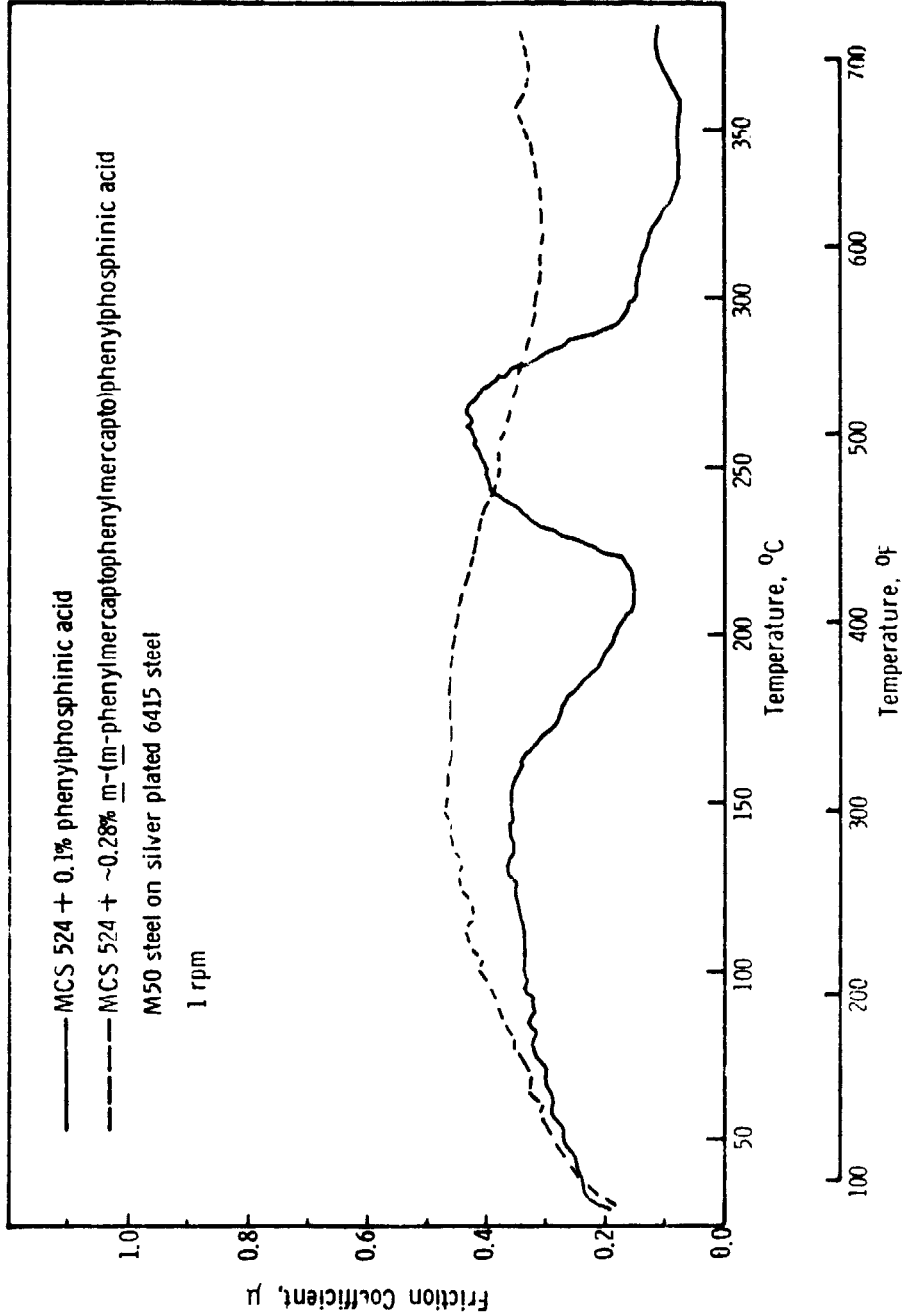
Figure E-12. Friction Curves for MCS 5.4 + 0.1% Phenylphosphinic Acid and MCS 524 + ~0.28% m-(m-Phenylmercaptophenylmercapto)- phenylphosphinic Acid

205
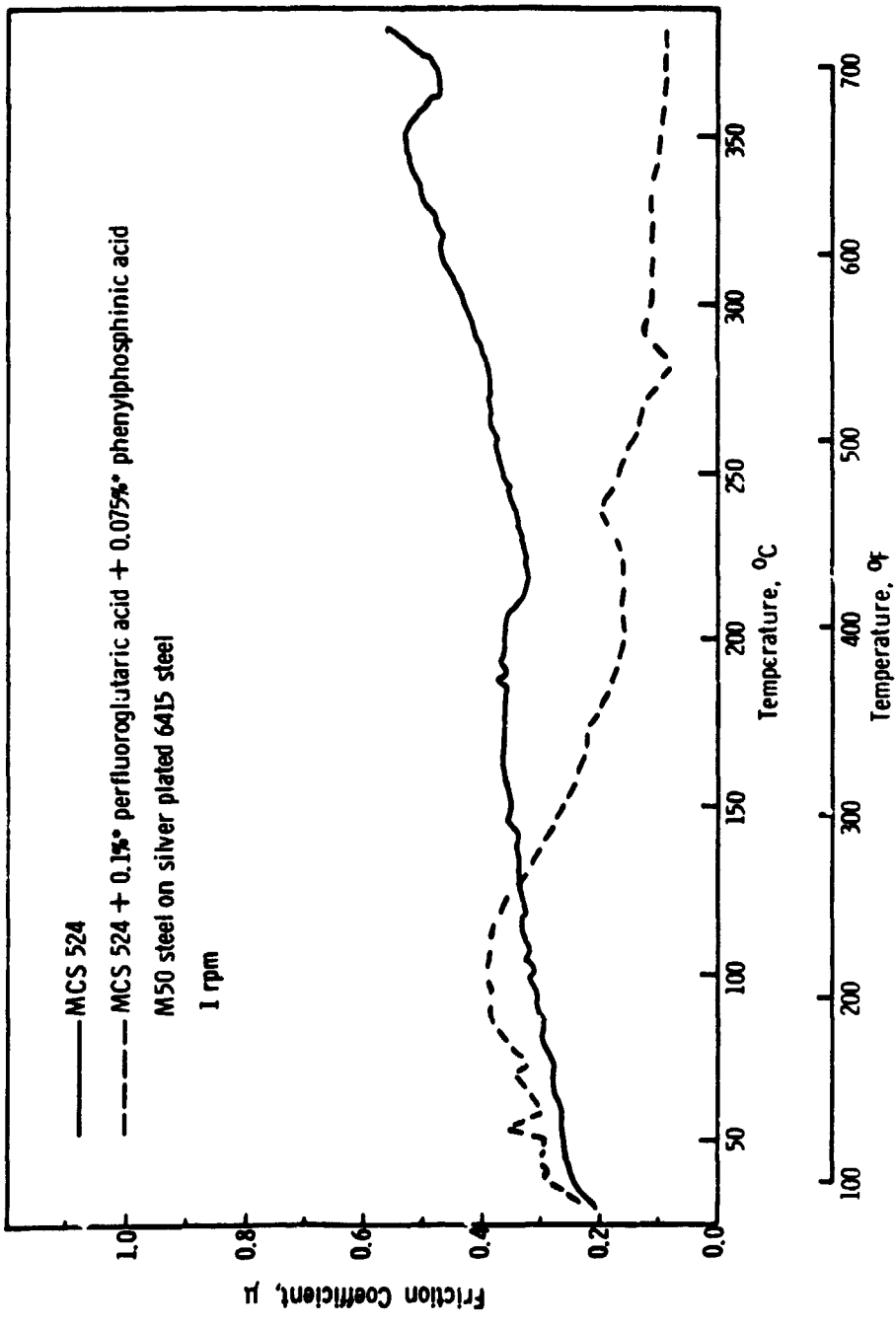
Figure E-13.   Friction Curves for MCS 524 and MCS 524 + 0.18* Per-
fluoroglutaric Acid + 0.075%* Phenylphosphinic Acid

*Initial additive charge.

206
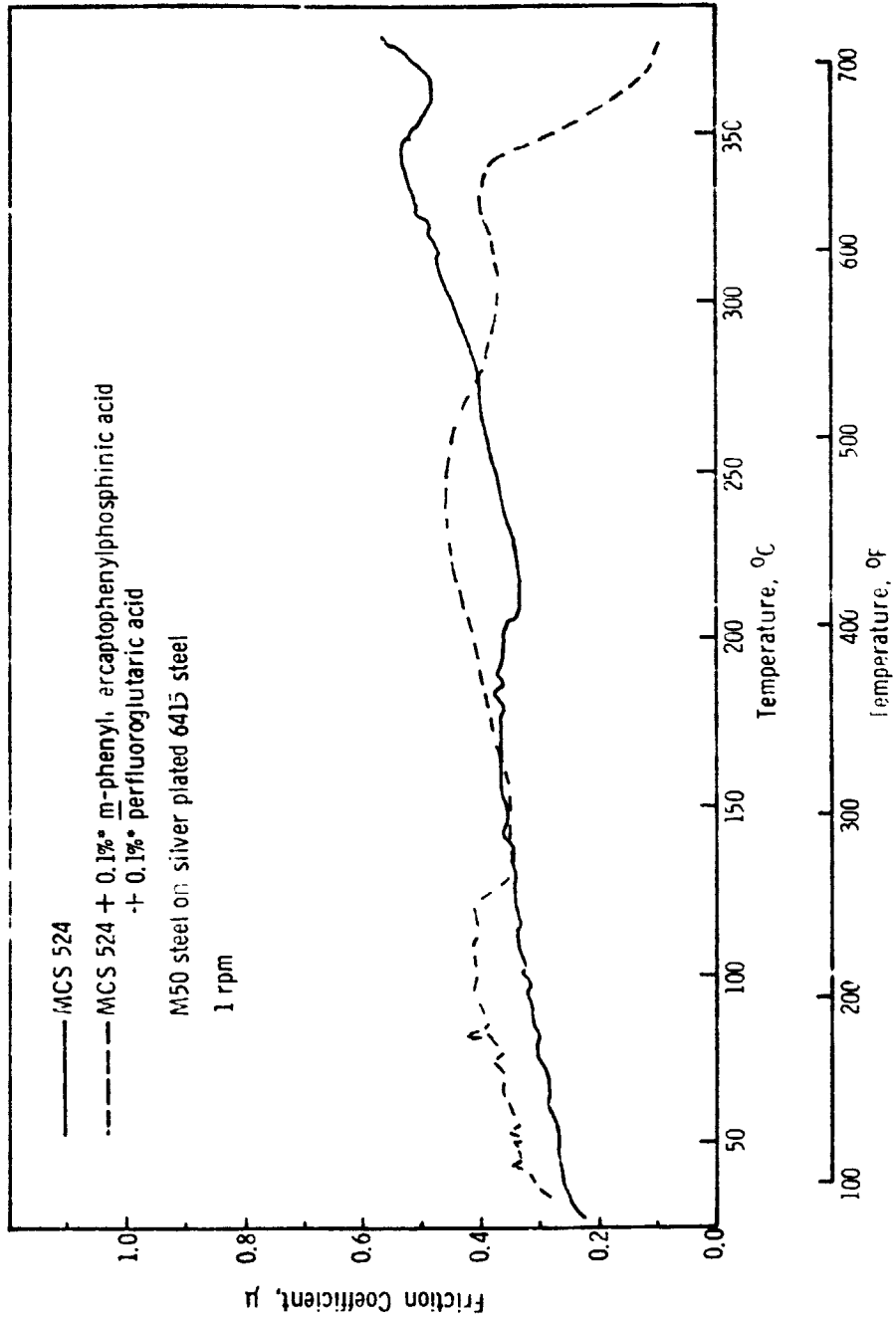
Figure E-14. Friction Curves for MCS 524 and MCS 524 + 0.1%* m-Phenylmer-captophenylphosphinic Acid + 0.1%* Perfluoroglutaric Acid

----
*Initial additive charge.

207
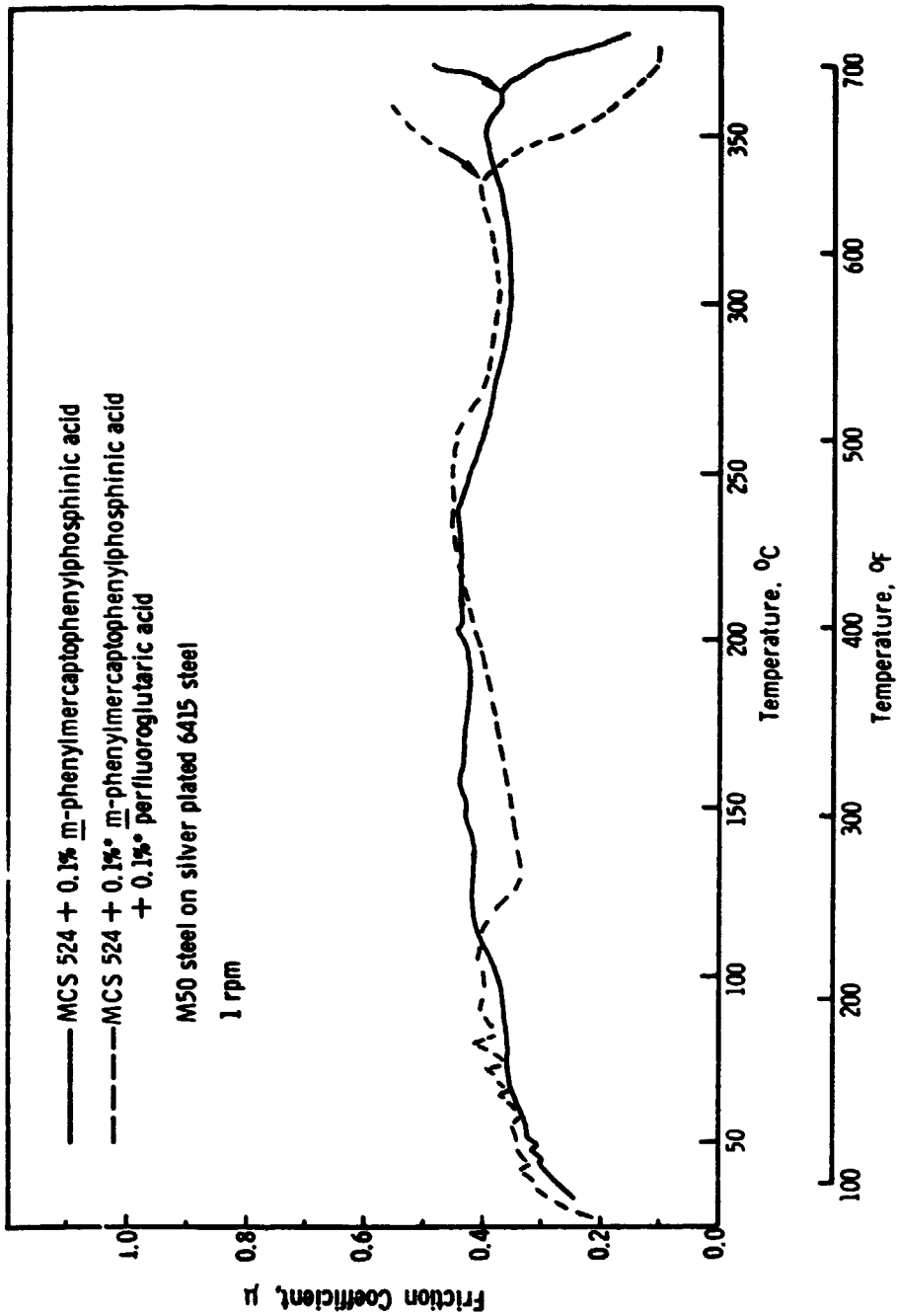
Figure E-15. Friction Curves for MCS 524 + 0.1% m-Phenylmercaptophenylphosphinic Acid and MCS 524 + 0.1* m-Phenylmercaptophenylphosphinic Acid + 0.1%* Perfluoroglutaric Acid

*Initial additive charge.

208
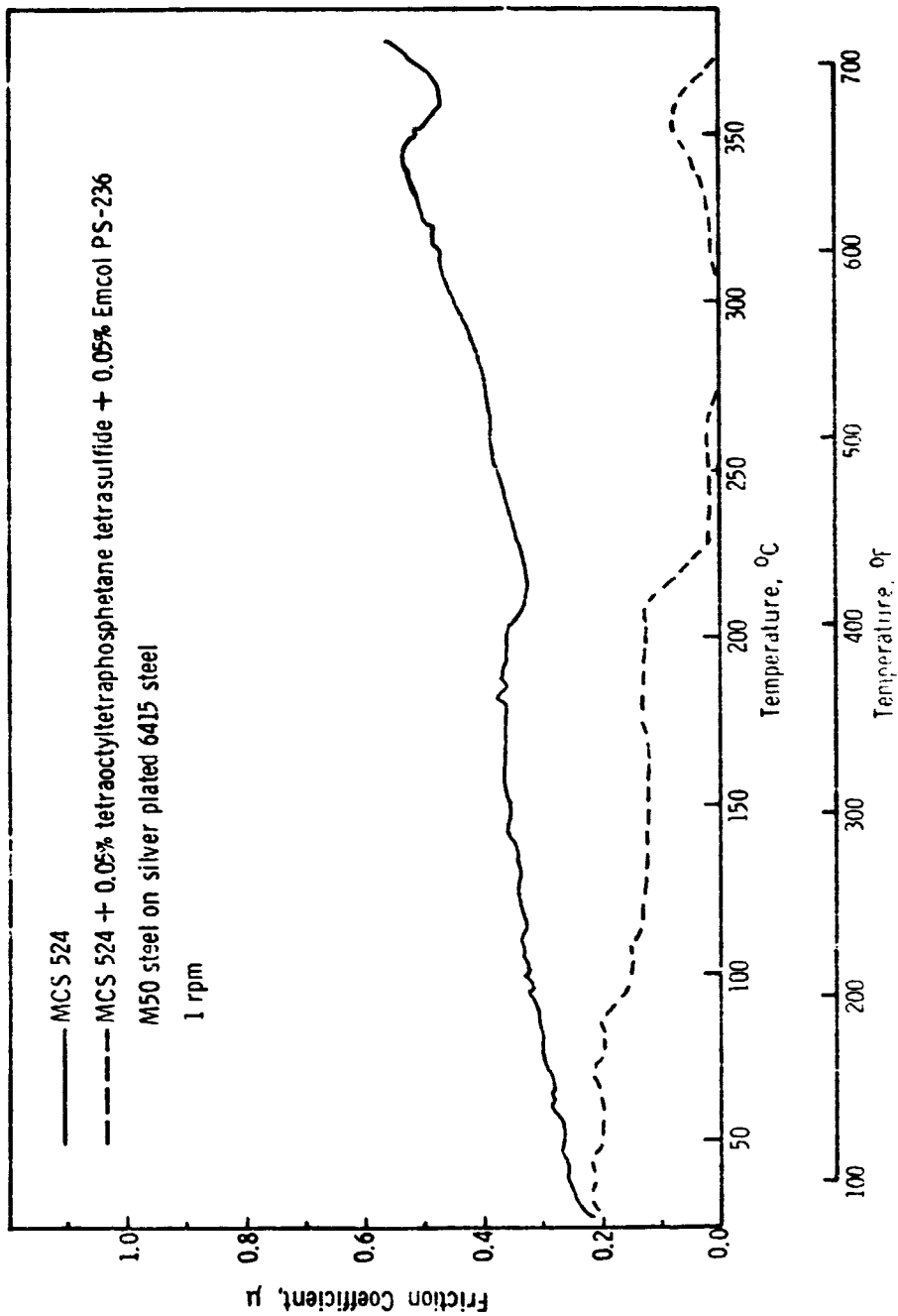
Figure E-16. Friction Curves for MCS 524 and MCS 524 + 0.05% Tetraoctyl-tetraphosphetane Tetrasulfide + 0.05% Emcol PS-236
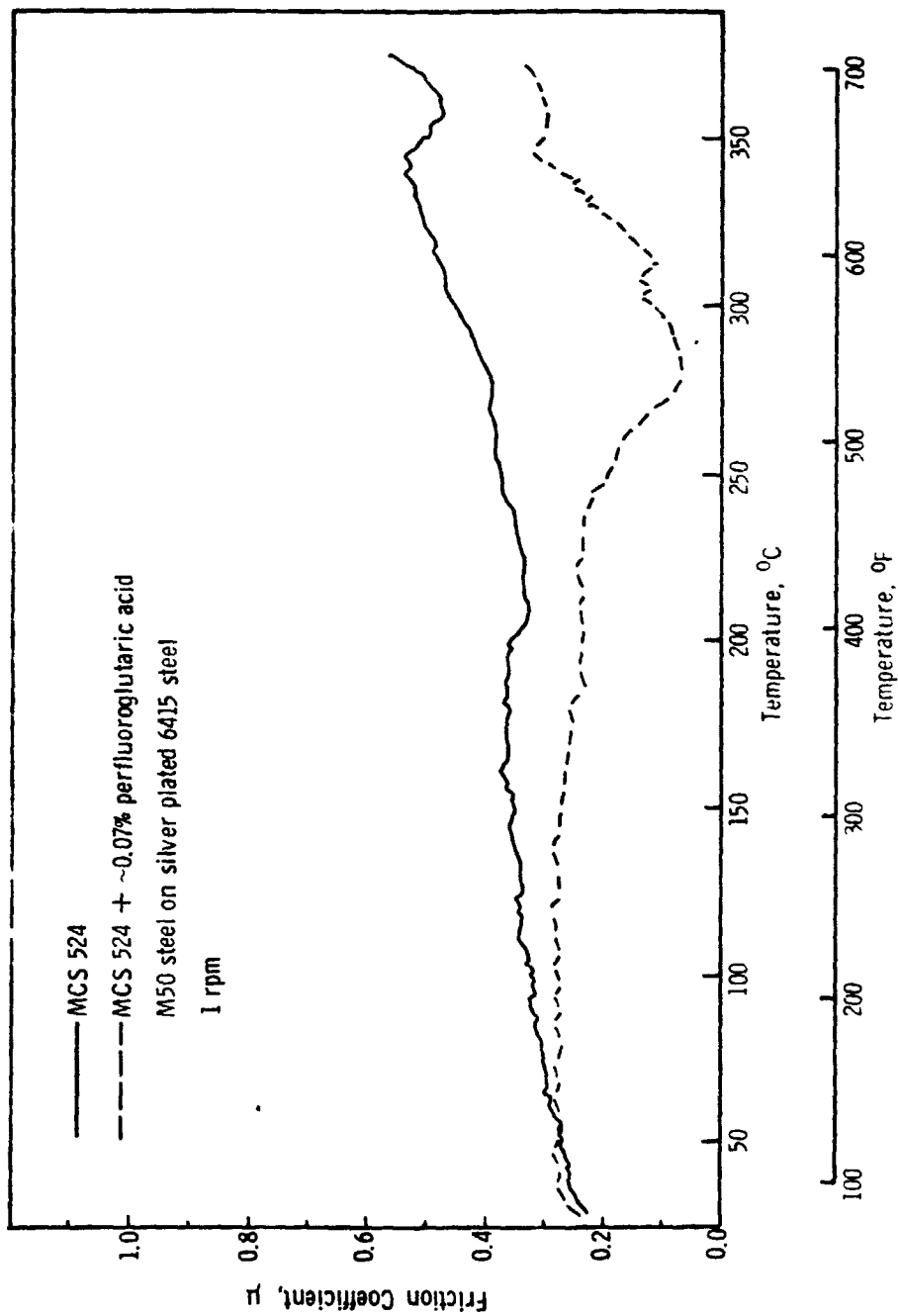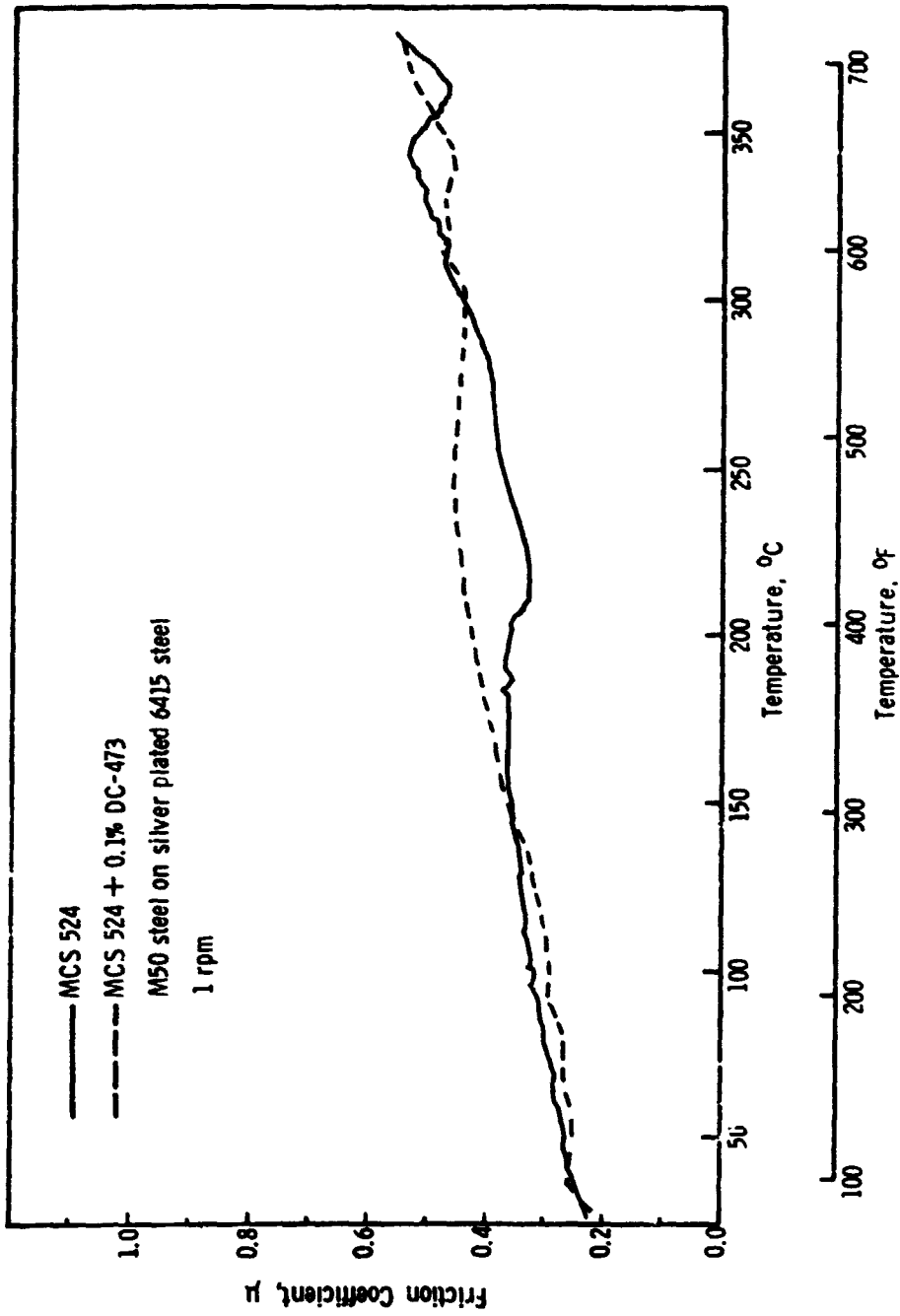
Figure II-17. Friction Curves for MCS 524 and MCS 524 + 0.1% DC-473

210
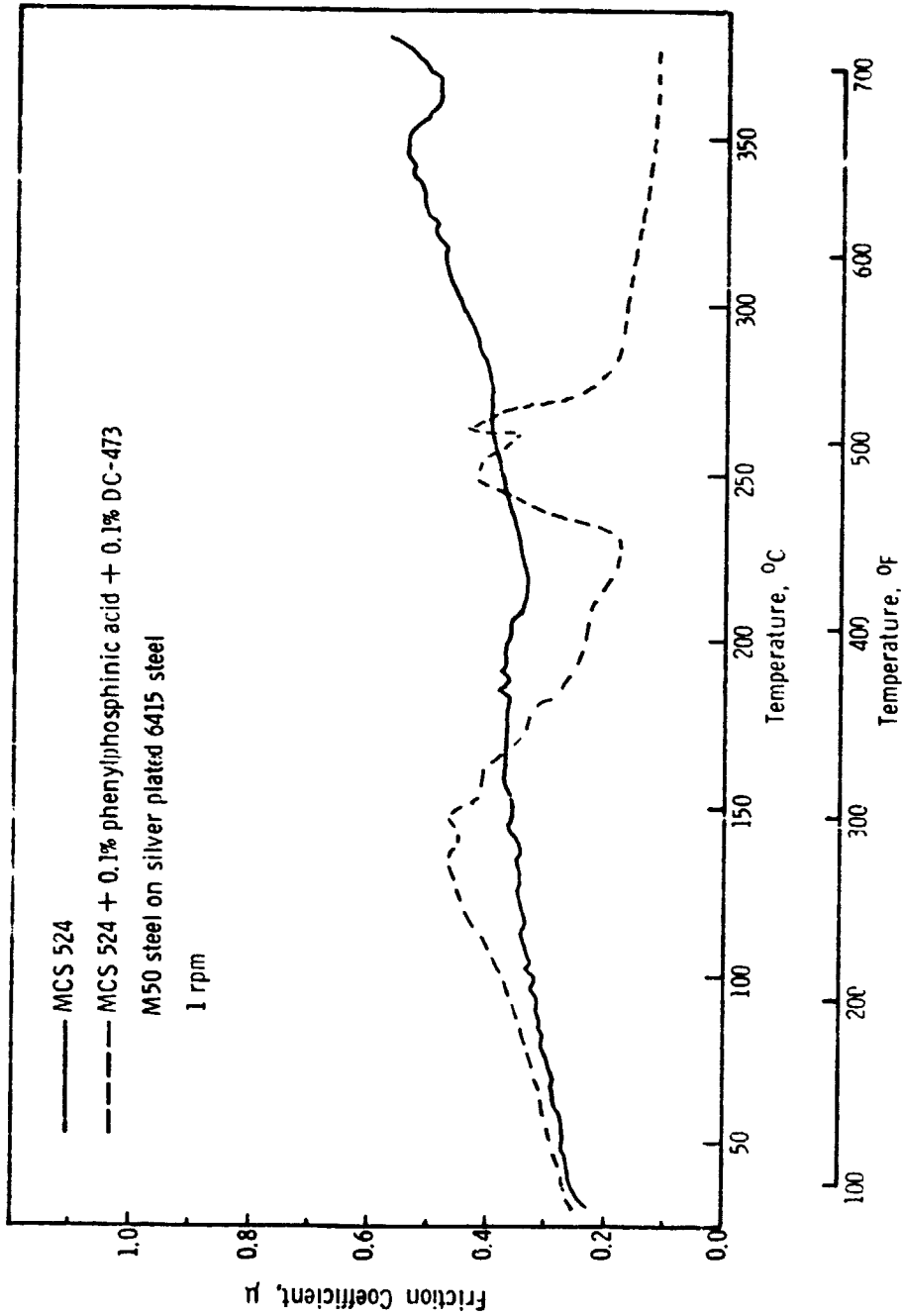
Figure E-18. Friction Curves for MCS 524 and MCS 524 + 0.1% Phenylphosphinic Acid + 0.1% DC-473

211
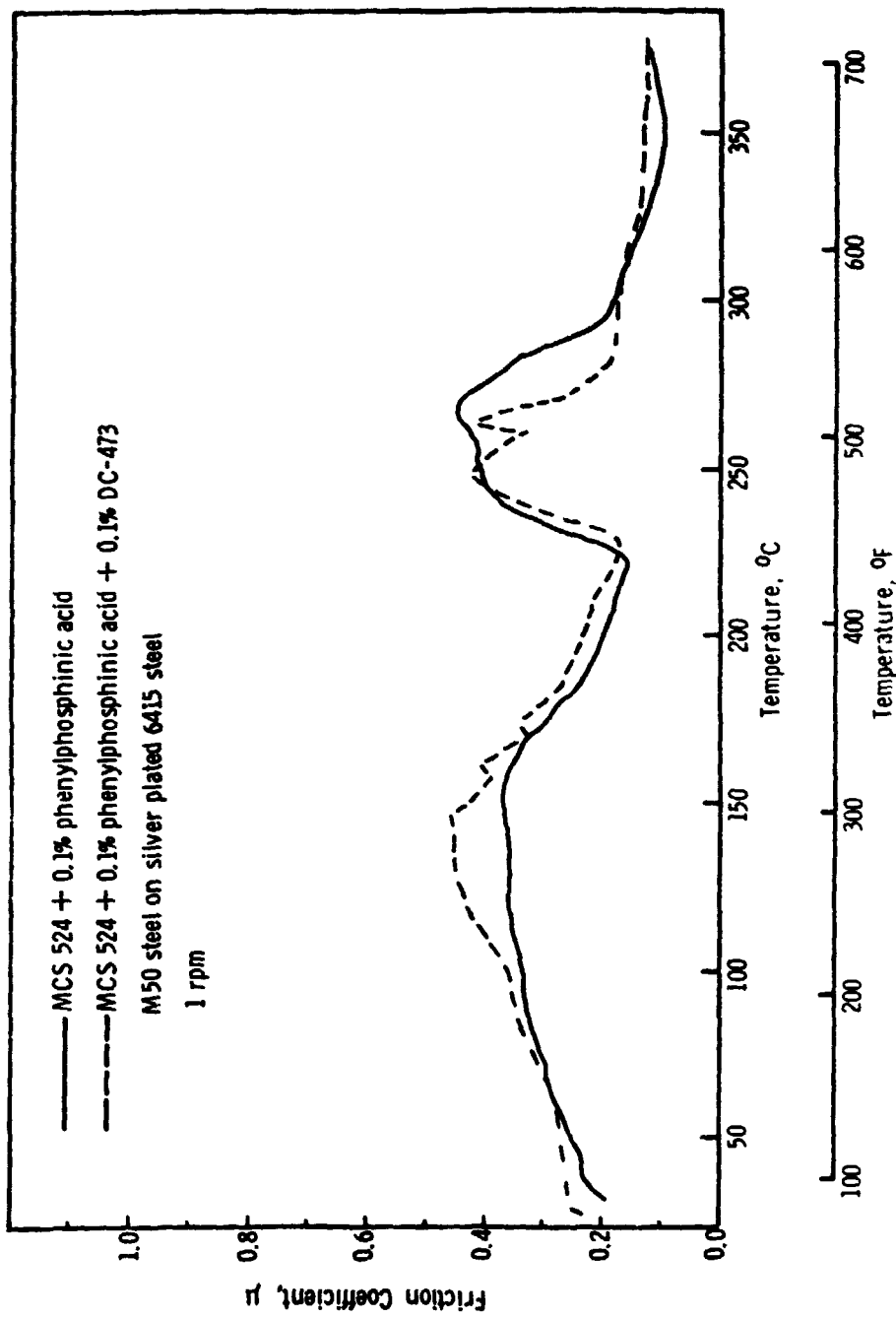
Figure E-19. Friction Curves for MCS 524 + 0.1% Phenylphosphinic Acid
and MCS 524 + 0.1% Phenylphosphinic Acid + 0.1% DC-473

212
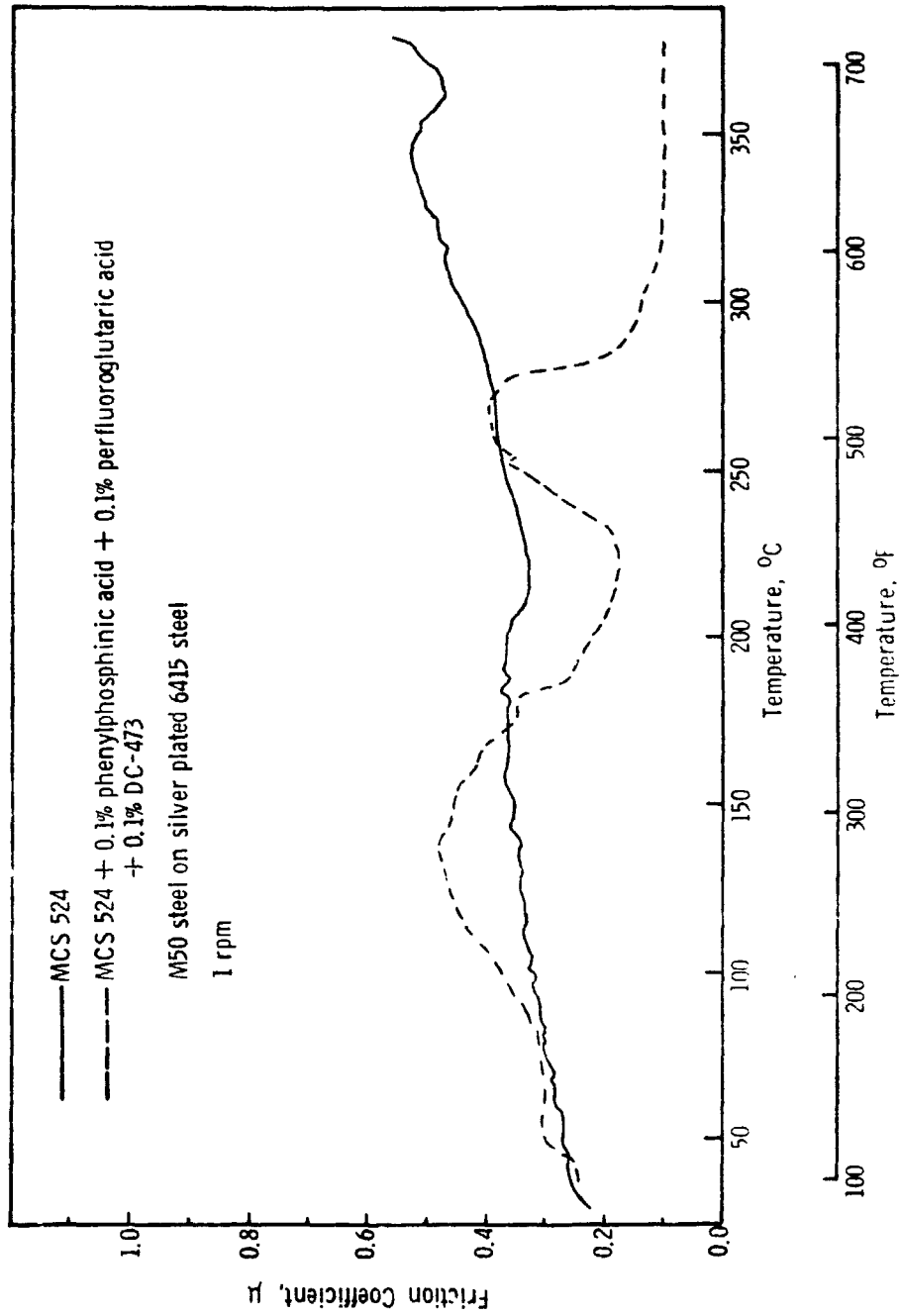
Figure E-20. Friction Curves for MCS 524 and MCS 524 + 0.1% Phenylphos-phinic Acid + 0.1% Perfluoroglutaric Acid + 0.1% DC-473

213
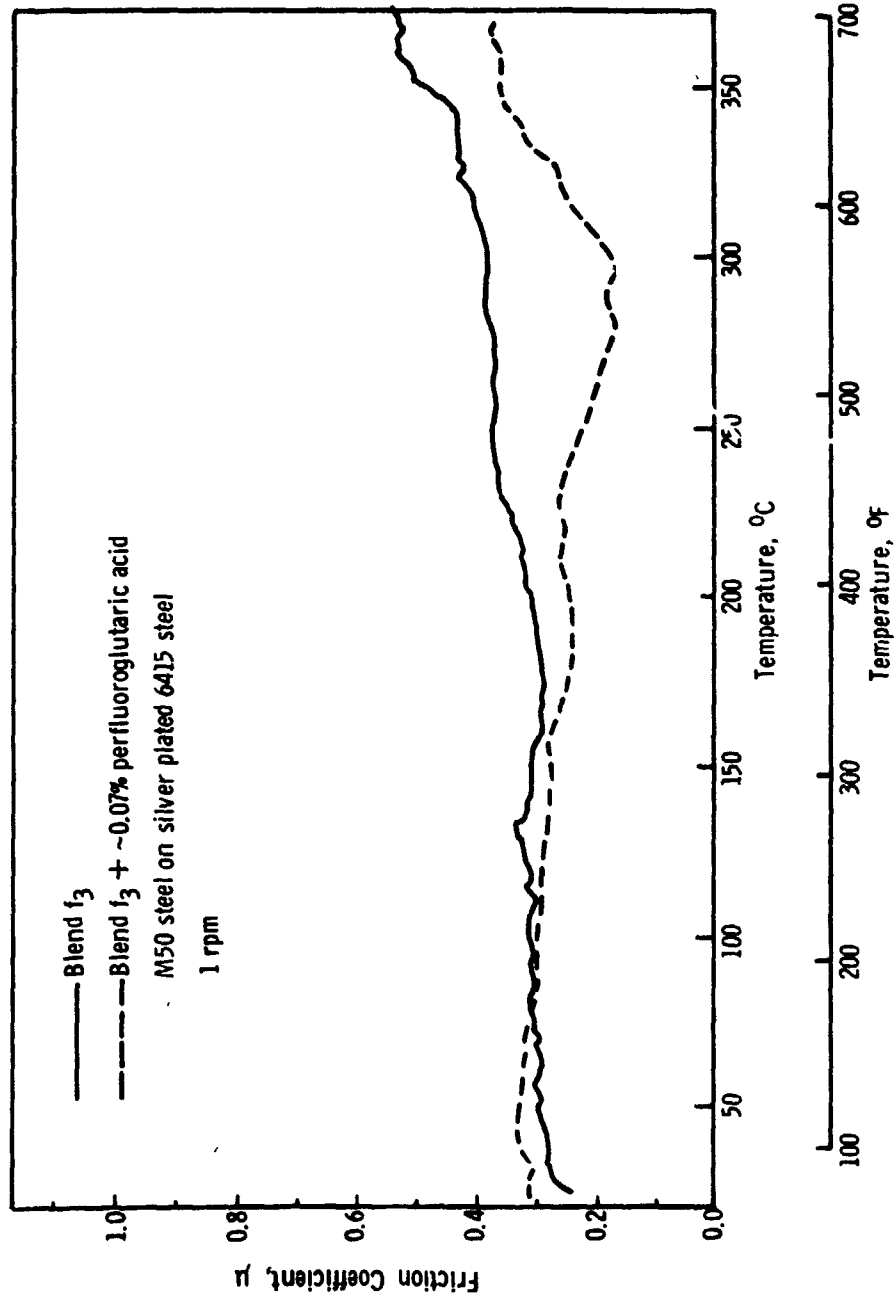
Figure E-21. Friction Curves for Blend f_3 and Blend f_3 + ~0.07% Perfluoroglutaric Acid

214
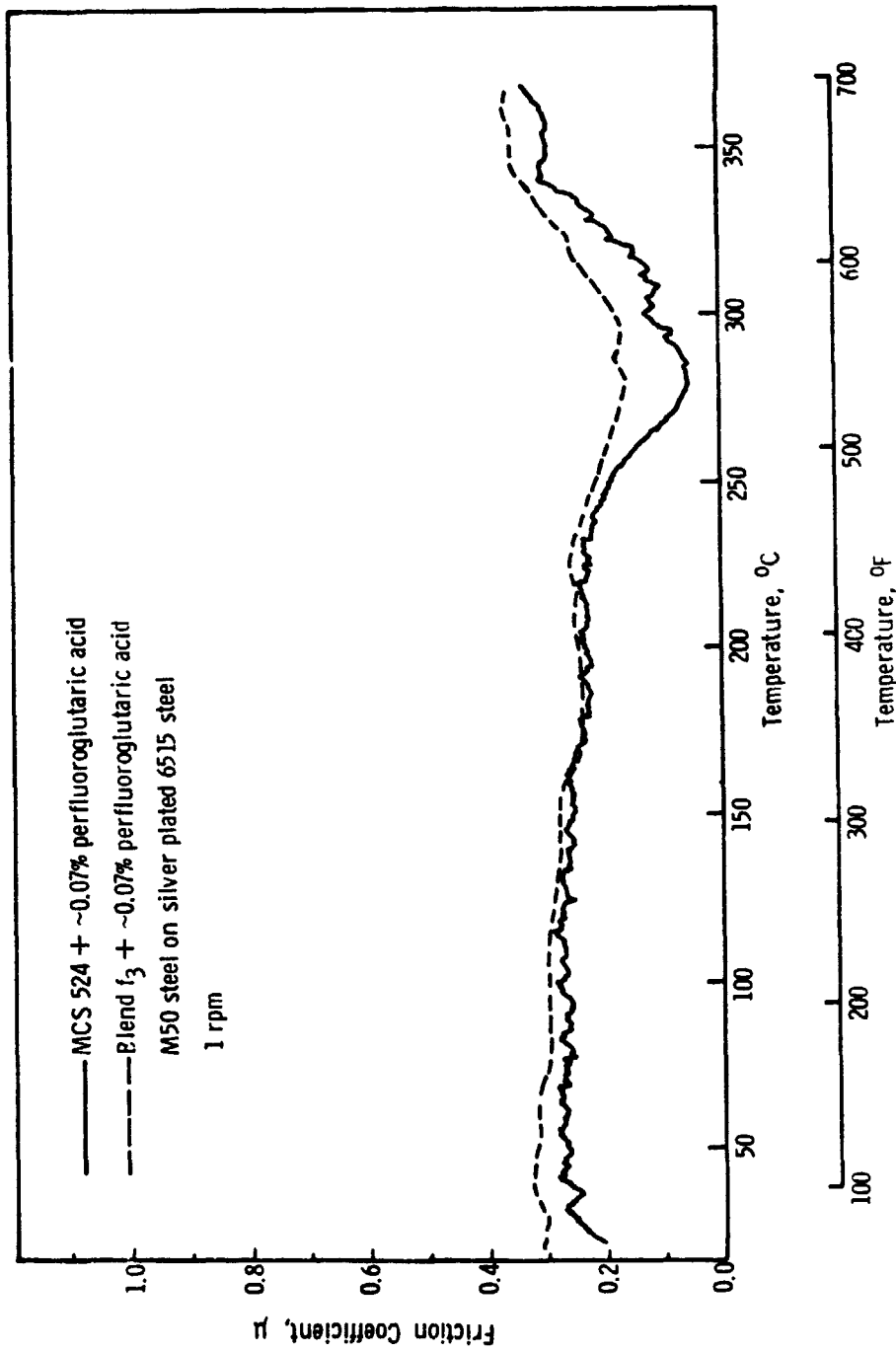
Figure E-22. Friction Curves for MCS 524 + ∿0.07% Perfluoroglutaric Acid and Blend f₃ + ∿0.07% Perfluoroglutaric Acid

APPENDIX F:

X-Y RECORDINGS OF RUB-BLOCK TESTS, M50

ON M50 IN AIR, 316°C (ONE TEST AT 260°C)
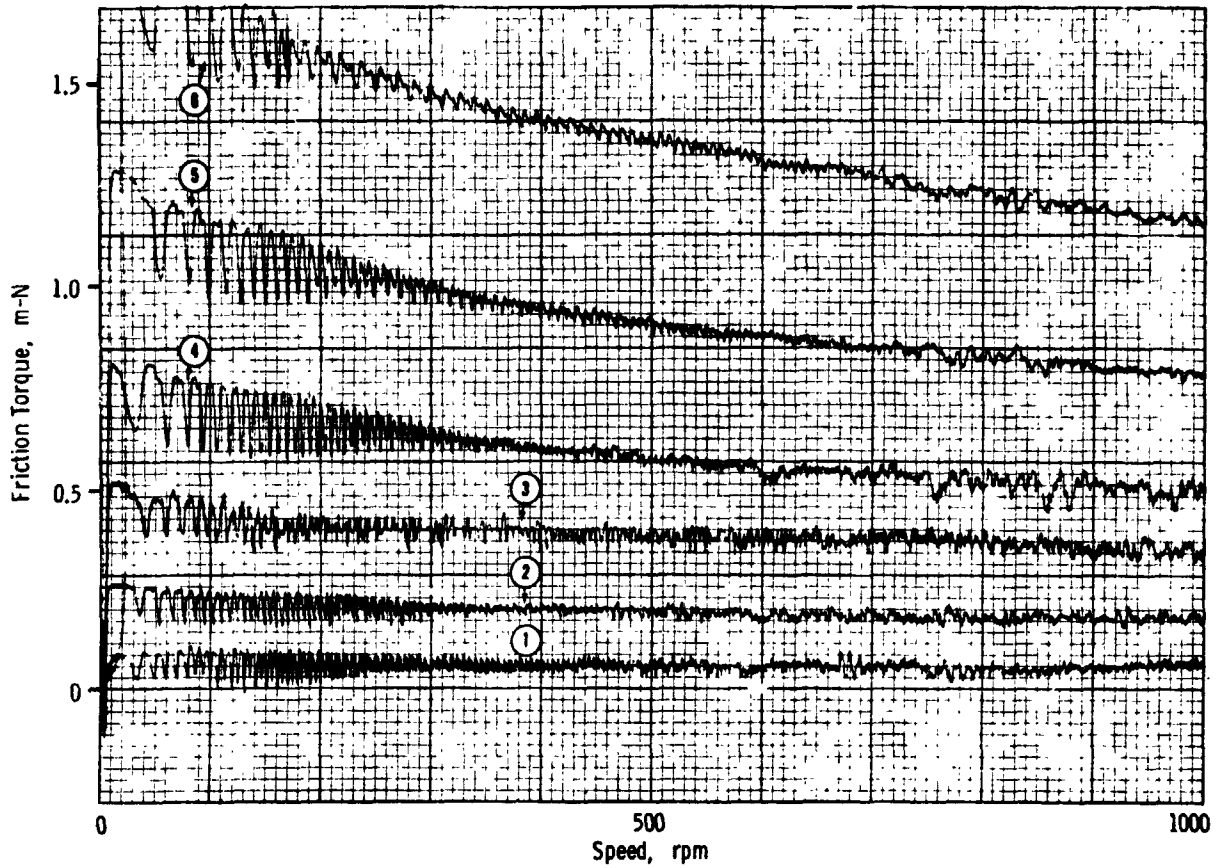
Loads, N/m^2

1. 2.07 x 10^5 (30 psi) (contact)
2. 2.76 x 10^5 (40 ")
3. 3.79 x 10^5 (55 ")
4. 5.17 x 10^5 (75 ")
5. 7.24 x 10^5 (105 ")
6. 1.03 x 10^6 (150 ")

Test Temp.: 260°C (500°F)

Atmosphere: air

Figure F-1.   RBT No. 22, Fluid: Skylube 450
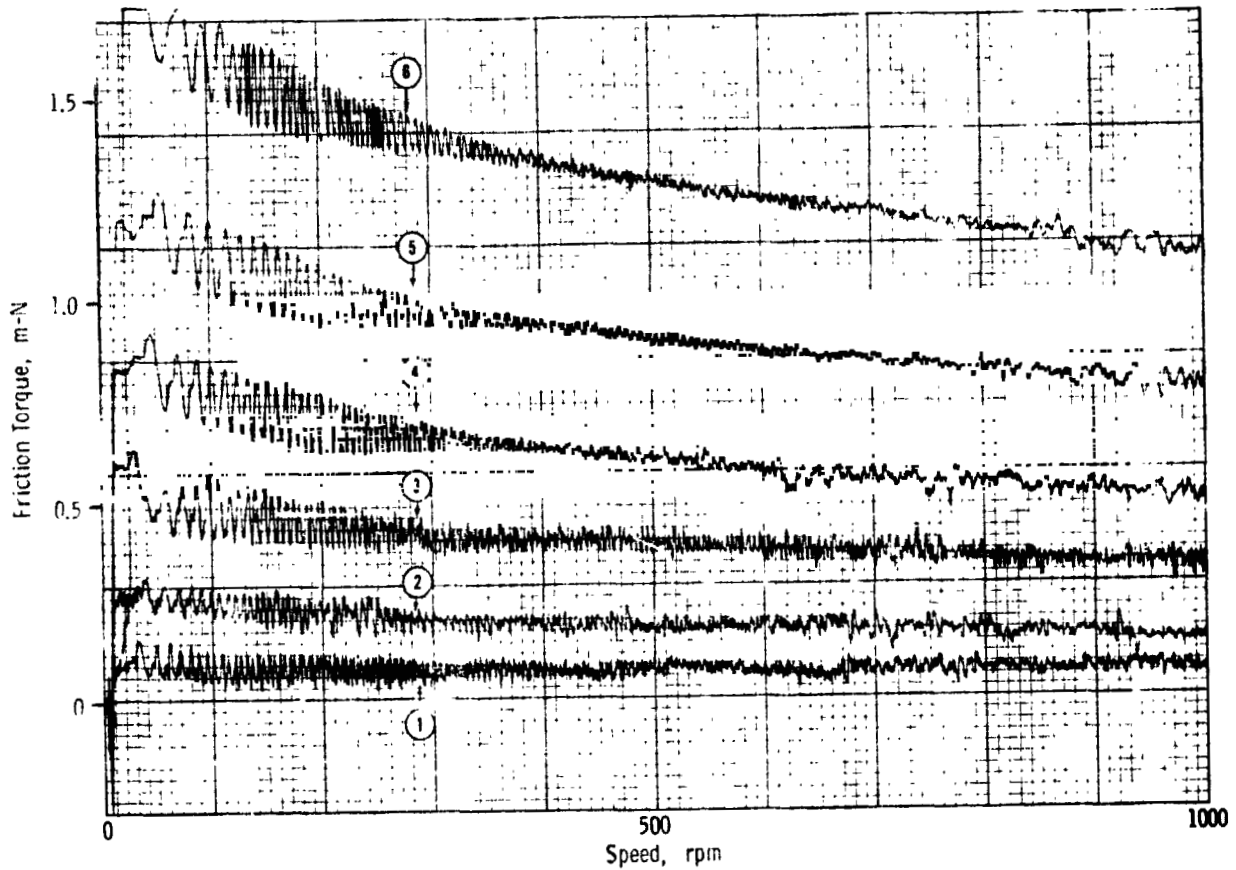
Loads, N/m²

1. 2.07 x 10⁵ (30 psi) (contact)
2. 2.76 x 10⁵ (40 ")
3. 3.79 x 10⁵ (55 ")
4. 5.17 x 10⁵ (75 ")
5. 7.24 x 10⁵ (105 ")
6. 1.03 x 10⁶ (150 ")

Test Temp.:   316°C (600°F)

Atmosphere: air

Figure F-2.   RBT No. 24, Fluid: MCS 524
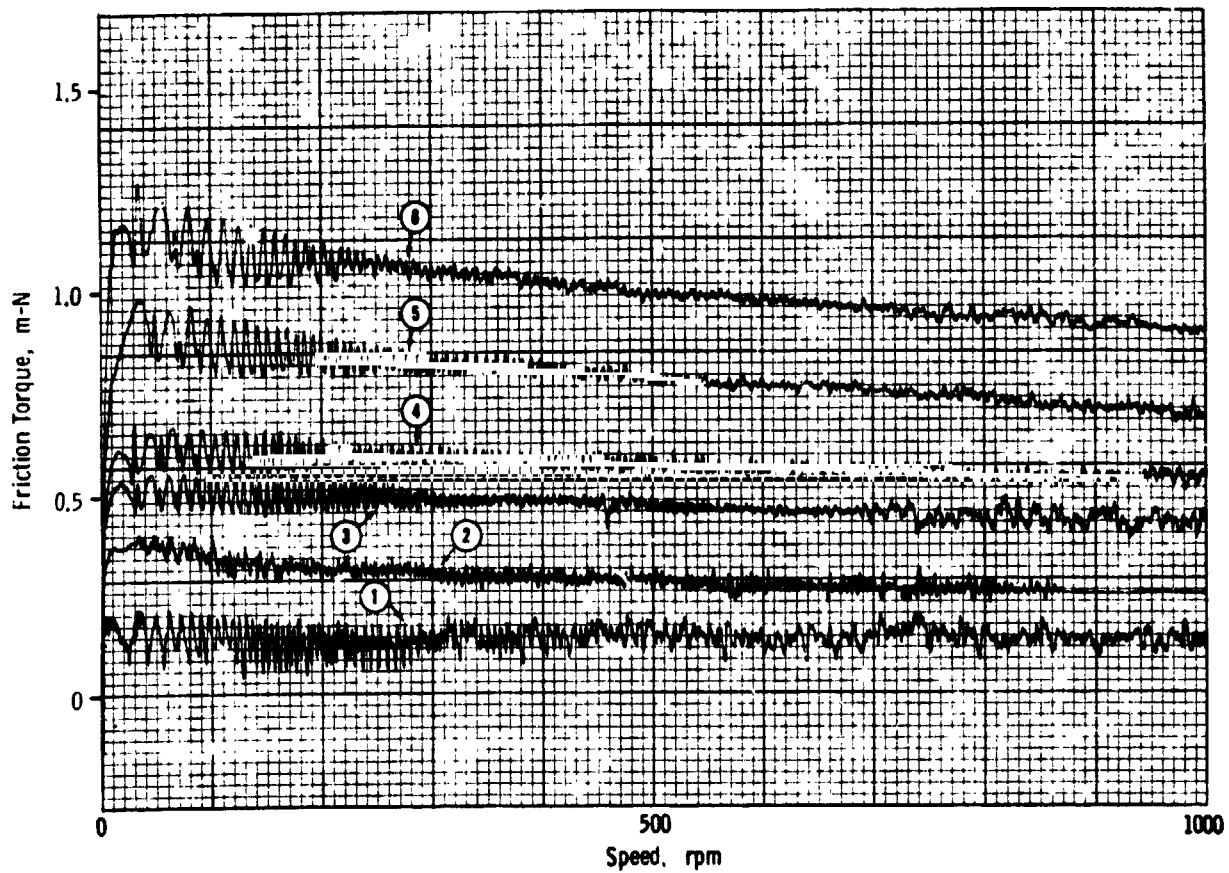
Figure F-3. RBT No. 26, Fluid: FH-140

Loads, N/m^2

1. 2.07×10^5 (30 psi) (contact)
2. 2.76×10^5 (40 ")
3. 3.79×10^5 (55 ")
4. 5.17×10^5 (75 ")
5. 7.24×10^5 (105 ")
6. 1.03×10^6 (150 ")

Test Temp.: 316°C (600°F)

Atmosphere: air

Figure F-3. RBT No. 26, Fluid: FH-140
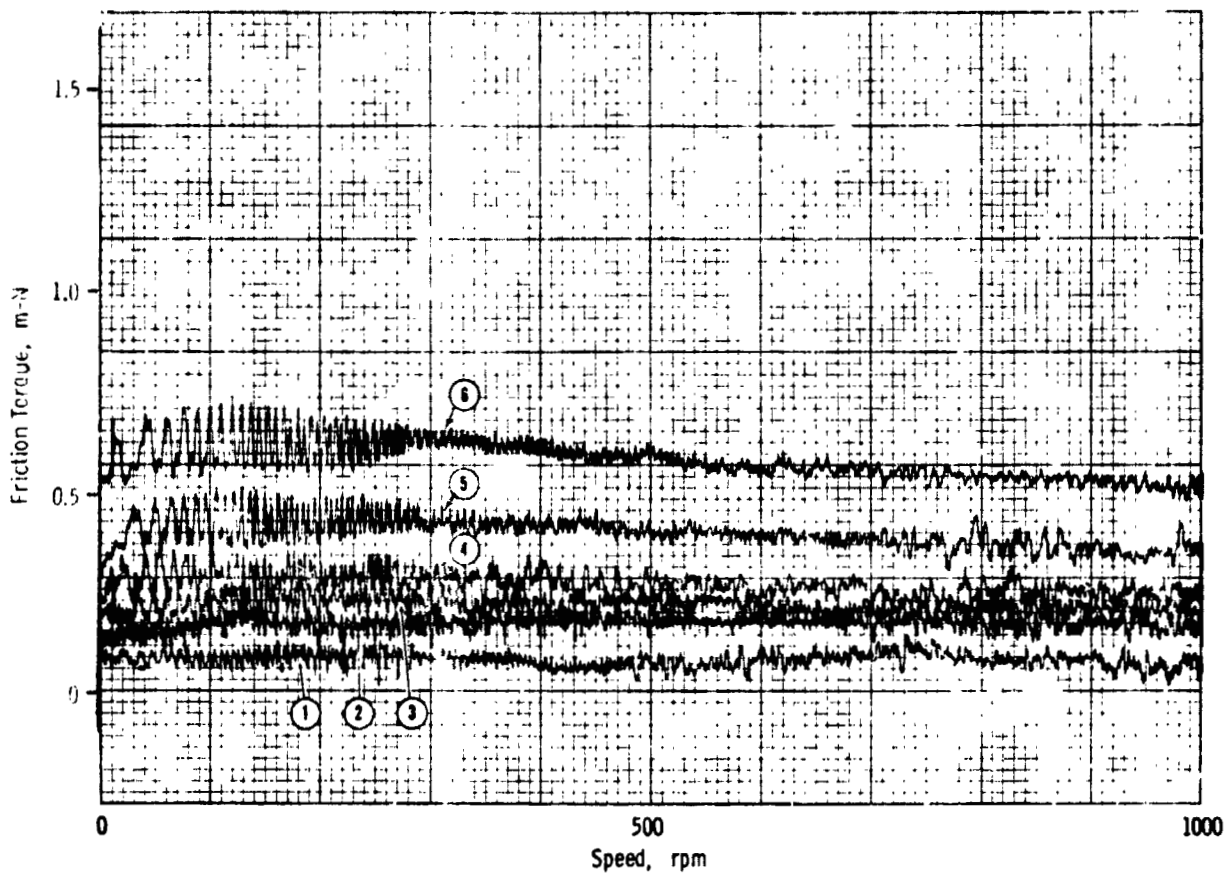
Loads, N/m^2

1. 2.07×10^5 (30 psi) (contact)
2. 2.76×10^5 (40 ")
3. 3.79×10^5 (55 ")
4. 5.17×10^5 (75 ")
5. 7.24×10^5 (105 ")
6. 1.03×10^6 (150 ")

Test Temp.: 316°C (600°F)

Atmosphere: air

Figure F-4. RET No. 27, Fluid: MCS 524
+ 0.05% Trichloroacetic Acid
+ 0.1% A-88
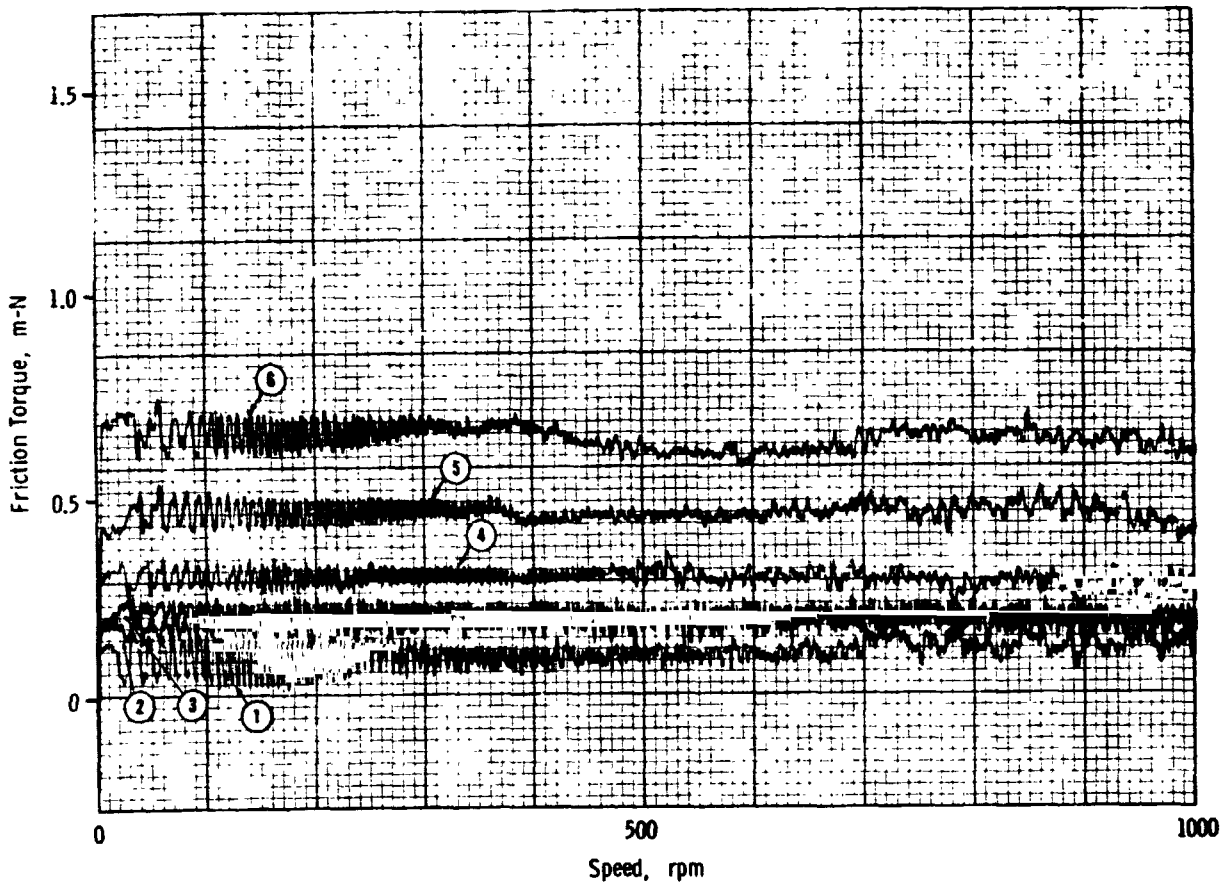
Figure F-5. RBT No. 30, Fluid: MCS 524
+ ~0.07% Perfluoroglutaric Acid
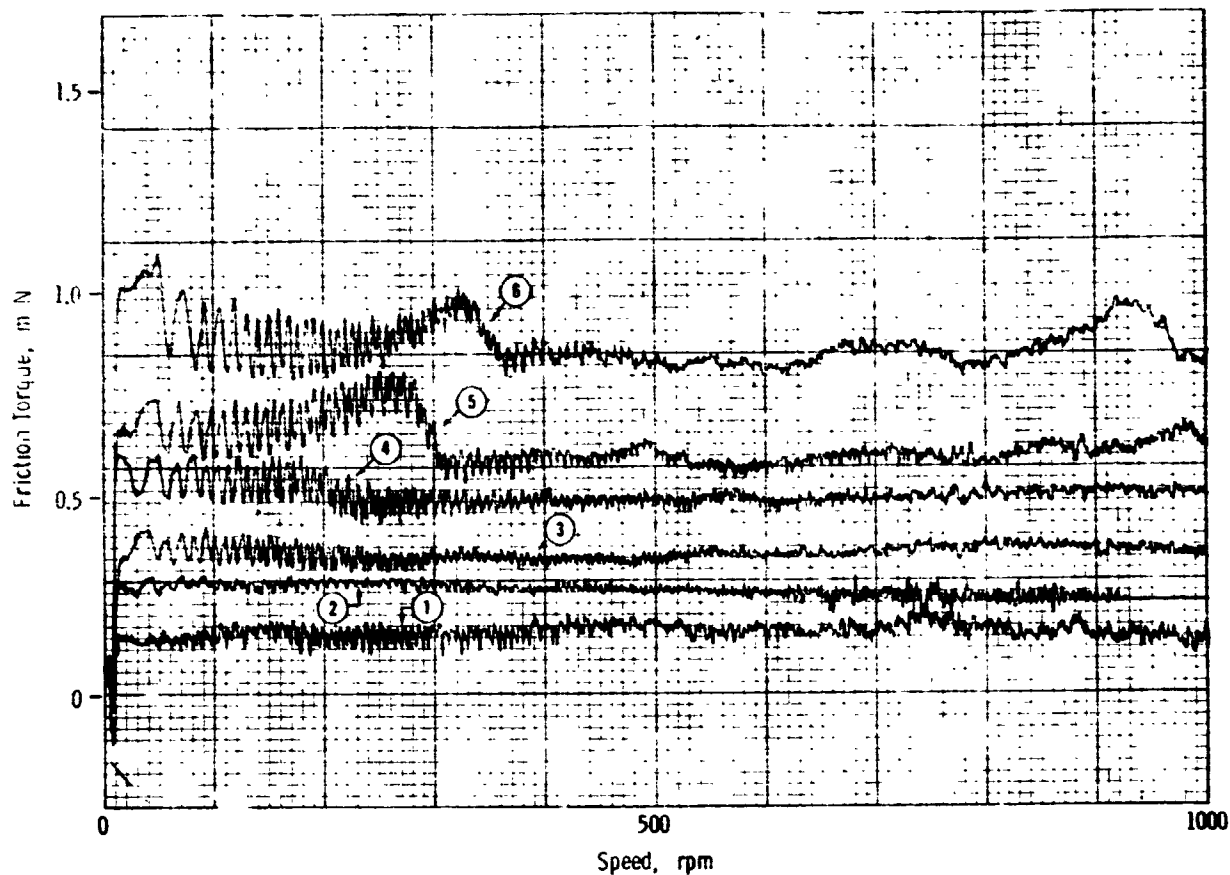
Loads, N/m^2

1. 2.07 x 10^5 (30 psi) (contact)
2. 2.76 x 10^5 (40   ")
3. 3.79 x 10^5 (55   ")
4. 5.17 x 10^5 (75   ")
5. 7.24 x 10^5 (105   ")
6. 1.03 x 10^6 (150   ")

Test Temp.:   316°C (600°F)

Atmosphere: air

222

Loads, N/m²

1. 2.07 x 10⁵   (30 psi) (contact)
2. 2.76 x 10⁵   (40 ")
3. 3.79 x 10⁵   (55 ")
4. 5.17 x 10⁵   (75 ")
5. 7.24 x 10⁵ (105 ")
6. 1.0? x 10⁶ (150 ")

Test Temp.:   316°C (600°F)

Atmosphere: air

Figure F-6.   RBT No. 25, Fluid: MCS 524
              + 0.1% Phenylphosphinic Acid
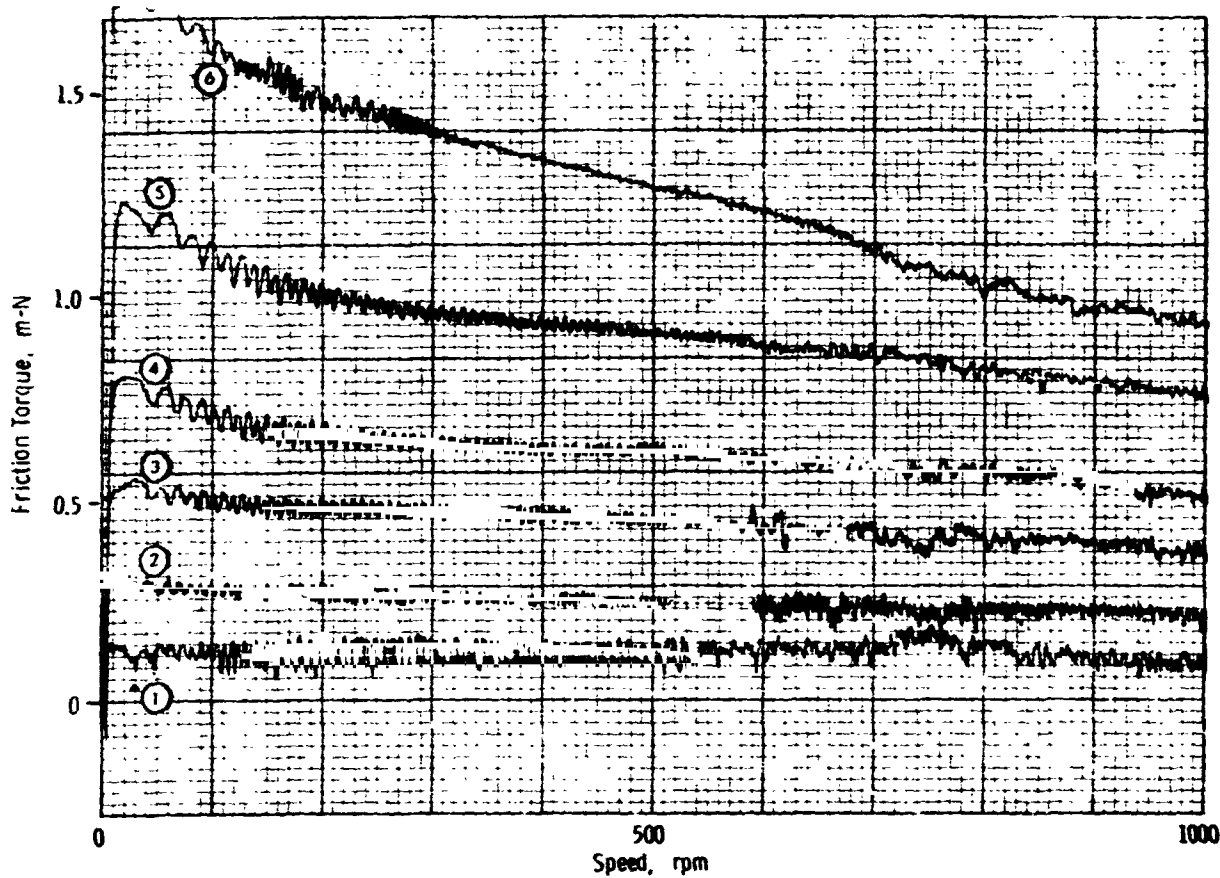
Figure F-7. RBT No. 28, Fluid: MCS 524 + 0.1% m-
Phenylmercaptophenylphosphinic Acid
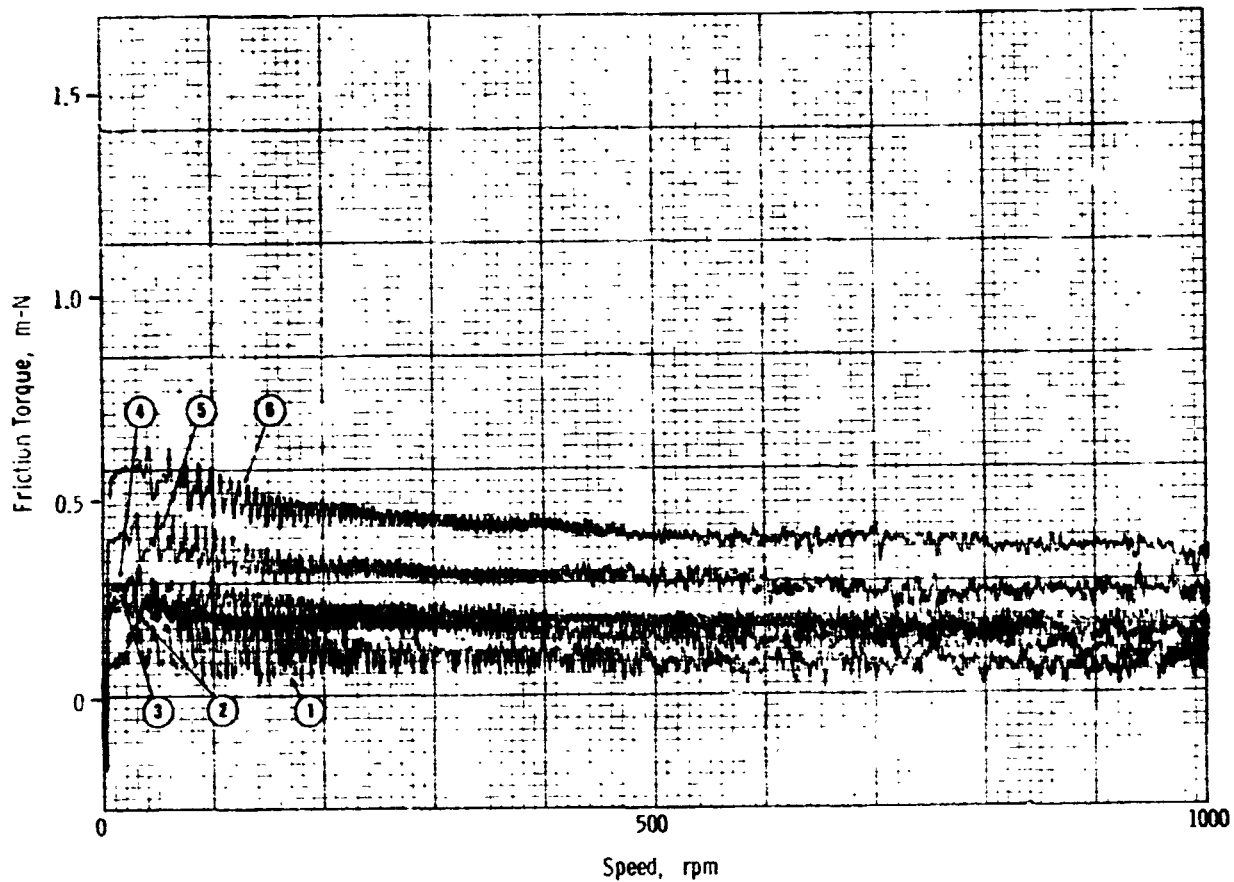
Loads, N/m2

1. 2.07 x 10^5 (30 psi) (contact)
2. 2.76 x 10^5 (40 ")
3. 3.79 x 10^5 (55 ")
4. 5.17 x 10^5 (75 ")
5. 7.24 x 10^5 (105 ")
6. 1.03 x 10^6 (150 ")

Test Temp.:   316°C (600°F)

Atmosphere: air

Loads, N/m^2

1. 2.07×10^5 (30 psi) (contact)
2. 2.76×10^5 (40 ")
3. 3.79×10^5 (55 ")
4. 5.17×10^5 (75 ")
5. 7.24×10^5 (105 ")
6. 1.03×10^6 (150 ")

Test Temp.: 316°C (600°F)

Atmosphere: air

Figure F-8. RBT No. 29, Fluid: MCS 524 + 0.1% m-(m-Phenyl-mercaptophenylmercapto)phenylphosphinic Acid
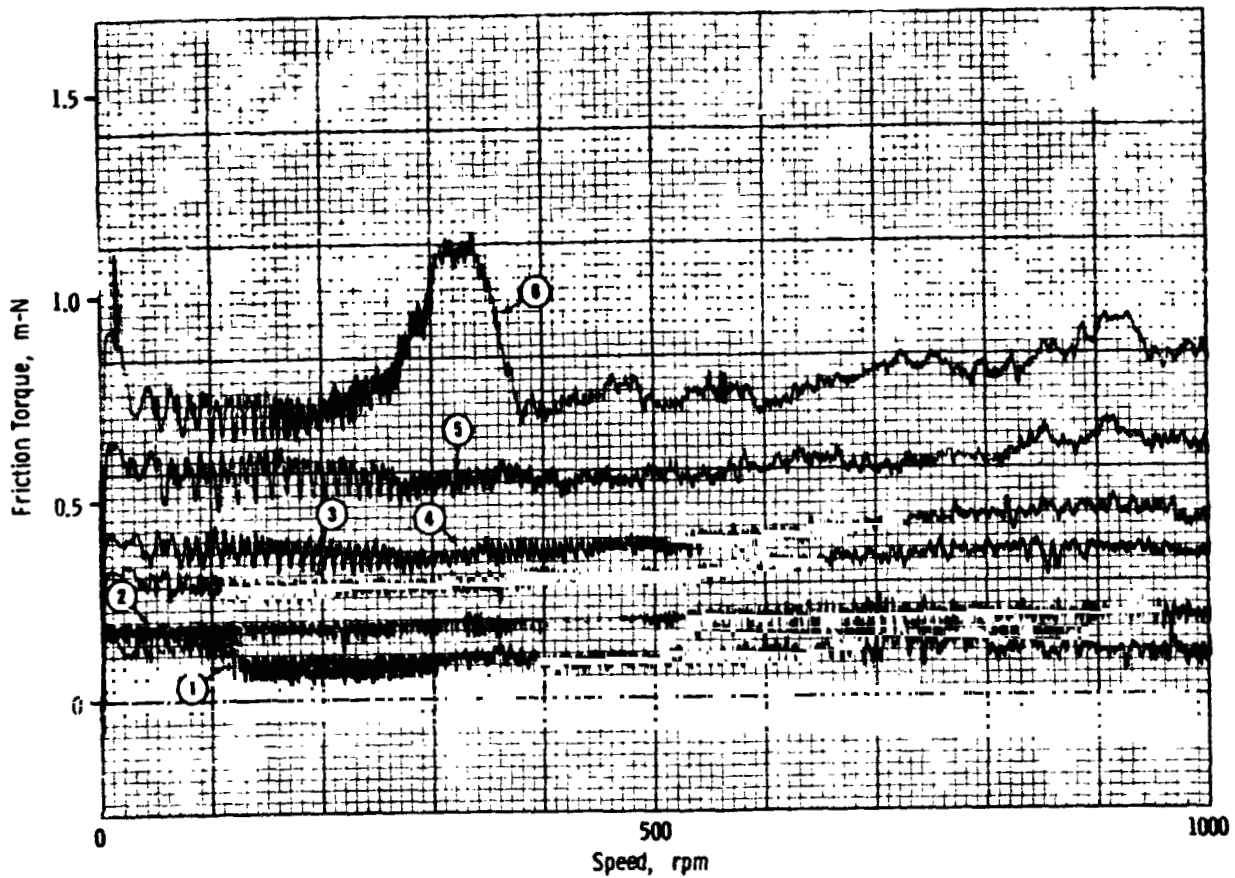
Loads, N/m²

1. 2.07 x 10⁵ (30 psi) (contact)
2. 2.76 x 10⁵ (40 ")
3. 3.79 x 10⁵ (55 ")
4. 5.17 x 10⁵ (75 ")
5. 7.24 x 10⁵ (105 ")
6. 1.03 x 10⁶ (150 ")

Test Temp.: 316°C (600°F)

Atmosphere: air

Figure F-9. RBT No. 31, Fluid: MCS 524 + 0.1%* Perfluoro-
glutaric acid + 0.075%* Phenylphosphinic Acid
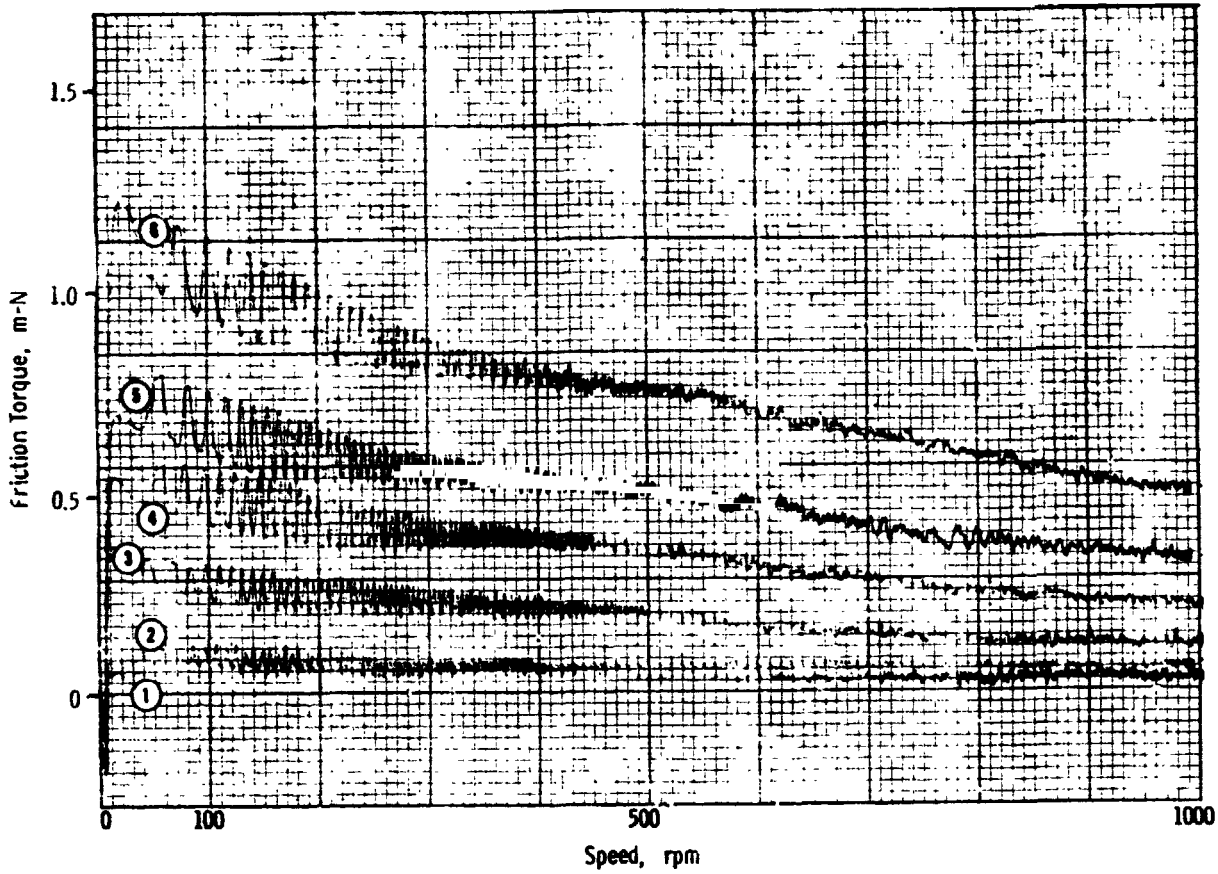
---

* Initial additive charge.

226

Loads, N/m^2

1. 2.07 x 10^5 (30 psi) (contact)
2. 2.76 x 10^5 (40 ")
3. 3.79 x 10^5 (55 ")
4. 5.17 x 10^5 (75 ")
5. 7.24 x 10^5 (105 ")
6. 1.03 x 10^6 (150 ")

Test Temp.: 316°C (600°F)

Atmosphere: air

Figure F-10. RBT No. 59, Fluid: MCS 524 + 0.1%* m-Phenyl-
mercaptophenylphosphinic Acid + 0.1%* Per-
fluoroglutaric Acid

---

*Initial additive charge.
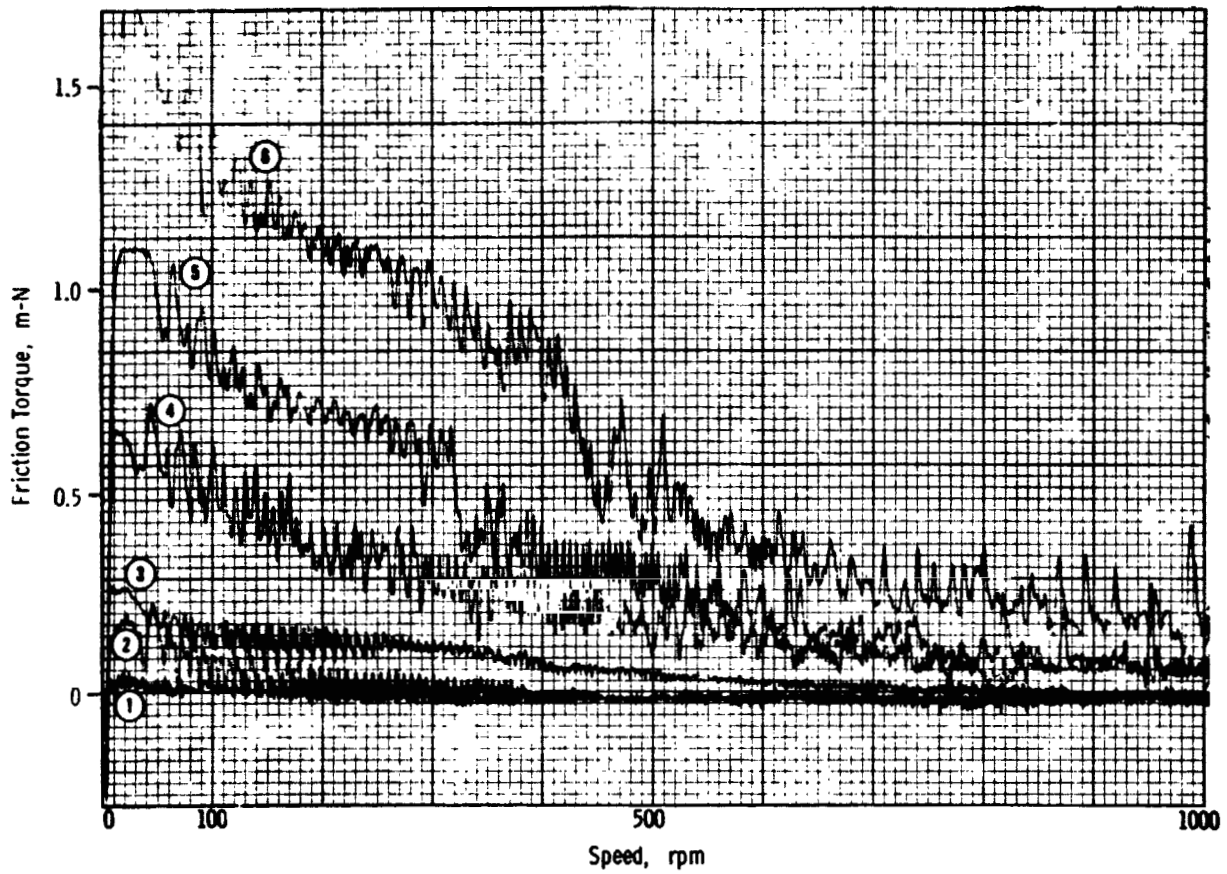
Loads, N/m^2

1.	2.07×10^5	(30 psi) (contact)
2.	2.76×10^5	(40 ")
3.	3.79×10^5	(55 ")
4.	5.17×10^5	(75 ")
5.	7.24×10^5	(105 ")
6.	1.03×10^6	(150 ")

Test Temp: 316°C (600°F)

Atmosphere: air

Figure F-11.   RBT No. 55, Fluid: MCS 524 + 0.1% Phenyl-
phosphinic Acid + 0.1% DC-473
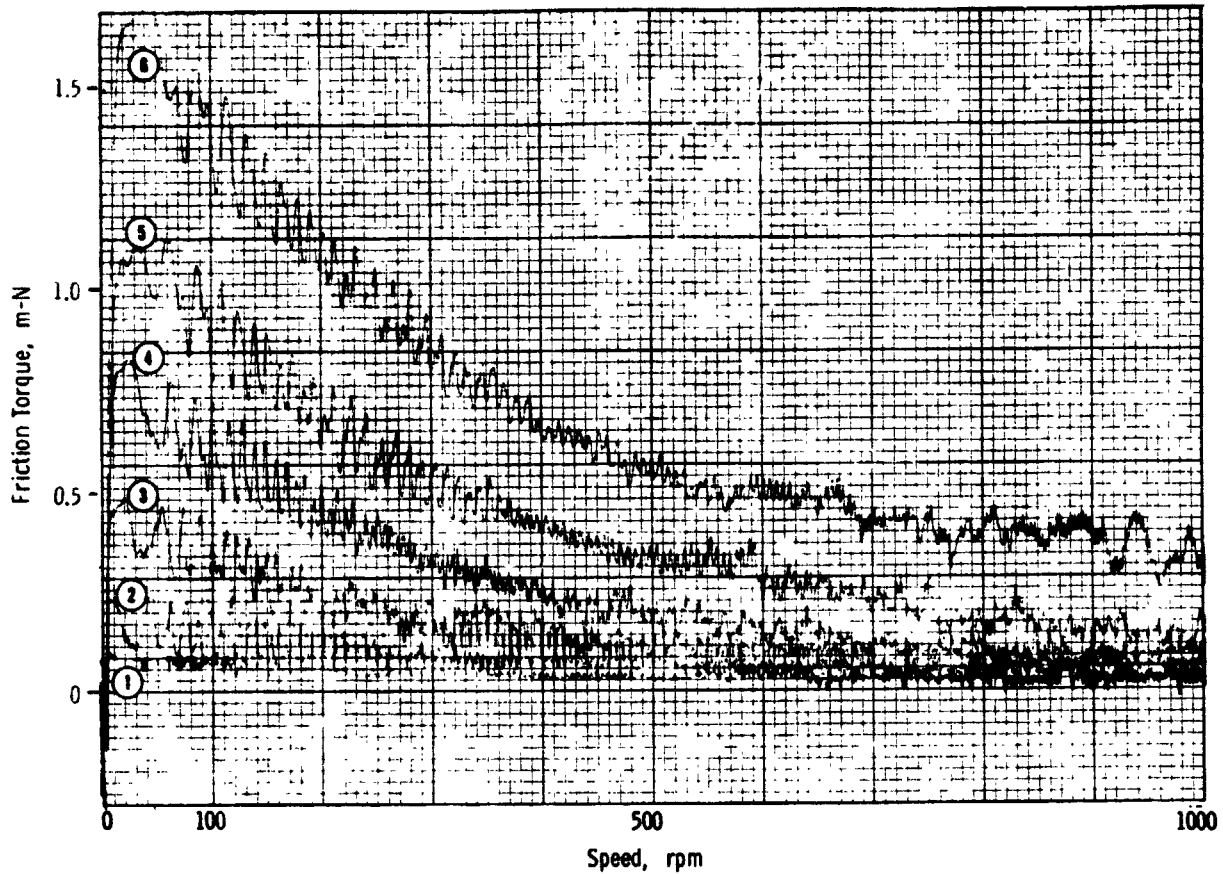
Figure F-12. RBT No. 62, Fluid: MCS 524 + 0.1% Phenyl-phosphinic Acid + 0.1% Perfluoroglutaric Acid + 0.1% DC-473

Loads, N/m^2

1. 2.07 x 10^5 (30 psi) (contact)
2. 2.76 x 10^5 (40 ")
3. 3.79 x 10^5 (55 ")
4. 5.17 x 10^5 (75 ")
5. 7.24 x 10^5 (105 ")
6. 1.03 x 10^6 (150 ")

Test Temp.: 316°C (600°F)

Atmosphere: air

229

APPENDIX G:

X-Y RECORDINGS OF RUB-BLOCK TESTS, M50 ON M50,

INERTED (N_2), 343°C (ONE TEST AT 316°C)

PRECEDING PAGE BLANK NOT FILMED

Loads, N/m²

1. 2.07 x 10⁵ (30 psi) (contact)
2. 2.76 x 10⁵ (40 ")
3. 3.79 x 10⁵ (55 ")
4. 5.17 x 10⁵ (75 ")
5. 7.24 x 10⁵ (105 ")
6. 1.03 x 10⁶ (150 ")

Test Temp.: 343°C (650°F)

Atmosphere: nitrogen

M50 on M50

Figure G-1. RBT No. 34, Fluid: MCS 524
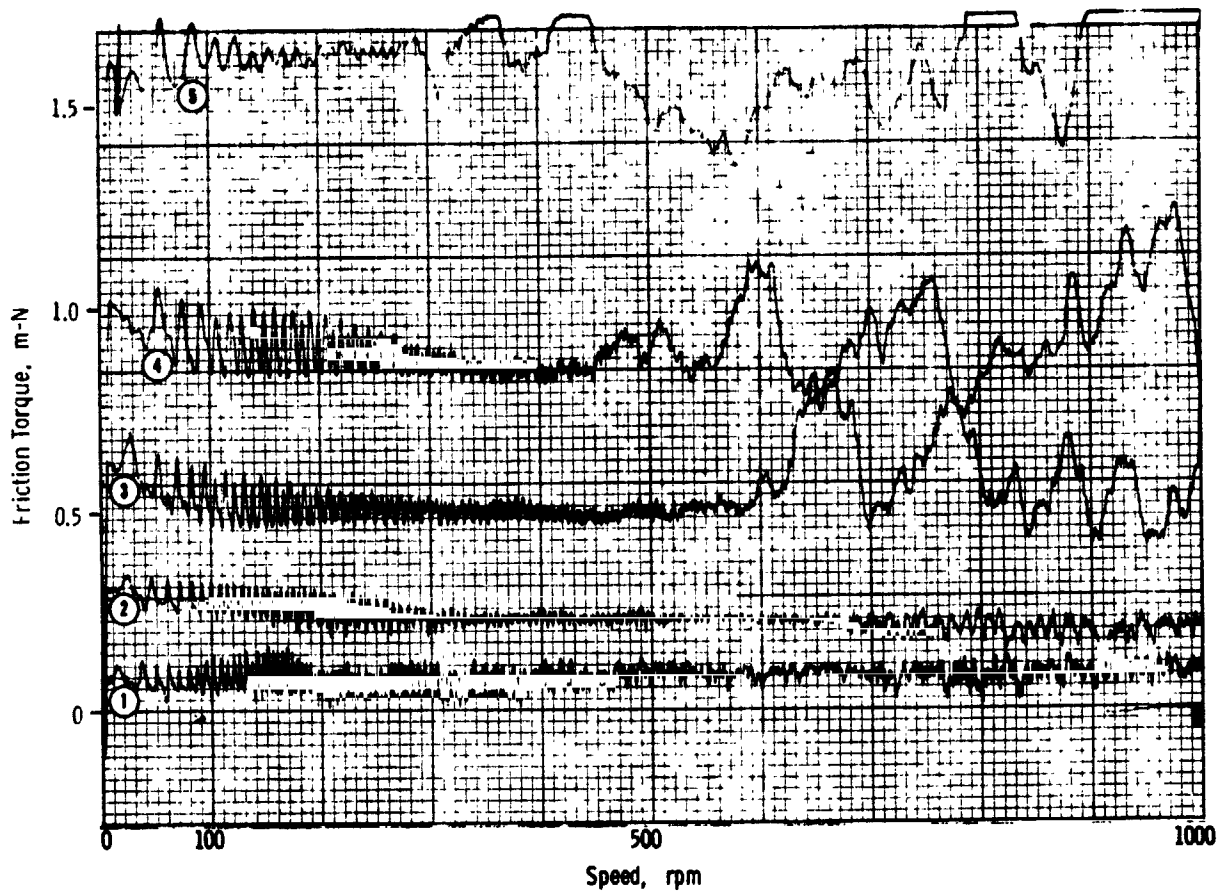
Figure G-2. RBT No. 33, Fluid: MCS 524

Loads, N/m^2

1. 2.07×10^5 (30 psi) (contact)
2. 2.76×10^5 (40 ")
3. 3.79×10^5 (55 ")
4. 5.17×10^5 (75 ")
5. 7.24×10^5 (105 ")
6. 1.03×10^6 (150 ") - not run

Test Temp.: 316°C (600°F)

Atmosphere: nitrogen

M50 on M50

Figure showing Friction Torque (m-N) versus Speed (rpm).

Loads, N/m^2

1. 2.07×10^5 (30 psi) (contact)
2. 2.76×10^5 (40 ")
3. 3.79×10^5 (55 ")
4. 5.17×10^5 (75 ")
5. 7.24×10^5 (105 ")
6. 1.03×10^6 (150 ") - not run

Test Temp.: 343°C (650°F)

Atmosphere: nitrogen

M50 on M50

Figure G-3. RBT No. 35, Fluid: FH-140
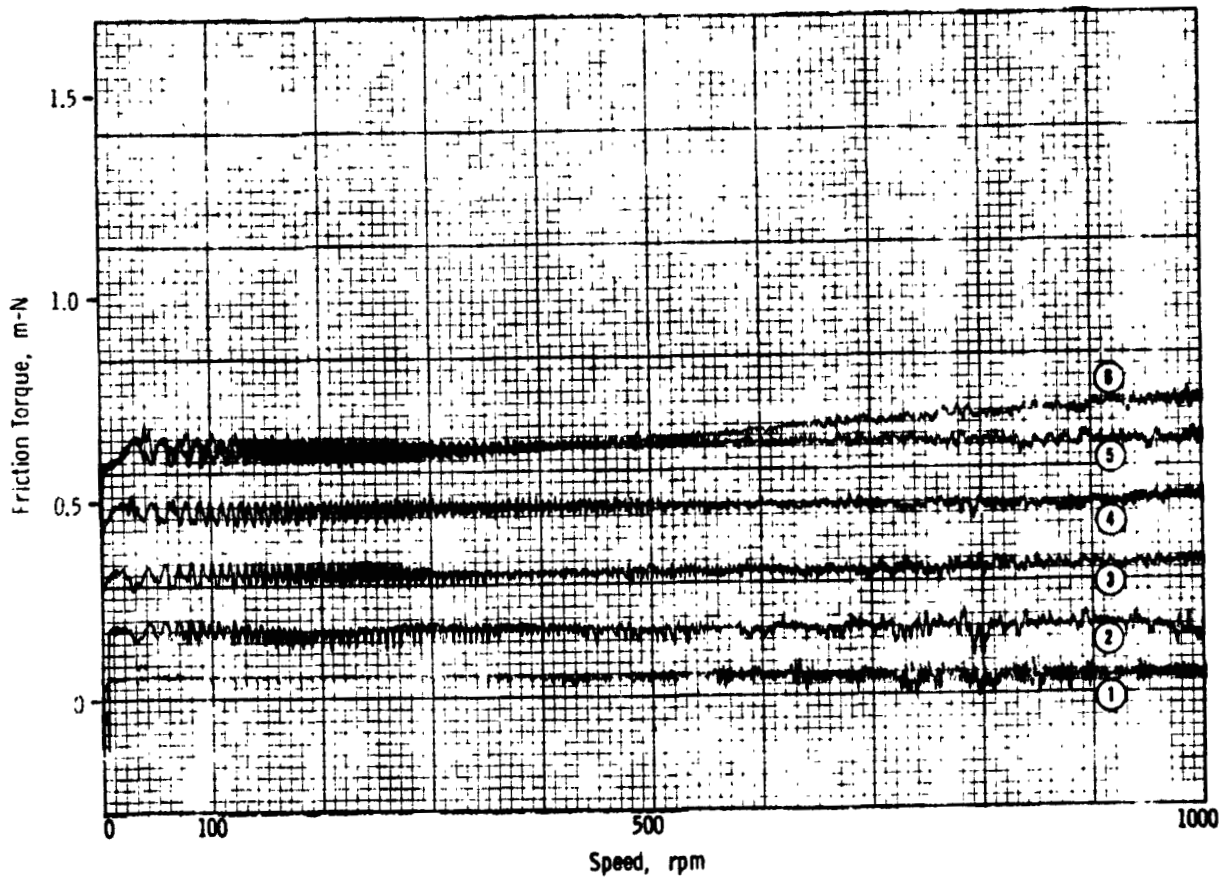
234

Loads, N/m^2

1. 2.07×10^5 (30 psi) (contact)
2. 2.76×10^5 (40 ")
3. 3.79×10^5 (55 ")
4. 5.17×10^5 (75 ")
5. 7.24×10^5 (105 ")
6. 1.03×10^6 (150 ")

Test Temp.:   343°C (650°F)

Atmosphere: nitrogen

M50 on M50

Figure G-4.   RBT No. 37, Fluid: MCS 524 + 0.05%
              Trichloroacetic Acid + 0.1% A-88
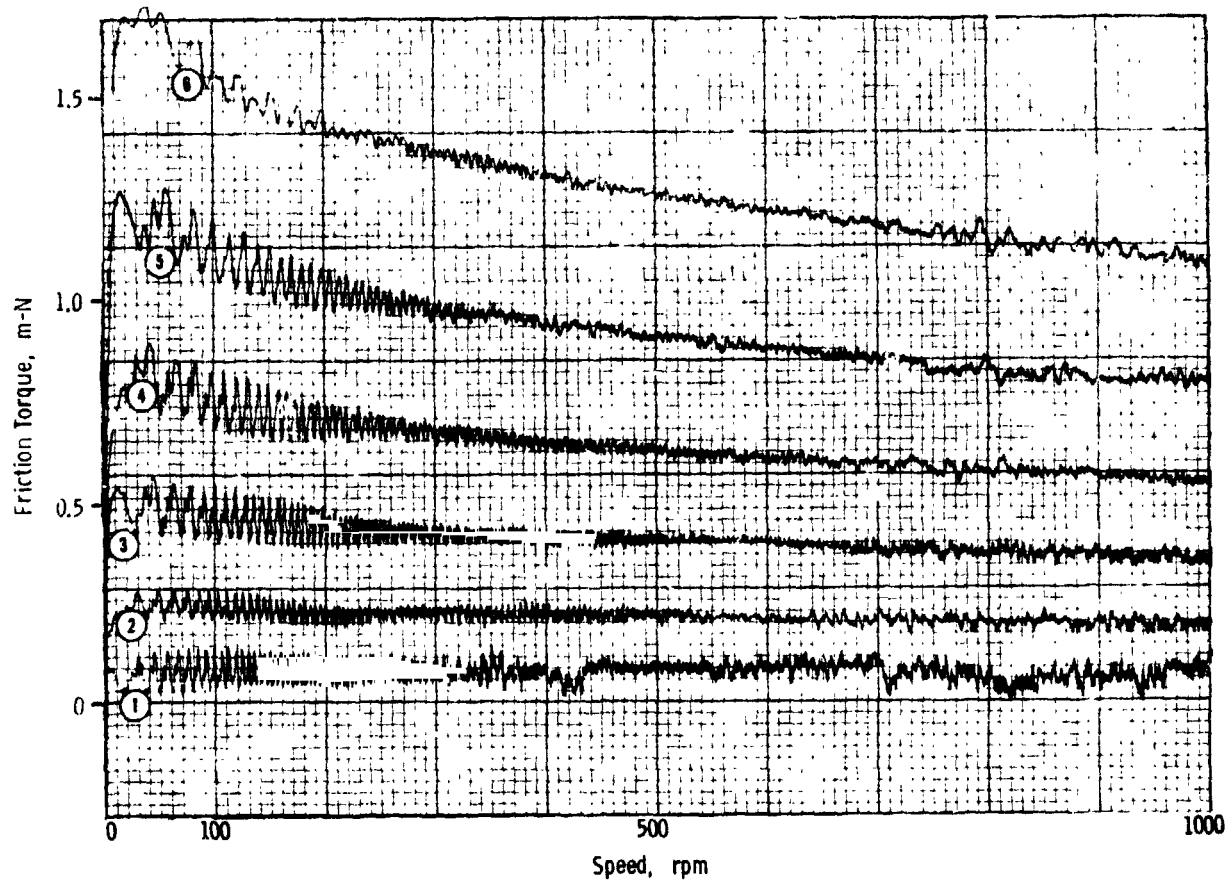
Figure G-5. RBT No. 38, Fluid: MCS 524
+ ∿0.07% Perfluoroglutaric Acid
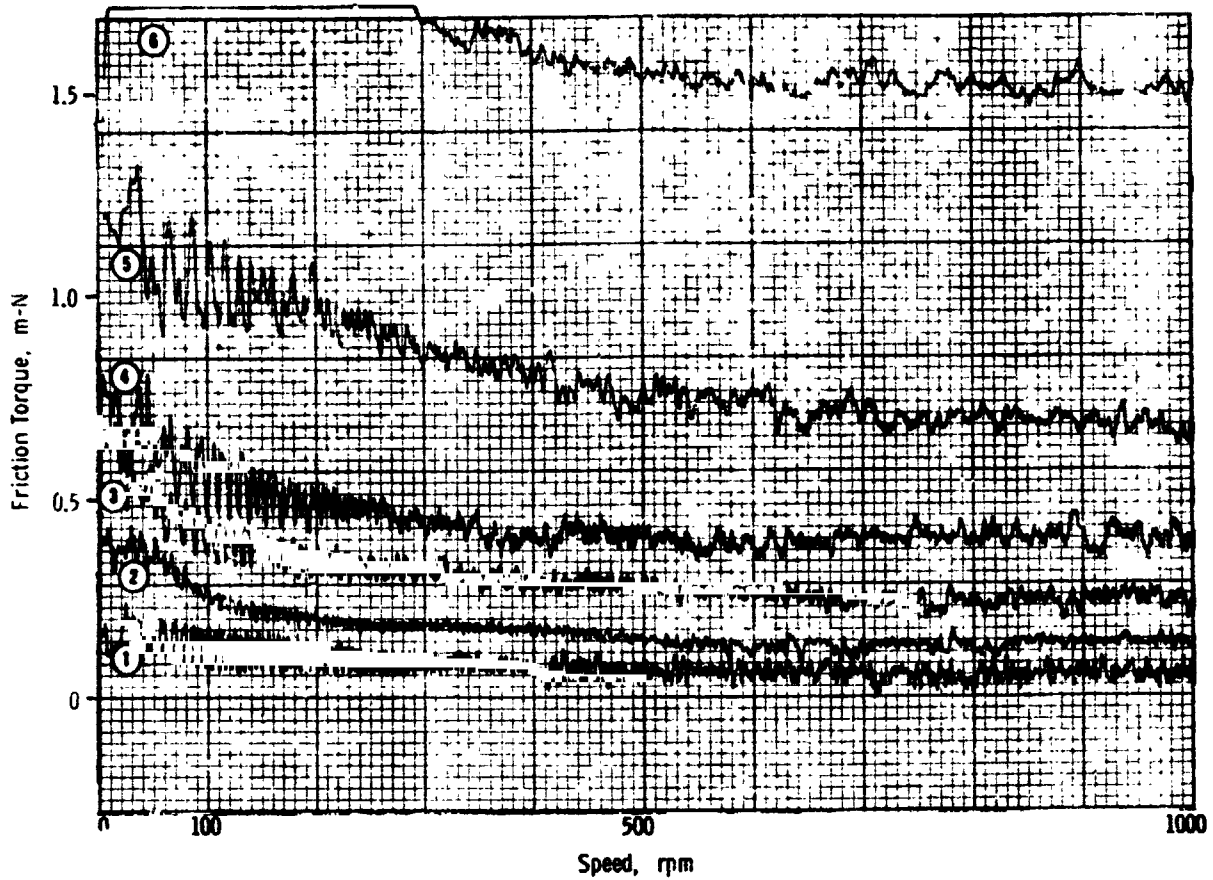
Loads, N/m²

1. 2.07×10^5 (30 psi) (contact)
2. 2.76×10^5 (40 ")
3. 3.79×10^5 (55 ")
4. 5.17×10^5 (75 ")
5. 7.24×10^5 (105 ")
6. 1.03×10^6 (150 ")

Test Temp.: 343°C (650°F)

Atmosphere: nitrogen

M50 on M50

236

Loads, N/m^2

1. 2.07×10^5 (30 psi) (contact)
2. 2.76×10^5 (40 ")
3. 3.79×10^5 (55 ")
4. 5.17×10^5 (75 ")
5. 7.24×10^5 (105 ")
6. 1.03×10^6 (150 ")

Test Temp.: 343°C (650°F)

Atmosphere: nitrogen

M50 on M50

Figure G-5. RBT No. 40, Fluid: MCS 524
± 0.1% Phenylphosphinic Acid
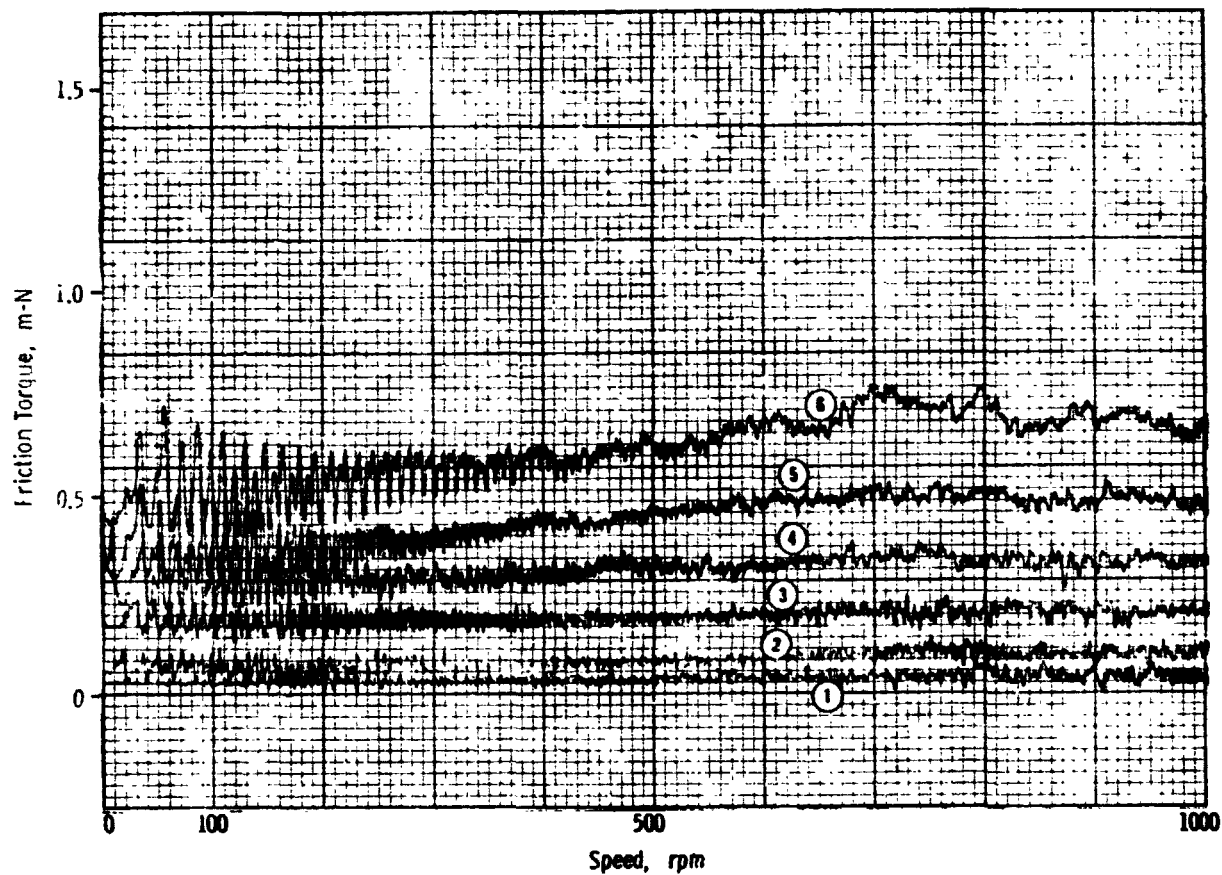
Figure G-7. RBT No. 41, Fluid: MCS 524 + 0.1%
m-Phenylmercaptophenylphosphinic Acid
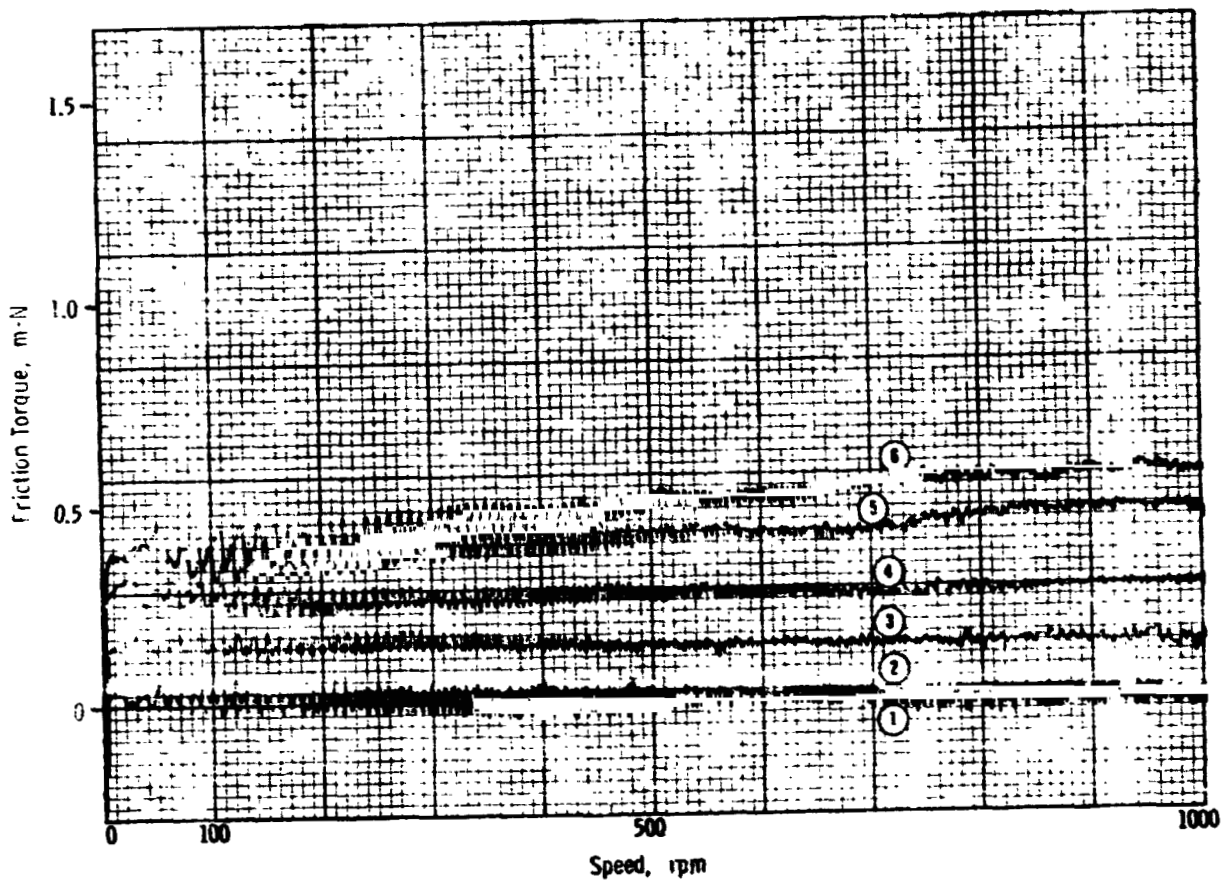
Loads, N/m²

1.   2.07 x 10⁵   (30 psi)   (contact)
2.   2.76 x 10⁵   (40   ")
3.   3.79 x 10⁵   (55   ")
4.   5.17 x 10⁵   (75   ")
5.   7.24 x 10⁵   (105   ")
6.   1.03 x 10⁶   (150   ")

Test Temp.:   343°C (650°F)

Atmosphere: nitrogen

M50 on M50

238

Loads, N/m^2

1. 2.07×10^5 (30 psi) (contact)
2. 2.76×10^5 (40 ")
3. 3.79×10^5 (55 ")
4. 5.17×10^5 (75 ")
5. 7.24×10^5 (105 ")
6. 1.03×10^6 (150 ")

Test Temp.: 343°C (650°F)

Atmosphere: nitrogen

M50 on M50

Figure G-8. RBT No. 56, Fluid: MCS 524 + 0.1%
m-(m-Phenylmercaptophenylmercapto)-
phenylphosphinic Acid

239

Loads, N/m²

1. 2.07 x 10⁵ (30 psi) (contact)
2. 2.76 x 10⁵ (40 ")
3. 3.79 x 10⁵ (55 ")
4. 5.17 x 10⁵ (75 ")
5. 7.24 x 10⁵ (105 ")
6. 1.03 x 10⁶ (150 ")

Test Temp.: 343°C (650°F)

Atmosphere: nitrogen

M50 on M50

Figure G-9. RBT No. 39, Fluid: MCS 524 + 0.075%* Phenyl-
phosphinic Acid + 0.1%* Perfluoroglutaric Acid

─────────────

*Initial additive charge.

240

Loads, N/m²

1. 2.07×10^5 (30 psi) (contact)
2. 2.76×10^5 (40 ")
3. 3.79×10^5 (55 ")
4. 5.17×10^5 (75 ")
5. 7.24×10^5 (105 ")
6. 1.03×10^6 (150 ")

Test Temp.: 343°C (650°F)

Atmosphere: nitrogen

M50 on M50

Figure G-9. RBT No. 39, Fluid: MCS 524 + 0.075%* Phenyl-
phosphinic Acid + 0.1%* Perfluoroglutaric Acid

─────────────

*Initial additive charge.

240
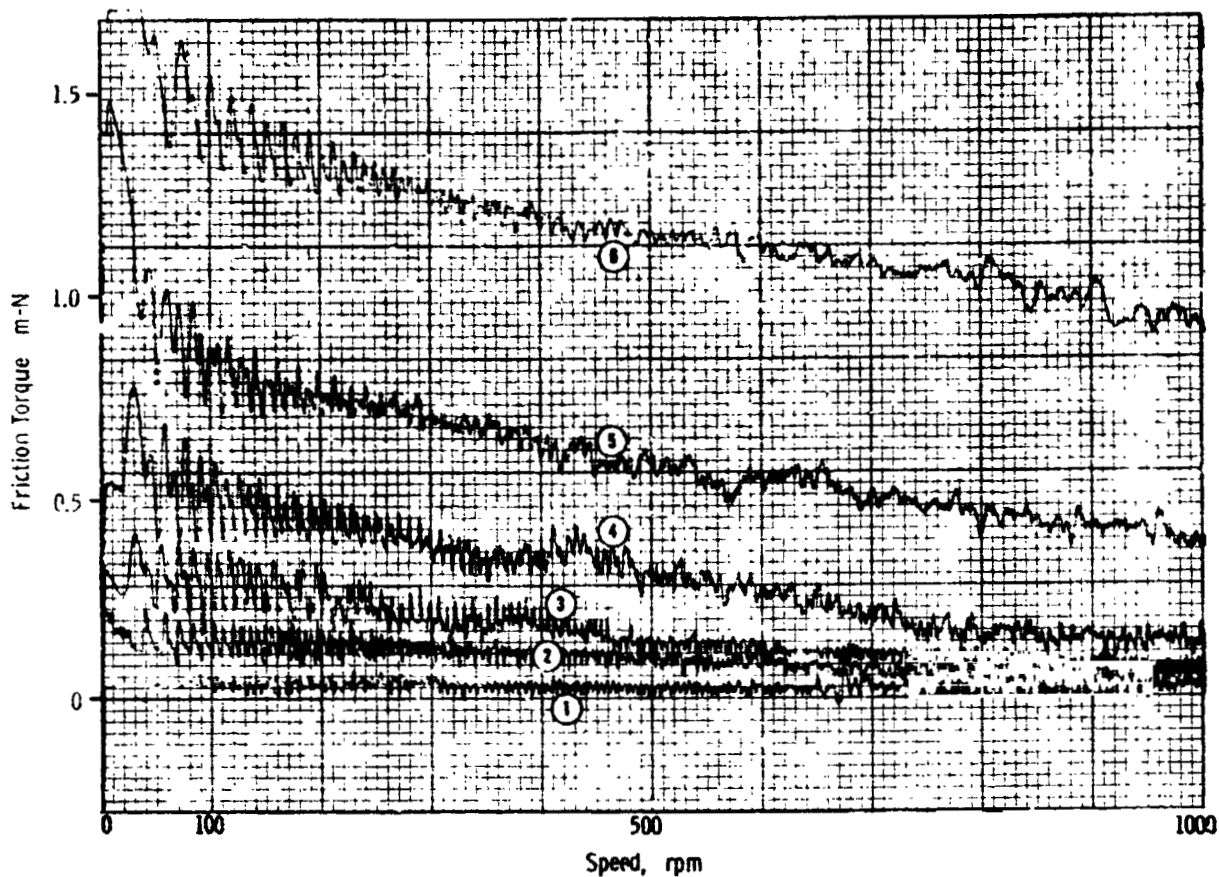
Loads, N/m²

1. 2.07×10^5 (30 psi) (contact)
2. 2.76×10^5 (40 ")
3. 3.79×10^5 (55 ")
4. 5.17×10^5 (75 ")
5. 7.24×10^5 (105 ")
6. 1.03×10^6 (150 ")

Test Temp.: 343°C (650°F)

Atmosphere: nitrogen

M50 on M50

Figure G-10. RBT No. 43, Fluid: MCS 524 + 0.1%* m-Phenylmercaptophenylphosphinic Acid + 0.1%* Perfluoroglutaric Acid

_____

*Initial additive charge.
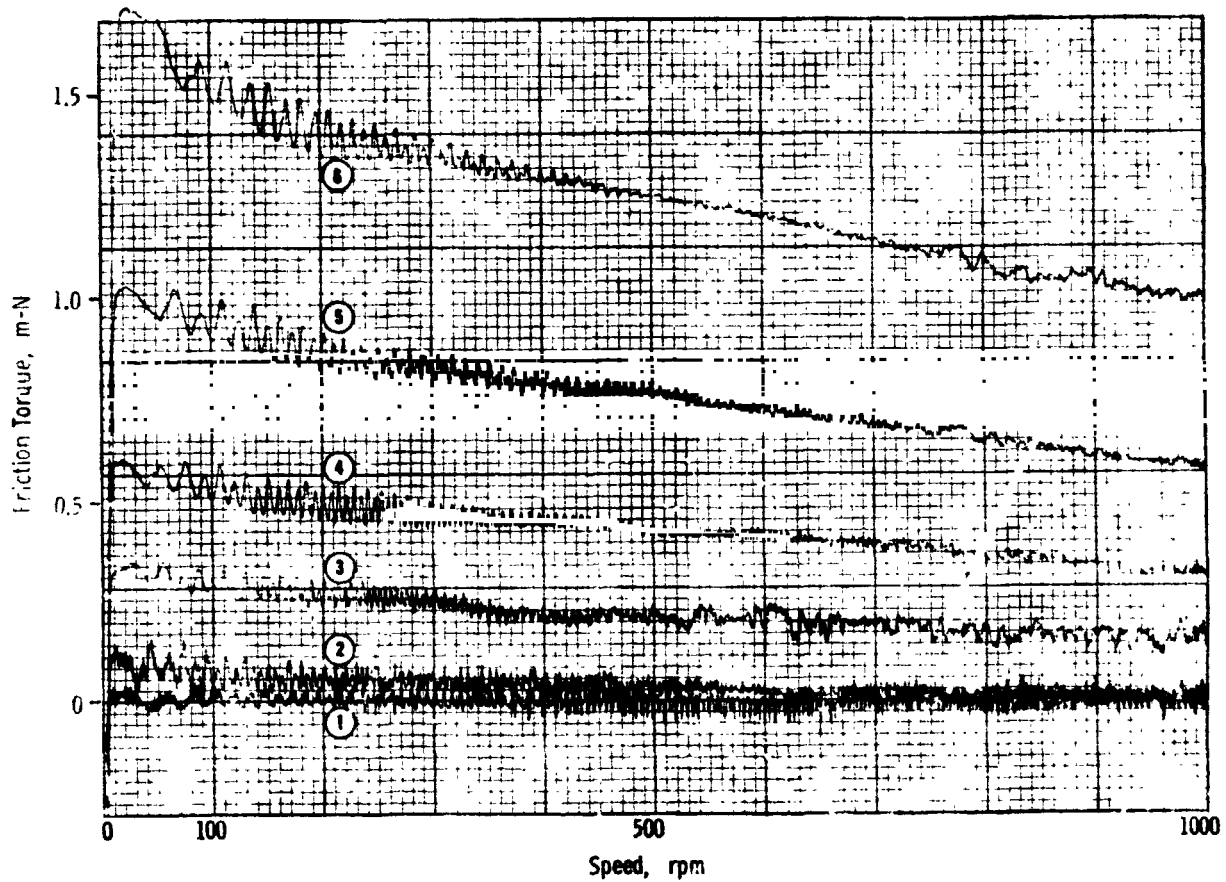
Loads, N/m²

1. 2.07 x 10⁵ (30 psi) (contact)
2. 2.76 x 10⁵ (40 ")
3. 3.79 x 10⁵ (55 ')
4. 5.17 x 10⁵ (75 ")
5. 7.24 x 10⁵ (105 ")
6. 1.03 x 10⁶ (150 ")

Test Temp.: 343°C (650°F)

Atmosphere: nitrogen

M50 on M50

Figure G-11. RBT No. 64, Fluid: MCS 524 + 0.1% A-88
+ 0.05% Trichloroacetic Acid + 0.1%
DC-473
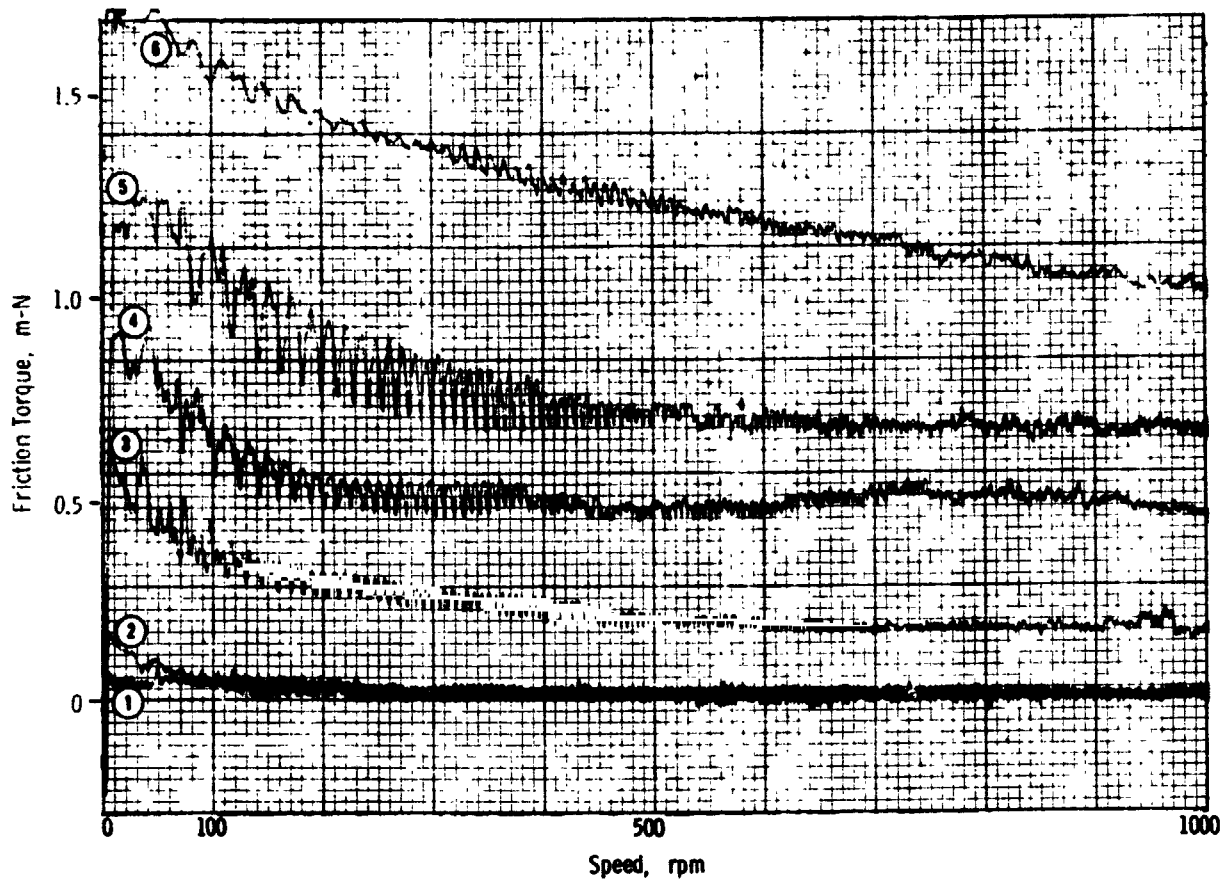
Figure G-12. RBT No. 53, Fluid: MCS 524 + 0.1%
Phenylphosphinic Acid + 0.1% DC-473
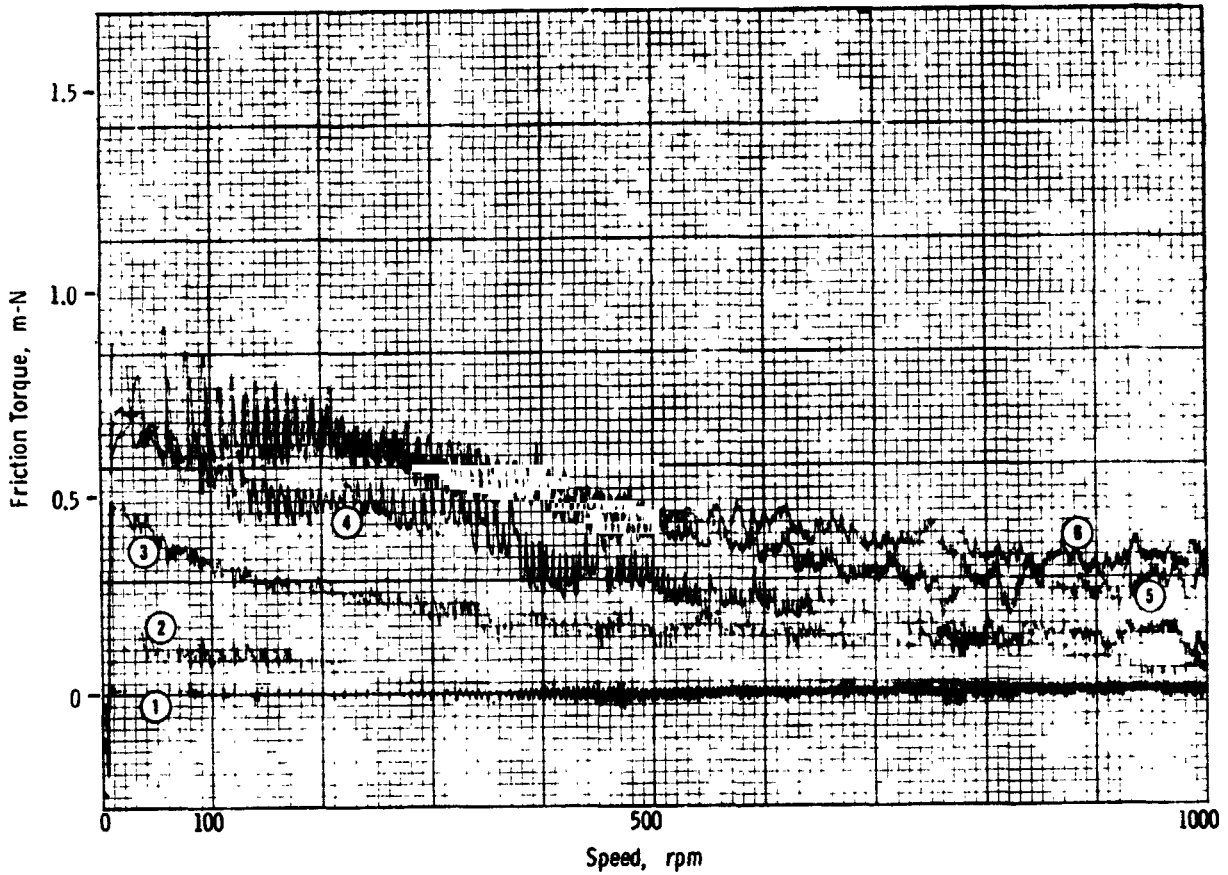
Loads, N/m^2

1. 2.07×10^5 (30 psi) (contact)
2. 2.76×10^5 (40 ")
3. 3.79×10^5 (55 ")
4. 5.17×10^5 (75 ")
5. 7.24×10^5 (105 ")
6. 1.03×10^6 (150 ")

Test Temp.: 343°C (650°F)

Atmosphere: nitrogen

M50 on M50

243

Loads, N/m^2

1. 2.07×10^5 (30 psi) (contact)
2. 2.76×10^5 (40 ")
3. 3.79×10^5 (55 ")
4. 5.17×10^5 (75 ")
5. 7.24×10^5 (105 ")
6. 1.03×10^6 (150 ")
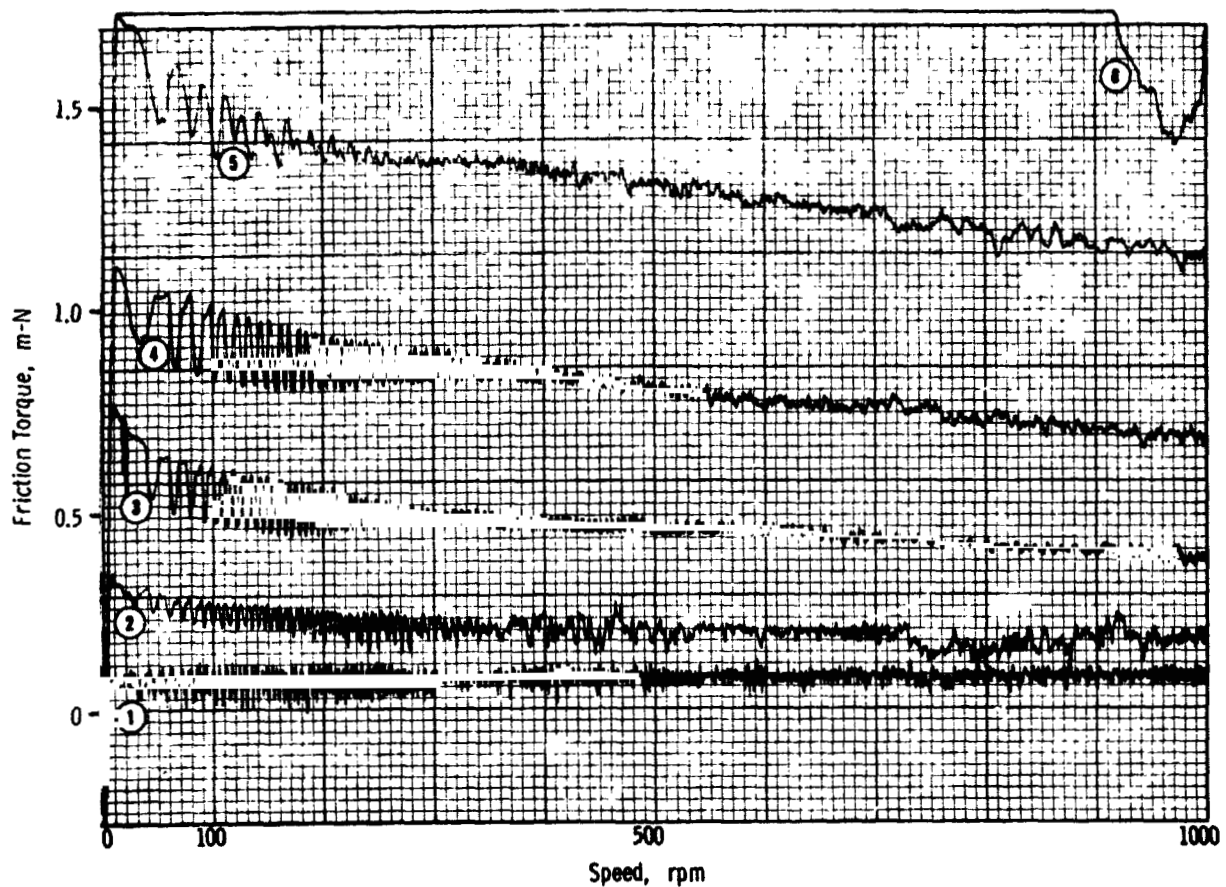
Test Temp.: 343°C (650°F)

Atmosphere: nitrogen

M50 on M50

Figure G-13. RBT No. 58, Fluid: MCS 524 + 0.1% Phenyl-
phosphinic Acid + 0.1% Perfluoroglutaric
Acid + 0.1% DC-473

APPENDIX H:

X-Y RECORDINGS OF RUB-BLOCK TESTS, TIN BRONZED

M2 ON TUNGSTEN CARBIDE, 260°C (ONE TEST AT 316°C)
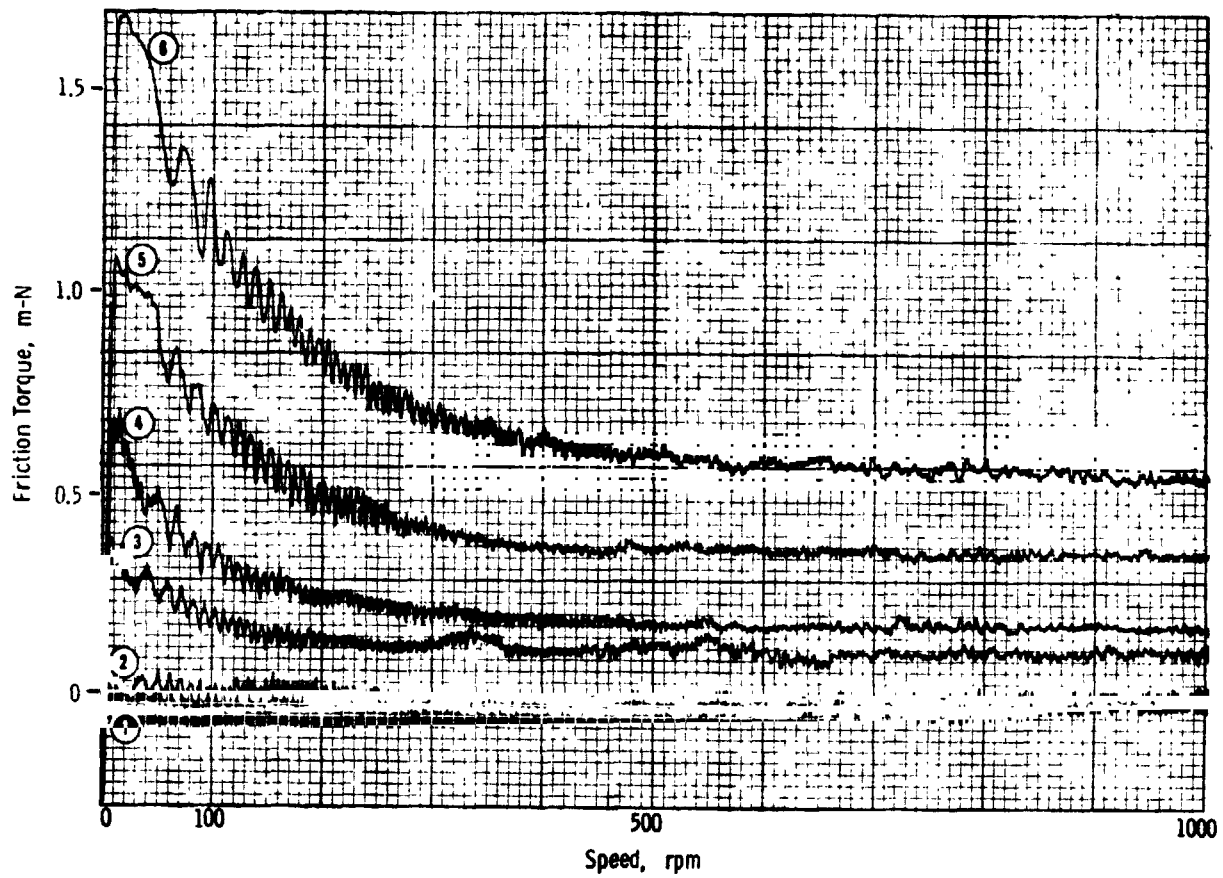
Loads, N/m2

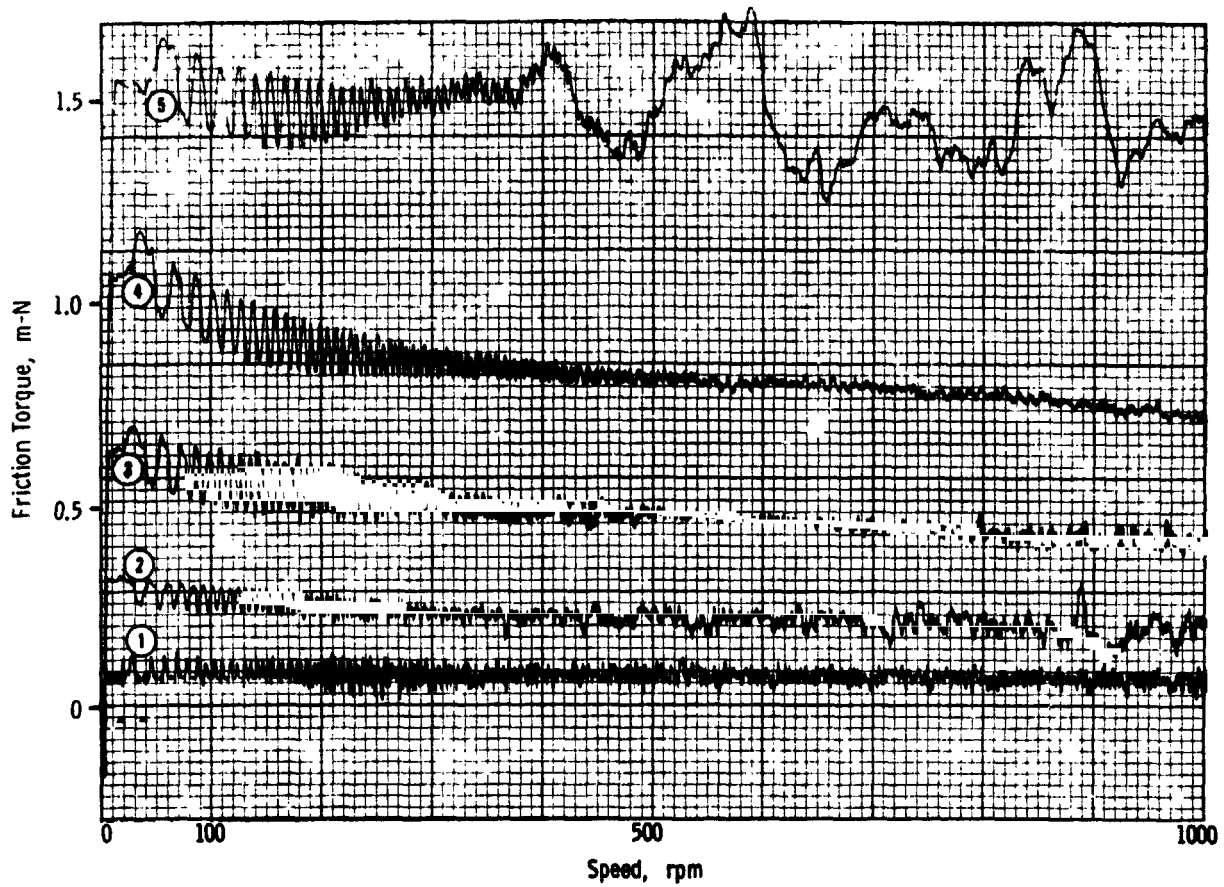1. 2.07×10^5 (30 psi) (contact)
2. 2.76×10^5 (40 ")
3. 3.79×10^5 (55 ")
4. 5.17×10^5 (75 ")
5. 7.24×10^5 (105 ")
6. 1.03×10^6 (150 ")

Test Temp.: 260°C (500°F)

Atmosphere: nitrogen

Tin bronzed M2 on tungsten carbide

Figure H-1.   RBT No. 51, Fluid: Skylube 450
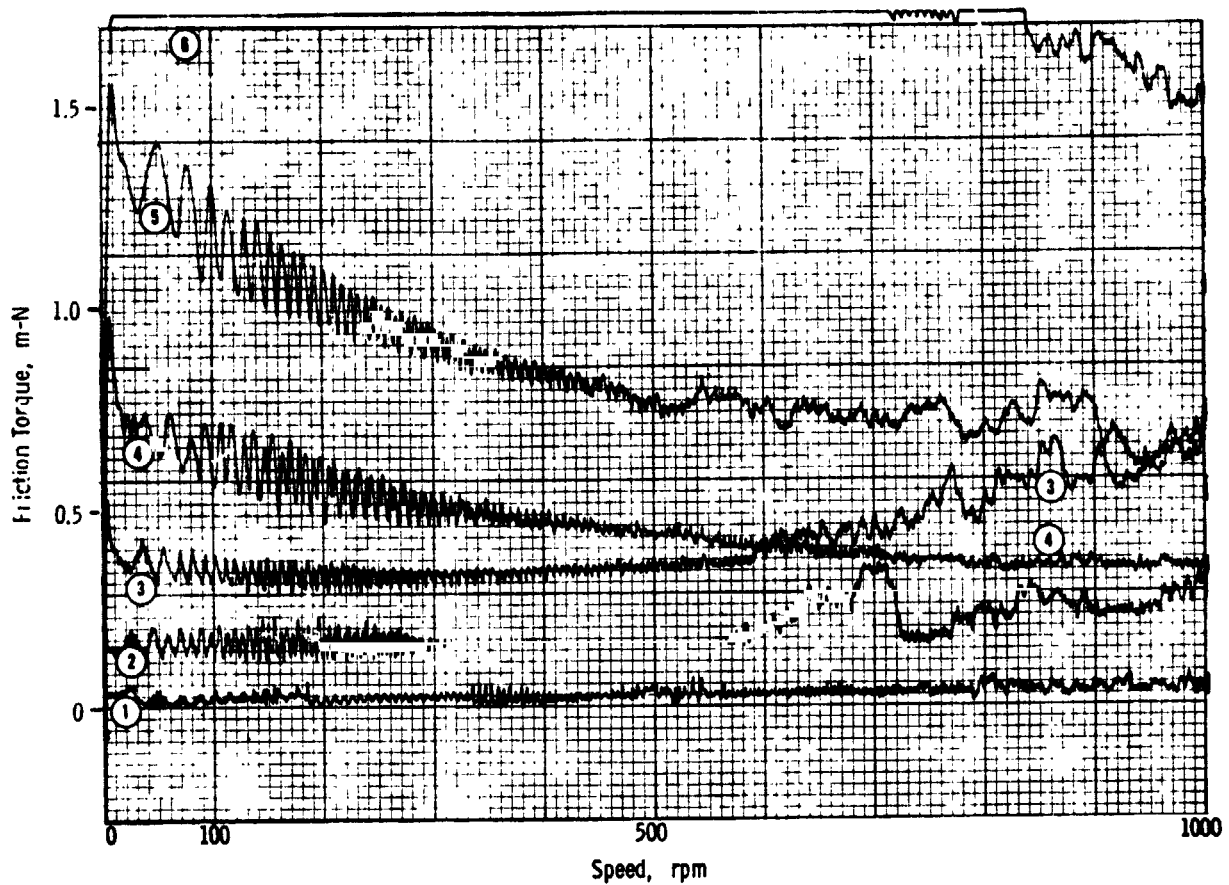
246

Figure H-2. RBT No. 46, Fluid: MCS 524

Loads, N/m²

1. 2.07 x 10⁵ (30 psi) (contact)
2. 2.76 x 10⁵ (40 ")
3. 3.79 x 10⁵ (55 ")
4. 5.17 x 10⁵ (75 ")
5. 7.24 x 10⁵ (105 ")
6. 1.03 x 10⁶ (150 ")

Test Temp.: 260°C (500°F)

Atmosphere: nitrogen

Tin bronzed M2 on tungsten carbide

247

Loads, N/m²

1. 2.07 x 10⁵ (30 psi) (contact)
2. 2.76 x 10⁵ (40 ")
3. 3.79 x 10⁵ (55 ")
4. 5.17 x 10⁵ (75 ")
5. 7.24 x 10⁵ (105 ")
6. 1.03 x 10⁶ (150 ")

Test Temp.: 260°C (500°F)

Atmosphere: nitrogen

Tin bronzed M2 on tungsten carbide

Figure H-2. RBT No. 46, Fluid: MCS 524

247

Loads, N/m²

1. 2.07 x 10⁵ (30 psi) (contact)
2. 2.76 x 10⁵ (40 ")
3. 3.79 x 10⁵ (55 ")
4. 5.17 x 10⁵ (75 ")
5. 7.24 x 10⁵ (105 ") - not run
6. 1.03 x 10⁶ (150 ") - not run

Test Temp.: 260°C (500°F)

Atmosphere: nitrogen

Tin bronzed M2 on tungsten carbide

Figure H-3. **RBT No. 45, Fluid: FH-140**
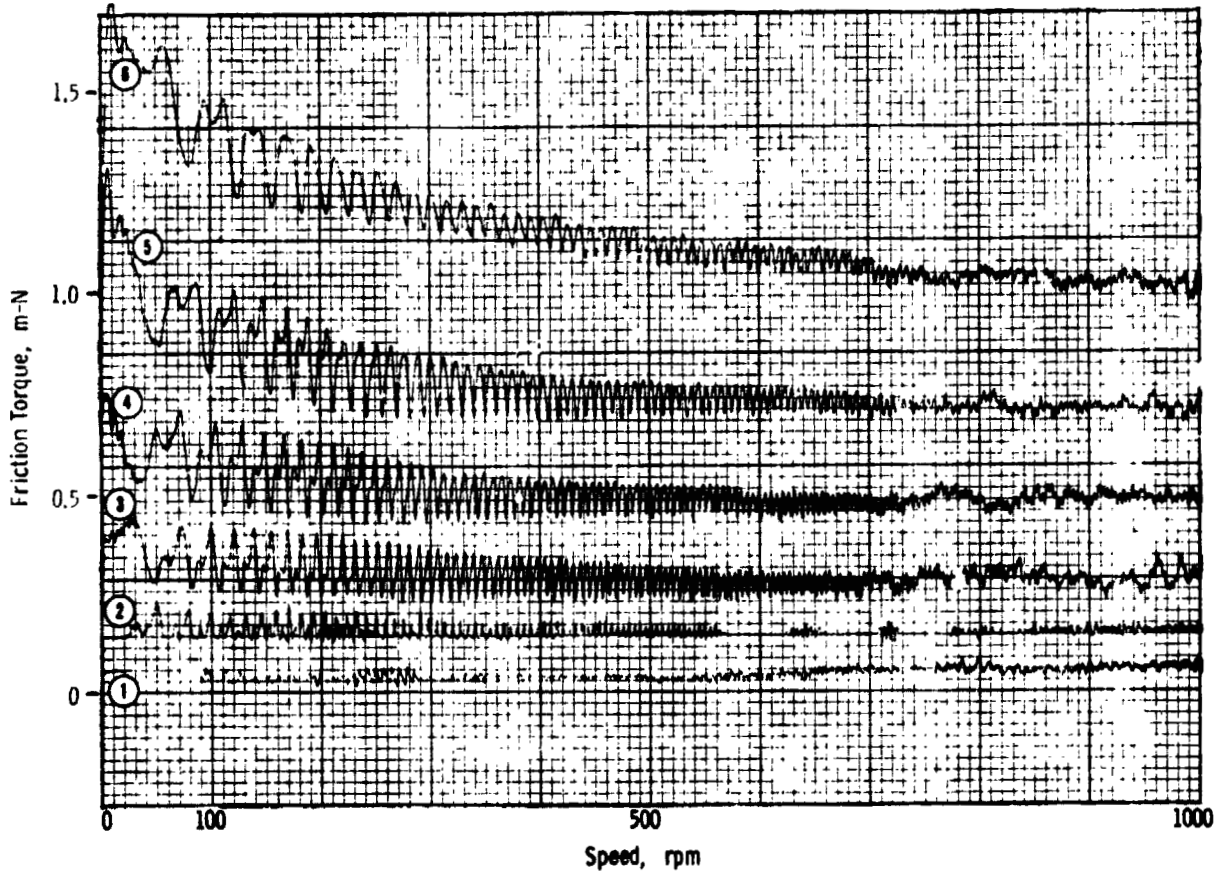
Loads, N/m^2

1. 2.07×10^5 (30 psi) (contact)
2. 2.76×10^5 (40 ")
3. 3.79×10^5 (55 ")
4. 5.17×10^5 (75 ")
5. 7.24×10^5 (105 ")
6. 1.03×10^6 (150 ")

Test Temp.: 316°C (600°F)

Atmosphere: nitrogen

Tin bronzed M2 on tungsten carbide

Figure H-4. RBT No. 44, Fluid: FH-140
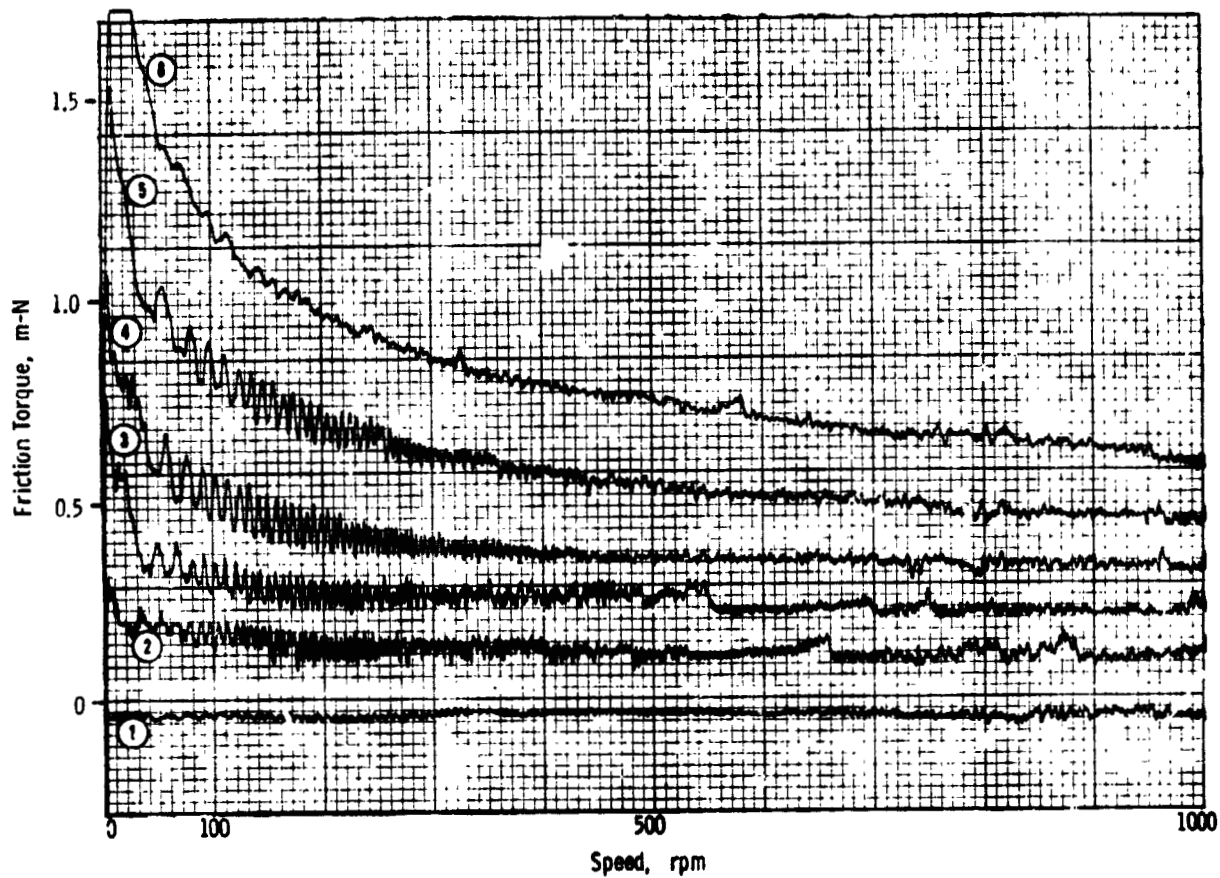
Loads, N/m^2

1. 2.07×10^5 (30 psi) (contact)
2. 2.76×10^5 (40 ")
3. 3.79×10^5 (55 ")
4. 5.17×10^5 (75 ")
5. 7.24×10^5 (105 ")
6. 1.03×10^6 (150 ")

Test Temp.: 260°C (500°F)

Atmosphere: nitrogen

Tin bronzed M2 on tungsten carbide

Figure H-5. RBT No. 49, Fluid: MCS 524 + 0.1% A-88
+ 0.05% Trichloroacetic Acid
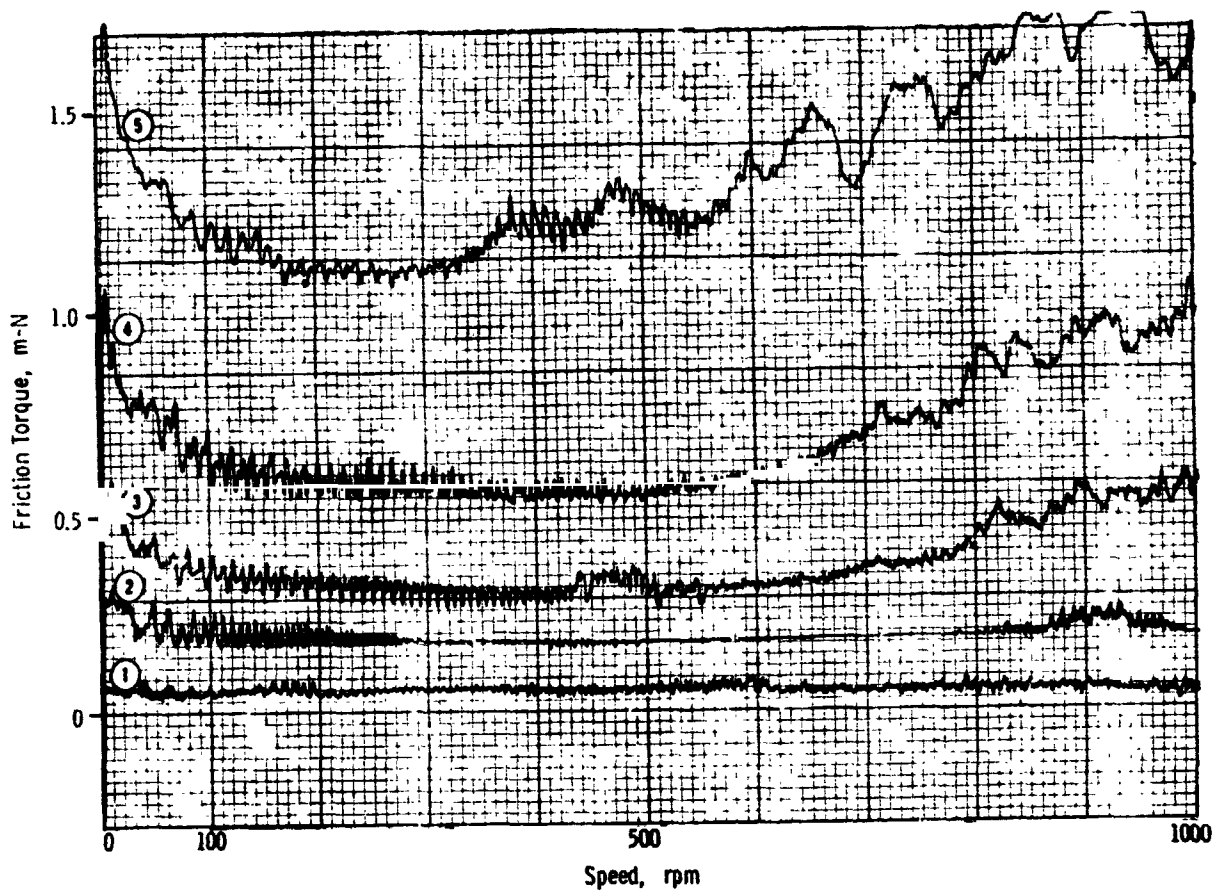
Loads, N/m²

1. 2.07 x 10⁵ (30 psi) (contact)
2. 2.76 x 10⁵ (40 ")
3. 3.79 x 10⁵ (55 ")
4. 5.17 x 10⁵ (75 ")
5. 7.24 x 10⁵ (105 ")
6. 1.03 x 10⁶ (150 ") - not run

Test Temp.: 260°C (500°F)

Atmosphere: itrogen

Tin bronzed M2 on tungsten carbide

Figure H-6. RBT No. 47, Fluid: MCS 524 +
∿0.07% Perfluoroglutaric Acid
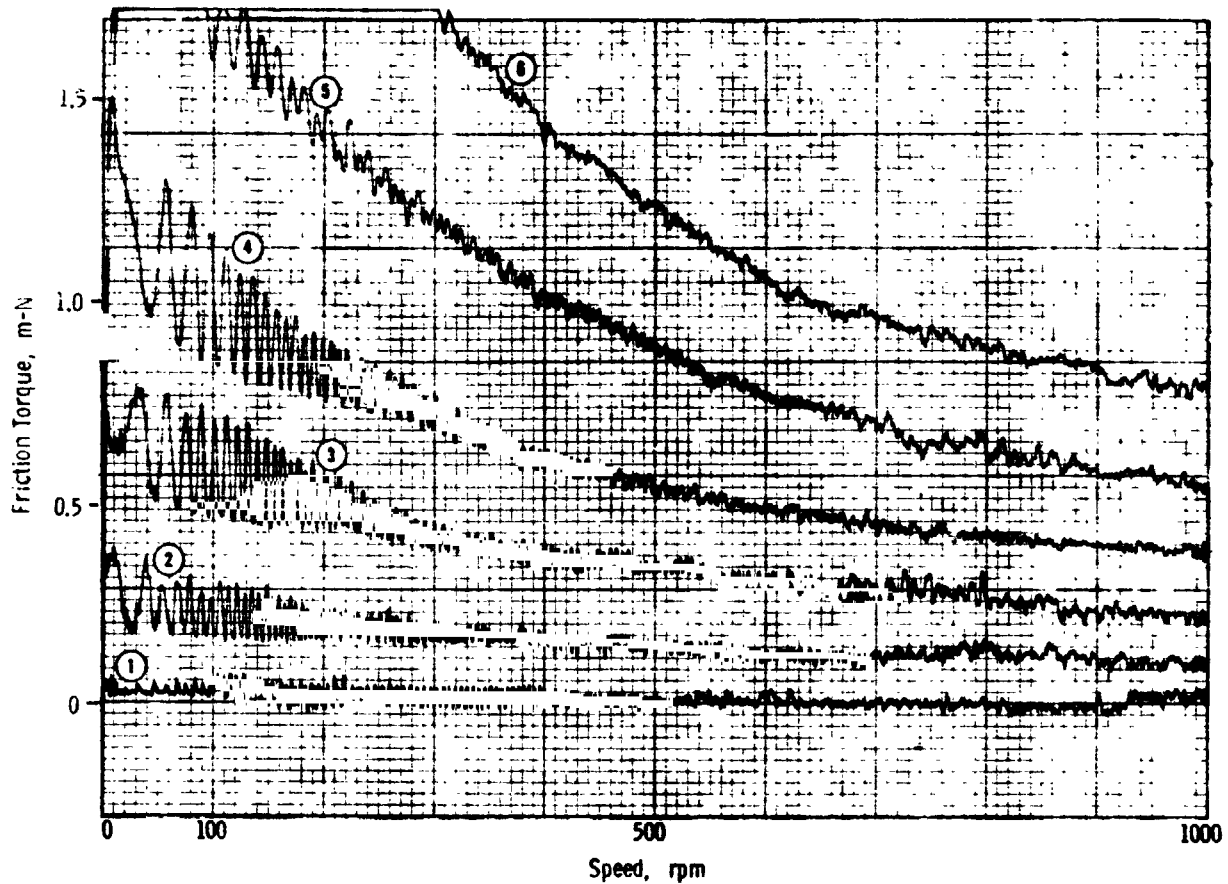
Loads, N/m^2

1.	2.07 x 10^5	(30	psi)	(contact)
2.	2.76 x 10^5	(40	"	)
3.	3.79 x 10^5	(55	"	)
4.	5.17 x 10^5	(75	"	)
5.	7.24 x 10^5	(105	"	)
6.	1.03 x 10^6	(150	"	)

Test Temp.: 260°C (500°F)

Atmosphere: nitrogen

Tin bronzed M2 on tungsten carbide

Figure H-7. RBT No. 50, Fluid: MCS 524 + 0.1%
Phenylphosphinic Acid
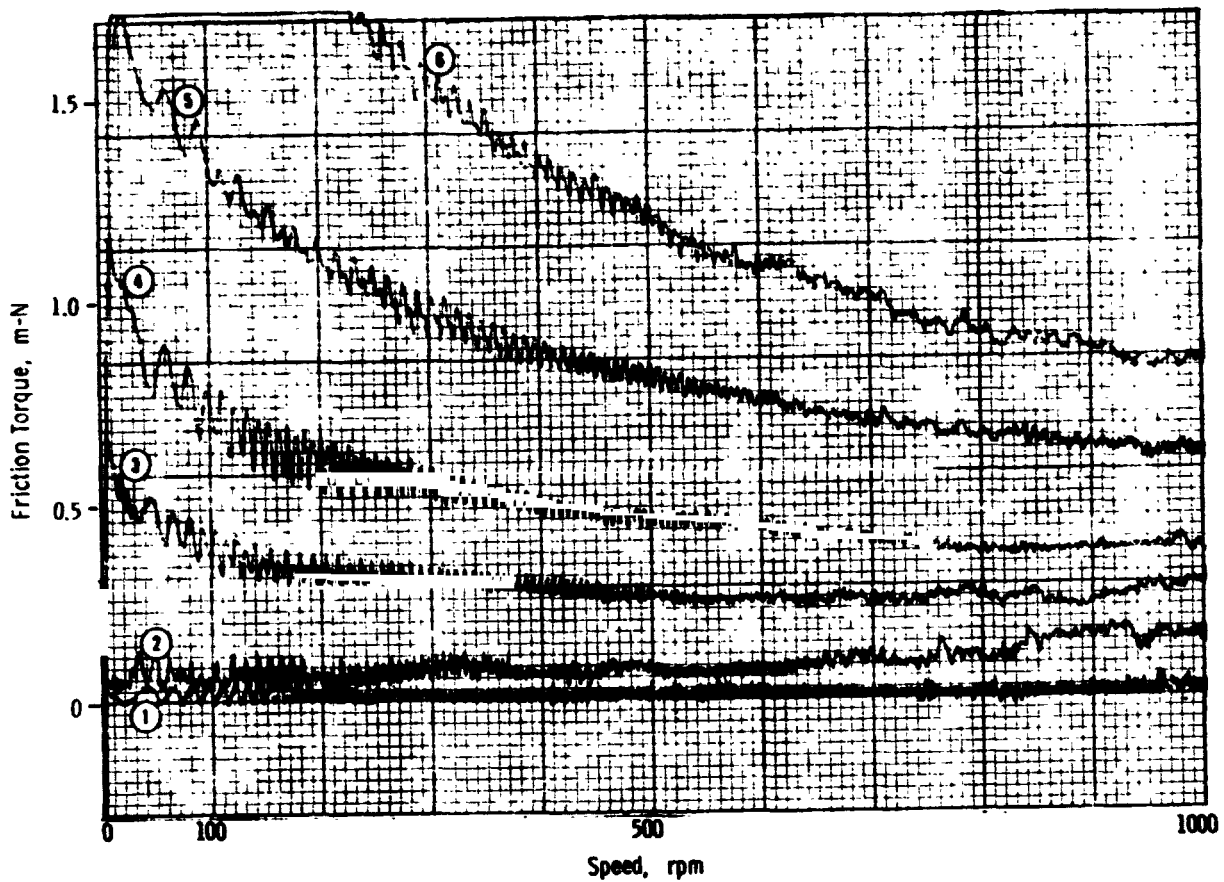
Loads, N/m^2

1. 2.07×10^5 (30 psi) (contact)
2. 2.76×10^5 (40 ")
3. 3.79×10^5 (55 ")
4. 5.17×10^5 (75 ")
5. 7.24×10^5 (105 ")
6. 1.03×10^6 (150 ")

Test Temp.: 260°C (500°F)

Atmosphere: nitrogen

Tin bronzed M2 on tungsten carbide

Figure H-8. RBT No. 54, Fluid: MCS 524 + 0.1%
m-Phenylmercaptophenylphosphinic
Acid

253

Loads, N/m²

1.	2.07 x 10⁵	(30 psi)	(contact)
2.	2.76 x 10⁵	(40 ")	
3.	3.79 x 10⁵	(55 ")	
4.	5.17 x 10⁵	(75 ")	
5.	7.24 x 10⁵	(105 ")	
6.	1.03 x 10⁶	(150 ")	- not run

Test Temp.:   260°C (500°F)

Atmosphere: nitrogen

Tin bronzed M2 on tungsten carbide

Figure H-9.   RBT No. 56, Fluid: MCS 524 + 0.1% m-(m-Phenylmercaptophenylmercapto)phenylphos-phinic Acid
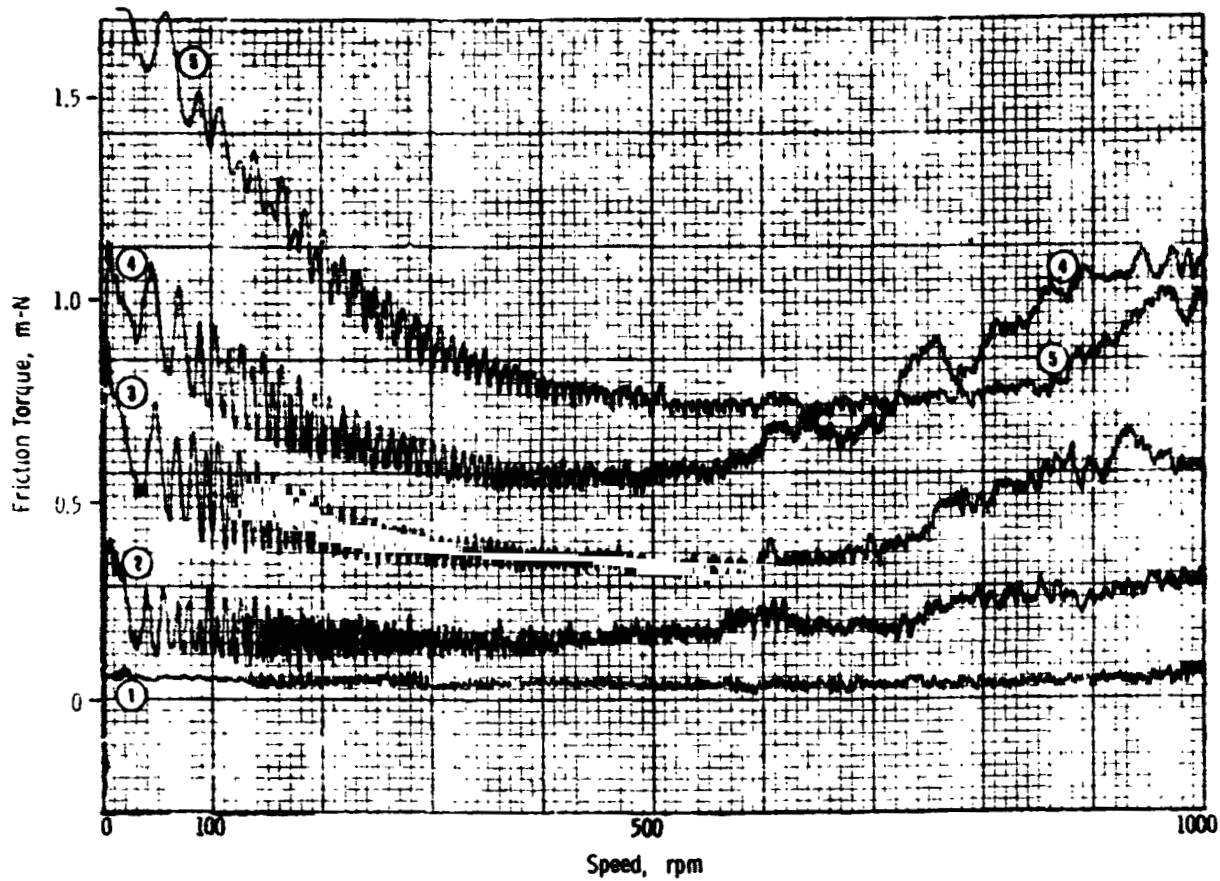
Loads, N/m^2

1. 2.07 x 10^5 (30 psi) (contact)
2. 2.76 x 10^5 (40 ")
3. 3.79 x 10^5 (55 ")
4. 5.17 x 10^5 (75 ")
5. 7.24 x 10^5 (105 ")
6. 1.03 x 10^6 (150 ") - not run

Test Temp.: 260°C (500°F)

Atmosphere: nitrogen

Tin bronzed M2 on tungsten carbide

Figure H-10. RBT No. 48, Fluid: MCS 524 + 0.075%*
Phenylphosphinic Acid + 0.1%* Per-
fluoroglutaric Acid

_____

*Initial additive charge.
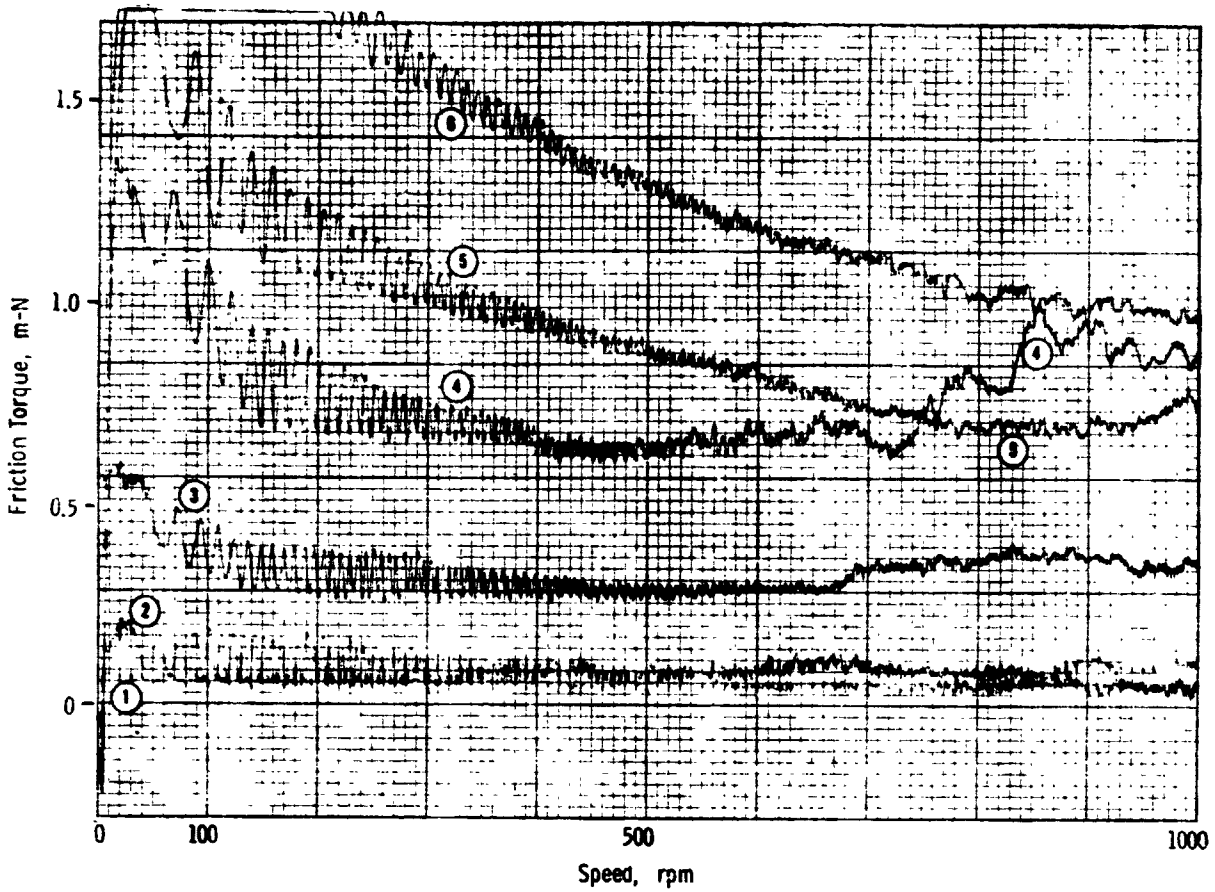
Loads, N/m^2

1. 2.07 x 10^5 (30 psi) (contact)
2. 2.76 x 10^5 (40   "   )
3. 3.79 x 10^5 (55   "   )
4. 5.17 x 10^5 (75   "   )
5. 7.24 x 10^5 (105   "   )
6. 1.03 x 10^6 (150   "   )

Test Temp.:   260°C (500°F)

Atmosphere: nitrogen

Tin bronzed M2 on tungsten carbide

Figure H-11.   RBT No. 60, Fluid: MCS 524 + 0.1%* m-
Phenylmercaptophenylphosphinic Acid
+ 0.1%* Perfluoroglutaric Acid

*Initial additive charge.

256
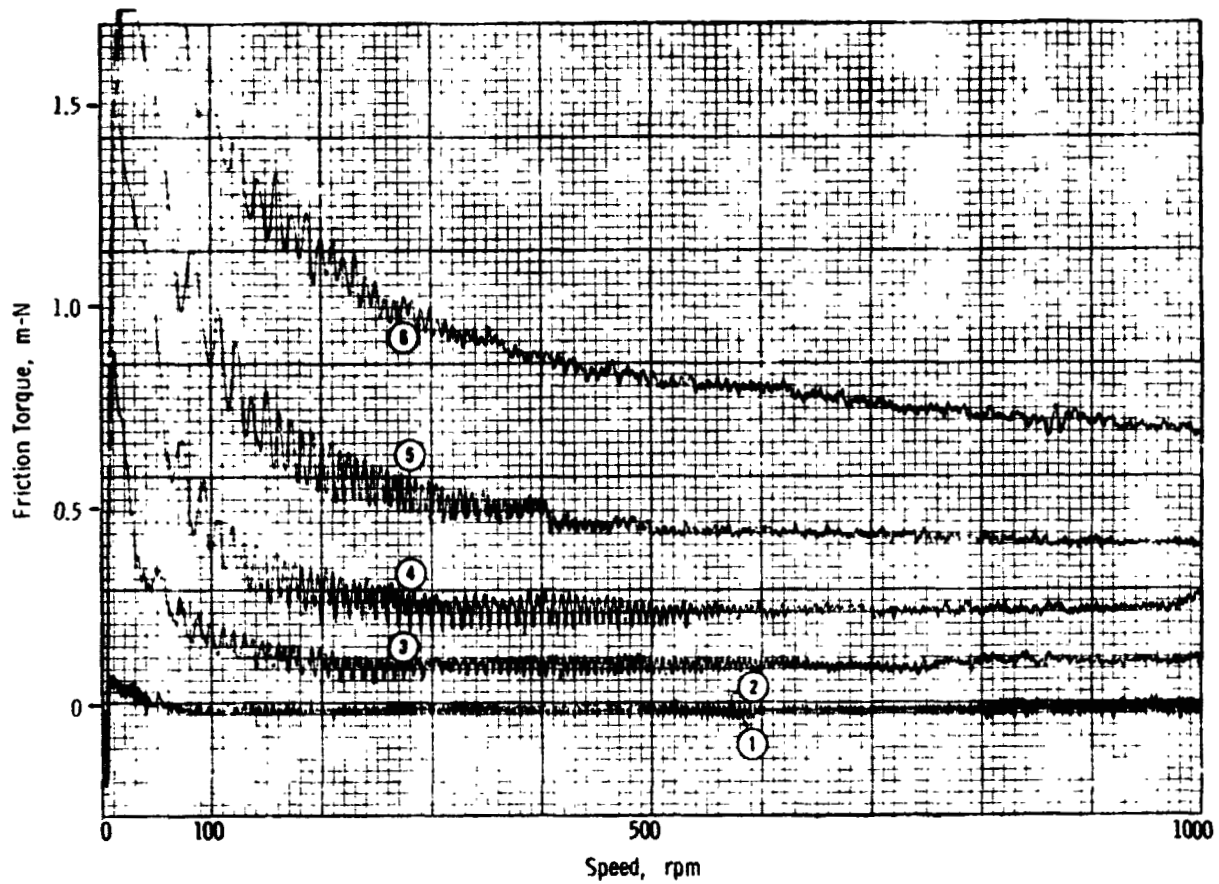
Loads, N/m^2

1. 2.07 x 10^5 (30 psi) (contact)
2. 2.76 x 10^5 (40 ")
3. 3.79 x 10^5 (55 ")
4. 5.17 x 10^5 (75 ")
5. 7.24 x 10^5 (105 ")
6. 1.03 x 10^6 (150 ")

Test Temp.: 260°C (500°F)

Atmosphere: nitrogen

Tin bronzed M2 on tungsten carbide

Figure H-12.   RBT No. 63, Fluid: MCS 524 + 0.1% A-88
               + 0.05% Trichloroacetic Acid + 0.1% DC-473
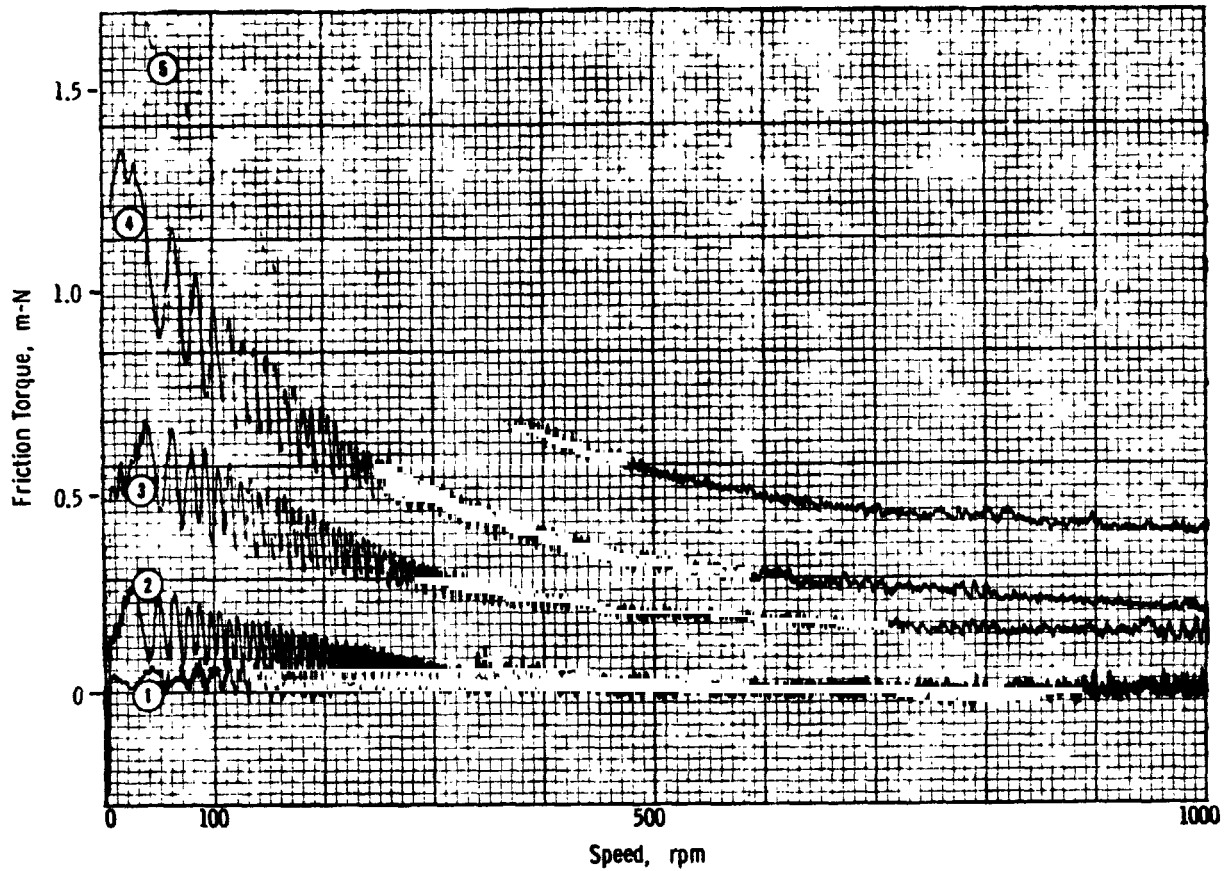
Loads, N/m^2

1. 2.07×10^5 (30 psi) (contact)
2. 2.76×10^5 (40 ")
3. 3.79×10^5 (55 ")
4. 5.17×10^5 (75 ")
5. 7.24×10^5 (105 ")
6. 1.03×10^6 (150 ") - not run

Test Temp.: 260°C (500°F)

Atmosphere: nitrogen

Tin bronzed M2 on tungsten carbide

Figure H-13. RBT No. 52, Fluid: MCS 524 + 0.1%
Phenylphosphinic Acid + 0.1% DC-473
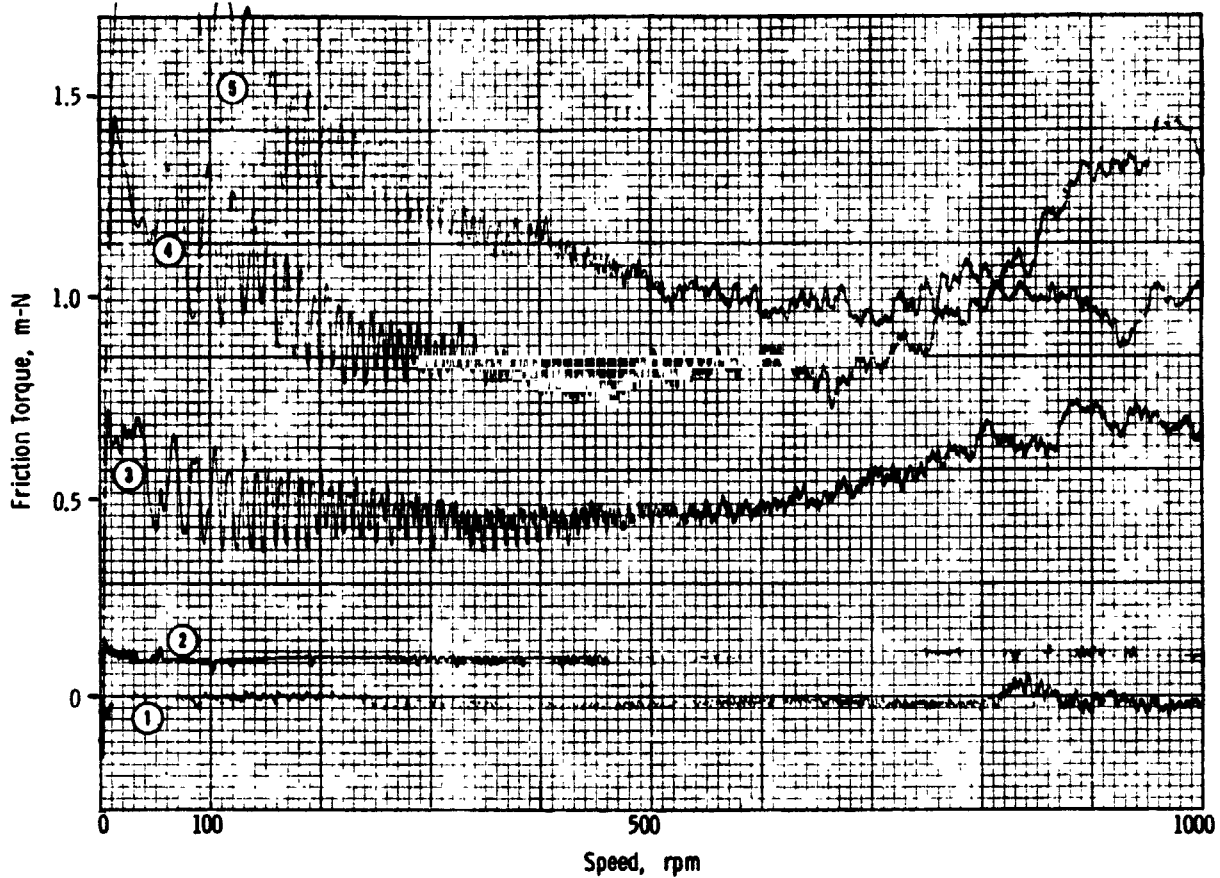
Loads, N/m^2

1. 2.07 x 10^5 (30 psi) (contact)
2. 2.76 x 10^5 (40 ")
3. 3.79 x 10^5 (55 ")
4. 5.17 x 10^5 (75 ")
5. 7.24 x 10^5 (105 ")
6. 1.03 x 10^6 (150 ") - not run

Test Temp.: 260°C (500°F)

Atmosphere: nitrogen

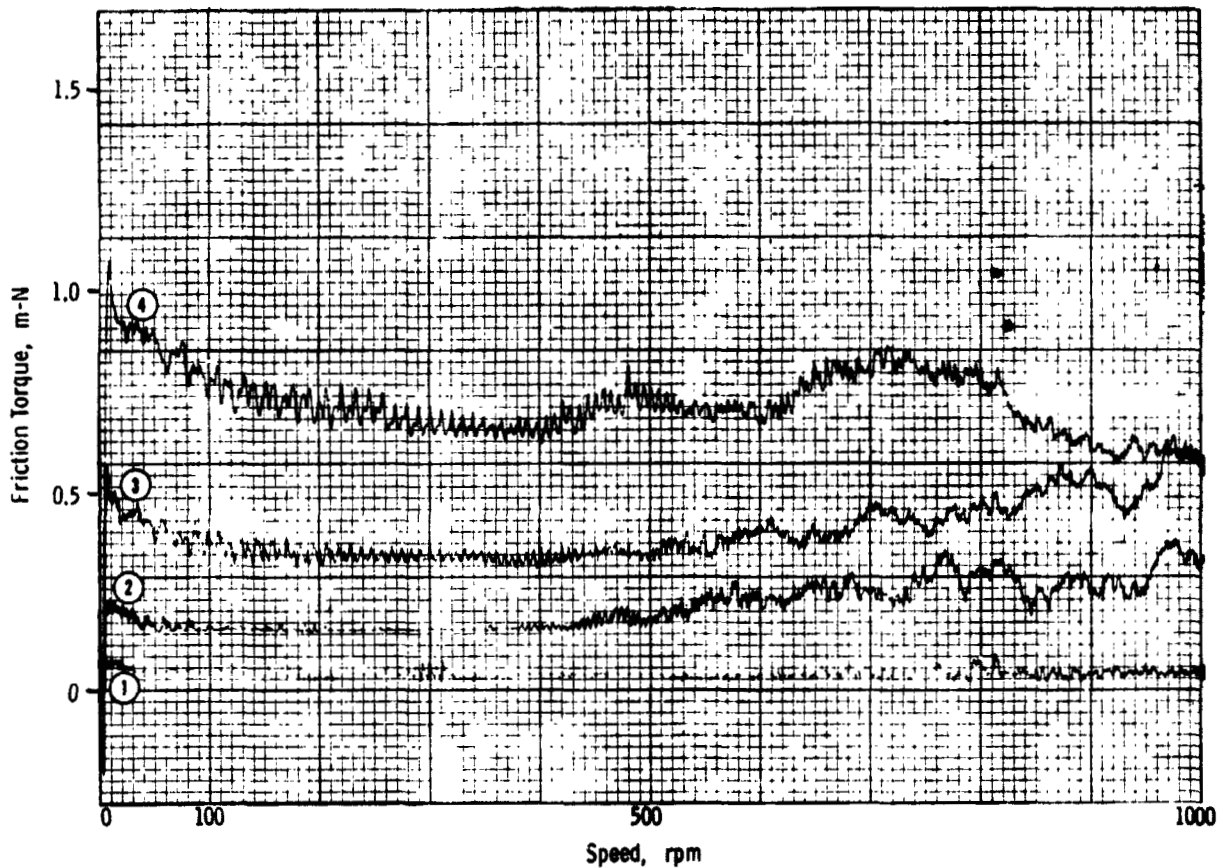Tin bronzed M2 on tungsten carbide

Figure H-14. RBT No. 61, Fluid: MCS 524 + 0.1% Phenyl-
   phosphinic Acid + 0.1% Perfluoroglutaric
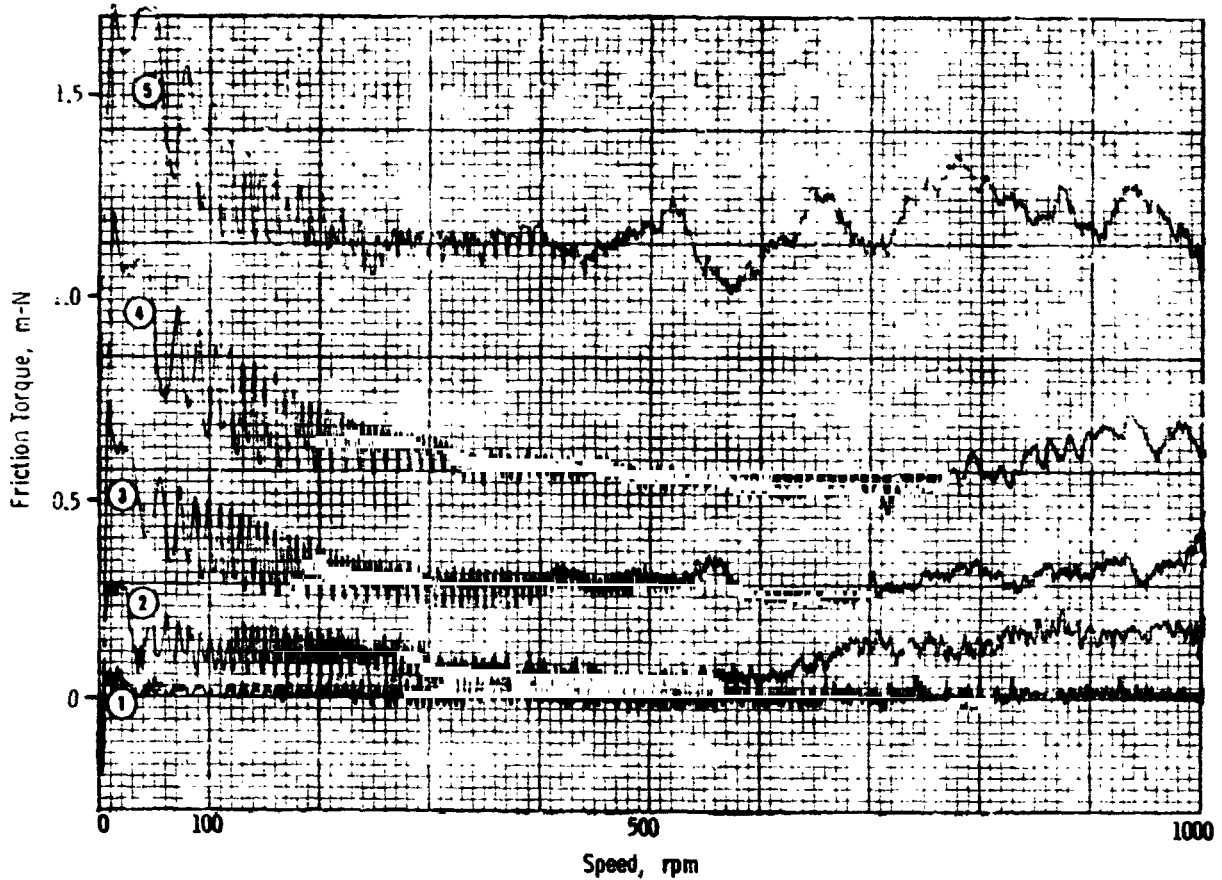   Acid + 0.1% DC-473

259

APPENDIX I: BEARING TEST PROCEDURES

DISASSEMBLY

Before beginning disassembly, the cold oil drain quantity was measured and consumption calculated. Appropriate fluid samples were retained for analysis and included in consumption calculations.

Fiber glass insulation was then removed and the test oil supply manifold assembly disconnected from the front cover and the individual jet pressure transducers. The front cover (#31)* was then removed by jackscrewing with several of the cover bolts (#53). [A part change was dictated here when the gasket (#30) repeatedly stuck tightly to both the housing and cover. The change to high temperature gasket material minimized the problem.]

Electrical leads to the bearing heaters (#31) were then disconnected and laid aside, and 1/4-28 nuts were installed and tightened on the bearing support-damper assembly carriers (not shown in drawing) to compress the belleville springs until the rollers cleared the housing. (All five carriers were retracted this way.)

Safety wire was removed next from the bearing torque transducer yoke (#82) to housing bracket (#63) connecting pin. [The yoke (#82) was modified to eliminate the ball lock pin (#83) which fell apart due to severe vibration during early MCS 524 tests.]

The SPIR-O-LOX retaining ring (#43) was then removed followed by the tabbed ring (#42) to allow removal of the slotted nuts.

Reaction wrench A along with shaft wrench B were then fastened in position across the front of the head by two bolts (#53). The reaction wrench purpose was to hold the slotted nut (#44 bearing inner ring retaining nut) stationary while shaft wrench B was used to turn the main shaft assembly CCW and loosen the slotted nut. When loosening was accomplished, reaction wrench A was removed and reaction wrench C installed (again with shaft wrench B). Reaction wrench C held slotted nut (#41 liner retaining nut) in place while the shaft was turned CW to loosen the nut. Both slotted nuts were then removed and a special threaded puller was installed onto the test bearing (#45) inner ring threads. Turning the jackscrew in the puller against the shaft center then caused the entire bearing housing assembly to slide forward and off the shaft. Thermocouples (#46) were then removed by turning the twist lock thermocouple adapters (#47). Slotted nuts were then repositioned on the assembly along with the tabbed ring and SPIR-O-LOX ring for photography.

---

*The part numbers refer to drawing #MBT100700 of the test head on file at NASA Lewis Research Center, Cleveland, Ohio.

After photographing the complete bearing/housing/support-damper assembly, the safety wire on ten damper housing bolts (#28) was removed and the damper assembly, retaining rings (#23, #26), and heaters (#25, #27) were removed. Damper assembly carriers were also removed for cleaning. At this point, the bearing and housing were photographed also.

Slotted nut #44 was removed again to allow the headed pin (#33) to be taken out after safety wire was removed. Special wrench D was then utilized to remove the outer race retaining nut (#35). The inner rings were then pressed from liner (#40). This also allowed the cage to be removed. Finally, the outer race was pressed out of the housing (#24). At this point, the bearing was fully apart for photography.

All test fluid wetted parts were then removed for cleaning except for large parts such as the condenser or test housing (#19) and load piston (#56). (See cleaning procedure.) In cases where the next test used the same basic fluid (unless there was an additive version difference) and dirt or metal generation was minimal, cleaning was accomplished with solvent and minimum parts were removed.

Wear type failures and/or dirt generators required complete breakdown and cleaning of all test related parts.

PHOTOGRAPHY

The first step in photography occurred during disassembly. The complete bearing housing/damper assembly was photographed. A POLAROID MP-3 camera with type 52 film was used for black and white photos while KODACOLOR-X was used for color photos of this and other test bearing parts.

For the next photograph, the damper assembly, heaters, and retaining rings were removed from the bearing housing. The housing and bearing assembly were then photographed.

After test bearing disassembly, the bearing was placed in the following format:

1. Outer race set up with <u>front</u> (surface facing inlet oil jets) oblique to the camera.

2. Cage assembly resting on one edge of outer race with <u>rear</u> side oblique to the camera.

3. Rear inner ring supported to right of outer race.

4. Front inner ring supported to left of outer race (thrust loaded ring).

262

After taking this overall view, other close-up shots (such as cage wear area or ball pocket areas) were made.

Various other photographs were made as necessary.

CLEANING

Cleaning of test oil wetted parts was accomplished by one of three different methods.

The first method involved flushing with solvents. In most cases this included the test oil vapor condenser. Hexane, then acetone, then hexane rinses were employed followed by air drying.

The second method consisted of spraying off oil deposits with stoddard solvent, then air drying. An OAKITE 77 bath with ultrasonic capability and heated to 82°C was then used to soak parts for 1-48 hours or more. Copious amounts of hot water were then used to remove all OAKITE residue. If deposits were not removed completely at this time, kitchen cleanser and appropriate brushes were used to remove them. Finally, thorough rinsing with hot water, then acetone to flash dry, and finally stoddard solvent was accomplished.

If hard deposits were not removed by these methods, a third method was employed using #240 silicon carbide paper or wire brush wetted with stoddard solvent. Frequent changes of solvent and abrasive paper were used until the desired removal of deposits was accomplished. This method was generally used on large flat or round parts such as the test housing interior, front cover, and oil reservoir. Cleaning was done until a uniform metal finish was exposed.

When it was desired to give the condenser a more thorough cleaning, the OAKITE 77 bath was used followed by hot water rinsing, then acetone, then air drying. Abrasives were not used for cleaning the condenser.

Filter cleaning was accomplished first by ultrasonic agitation in tri-solvent (equal parts acetone, chloroform and toluene) to remove metallic and oily residue. Fifteen to twenty percent sodium hydroxide solution was next used in the ultrasonic cleaner bath. Following hot water flushing, a strong detergent solution was used in the ultrasonic bath followed again by hot water flushing. This was then followed by several acetone flushes aided by ultrasonic action. Finally, the filter was dried by blowing with filtered nitrogen gas.

Extreme difficulty was encountered in cleaning deposits from head parts after some extremely dirty tests. For test 12 and following,

it was decided to have test bearing housing parts nickel plated to present a uniform surface that would be easier to clean. Removing the silver plating from the bearing retainer nuts makes test oil silver content analysis a better indicator of silver removal from the test bearing cage.

Small parts such as bolts and nuts were cleaned ultrasonically using appropriate solvents or solutions. Stubborn deposits were removed by abrasive methods such as method three or by wire brushing.

Cleaning of shaft cavities was accomplished with brushes, solvent, and air drying. The center oil jet annulus was the most difficult portion of this.

ASSEMBLY

For assembly all parts were once again inspected to assure clean surfaces. The new test bearing was then solvent cleaned of preservative grease. Then the inner rings were heated along with the bearing housing in an 82-93°C oven for 20-30 minutes. Upon removal from the oven, the outer race was lightly tapped into the bearing housing (#24) using a press sleeve and with serial number to the rear. The rear inner ring (one with annular groove and oil grooves) was then placed on the liner (#40) and the cage assembled into the bearing. The front inner ring was then aligned carefully with grind marks in relation to the rear ring grind marks and tapped into place with a drift. All parts were prelubed with test fluid before assembly. Light bearing prelube followed.

After assembly of the bearing, a paste of graphite and test fluid was used to lubricate the threads of slotted nuts (#35 and #44) before installation. The outer race slotted nut (#35) was then tightened until one of the holes in the housing matched the hole in the slotted nut. The headed pin (#33) was then inserted and safety wired. The inner ring retaining nut (#44) was now installed finger tight.

Heaters (#25, #27) and their retainer plates (#23, #26) were installed in conjunction with the damper housing using stainless steel bolts and washers and nuts. Finally, these were secured by fastening safety wire around the exposed thread above the nut and tying these together. The damper assembly carriers were then installed and retracted for installation in the test housing.

The entire assembly was then checked for proper assembly and smooth bearing operation before proceeding with installation. The three thermocouples were then installed and locked in place before the assembly could be inserted into the housing. Prelubing the shaft preceded the next steps of careful alignment of

264

dowel pins (#52) with the corresponding liner slots and sliding
the entire assembly onto the shaft in the housing. After again
checking alignment, the liner retaining nut (#41) was installed
and tightened to 169.5 N-m (125 ft lb). The inner ring re-
taining nut (#44) was then torqued to 203.4 N-m (150 ft lb).
After both slotted nuts were tightened, the tabbed ring (#42)
was located to lock the slotted nuts together, and finally, the
SPIR-O-LOX retaining ring (#43) was installed in the machined
groove in the outer slotted nut (#44).

Heater leads were then connected, taking care to support wires
well and eliminate points of strain as well as possible.

The torque transducer connecting link was then safety wired in
place by placing wire through the cotter pin hole and wiring
around the threaded rod (#81).

Careful positioning of all thermocouple wires was then checked
to eliminate binding or chafing possibilities.

Damper assembly carriers were released by loosening the two nuts
on each carrier leg. Nuts were then completely removed from the
carrier legs and carrier rollers were left contacting the test
housing inner diameter.

After a final check for free operation and installation of all
items, the front cover (#31) was installed with twelve bolts
(#53) and washers (#54). A new cover plate gasket (#30) was
used on most high temperature tests. Oil manifold installation
followed as did installation of remaining lines, meter, filter,
thermocouples, and other instrumentation.

Normal maintenance of the support system was also done at this
time.

STARTING THE TEST

An initial fluid fill of 7000 milliliters was charged to the
test oil reservoir. The test oil pump was then run and flow was
approximately adjusted for target amount. Integrity of line
assembly was observed and insulation was then installed on the
supply lines. Oil flow was then stopped. (Coinciding with oil
flow start, air flow to the labyrinth seal was begun and adjusted.
Various combinations of air flow to this seal and air bleed to the
support system were used to conserve test fluid. Most effective
were low differentials - usually 1 inch of oil on the test oil
side relative to the support side whenever possible.)

Support oil heaters were started approximately 30 minutes or
more before desired test start to allow visco   support oil to

265

be pumped readily. Test oil flow and outer race heaters were also started (flow-only method of circulating fluid for hot spot elimination) to bring oil inlet temperature to about 121°C before starting bearing rotation. Recorders were also turned on at this time.

When the warm-up period was complete, cooling water flow to support components was started. Test bearing rotation was slowly brought to 5,000 or 10,000 rpm and temperatures observed for 15 minutes or more before advancing speed further. Test bearing heat was also turned on as soon as 10,000 rpm conditions were attained. Usually contract speed conditions were reached in an hour or less (unless problems developed) and target contract temperatures were reached within about 30 minutes from that point. Attainment of target contract temperatures was taken as test time zero.

During the time required for warm-up, various test conditions were observed and recorded at intervals, when possible. Adjustments of torque equipment, flow rate, air flow, load setting, support oil pressures, ar other items were sometimes necessary. Because of short times in red between adjustments, readings of many items were omitted during warm-up. A continuous record was kept of 24 of these items on a strip chart recorder; however, the time interval of about eight minutes for a complete set of measurements was too slow for close monitoring of all variables during starting. Important temperatures, pressures, speed, vibration, and flow are items that were continuously observed by visual displays such as oscilloscope traces, meters, decade counter, etc. Test bearing temperatures were available at the temperature controller and at the select point potentiometer. Other temperatures were available at a select point potentiometer for instant readings. Numerous operational conditions were observable at various points with two inspections of the operation per day. Otherwise, shutdown alarm limits controlled shutdown. A total of 42 separate items were recorded at intervals beginning with the starting test time reading, and were kept on test log sheets.

When temperatures reached equilibrium, the torque system was recalibrated by hanging standard weights on the calibration weight holder (#84) and adjusting the span value. The initial torque reading was then zeroed and used as a base for subsequent readings. Due to the torque system zero drift, no accurate measurement of torque was possible.

RUNNING PROCEDURE

Running time began when equilibrium or target conditions were reached. (Exception was the first test when bearing heaters were unavailable.) A complete reading of test conditions was taken at this time. All running time was monitored by a timer in parallel with the drive motor startup.

Runs continued for the 100 hour contract time unless stopped due to fluid related failure or mechanical malfunction requiring shutdown.

Periodic recordings of test conditions were made along with occasional adjustments to controllers, flow valves, or other necessary changes to the test at contract conditions. Log sheet data included semicontinuous strip chart recordings and other parameters. The recorded points are listed in Tables I-1 and I-2.

Oil samples were generally taken before oil makeup was attempted. A zero time oil sample was obtained at the start of test. Other than this policy, no specific pattern for oil samples during the test was followed. The final oil sample was taken as near shutdown time as possible to obtain a representative sample.

During the test run, a number of important variables were monitored electronically (through pressure switches, chip detectors, vibration monitors, and strip chart recorder high and low alarms) to provide shutdown control when the unit was unattended. This system proved valuable, and troublesome. Shutdowns occurred for a number of reasons both fluid and system related. The most perplexing problem, however, was failure of relay switches in the control unit. Open relays were used in the control unit and at times these would malfunction due to dirt on or oxidation of contacts. Many times it was found on startup that the shutdown box would not reset, and cleaning and relay adjustment were required. Sealed relays were a long delivery item and were finally obtained during the last test. (They have since been installed for future use.)

SHUTDOWN PROCEDURE

Unattended malfunction type shutdowns were made by interrupting the console panic buttom circuit in order to stop rotation as quickly as possible. This broke all hold-in relays for pumps, heaters, and drive motors.

However, to provide test bearing oil flow for cooling, a timer was activated by the shutdown unit that closed the relays for

TABLE I-1. – TEST DATA RECORDED ON LOG SHEETS

Test Oil System	Source of Reading
Bearing temperature 1	Strip chart recorder; high S.D. alarm
2	Select point potentiometer
3	West temperature controller
Test oil in temperature	Strip chart recorder; low S.D. alarm
Test oil out temperature	Strip chart recorder; chip detector S.D.; high alarm S.D.
Force transducer temperature	Select point potentiometer
Test oil pressure jet 1	Transducer/strip chart recorder; low alarm S.D.
2	Transducer/strip chart recorder
3	" " " " "
4	" " " " "
Test compartment air pressure	Manometer (oil)
Labyrinth seal pressure	" "
Bearing speed	Speed chart recorder, decade counter
Test hours	Hour meter in series with drive motor
Test bearing load pressure	Test gauge, pressure T.D. to strip chart
Bearing torque	Transducer output meter, also strip chart, high S.D. alarm, oscilloscope output
Vibration level	D.C. signal to oscilloscope, also strip chart, high S.D.
Test oil heater input	Watt-hour meter
Test bearing heater input	" " "
Bearing power level	Wattmeter
Labyrinth seal air flow	Rotameter
Load piston air flow	"
Test oil flow	Strip chart recorder, meter, low S.D. alarm
Date	
Time	
Miscellaneous test observations	

TABLE I-2. - TEST DATA RECORDED ON LOG SHEETS

Support System	Source of Reading
Inlet temperature (main supply)	Select point potentiometer
Outlet temperature (head)	Strip chart recorder, chip detector, S.D.
Adapter block outlet temperature	Select point potentiometer, chip detector S.D.
Gear box outlet temperature	Select point potentiometer, chip detector S.D.
Slave bearing temperature 1	Strip chart recorder
2	" " "
3	Select point potentiometer
4	" " "
Dynamatic H_2O outlet temperature	" " "
Roller bearing temperature,	
left	Strip chart recorder
right	Select point potentiometer
Support oil supply pressure	Gauge
" " jet pressure,	
Spline	"
Roller	"
Ball 1	"
Ball 2	"
Scavenged compartment pressure	Manometer (oil)

support oil pumps and the test oil pump. This timer at first was set for about 15 minutes (later reduced to about five minutes) to allow cooling of bearings after electronic shutdown.

Emergency shutdowns made by operator were done by manually switching off heaters and drive unit shutdown. Oil flow was then continued for bearing cooling as long as judged necessary (usually about five minutes).

Normal shutdowns were made similarly except that the bearing was normally run at low speed (5000 to 1000 rpm) to allow better cooling. After about five minutes all pumps, motors, and water and air valves were shut off. Recorders were left on for varying periods before they were shut off. The final oil sample was taken while oil was being drained.

APPENDIX J: CHARACTERIZATION OF FILTER PLUGGINGS AND TWO SLUDGES FROM BEARING TEST 12

Location of Solids	Analytical Method	Major Metals, Crystalline Products	% C	% H	% N	% P	% Ash	Other Results
Filter plugging #1	XRF	Ag, Fe, Ni, Zn, Ca, Cu, P, S	40.4	3.1	0.1		51.9	
	XRD	Amorphous + at least one crystalline compound; no metallic silver						
	IR							Monosubstituted aryl acid; salt of this acid; acid not identified. Aliphatic peak. Carbonyl peak.
Filter plugging #2	XRF	Ag, Fe, Cr, Ni, Cu, Ca, P, S	43.7	2.5	0.1		40.9	
	XRD	Amorphous; no metallic silver						
Sludge from outer bearing housing	XRD	Amorphous	49.9	3.2	0.0	2.1	27.4	
Sludge from inner bearing hub	XRD	Amorphous	50.5	4.1	0.3	0.7	35.7	

271

APPENDIX K: CHARACTERIZATION OF SOLIDS FROM BEARING TEST 13

Filter plugging #1:

Major metals by XRF: Fe, Ag, Mo, Ni, Cr

% C: 15.32

% H: 1.4

% N: 0.07

% Ash: 81.6

XRD: Major line at d = 3.35 $\overset{\circ}{A}$
       Minor line at d = 2.15 and 2.09 $\overset{\circ}{A}$

Filter Plugging #2:

Major metals by XRF: Fe, Ag, Mo, Ni, Cr

% C: 16.8

% H: 1.8

% N: 0.02

% Ash: 76.9

XRD: Major line at d = 3.35 $\overset{\circ}{A}$
       Minor line at d = 2.15 $\overset{\circ}{A}$

APPENDIX L: PUMP TEST APPARATUS

The hydraulic pump selected was a Vickers modified PV3-044 aircraft pump of inline design. Commercially available hydraulic pumps for high temperature operation are extremely limited. In fact, the primary reason for selecting the Vickers pump is the availability of spare parts. The variable volume pressure compensated piston pump of inline design has the rubbing and rotating groups constructed with high temperature materials. Referring to Figure L-1, the exploded view of the pump, the specified high temperature components are:

No. 28   Valve plate containing the inlet and outlet parting is made of ASA 8620 steel carburized to 50 mils (R_c 60); the valve plate area (rubbing area with cylinder barrel) is coated with a tungsten carbide flame spray.

No. 45   Cylinder barrel of M2 tool steel coated with tin bronze.

No. 46   Piston and shoe assembly has M2 tool steel pistons plated with tungsten carbide and M50 tool steel shoes with tin bronze plating on the shoe thrust pads.

No. 51   Wear plate of sintered tungsten carbide.

No. 50   Shoe hold-down plate of M2 tool steel.

No. 47   Retainer of steel with proprietary coating.

No. 65   Tail bearing with M50 balls and races with silver plated steel cage.

Otherwise, the remainder of the parts are low temperature alloys seen in commercial aircraft.

The hydraulic test st. ' is similar to that shown in Figure L-2 but with the high temp. ture modifications as shown in the hydraulic circuit of Figure L-3.

Concern that Viton seals would not perform satisfactorily at the peak 260°C operating temperature led to a test of two Viton compounds in an O-ring compression/immersion test (70 hours at 260°C in MCS 524). The results were as follows:
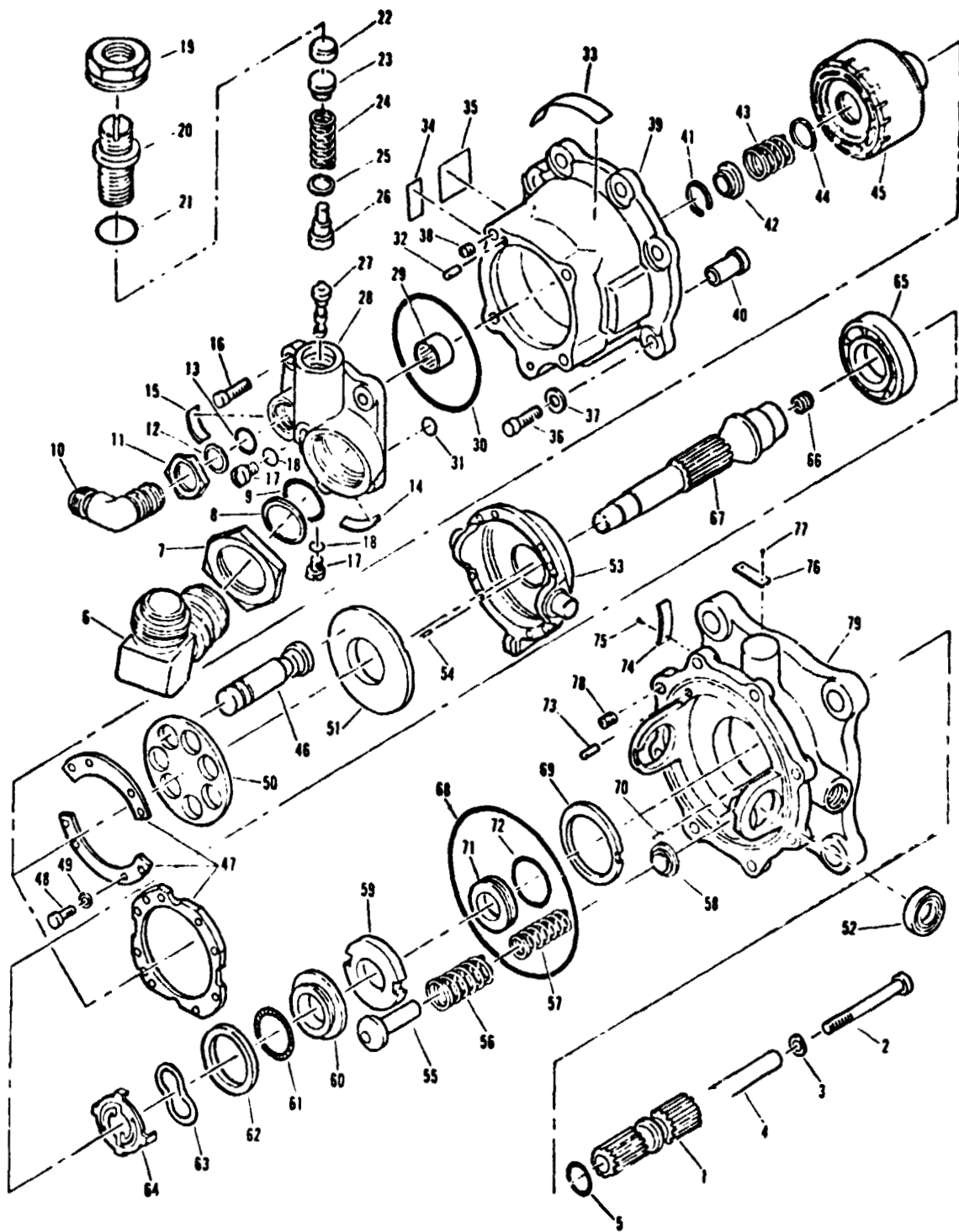
Figure L-1. Vickers PV3-044 Hydraulic Pump, Exploded View
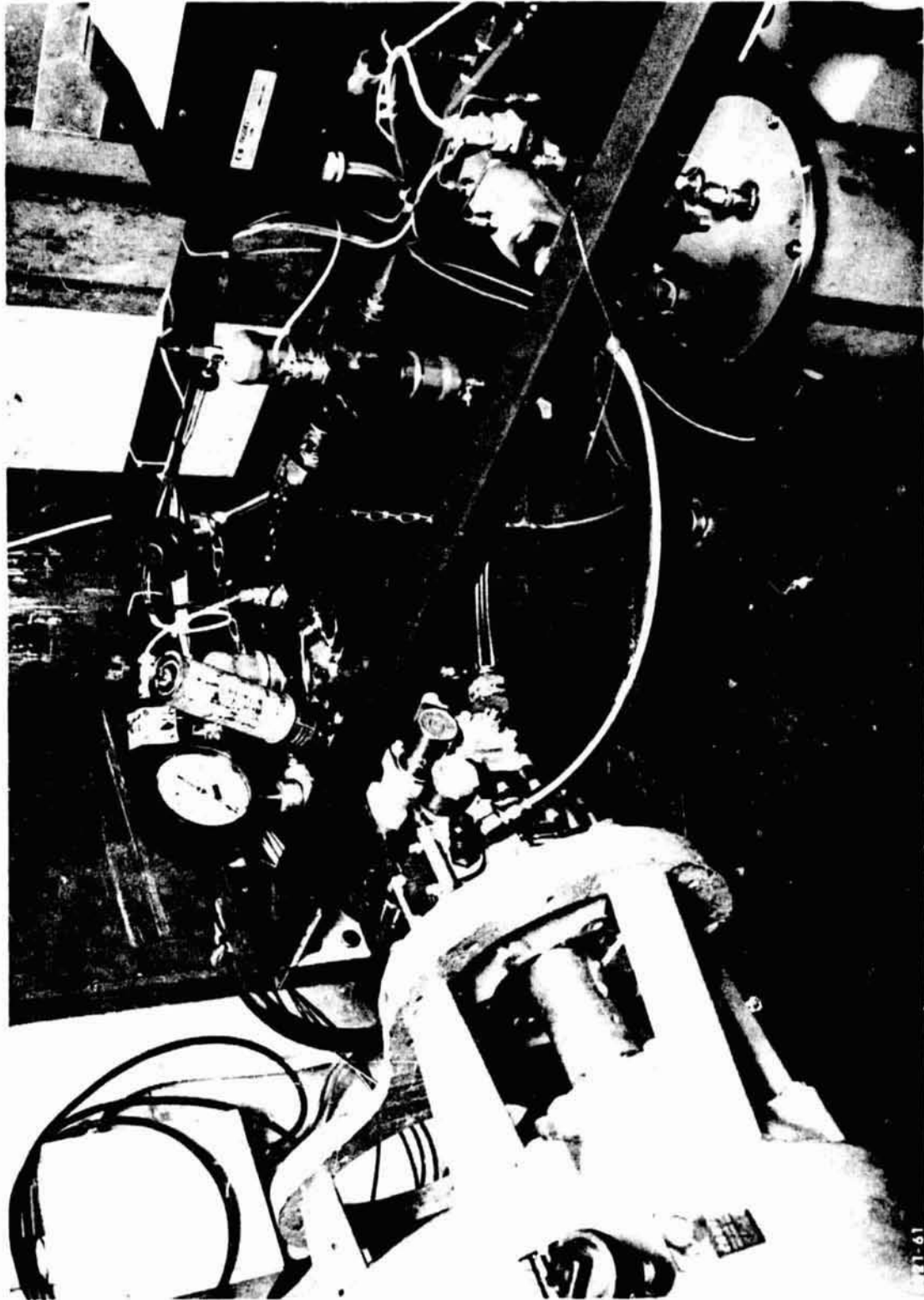
Figure L-2. High Temperature Pump Stand
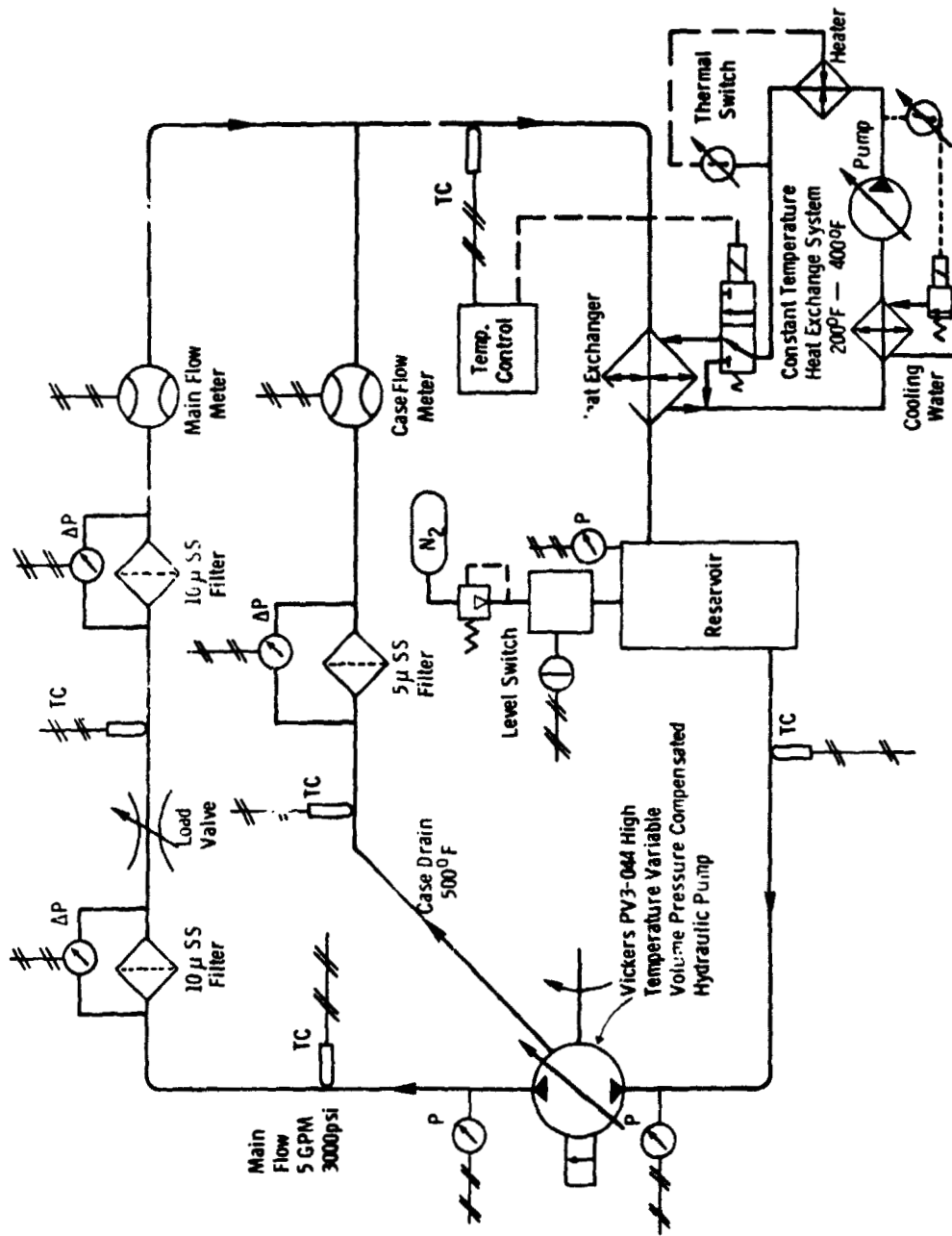
Figure L-3. High Temperature Pump Stand

Parker Compound	Shore Hardness		Final Condition
	Initial	Final	
V747-75 (new)	74	68	As new
77-545 (old)	71	94	Severe cracking, setting

The V747-75 compound, which was the compound specified in the hydraulic pump O-rings, does appear to be far superior to the older compound and should be acceptable for use in the 100 hour (max) pump tests employing C-ether formulations.

279

APPENDIX M: HYDRAULIC PUMP QUALIFICATION

The high temperature PV3-044-28 Vickers pump was inspected and found to be suitable for initial testing with Mil-H-83282 (fluid used was MLO 72-34). A successful one hour test was run as follows:

$$\text{case temperature} = 260°C$$
$$\text{rpm} = 4600$$
$$\text{outlet pressure} = 1.97 \times 10^7 \text{ N/m}^2 \text{ (2850 psig)}$$
$$\text{main flow} = 2.52 \times 10^{-4} \text{ m}^3/\text{sec (4 gal/min)}$$
$$\text{case flow} = 1.04 \times 10^{-4} \text{ m}^3/\text{sec (1.65 gal/min)}$$

There was a slight degradation in the 149°C (300°F) pump characteristic as seen from Figures M-1 and M-2. Visual inspection following testing showed the only potential problem to be wear between the piston shoes and wear plate and between the cylinder barrel and valve plate. The wear at these interfaces was primarily on the tin bronze with little effect on the tungsten carbide. The bronze suffered very slight metal removal. The surfaces had a matte copper-colored appearance indicative of copper transfer. The slight reduction in the 149°C pressure-flow pump characteristic could be due to wear or to geometry changes in the pump accompanying thermal cycling.

PRECEDING PAGE BLANK NOT FILMED

Figure M-1. Variation of Pump Flows with Outlet Pressure at
149°C and 260°C Inlet Temperature Before One
Hour 260°C Test. Pump - Vickers PV3-044-29;
Pump Speed - 4600 rpm; MLO 72-34 Fluid

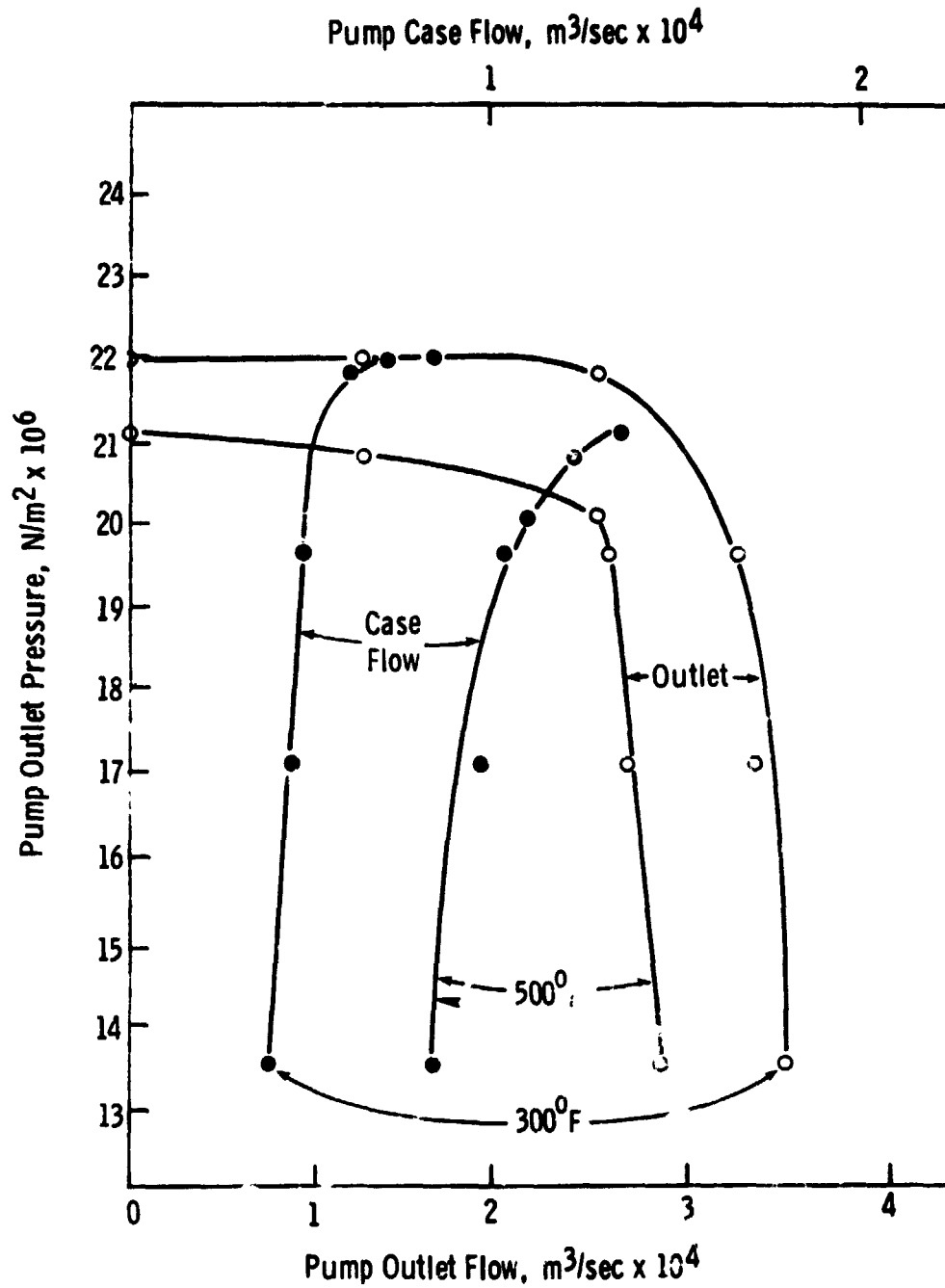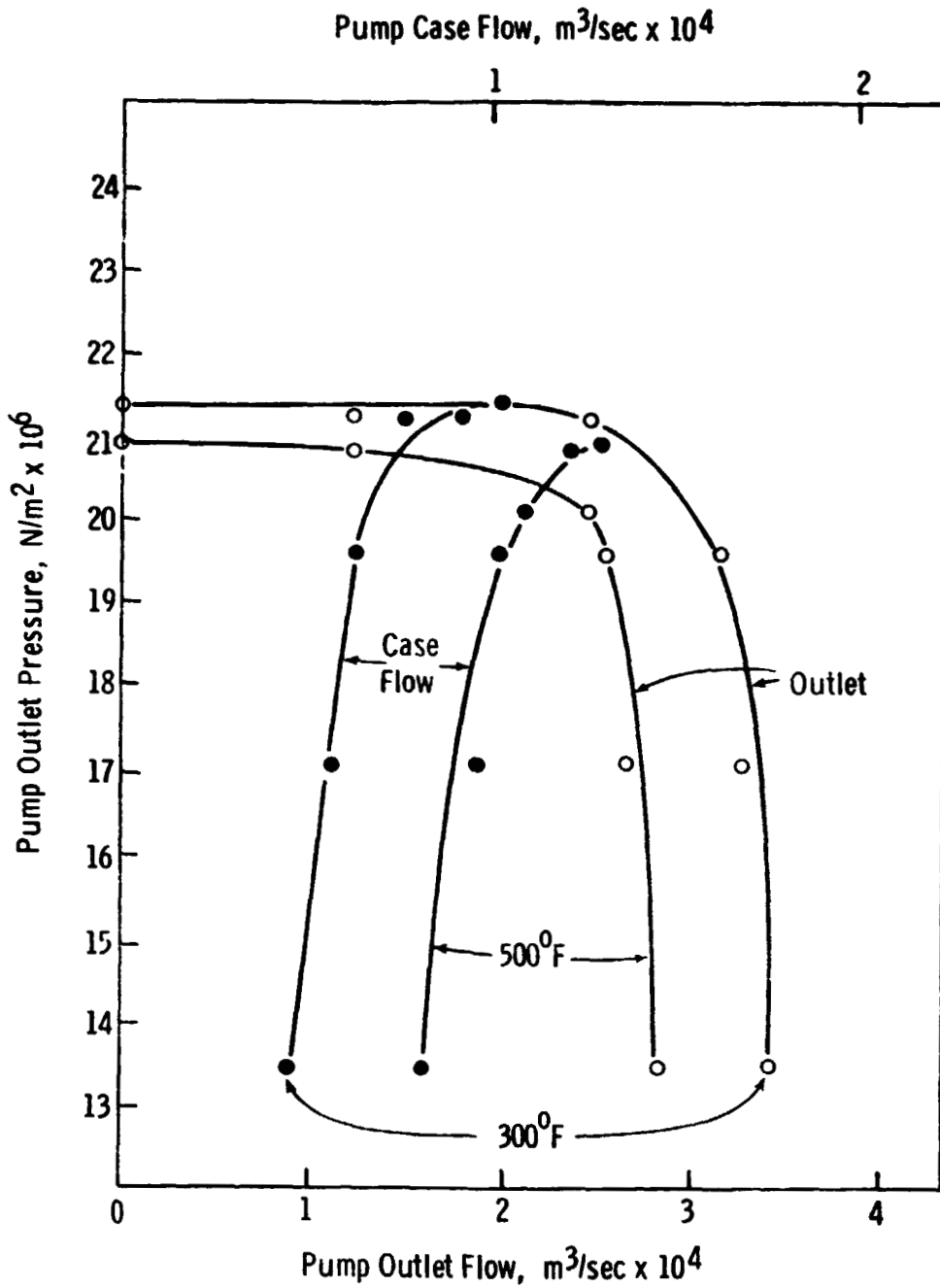Figure M-2. Variation of Pump Flows with Outlet Pressure at 149°C and 260°C Inlet Temperature After One Hour 260°C Test. Pump - Vickers PV3-044-28; Pump Speed - 4600 rpm; MLO 72-34 Fluid

C-4

APPENDIX N: NEW TECHNOLOGY APPENDIX

Inventions, innovations and improvements achieved during the contract include:

		Page No.
1)	The novel compound 1-(m-phenylmercaptophenyl)-3-phenyltetramethyldisiloxane	11, 12, 161
2)	The novel compound 1,3-bis(m-phenylmercaptophenyl)-tetramethyldisiloxane	11, 12, 159
3)	The novel compound (m-phenylmercaptophenyl)-dimethylchlorosilane	158
4)	Low pour point blends containing (1) and/or (2) above and C-ethers	14, 15, 16, 17
5)	A new all C-ether low pour point fluid (blend b)	14-17, 19
6)	The novel compound m-(m-phenylmercaptophenylmercapto)-phenylphosphinic acid	155
7)	The novel compound m-phenylmercaptophenylphosphinic acid	155
8)	Blends of (6) or (7) in C-ethers	
9)	A new apparatus for measuring surface tension	30

Items 1-4 above are claimed in a patent issued to Monsanto Company (U.S. 3,767,691 of October 23, 1973). Patent applications will be filed on items 5, 6 and 8.

PRECEDING PAGE BLANK NOT FILMED

SYMBOLS AND ABBREVIATIONS

Symbol	Meaning
A-88	proprietary Monsanto additive
DN	bearing velocity (diameter in mm x rpm)
DSC	differential scanning calorimetry
EP	extreme pressure
FH-140	C-ether base stock (lower viscosity than MCS 524)
4-ring oxy disiloxane	1,3-bis(m-phenoxyphenyl)tetramethyldisiloxane
4-ring sulfur disiloxane	1,3-bis(m-phenylmercaptophenyl)-tetramethyldisiloxane
MCS 524	reference C-ether base stock plus antifoam
m	meta
mm...	consecutive meta orientation from the left side of the structure
NMP	N-methylpyrrolidone
O & C	oxidation-corrosion
OES	optical emission spectroscopy
PFGA	perfluoroglutaric acid
φ	substituted benzene ring (see below)
PPA	phenylphosphinic acid
PMPMPPA	m-(m-phenylmercaptophenylmercapto)-phenylphosphinic acid
PMPPA	m-phenylmercaptophenylphosphinic acid
PPM or ppm	parts per million
P/N	part number
PV	pressure x velocity
RBT	rub-block test
rms	root mean square

Symbol	Meaning
TAN	total acid number (mg KOH/g)
TCA	trichloroacetic acid
tetrasulfide	tetraoctyltetraphosphetane tetrasulfide
THF	tetrahydrofuran
3-ring sulfur disiloxane	1-(m-phenylmercaptophenyl)-3-phenyltetramethyldisiloxane
2-ring disiloxane	1,3-bis(phenyl)tetramethyldisiloxane
2-ring sulfur silyl	3-trimethylsilyldiphenyl sulfide
XRD	x-ray diffraction
XRF	x-ray fluorescence
μ	coefficient of friction

- -

Chemical formulas using ϕ = substituted benzene ring:

$\phi PO_2 H_2$	phenylphosphinic acid
(m) $\phi S\phi PO_2 H_2$	m-phenylmercaptophenylphosphinic acid
(mm) $\phi S\phi S\phi PO_2 H_2$	m-(m-phenylmercaptophenylmercapto)-phenylphosphinic acid
(m) $\phi O\phi S\phi$	3-phenylmercaptodiphenyl ether
(mm) $\phi S\phi O\phi S\phi$	3,3'-bis(phenylmercapto)diphenyl ether
(m) $\phi S\phi Si(CH_3)_3$	3-trimethylsilyldiphenyl sulfide
(mm) $\phi S\phi O\phi Si(CH_3)_3$	3-trimethylsilyl-3'-phenylmercapto-diphenyl ether
$[\phi Si(CH_3)_2]_2 O$	1,3-bis(phenyl)tetramethyldisiloxane
(m) $\phi S\phi Si(CH_3)_2 -O-Si(CH_3)_2 \phi$	1-(m-phenylmercaptophenyl)-3-phenyltetramethyldisiloxane
(mm) $[\phi S\phi Si(CH_3)_2]_2 O$	1,3-bis(m-phenylmercaptophenyl)-tetramethyldisiloxane
(mm) $[\phi O\phi Si(CH_3)_2]_2 O$	1,3-bis(m-phenoxyphenyl)tetramethyl-disiloxane

288

REFERENCES

1. Bisson, Edmund E., and Anderson, William J., "Advanced Bearing Technology," NASA SP-38, 1-13 (1964). This topic is also discussed in reference 18 below.

2. Contract NAS3-6267, "Supersonic Transport Lubrication System Investigation," SKF Industries, Inc.

3. Contract NAS3-7263, "Evaluation of Hydraulic Fluids for Use in Advanced Supersonic Aircraft," Republic Aviation.

4. Contract NAS3-11171, "High Temperature Lubricant Screening Tests," SKF Industries, Inc.

5. Contract AF 33(657)-8893, "Research to Develop a Gas Turbine Engine Lubricant Based on Polyphenyl Ethers," Monsanto Research Corp.

6. McHugh, Kenneth L., and Stark, Louis R., "Properties of a New Class of Polyaromatics for Use as High Temperature Lubricants and Functional Fluids," ASLE Trans., 9, 13-23 (1966).

7. Clark, Frank S., "Polyphenyl Thioether Lubricating Compositions," U.S. Patent 3,677,944, July 18, 1972.

8. Johnson, Robert L., Loomis, William R., and Ludwig, Lawrence P., "Bearings, Lubricants and Seals for Actuators and Mechanisms," NASA Space Shuttle Technology Conference, Vol II-Structure and Materials, NASA TM-X-2273, 1971, pp. 616-632.

9. Lewis, Richard N., "High Temperature Fluids," U.S. Patent 3,114,759, December 17, 1963.

10. Askwith, T. C., Cameron, A., and Crouch, R.F., "Chain Length of Additives in Relation to Lubricants in Thin Film and Boundary Lubrication," Proc. Roy. Soc. A., 291, 500-19 (1966).

11. Grew, W., and Cameron, A., "Friction Transition Temperature Effect of Matching Surfactant and Carrier," Nature, 214, 429 (1967).

12. Gray, V.R., "Contact Angles, Their Significance and Measurement," in Wetting, S.C.I. Monograph No. 25, Society of Chemical Industry and Gordon and Breach, Science Publishers, Inc., New York, 1967, pp. 102-4.

13. Sugden, Samuel, "The Determination of Surface Tension from the Maximum Pressure in Bubbles," J. Chem. Soc., 1922, 858; also 1924, 27.

14. Cuny, K. H., and Wolk, K.L., "Präzisierung der Blasendruck-methode zur Bestimmung der Oberflächenspannung von Flüssig-keiten," Ann. Phys., ser. 6, 17, 57-77 (1956).

15. Jones, William R., Jr., and Wedeven, Lavern D., "Surface Tension Measurements in Air of Liquid Lubricants to 200°C by the Differential Maximum Bubble Pressure Technique," NASA TN D-6450, 1971.

16. Matveevsky, R. M., "The Temperature of Tribochemical Reaction Between E.P. Additives and Metals," Tribology, 4, 97 (1971).

17. Foord, C. A., Hammann, W. C., and Cameron, A., "Evaluation of Lubricant Using Optical Elastohydrodynamics," ASLE Trans., 11, 31-43 (1968).

18. Jones, William R., Jr., "Boundary Lubrication of Formulated C-ethers in Air to 300°C. II, Organic Acid Additives," NASA TN D-7524, 1973.

19. Bascom, Willard D., Cottington, Robert L., and Singleterry, Curtis R., "Dynamic Surface Phenomena in the Spontaneous Spreading of Oils on Solids," in Contact Angle, Wettability and Adhesion: Advances in Chemistry Series No. 43, American Chemical Society, Washington, D.C., 1964, pp. 355-379.

20. Federal Test Method Standard No. 791B, Method 6508.1.

21. Fein, R. S., and Kreuz, K. L., "Chemistry of Boundary Lubrication of Steel by Hydrocarbons," ASLE Trans., 8, 29 (1965).

22. Goldman, I. B., Appledorn, J. K., and Tao, F. F., "Scuffing as Influenced by Oxygen and Moisture," ASLE Trans., 13, 29-38 (1970).

23. Lewis, Richard N., "Methylphenylpolysiloxanes," J. Am. Chem. Soc., 70, 1115 (1948).

24. Andrianov, K. A., and Delazari, N. V., "Synthesis of Some Organosilicon and Titanoörganic Compounds," Doklady Akad. Neuk, S.S.S.R., 122, 393-6 (1958); Chem. Abst., 53, 2133d (1959).